

Biocatalytic and Organocatalytic Approaches to Ketodiol Synthesis

A Thesis Submitted to University College London

By

James Galman

For the Degree of

DOCTOR OF PHILOSOPHY

Christopher Ingold Laboratories

Department of Chemistry

University College London

20 Gordon Street

London

WC1H 0AJ

I, **James Galman** confirm that the work presented in this thesis is in partial fulfillment of the requirements for the degree of Doctorate of Philosophy represents my own work. Where information has been derived from other sources, I confirm that this has been indicated in the thesis.

Signature_____

Abstract

The enzyme transketolase (TK) (EC2.2.1.1) catalyses a reversible asymmetric carbon-carbon bond forming reaction, where a two carbon ketose donor is transferred to an aldose acceptor. The use of hydroxypyruvate (HPA), a non-phosphorylated ketol donor with subsequent loss of carbon dioxide renders the reaction irreversible generating the dihydroxyketone product. Several years ago the TK gene from the plasmid of *E. coli* (BJ502/pKD112A) was incorporated into a high copy plasmid leading to the overexpression of the protein in *E. coli*, a suitable host for industrial processes. The TK condensation of HPA with glycolaldehyde and propanal, in analogous but separate experiments, has been described in the literature. The on-going development of the enzyme TK as a practical biocatalyst performed on a small scale recently led to the discovery of the first biomimetic TK reaction.

The aims of the PhD project were principally two-fold; to explore both biomimetic and biocatalytic routes to α,α' -dihydroxyketones. Firstly, investigation of the new one pot synthesis of racemic dihydroxyketones; in terms of substrate scope of the reaction, including aromatic, aliphatic hydrophobic aldehydes as substrates. Donors other than hydroxypyruvate (HPA) were also investigated to assess the general synthetic utility of the reaction. Reaction optimisation studies and preliminary mechanistic studies were performed. In addition, investigations into the development of an asymmetric organocatalytic reaction were pursued. Secondly, libraries of TK mutants were also screened against a range of non-natural substrates. A colorimetric assay for screening active mutants in a 96 well plate format was used to identify successfully a number of active mutants with enhanced substrate specificity towards novel cyclic and aromatic acceptor molecules, as well as being used for determining initial rate velocities. A chiral assay as a means to determine the absolute stereochemistry, using chiral derivatising agents (CDAs) was established which was used with HPLC for successful characterisation of the dihydroxyketone motifs.

Chapter 1 of this thesis is an introduction to the important role of thiamine dependent enzymes in synthesis, in particular transketolase: the structure, mechanism and its usage in industry is covered. Chemical synthetic routes to ketodiol motifs are also mentioned. Chapter 2 presents the use of a novel chiral assay to determine absolute stereochemistries achieved in biocatalytic or biomimetic reactions. Chapter 3 describes studies of stereoselectivities with active point single TK mutants on cyclic aldehydes. Chapter 4 covers the use of aromatic acceptor substrates with transketolase. Chapter 5 describes investigation into novel asymmetric biomimetic routes to ketodiol synthesis and finally Chapter 6 concludes the studies and encourages further research.

Contents

Abstract	3
Contents	4
Contents of Schemes, Tables and Figures	7
Abbreviations	12
Acknowledgements	15
Chapter 1.0 Introduction	16
1.1 Enzymes used as biocatalysis in synthesis	17
1.1.0 Thiamine-dependent enzymes	18
1.1.1 Benzoylformate decarboxylase (BFD)	18
1.1.2 Benzaldehyde lyase (BAL)	20
1.1.3 Pyruvate decarboxylase (PDC)	22
1.2 Transketolase and the transketolase reaction	24
1.2.1 X-ray crystal structure of <i>saccharomyces cerevisiae</i> transketolase	25
1.2.2 Substrate binding in thiamin diphosphate-dependant transketolase	26
1.2.3 Site directed mutagenesis on selected amino acid residues with catalytic activity	29
1.2.4 Amino acid residue Asp477 responsible for enantioselectivity	30
1.2.5 Protocols for the transketolase reaction	31
1.2.6 Transketolase: A biocatalyst for asymmetric carbon-carbon bond synthesis and applications in organic syntheses using yeast, spinach and <i>E.coli</i> TK.	31
1.2.7 Transketolase in synthesis	37
1.3. Synthesis of acyclic α,α'-dihydroxyketones	39
1.3.1 Addition of 2-lithio-1,4-dioxane to aldehydes/ketones followed by peracid oxidation	39
1.3.2 Chloroalkyl <i>p</i> -tolyl sulfoxides as hydroxycarbonyl anion equivalents	40
1.3.3 The ruthenium-catalysed oxidation of allenes	41
1.3.4 A double hydroxylation of enol silyl ethers	42
1.3.5 The SAMP/RAMP-hydrazone methodology	43
1.3.6 Aims of Research	46
Chapter 2.0 The modified Mosher's method	47
2.1 Determination of the absolute stereochemistry of chiral carbinol carbons	48

2.2	Determining the absolute stereochemistry of chiral carbinols using Mosher's ester analysis	48
2.2.1	¹⁹ F Chemical shifts of α -methoxy- α -trifluoromethylphenylacetate (MTPA) derivatives	50
2.2	Modified Mosher's method on the absolute stereochemistry of β -chiral primary alcohols	51
2.3	Application of a modified Mosher's method for the determination of chiral 1,3-dihydroxy ketones	55
2.4	Summary	59
Chapter 3.0 Aliphatic aldehydes used in the TK reaction		60
3.1	UCL developments prior to thesis research	61
3.1.1	Directed evolution of TK substrate specificity towards the non-phosphorylated substrate, glycolaldehyde	62
3.1.2	Directed evolution of TK substrate specificity towards an aliphatic aldehyde propanal	64
3.1.3	The colorimetric assay for screening transketolase activity	64
3.1.4	Investigating cyclic aldehydes with evolved TK enzymes	68
3.2	Active mutant identification with cyclic substrates	70
3.3	Obtaining <i>E. coli</i> TK cell-free lysates	73
3.4	Cyclopropanecarboxaldehyde as an acceptor substrate for the TK Reaction	74
3.5	Cyclopentanecarboxaldehyde as an acceptor substrate for the TK Reaction	76
3.6	Cyclohexanecarboxaldehyde as an acceptor substrate for the TK Reaction	80
3.7	Initial relative rates of D469T	83
3.8	Synthesis of 3,4-dimethyl-3-cyclohexene-1-carboxaldehyde and the formation of the ketodiol product	84
3.9	The colorimetric screening of library D469 with aldehyde 104	86
3.10	Aldehyde 104 as acceptor substrate for the TK reaction	91
3.11	Summary	92
Chapter 4.0 Aromatic aldehydes used in the TK reaction		93
4.1	Aromatic aldehydes used as novel substrates in the TK reaction	94
4.2	The colorimetric screening of library D469 with benzaldehyde	95
4.3	Benzaldehyde as an acceptor substrate for the TK reaction	96
4.4	Furfural as an acceptor substrate for the TK reaction	99

4.5	Phenylacetaldehyde as an acceptor substrate for the TK reaction	101
4.6	2-Phenylpropionaldehyde as an acceptor substrate for the TK reaction	104
4.7	Substrate specific activity, Initial rates of reaction of Phenylacetaldehyde and 2-Phenylpropionaldehyde	109
4.8	Other aromatic aldehydes used as acceptor substrate molecules	110
4.9	Summary	111
Chapter 5.0 Biomimetic TK Reaction		112
5.1	Reporting the first pioneering biomimetic transketolase reaction	113
5.1.1	Biomimetic TK research performed prior to PhD studies	113
5.2	Preparation of lithium hydroxypyruvate as a ketol donor from bromopyruvic acid	115
5.2.1	Other alkaline metal hydroxypyruvates and its reactivity in ketodiol synthesis	116
5.3	Aliphatic aldehydes as acceptor molecules for the biomimetic TK reaction	117
5.4	Aromatic aldehydes as acceptor molecules for the biomimetic TK reaction	119
5.5	Mechanistic implications	122
5.5.1	Postulated reaction mechanism	122
5.5.2	NMR investigations using bromopyruvate and hydroxypyruvate	122
5.5.3	Synthesis of [1- ² H]-cyclohexancarboxyaldehyde and its use in ketodiol synthesis	125
5.5.4	Deuterium oxide experiments used in ketodiol synthesis	127
5.6	Cinchona alkaloid catalysts for ketodiol synthesis	129
5.6.1	Synthesis of cinchona alkaloid catalysts	132
5.6.2	Organocatalytic TK reaction using the cinchona alkaloid catalysts	133
5.7	Chiral diamine catalysts for ketodiol synthesis	135
5.7.1	Synthesis of chiral diamine catalysts for the biomimetic TK reaction	136
5.7.2	Organocatalytic reaction using the diamine catalyst for the TK reaction	138
5.8	Summary	139
Chapter 6.0 Conclusions and Future work		141
Chapter 7.0 Experimental		145
Publications from PhD research		196
References		228

Contents of Schemes, Tables and Figures.

Scheme 1: The pathway for microbacterial production of 3-dehydroxyshikimate by using recombinant <i>E.coli</i> KDPGal	17
Scheme 2: Chemoenzymatic pathway for the production of a 7 membered azasugar	18
Scheme 3: The catalytic mechanism of BFD generating benzaldehyde and 15	19
Scheme 4: The generation of (<i>R</i>)-Benzoin products 16	19
Scheme 5: Cross coupling of an aromatic aldehyde with acetaldehyde to generate 17	19
Scheme 6: Self condensation reaction with BFD	20
Scheme 7: General carboligation with BAL	20
Scheme 8: Catalytic cycle of BAL using ThDP	21
Scheme 9: Synthesis of enantiopure 19 that can be used as chiral synthons.....	22
Scheme 10: The production of ephedrine 23 and pseudoephedrine 24 from 15	22
Scheme 11: General reaction mechanism for (<i>R</i>)- 15 synthesis	23
Scheme 12: Carboligation of propanal and pyruvate 3	23
Scheme 13: Transfer of a ketol unit to an aldose sugar phosphate molecule	24
Scheme 14: The ThDP mechanism of TK	25
Scheme 15: Irreversible Condensation reaction of Li-27	31
Scheme 16: The yeast TK biotransformation reaction using Li-27 and 28	32
Scheme 17: The yeast TK reaction using a non- α -hydroxyaldehyde with Li-27	34
Scheme 18: TK-catalysed reaction with Li-27 and (<i>R</i>)- α -hydroxyaldehyde	35
Scheme 19: Retrosynthesis of (+)-exo-Brevicomine.....	38
Scheme 20: Retrosynthesis and synthesis of an ulosonic acid analogue	38
Scheme 21: Synthesis of novel <i>N</i> -hydroxypyrrolidine.....	39
Scheme 22: Multi-step synthesis of ketodiol 46	40
Scheme 23: Chloroalkyl <i>p</i> -tolyl sulfoxides used in the synthesis of ketodiol 50	40
Scheme 24: Ruthenium catalysed oxidation of allenes to ketodials 52 and 53	41
Scheme 25: The synthesis of corticosteroids	42
Scheme 26: Preparation of α -silyoxy and α -hydroxy ketones	42
Scheme 27: Mechanistic pathway for the generation of α -silyoxy and α -hydroxy ketones 65	42
Scheme 28: Two approaches for the synthesis of 2,2-dimethyl-1, 3-dioxan-5-one. DMP=2,2-dimethoxypropane, PTSA = <i>p</i> -toluenesulfonic acid.	43
Scheme 29: The asymmetric synthesis of 4-substituted 2,2-dimethyl-1,3-dioxane-5 ones.....	44
Scheme 30: Cleavage of chiral auxiliary and acetal protecting group to afford ketodiol product.....	44
Scheme 31: Formation of disubstituted 2,2-Dimethyl-1,3-dioxane-5-ones.....	45
Scheme 32: Symmetric synthesis of α,α' -quaternary 2-keto-1,3-diols	45
Scheme 33: The synthesis of (<i>R</i>)- and (<i>S</i>)- Mosher's ester from the stereogenic carbinol centre	48
Scheme 34: TK-catalysed reaction with propanal and Li-27	55
Scheme 35: Ender's chiral auxiliary methodology	55
Scheme 36: Biotransformation of glycolaldehyde with Li-27 as substrate using mutant <i>E.coli</i> TK	62
Scheme 37: The oxidation of 83 to the diketone 86 generating red coloration.....	65
Scheme 38: The oxidation of the ketodiol to the diketone 87 or ketone-aldehyde 88 ..	65
Scheme 39: Biotransformations using <i>E.coli</i> TK to generate 30r and 30s	66
Scheme 40: The objectives	69
Scheme 41: Potential routes to biologically active compounds.....	69
Scheme 42: The biomimetic formation of 30v	74
Scheme 43: Benzoylation of 30v and HPLC data of 94a	75
Scheme 44: Formation of the (<i>S</i>)-MTPA ester 95	76
Scheme 45: Biomimetic formation of 30x	77
Scheme 46: Benzoylation of 30x and HPLC data of 96	77

Scheme 47: Formation of (<i>S</i>)-MTPA and (<i>R</i>)-MTPA ester, 97 and 98	79
Scheme 48: Biomimetic formation of ketodiol 30y	80
Scheme 49: Acetylation of ketodiol 30y	81
Scheme 50: Benzoylation of ketodiol 30y	81
Scheme 51: Formation of the (<i>S</i>)-MTPA ester 101	82
Scheme 52: Formation of aldehyde 104 via ionic liquid	84
Scheme 53: Biomimetic reaction of aldehyde 104	85
Scheme 54: Benzoylation of ketodiol 105	85
Scheme 55: The biotransformation of 104 and Li-27 to generate ketodiol 105	87
Scheme 56: Formation of (<i>S</i>)-MTPA ester 107	88
Scheme 57: Diels-Alder formation of (<i>1R</i>)- 104	89
Scheme 58: The formation of the benzoylated product 106	90
Scheme 59: Formation of (<i>1S</i> , <i>1'R</i>)- 106	91
Scheme 60: Formation of 30Ar1 and 110 in water	96
Scheme 61: The generation of glycolaldehyde in situ via decarboxylation of a β-ketocarboxylic acid	97
Scheme 62: Mechanism for the generation of the proposed structure of the by-product formed	97
Scheme 63: Formation of (<i>R</i>)-MTPA ester 115	98
Scheme 64: Acetylation of 30Ar1 and a spectrum of the separated isomers 116	98
Scheme 65: Mechanism of ketodiol 30Ar2 rearranged to 117	99
Scheme 66: Formation of (<i>S</i>)-MTPA ester 119	100
Scheme 67: DCC coupling forming (<i>S</i>)-MTPA ester of 30Ar2	100
Scheme 68: Formation of 30Ar3 and acetylated product 121 (spectra of inseparable Isomers)	101
Scheme 69: Generation of a mono-, dibenzoylated products (spectra of separated isomers of 123)	102
Scheme 70: Rearrangement mechanism of 30Ar3	103
Scheme 71: Formation of the (<i>S</i>)-MTPA ester 126	103
Scheme 72: Benzoylation of 30Ar4	105
Scheme 73: Formation of (<i>S</i>)-MTPA ester 128	106
Scheme 74: Retrosynthesis of (<i>4R</i>)- 30Ar4	107
Scheme 75: Formation of (<i>R</i>)-aldehyde 131	108
Scheme 76: Formation of benzoylated (<i>4R</i>)- 132	108
Scheme 77: Biomimetic reaction using 146 as catalyst	113
Scheme 78: Mechanistic investigation of the formation of Li-27	115
Scheme 79: The formation of hydroxypyruvate salt	116
Scheme 80: The direct aldol condensation of pyruvate and an aliphatic aldehyde in polar solvent	118
Scheme 81: Reactions of α-keto acids	118
Scheme 82: The formation of ketodiol product 30Ar1 and the rearranged product 110	119
Scheme 83: Mechanism for the rearrangement of ketodiol to generate 165	121
Scheme 84: Postulated biomimetic reaction mechanism	122
Scheme 85: Formation of deuterated aldehyde 176	125
Scheme 86: Biomimetic reaction involving deuterated aldehyde 176	126
Scheme 87: Pathway favoring kinetic enolate 30yDH and 30yDD	128
Scheme 88: Using quindine as a catalyst for biomimetic TK reaction	129
Scheme 89: Formation of the Mosher's ester 101	130
Scheme 90: Formation of quinine analogues	132
Scheme 91: Catalyst used in direct aldol condensation	135

Table 1: The kinetic data of several TK mutants with Xu5P and R5P as acceptor substrates	29
Table 2: Reported results of α -hydroxyaldehydes as acceptor molecules with yeast TK. Whitesides <i>et al.</i> (pink), biotransformation conditions; Li-27 (10 mM), aldehyde (50-130 mM), pH maintained by addition of Li-27 , 10-30U TK added. Effenberger <i>et al.</i> (blue), biotransformation conditions: 25-50 mM scale, equimolar reagents, Tris.HCl buffer (0.5 M, pH 7.6) incubated at 30 °C, unspecified amount of enzyme used. ^{42, 44}	33
Table 3: V_{rels} of non- α -hydroxyaldehydes using yeast TK. Demuynck <i>et al.</i> biotransformation conditions; TK (1 U ml ⁻¹), gly-gly buffer 0.1 M at pH 7.5, aldehyde (60-200 mM), and Li-27 (7.5 mM).....	34
Table 4: The Spinach TK reaction with various acceptor aldehydes. Demuynck <i>et al.</i> biotransformation conditions; Spinach TK (250 U), Tris buffer 0.1 M at pH 7.5, Li-27 (100 mM), aldehyde (100 mM)	35
Table 5: The relative rates of various substrates for the TK reaction	36
Table 6: <i>E. coli</i> TK with various acceptor molecules. Turner <i>et al.</i> ⁵¹ biotransformation reaction; Li-27 (7.5 mM), gly-gly buffer (70 mM at pH 7.6), aldehyde (100mM) TK (3U) in 1 ml.....	37
Table 7: Examples of the synthesis of ketodiols using chloroalkyl <i>p</i> -tolyl sulfoxides .	41
Table 8 : The performance of selected TK mutants	63
Table 9: The specific substrate activities of the formation of 30s and 30r	67
Table 10: Kinetic parameters for WT and D469T-TK	68
Table 11: The calculated TK protein concentration in lysates	74
Table 12: The percentage yields obtained from acceptor substrate 89	75
Table 13: The <i>ees</i> obtained from selected D469 mutants of 30v	76
Table 14: The percentage yields obtained from acceptor substrate 90	78
Table 15: The <i>ees</i> obtained from selected D469 mutants of 30x	78
Table 16: The percentage yields of ketodiol product 30y	81
Table 17: The <i>ees</i> obtained from selected D469 mutants of 30y	82
Table 18: The kinetic kinetic data obtained for D469T on various acceptor substrates	83
Table 19: The relative activities and total expressed protein of D469 TK mutants	87
Table 20: Other aromatic substrates used as substrates	94
Table 21: The yields of the biotransformation product 30Ar1 and 110 using several TK mutants	96
Table 22 The percentage <i>ees</i> of ketodiol 30Ar1 upon formation of 116	98
Table 23: Isolated biotransformation yields of 30Ar2 and by-product 117 using several TK mutants	99
Table 24: Yields of ketodiol 30Ar3 generated.....	102
Table 25: The percentage <i>ees</i> of ketodiol 30Ar3 generated.....	103
Table 26: The yields of the biotransformation product 30Ar4	105
Table 27: The percentage <i>ees</i> of 30Ar4	107
Table 28: The diastereoselectivities generated from WT and D469 TK mutants.....	108
Table 29: The D469T kinetic and specific activity data on substrates 93 and 133	110
Table 30: Catalysts used for the biomimetic TK reaction	114
Table 31: The formation of HPA salt and the ketodiol product 30v	117
Table 32: The TK biomimetic reaction of ketodiol 30	119
Table 33 Aromatic aldehydes used in the biomimetic TK reaction conducted pH 7.0	121
Table 34: Biomimetic reaction with acceptor aldehyde 91 with various catalysts	133
Table 35: The reactions were conducted with 30 mol% of the diamine, 1.0 eq. of aldehyde and 5.0 eq. of methyl vinyl ketone in EtOH at 0 °C.....	135
Table 36: Diamine/TFA-catalysed aldol reaction with various arylaldehydes in water	136
Table 37: Formation of (<i>S</i>)-Boc-proline.....	136
Table 38: The reduction of the amide 187 to the diamine catalyst 188	137
Table 39: Generation of diamine 190	137
Table 40: Entries 1-6; diamine cat. (1 eq.), aldehyde (1 eq.), Cs-27	138

Figure 1: Structure of ThDP, amPyr = aminopyrimidine ring, Thiaz = thiazolium ring,	18
Figure 2: The chemical structure of ThDP	25
Figure 3: X-ray crystal structure of <i>Saccharomyces cerevisiae</i> TK with ThDP, Ca ²⁺ and E4P (1NGS.pdb) from www.rcsb.org/pdb	26
Figure 4: Selected amino acid residues and the hydrogen bonding distances.....	27
Figure 5: Schematic interaction of ThDP with E4P	27
Figure 6: Crystal structure of Xu5P-ThDP adduct with an out-of-plane distortional angle (25-30°) (2R8O.pdb) from www.rcsb.org/pdb.....	28
Figure 7: (A) WT amino acid residues hydrogen bond to E4P (B) Mutant amino acid residues hydrogen bonding to E4P (mutagenesis performed by pyMOL) ...	30
Figure 8: Depletion of HPA towards D-, L- and DL-glyceraldehyde. Reprinted from "Transketolase from <i>Escherichia coli</i> : A practical procedure for using the biocatalyst for asymmetric carbon-carbon bond synthesis" with permission from Elsevier	36
Figure 9: The two enantiomers of thalidomide.....	48
Figure 10: Common conformational representations of the MTPA-esters.....	49
Figure 11: Configuration-correlation models where (<i>R</i>)-MTPA diastereomer is downfield relative	51
Figure 12: Configuration-correlation models where <i>S</i> -MTPA diastereomer is downfield relative to alternate diastereomer	51
Figure 13: Conformational representation of the interaction between γ , δ substituents and the aryl group of MTPA, an example of borneol an exception to this model.....	52
Figure 14: Investigating the stereochemistry steroid 88	52
Figure 15: ABX splitting pattern of diastereotopic protons. Reprinted from "Application of Modified Mosher's Method for Primary Alcohols with a Methyl Group at C2 Position", with permission from Chemical and Pharmaceutical Bulletin.....	53
Figure 16: Chemical shift differences $\Delta\delta$ of oxymethylene protons of MTPA.....	53
Figure 17: Retrosynthesis of bioactive natural product from 2-methyl-1, 2-butanediol	54
Figure 18: The ¹ H NMR AB-spectra of diastereotopic oxymethylene protons, the arrows represent the anisotropic interaction of the aryl ring and the hydroxyl group. Reprinted from "Stereochemical assignment of naturally occurring 2,3-epoxy-2-methylbutanoate esters", with permission from John Wiley and Sons. ⁸⁴	54
Figure 19: A conformational model proposed for the analysis of the diastereomeric MTPA ester	58
Figure 20: Configuration correlation models of MTPA esters where R is small R ₁ \approx R ₂	59
Figure 21: Location of structurally defined and phylogenetic sites relative to the ThDP cofactor in the <i>E.coli</i> TK active site.....	62
Figure 22: The interaction with A29 (A) and the postulated interaction with A29E (B) crude mutagenesis performed using pyMol (1NGS.pdb, from www.rcsb.org/pdb)	63
Figure 23: Clustered enzyme mutants responsible for catalysis in the active site of TK using pyMOL (1NGS.pdb, from www.rcsb.org/pdb).....	67
Figure 24: Enzyme active site to <i>E.coli</i> TK highlighting position of D469.....	70
Figure 25: ODs of selected D469 <i>E.coli</i> TK with substrates 89, 90, 91	71
Figure 26: Colorimetric plates screened against the cyclic aldehydes	72
Figure 27: Top view of a 7.5% SDS-page gel of TK variants, WT-TK, and purified TK. The enzyme was purified using a XK 16/20 chromatographic column. The dark band represents the denatured TK protein monomer at 75kDa. The samples are as follows: (1) Protein standard marker; (2) WT; (3) D469L; (4) H4; (5) H26Y; (6) D469T; (7) Purified TK; (8) D469E; (9) D469S; (10) G6	73
Figure 28: (A) racemate 94 ; (B) D469T product with added racemate; (C) D469T product.....	75
Figure 29: ¹ H NMR region 5.0 to 5.5 ppm of (<i>S</i>)-MTPA ester 95	76

Figure 30: (A) racemate of 96 ; (B) D469T product with added racemate 96 ; (C) D469T product.....	78
Figure 31: (A) SMTPA ester of D469T (B) racemic (<i>S</i>)-, (<i>R</i>)-MTPA esters, (C) (<i>R</i>)-MTPA ester D469T	79
Figure 32: RP5 furanose form in enzyme active site with ThDP	80
Figure 33: (A) racemate 30y ; (B) D469T product with added racemate 30y ; (C) D469T product.....	82
Figure 34: ¹ H NMR of H _a H _b from 101	82
Figure 35: HPLC trace of 4 isomers of 106	86
Figure 36: Colorimetric assay on D469 library with aldehyde 104	86
Figure 37: Comparison of WT-TK and D469T-TK mutant by TLC	87
Figure 38: HPLC traces of monobenzoylated products 105	88
Figure 39: ¹ H NMR spectra of H _a and H _b of 107	89
Figure 40: Retrosynthesis of (<i>1'R</i>)- 105	89
Figure 41: Spectra (A) Biomimetic, 2 major peaks and (B) D469T product, 1 major peak.....	90
Figure 42: (A) D469 hydrogen bonding to R5P (B) D469/D469T steric clash to neighbouring side chains (C) D469T hydrogen bonding to R5P (a crude pyMOL mutagenesis (1NGS.pdb, taken from www.rcsb.org/pdb).....	91
Figure 43: The colorimetric assay screening library D469 for active TK mutants with benzaldehyde.....	95
Figure 44: TLC plate showing the biotransformation products of D469T	97
Figure 45: NMR spectra of (<i>R</i>)-MTPA ester of 115	98
Figure 46: ¹ H NMR representing H _A and H _B of 119	100
Figure 47: ¹ H NMR of H _a and H _b of 120	101
Figure 48: ¹ H NMR spectrum of H _A and H _B of 126	104
Figure 49: ¹ H NMR spectra of biomimetic (A) and ¹ H NMR of D469T (B).....	104
Figure 50: Spectrum A (127 obtained from D469T) Spectrum B (127 Racemate from biomimetic).....	106
Figure 51: ¹ H NMR of H _a and H _b of 128	106
Figure 52: HPLC traces of 30Ar4	108
Figure 53: Acceptor substrates	109
Figure 54: Further biotransformations	109
Figure 55: Various aldehyde acceptors used in the TK reaction.....	111
Figure 56: Li-27 existing in <i>gem</i> -diol and keto form.....	116
Figure 57: Pyruvic acid and lithium monohydrate salt in different forms	116
Figure 58: ¹ H NMR of 30Ar1 and 110	120
Figure 60: The major forms of pyruvates existing in water	124
Figure 61: A donor acceptor substrate	124
Figure 62: ¹ H NMR spectra of ketodiols production with aldehyde (A); generated ketodiols product at pH 8.0 with 176 (B); and at pH 9.7 with 176 (C)	126
Figure 63: NMR spectra of ketodiols production (A) H ₂ O solution at pH 8.00; (B) D ₂ O solution at pH 7.00; (C) D ₂ O solution at pH 8.00	127
Figure 64: Deuterated containing compounds 30yDH and 30yDD	128
Figure 65: The cinchona alkaloids.....	129
Figure 66: Diacetylated racemic ketodiols product (A) and quinidine catalysed product (B).....	130
Figure 67: A donor acceptor substrate	124
Figure 68: The HPLC trace of quinidine catalysed biomimetic reaction.....	132
Figure 69: The HPLC trace of the biomimetic reaction using catalyst 183 , 20 mol%	133
Figure 70: A postulated intermediate for the generation of ketodiols using 183	134
Figure 71: Screening of commercially available cinchona alkaloids	134
Figure 72: The proposed reaction intermediate for the generation of (<i>S</i>)- 30y	139
Figure 73: An X-ray crystal structure of a trapped F6P-ThDP intermediate	143
Figure 74: Phenylpyruvate 191 and Mercaptopyruvate 192	144
Figure 75: ¹ H NMR spectra of compound 97	166
Figure 76: ¹ H NMR spectra of compound 98	167

Abbreviations

Å	Angstrom
AcOH	Acetic acid
Ar	Aromatic
Arg	Arginine
Asp	Aspartic Acid
BAL	Benzaldehyde lyase
Boc	tert-Butyloxycarbamate
BOP-Cl	Bis (2-oxo-3-oxazolidinyl) phosphinic chloride
BFD	Benzoylformate decarboxylase
BKD	1,3-Dihydroxy-1-phenyl-propan-2-one
BzCl	Benzoyl chloride
br	Broad
cat.	Catalyst
CDCl ₃	Deuterated chloroform
CHCl ₃	Chloroform
CH ₂ Cl ₂	Dichloromethane
d	Doublet
dd	Doublet of doublets
δ	Chemical Shift in ppm
δ _{Low}	Low field protons
δ _{high}	High field protons
Δδ _H	Chemical shift difference
DCC	Dicyclohexylcarbodiimide
DHE	α,β-Dihydroxyethyl-
DHE–ThDP	α,β-Dihydroxyethyl- thiamine diphosphate intermediate
DMAP	Dimethylaminopyridine
DMF	Dimethylformamide
DMPU	1,3-Dimethyl-2-oxo-hexahydropyrimidine
DMSO	Dimethylsulfoxide
ee	Enantiomeric excess
eq	Equivalence
<i>E. coli</i>	<i>Escherichia coli</i>
EtOAc	Ethyl Acetate
E4P	Erythrose-4-phosphate
FAB	Fast atom bombardment
F6P	Fructose-6-phosphate

GC	Gas chromatography
Glu	Glutamic acid
Gly-gly	gly-glycine
h	Hour(s)
His	Histidine
HPA	β -Hydroxypyruvic acid
HPLC	High performance liquid chromatography
IDH	Iditol dehydrogenase
IR	Infra-red
LB	Luria-Bertani
m	Multiplet (NMR)
mg	Milligram
Mg ²⁺	Magnesium
min	Minute(s)
mmol	Millimoles
MOPS	3-(N-morpholino)propanesulfonic acid
MTPA	α -Methoxy- α -trifluoromethylphenylacetic acid
MTPA-Cl	α -Methoxy- α -trifluoromethylphenylacetic acid chloride
NaCNBH ₃	Sodium cyanoborohydride
NaOH	Sodium hydroxide
NADH	Reduced nicotinamide adenine dinucleotide
NMM	<i>N</i> -methylmorpholine
NMR	Nuclear magnetic resonance
NEt ₃	Triethylamine
OD	Optical density
PDC	Pyruvate decarboxylase
PEP	Phosphophenol pyruvate
pK _a	Acid dissociation constant
PKD	1,3-Dihydroxy-pentan-2-one
POX	Pyruvate oxidase
PDH	Pyruvate dehydrogenase
PTSA	<i>p</i> -Toluenesulphonic Acid or <i>p</i> TsOH
q	quartet
QN	Quinine
QD	Quinidine
R	Unspecified carbon substituent
(<i>R</i>)	Rectus (clockwise direction) chirality
R _f	Retention factor

rt	Room temperature
s	Strong Intensity (IR)
s	Singlet (NMR)
(S)	Sinister (counter-clockwise direction) chirality
SAMP	(S)-1-amino-2-methoxy-methylpyrrolidine
Ser	Serine
t	Triplet (NMR)
TBS	<i>tert</i> -butyldimethylsilyl (protecting group)
TBSOTf	<i>tert</i> -butyldimethylsilyl trifluoromethanesulfonate
ThDP	Thiamine diphosphate
TLC	Thin layer chromatography
TFA	Trifluoroacetic acid
TK	Transketolase
Tris	Tris(hydroxymethyl)methylamine
<i>t</i> -BuLi	<i>tert</i> -Butyllithium
THF	Tetrahydrofuran
UV	Ultraviolet
V_{rel}	Relative Velocities
K_M	Michaelis Constant – concentration at which rate of enzyme reaction is half V_{max}
V_{max}	Maximum rate
WT-TK	Wild type transketolase
Xu5P	Xylulose-5-phosphate
λ_{max}	Wavelength at maximum absorbance (UV)

Acknowledgements

I would like to express my sincere thanks to:

My supervisor Helen Hailes for her guidance and patience throughout my tenure as a PhD student, and to EPSRC for financial support. I would like to express my gratitude to the past and present Hailes/Tabor research groups for the 'laughs', the 'drama' and the camaraderie for making my research studies worthwhile.

Special thanks to Mark E.B. Smith, Armando Cazares, Phattaraporn Morris, Lydia Crago, Jimmy Ho, Eun-Ang Raiber and Elisabetta Greco for their expertise and corroborative efforts that helped me with my PhD. I would especially like to acknowledge my brothers; Jeremy and Jeffrey and my parents; Gloria and Rodolfo Galman for their kind support, encouragement and understanding during the difficult times in writing my thesis.

Maraming salamat sa inyong lahat, Mahal Kita! <3

'Quod me non necat me certe fortiozem facit'

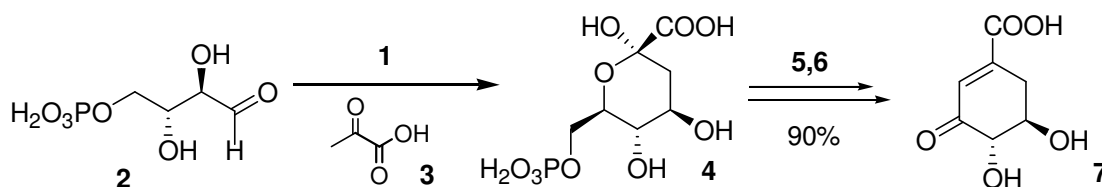
Chapter 1.0

Introduction

1.1 Enzymes used as biocatalysts in synthesis

Enzymes are highly suited to the on-going 'Green Chemistry' initiative first proposed by P.T Anastas of 'designing new products and processes that reduce or eliminate the use and generation of hazardous substances'.¹ Enzymes by their nature are biodegradable, renewable sources and utilize water as the reaction solvent. Reactions catalyzed by enzymes are the most mild, effective and selective 'green' processes available to date. The advantages of using biocatalysts include; high regio- and stereoselectivity, substrate versatility, and the production of fewer by-products that can be considered detrimental to the environment. Enzyme catalysed formation of C-C bonds is important in synthetic organic chemistry, providing efficient access to stereospecific motifs, which may require a number of synthetic steps to produce using chemical transformations.

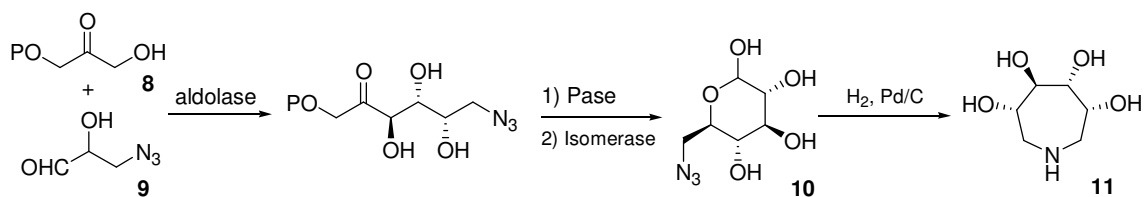
In light of the demand for enantiomerically pure compounds for pharmaceutical purposes, the benefits of using enzymes are obvious. One example reported by Frost *et al.*² is the novel synthesis of shikimic acid an essential precursor to the production of tamiflu. The success of this shikimic pathway is dependent on the directed evolution of 2-keto-3-deoxy-6-phosphogalactonate aldolase **1** (KDPGal) to generate 3-deoxy-D-*arabino*-heptulosonate 7-phosphate **4**, from pyruvate **3**, and a non-natural substrate D-erythrose-4-phosphate **2**. The KDPGal variant was overexpressed in *E. coli* and incubated with pyruvate **3**, and **2**, 3-dehydroquininate synthase **5**, and 3-dehydroquininate dehydratase **6** which catalyzed the formation of enantiomerically pure 3-dehydroxyshikimate **7** in 90% yield (Scheme 1).



Scheme 1: The pathway for microbacterial production of 3-dehydroxyshikimate by using recombinant *E.coli* KDPGal

In carbohydrate chemistry in particular, the usage of a plethora of protecting groups is typically required for chemical preparation due to the multiple hydroxyl groups. A variety of enzymes such as lyases and aldolases have been used to synthesize complex sugars and other biologically important natural compounds.³ One such example is the synthesis of aza sugars which are known as potential enzyme inhibitors and therapeutic agents. Ketoses containing an azido group can be generated by an enzymatic aldol condensation between dihydroxyacetone phosphate **8** as a donor molecule with an azido containing acceptor aldehyde **9**.^{3c} Then treatment with acid

phosphatase and an isomerase to generate 6-azido-6-deoxyaldopyranose **10**, which upon reductive amination afforded the 7-membered azasugar **11** (Scheme 2).



Scheme 2: Chemoenzymatic pathway for the production of a 7 membered azasugar

1.1.0 Thiamine-dependent enzymes

Thiamine-dependant enzymes have been used on an industrial since the early 1920's as catalysts, in a baker's yeast whole cell biotransformation of (*R*)-phenylacetyl carbinol, a precursor to (-)-ephedrine. However it was not until 1937 that the structure of thiamin diphosphate (ThDP) was first determined.⁴ In most ThDP (Fig. 1) dependent enzymes the haloenzyme catalyses a carbon-carbon bond cleavage of a donor substrate forming a reactive intermediate which condenses with an acceptor molecule generating a new product with the regeneration of ThDP. The nature of the acceptor molecule determines if the enzyme is more specific in the reaction or more permissive. From an industrial stand point, enzymes that tolerate a large spectrum of substrates are of greater interest. Discussed below are several ThDP dependent enzymes, their substrate specificity and their industrial synthetic potential, with examples.

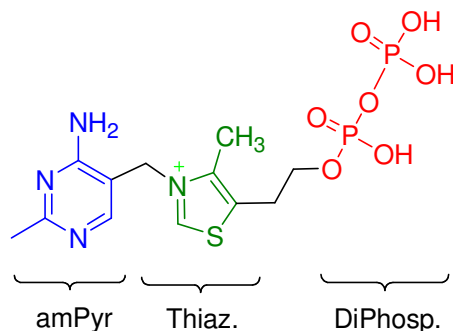
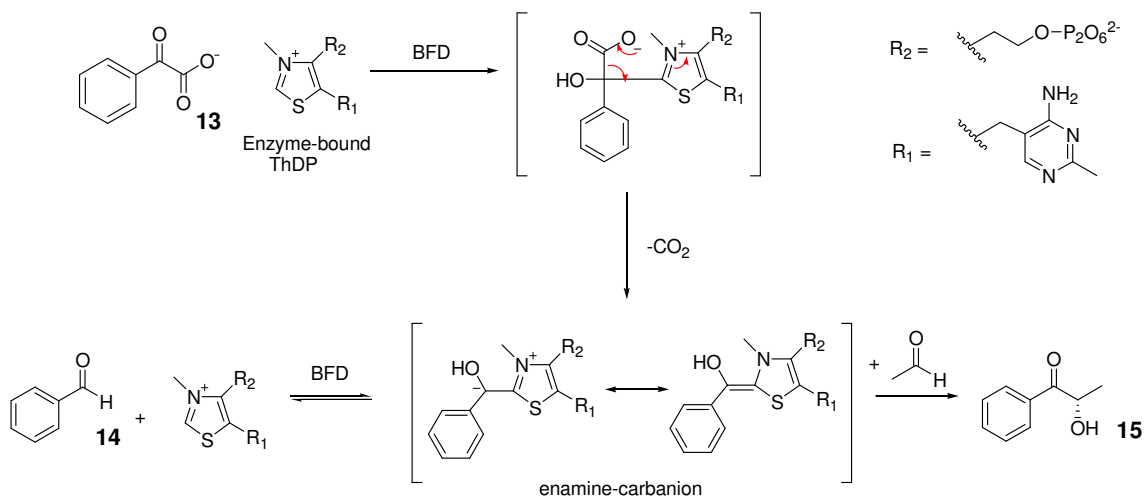


Figure 1: Structure of ThDP, amPyr = aminopyrimidine ring, Thiaz = thiazolium ring, Diphos = Diphosphate

1.1.1 Benzoylformate decarboxylase

Benzoylformate decarboxylase (BFD) (E.C. 4.1.1.7) involved in the mandelate biosynthetic pathway⁵ is a ThDP dependant enzyme purified and characterized from *Pseudomonas putida*,⁶ or from *Acinetobacter calcoaceticus*.⁷ BFD has been shown to exhibit various catalytic activities; a non oxidative decarboxylation of benzoyl formate **13** to form benzaldehyde **14** and catalyses the enantioselective acyloin formation of

(*S*)-2-hydroxypropiophenone **15**, (92% *ee*) from *Pseudomonas putida* BFD within a broad pH range (5-8) and temperature (20-40 °C) range (Scheme 3).⁸ Further (*S*)-**15** analogues have also been formed upon the ligation of acetaldehyde with different, aromatic, heteroaromatic, olefinic and cyclic aliphatic aldehydes, with high *ees* in the range of 87-99%.^{9,10}



Scheme 3: The catalytic mechanism of BFD generating benzaldehyde and 15

The carboligase activity of BFD from *Pseudomonas putida* has also been reported for the general C-C bond mediated synthesis of enantiomerically pure benzoin and substituted benzoin derivatives from aromatic aldehydes. The carboligation experiments were performed with benzaldehyde as the sole substrate and generated (*R*)-benzoin **16** in an optimized 70% yield and >99% *ee* (Scheme 4).



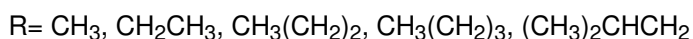
Scheme 4: The generation of (*R*)-benzoin products 16

The cross coupling of various aromatic aldehydes with acetaldehyde as acceptor, to generate (*S*)-2-hydroxy ketones using WT-BFD was achieved without the need for 2-ketoacids as substrate donor molecules (*c.f.* pyruvate decarboxylase (PDC)), and resulted in good to high conversions to (*S*)-2-hydroxypropanone derivatives on a preparative scale.¹¹ The highest *ees* were obtained using aromatic substrates containing substituents on the meta or para position on the aryl ring (Scheme 5).



Scheme 5: Cross coupling of an aromatic aldehyde with acetaldehyde to generate 17

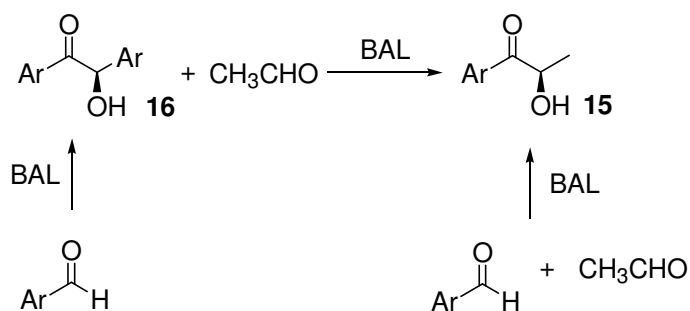
Ortho- substituted aromatic substrates were poorly accepted by WT-BFD, with the exception of 2-fluorobenzylaldehydes. This was attributed to steric and electronic effects.¹² The limitations with ortho-substituted aromatic aldehydes were circumvented by site directed mutagenesis via directed evolution.¹³ A BFD mutant L476Q, not directly involved in the binding of the acyl donor had an increased substrate specificity profile, and improved organic solvent toluene in aqueous media was observed. The same approach was applied to interchange BFD and PDC carboligation activity. The BFD variant A460I was used to decarboxylate pyruvate in the presence of long chain aliphatic substrates, giving (*R*)-acyloin products **18** in 34-85% *ee* (Scheme 6).¹²



Scheme 6: Self condensation reaction with BFD

1.1.2 Benzaldehyde lyase (BAL)

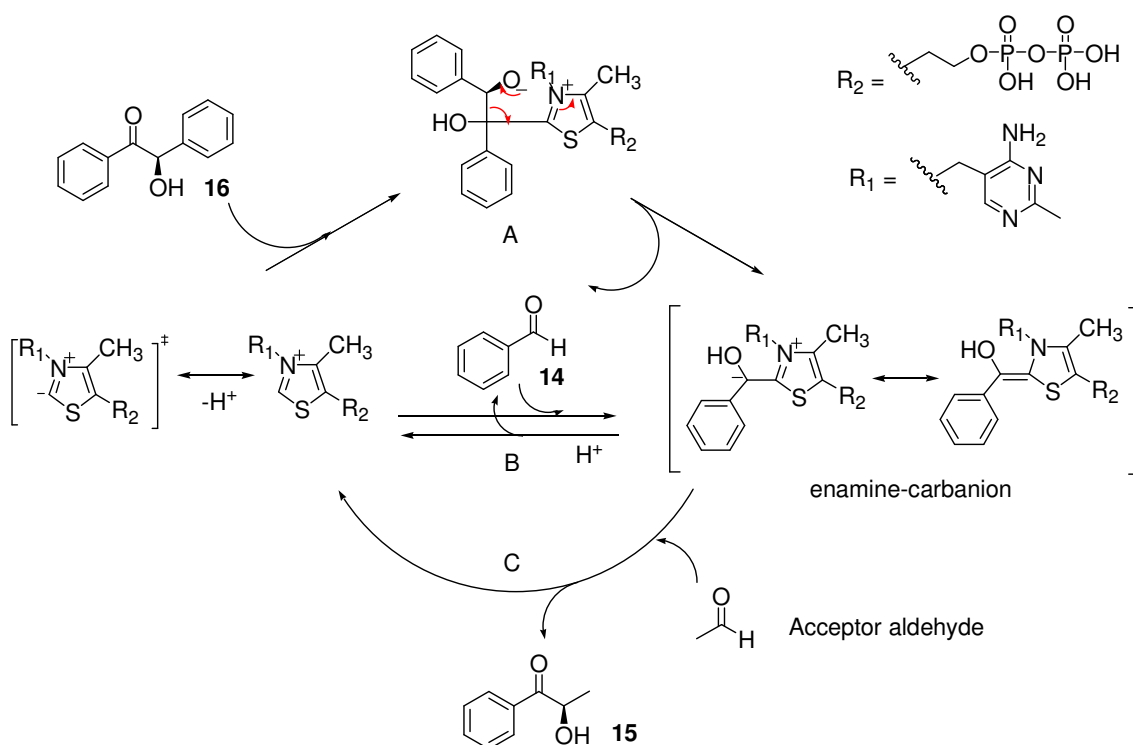
Benzaldehyde Lyase (BAL) (EC 4.1.2.38) from *Pseudomonas fluorescens* was first reported by Gonzales *et al.*¹⁴ The purified enzyme cleaved acyloin and benzyloin linkages using a bivalent ion and ThDP as a cofactor. It was first reported that BAL catalysed the carboligation of two aldehydes to afford the products (*R*)-**16** and (*R*)-**15**.¹⁵ Since then, the carboligation activity of BAL with a broad range of substrates has been explored (Scheme 7).



Scheme 7: General carboligation with BAL

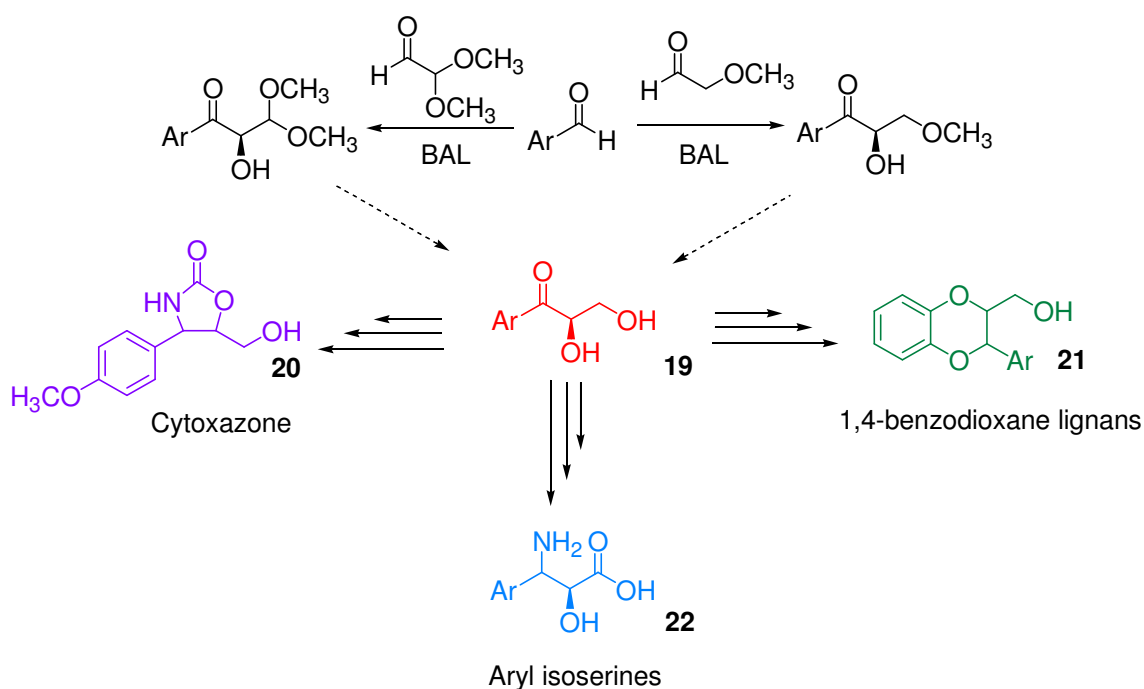
The mechanism of BAL is in accordance with other ThDP-dependent enzymes (Scheme 8). The first step involves the attack of the thiazolium ylid on the carbonyl carbon of the (*R*)-**16** to form adduct **A**. The nitrogen on the thiazolium ring acts as an electron sink which enables an electron rearrangement leading to the enamine-carbanion intermediate with the release of one benzaldehyde molecule **14**. The enamine intermediate can be generated upon attack of the ThDP ylid with a free benzaldehyde molecule. In the absence of an acceptor aldehyde the enamine intermediate is protonated and a benzaldehyde molecule is released with the

regeneration of ThDP (route **B**). In the presence of an acceptor molecule the carboligation reaction can occur, generating (*R*)-**15** as product and regenerating of the ThDP ylid (route **C**).



Scheme 8: Catalytic cycle of BAL using ThDP

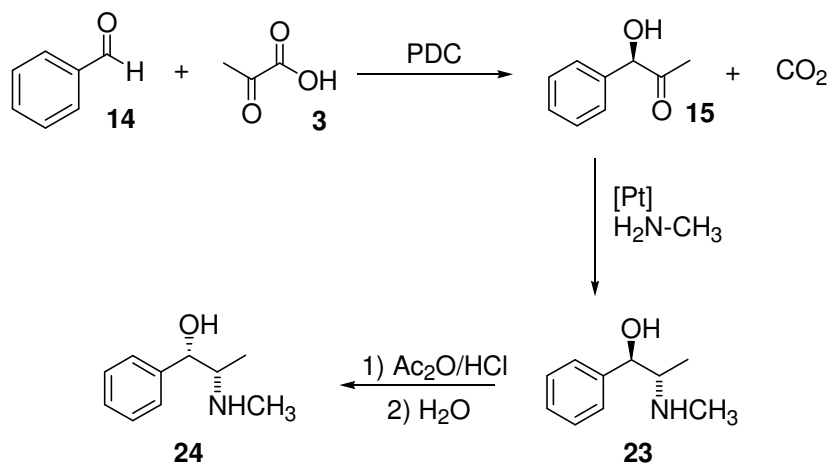
In contrast to BFD, BAL can accept ortho- substituted aromatics.¹⁵ Several synthetic benzoin derivatives were synthesized by BAL mediated self-condensation reaction in 96-99% *ee*,¹⁶ heterocyclic aldehydes had slightly lower *ees*; 92% *ee* for 2-furfuraldehyde and 91% *ee* for thiophene-2-carboxyaldehyde. Pyridine-3/4-carboxyaldehydes and sterically demanding aryl aldehydes, gave poor yielding benzoin condensation products.¹⁸ Unlike BFD, BAL has a wider substrate group tolerance for longer chain aliphatic aldehydes (e.g propanal and butyraldehyde) as an acyloin acceptor. The structural differences between BAL and BFD and the reason for the general *R*-specificity of BAL upon formation and cleavage of the 2-hydroxyketone is due to the wider overall shape of the binding site and the absence of an 'S-pocket' structural element in BAL, responsible for directing stereoselectivity.^{17,18} In another study, BAL has been used to form enantiopure 2,3-dioxygenated aryl propanones **19**, highly valuable chiral synthons used for the synthesis of cytotoxazone, a novel cytokine modulator **20**, lignans **21**, and aryl isoserines **22**. This involved the carboligation of aromatic aldehydes with methoxy and dimethoxyaldehydes generating (*R*)-2-hydroxy-3-methoxy-1-arylpropane-1-one derivatives in high yields in 89 - 98% *ee* (Scheme 9).



Scheme 9: Synthesis of enantiopure 19 that can be used as chiral synthons

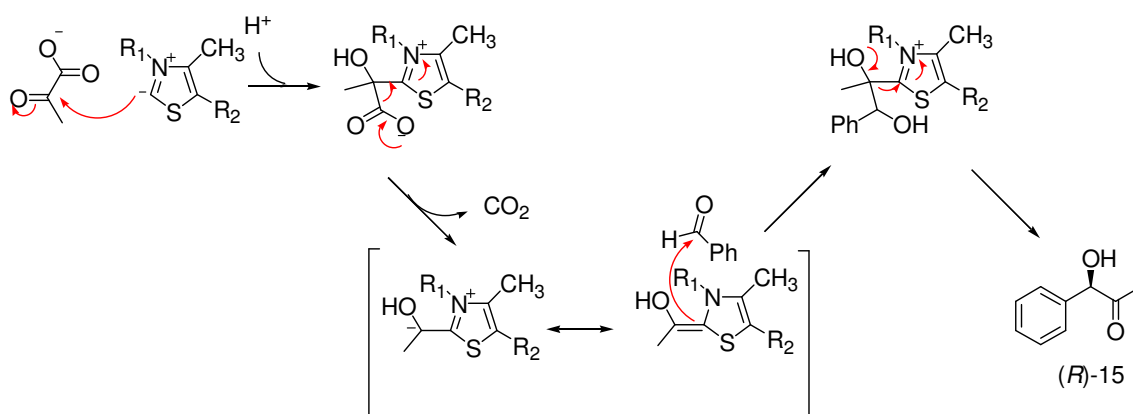
1.1.3 Pyruvate decarboxylase (PDC)

Pyruvate decarboxylase PDC [(E.C.4.1.1.1)] is an important enzyme in the glycolytic pathway and ethanol fermentation. PDC has been an important biocatalyst in carbonylation reactions such as (*R*)-**15**, a key intermediate for ephedrine **23** and pseudoephedrine **24** production (Scheme 10).¹⁹



Scheme 10: The production of ephedrine 23 and pseudoephedrine 24 from 15

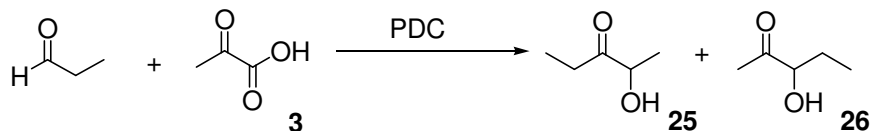
The PDCs used in biocatalysis are isolated from *Neurospora crassa*, *Zymomonas mobilis*, *Candida utilis*, and *Rhizopus javanicus*.²⁰ The mechanism for the formation of (*R*)-**15** involves the decarboxylation of pyruvic acid to form the reactive enamine for carbonylation with the acceptor molecule benzaldehyde.



Scheme 11: General reaction mechanism for (*R*)-15 synthesis

Various aldehydes have been explored to produce *S*-acetyl aromatic carbinols using *S. cerevisiae*. It was found that substrates containing ortho- substituents failed, whilst -CH₃, -CF₃, and -Cl substituents at the para- position generated higher yields than the meta- counterparts. Mono and disubstituted halogenated benzaldehyde derivatives were also investigated for the syntheses of novel (*R*)-15 analogs using purified PDC from yeast.²¹ The substrates containing the highest relative initial rates were 2-fluorobenzaldehyde and 2,3-difluorobenzaldehyde with high *ees* (>99%) but moderate yields (60% and 40% respectively).²¹

Further to this report Crout *et al.* used recombinant PDC from *Z. mobilis* to catalyse (*R*)-aromatic acyloin formations in high optical purity from *o*, *m*, *p*-halogenated aromatic aldehydes as acceptor molecules, with either pyruvate or acetaldehyde. Heterocyclic aldehydes, including furfural aldehydes and thiophene-3-aldehyde, were poor substrates but gave products in relatively high 80-90% *ees*. The acyloin reaction was also carried out with aliphatic aldehydes. Only propanal gave the acyloin product with pyruvate generating 2-hydroxypentan-3-one **25** and 3-hydroxypentan-2-one **26** in equal amounts with no self condensation product isolated (Scheme 12).²²

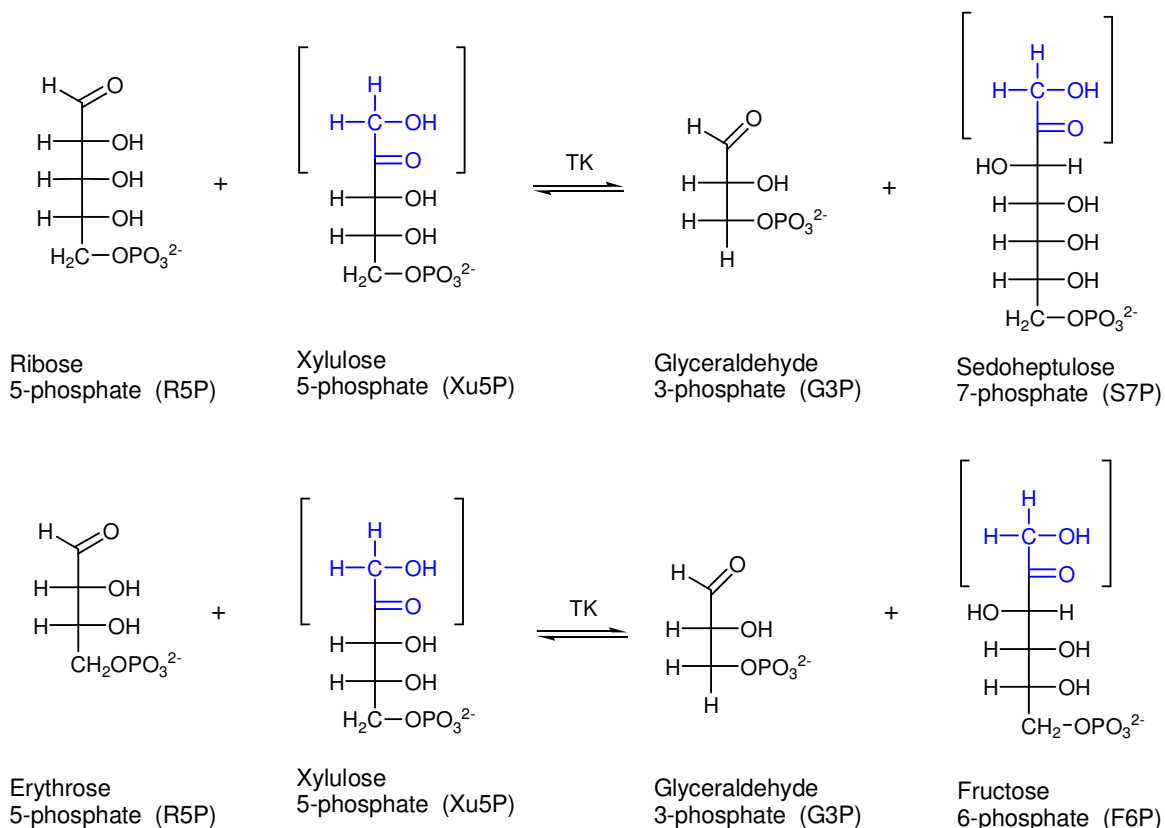


Scheme 12: Carbonylation of propanal and pyruvate 3

Other ketoacids were explored, such as 3-hydroxypyruvate (HPA), but they failed to generate acyloin product. The keto acid can selectively be decarboxylated by *Z. mobilis* PDC to generate glycolaldehyde, however no acyloin product was afforded with either aromatic or aliphatic aldehydes.

1.2 Transketolase and the transketolase reaction

Transketolase (TK) [E.C.2.2.1.1] is an important and versatile enzyme in the non-oxidative branch in the pentose phosphate pathway in animals and the Calvin Cycle of photosynthesis.²³ *In vivo* the enzyme reversibly transfers a two carbon ketol unit to the carbon terminus of aldose sugars; erythrose-4-phosphate (E4P) and ribose-5-phosphate (R5P) which affords fructose-6-phosphate (F6P) and sedoheptulose-7-phosphate (S7P) respectively (Scheme 13). In the Calvin Cycle, TK catalyses the reverse reaction.



Scheme 13: Transfer of a ketol unit to an aldose sugar phosphate molecule

The TK enzyme has been shown to be dependant on cofactor thiamine pyrophosphate (ThDP) and a bivalent metal ion (Ca^{2+} , Mg^{2+} , Co^{2+} , Mn^{2+} , Ni^{2+}) for enzymatic activity, but the activity is independent of the nature of the bivalent metal ion used.²⁴ From mechanistic studies, catalysis is initiated by the deprotonation of carbon-2 of the thiazolium ring of ThDP (Fig. 2).

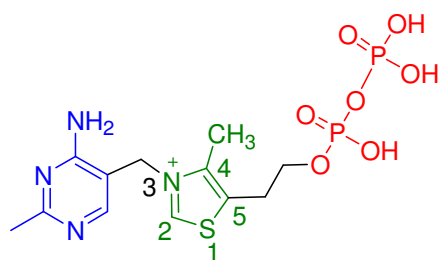
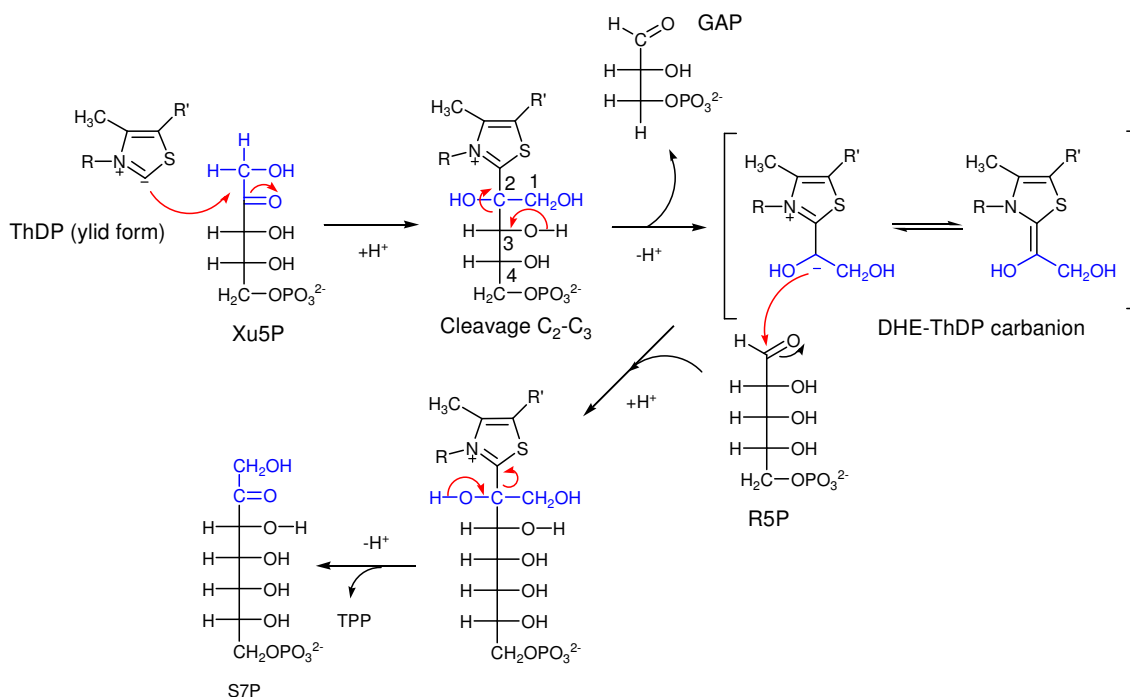


Figure 2: The chemical structure of ThDP

The reactive ThDP ylid attacks the carbonyl group of a donor Xu5P substrate. The C2-C3 bond cleavage of the ketose sugar yields glyceraldehyde-3-phosphate (GAP) and an enzyme bound α,β -dihydroxyethyl-ThDP (DHE-ThDP) resonance stabilised carbanion intermediate. The DHE-ThDP carbanion then attacks the aldehyde of the aldose sugar ribulose-5-phosphate (R5P) forming sedoheptulose-7-phosphate ((S7P)-ThDP) adduct. ThDP is finally eliminated by cleavage of the thiazolium ring yielding the S7P product (Scheme 14).²⁵



Scheme 14: The ThDP mechanism of TK

1.2.1 X-ray crystal structure of *saccharomyces cerevisiae* transketolase

TK is a member of a group of transferases, composed of two identical subunits, each with a molecular mass of 74.2 kDa.²⁶ X-ray crystallographic studies on *Saccharomyces cerevisiae* TK indicated that each monomer of the dimeric TK enzyme consists of three domains: N-, or PP- domain (residues 3-322); the middle section, or Pyr-domain (323-538), and the C-domain (539-680).²⁷ The first two domains are involved in the catalytic profile of the enzyme and coenzyme binding, while the role of the C-domain is relatively

unclear. At the interface lie the cofactors ThDP and a bivalent metal ion (calcium) in a deep cleft between the subunits (Fig. 3).

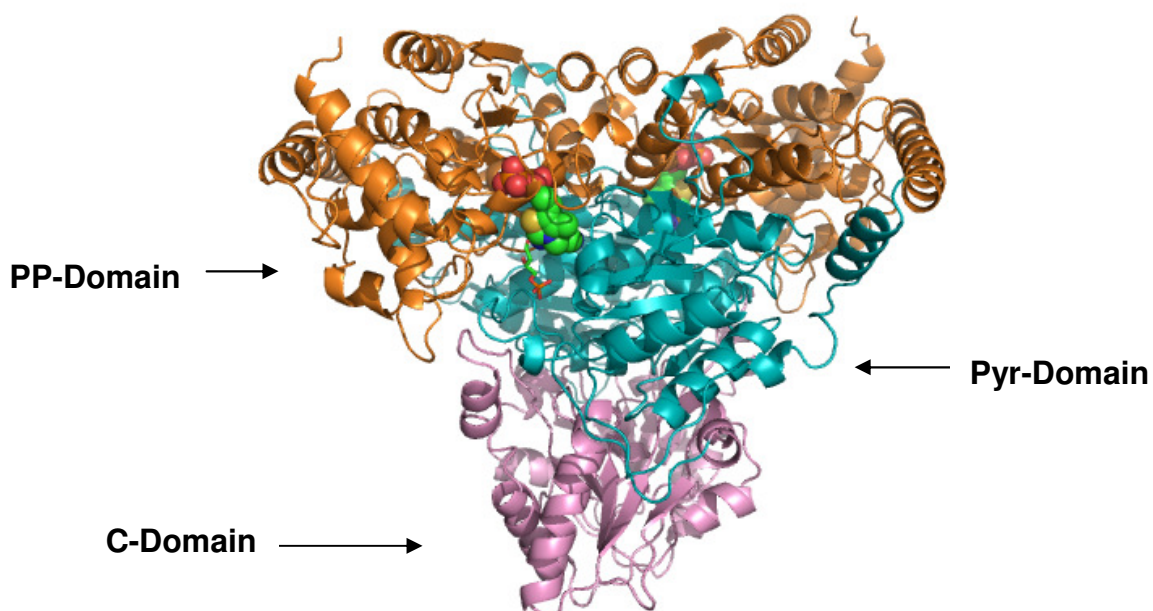


Figure 3: X-ray crystal structure of *Saccharomyces cerevisiae* TK with ThDP, Ca²⁺ and E4P (1NGS.pdb) from www.rcsb.org/pdb

The thiazolium ring is bound to both subunits, held together by hydrophobic interactions from nearby aromatic residues, Tyr 442/445 and Tyr-446. Only the C2 atom of the thiazolium ring of ThDP is exposed and bound covalently to the donor substrate in solution. The ThDP diphosphate group hydrogen bonds with His residues (69 and 263) and a Gly residue (158) and an electrostatic interaction with the calcium ion is also present

1.2.2 Substrate binding in thiamin diphosphate-dependant transketolase

A TK crystal structure with bound acceptor substrate molecule, erythrose-4-phosphate (E4P) present in the active site was first studied by Schneider and coworkers.²⁸ E4P was generated from the enzymatic cleavage of donor substrate fructose-6-phosphate (F6P). The X-ray crystal structure identified amino acid residues at the active site primarily involved in substrate binding. E4P is projected from the surface of the protein into the enzyme cleft; with the phosphate group hydrogen bonding with conserved residues Arg359, Ser386, Arg528, and His469 at the entrance of the cleft assessible to solvents. The side chains Arg528, His469 and Ser386 are within hydrogen bond distances to the substrate's phosphate group.²⁸ Another polar interaction occurs between the hydroxyl group of E4P and the Asp477 residue, and the aldehydic oxygen atom can interact with two His residues which are conserved in known transketolases sequenced thus far (Fig.4).

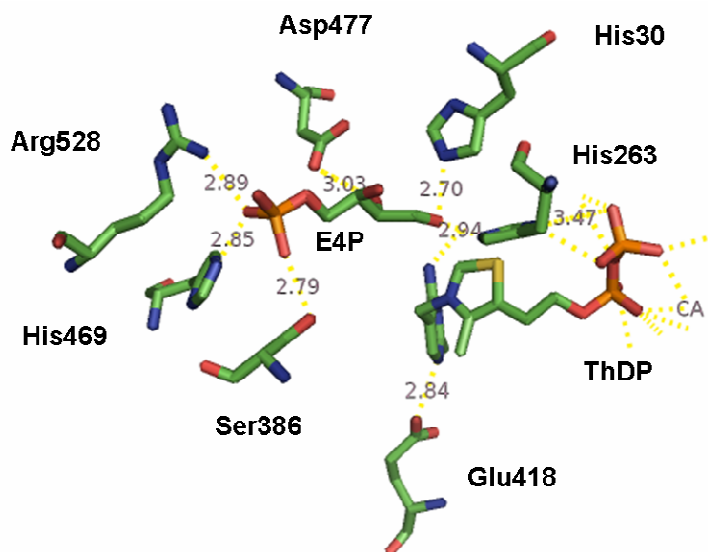


Figure 4: Selected amino acid residues and the hydrogen bonding distances (1NGS.pdb) from www.rcsb.org/pdb

Analyses of the quaternary complex of TK revealed that the substrates bind in a narrow channel. The substrate extends until it is in contact with the C2 carbon atom of ThDP which is located at the end of the interior protein channel. It is not possible for both the donor and acceptor molecule to enter and covalently bind in the active site simultaneously, hence a Bi Bi Ping Pong mechanism was proven.²⁹ The aldehydic carbon cannot interact with the C2 carbon of the thiazolium ring which is at a distance of 4.16 Å. There is however, a small enough pocket for an α,β -dihydroxyethyl (DHE) group to generate a DHE-ThDP-carbanion intermediate, reducing the distance to 3.2 Å between the acceptor substrate and this reactive intermediate to covalently bond (Fig. 5). This is made possible with a few side chain rotations but no necessary side chain rearrangement of the amino acid residue is required.

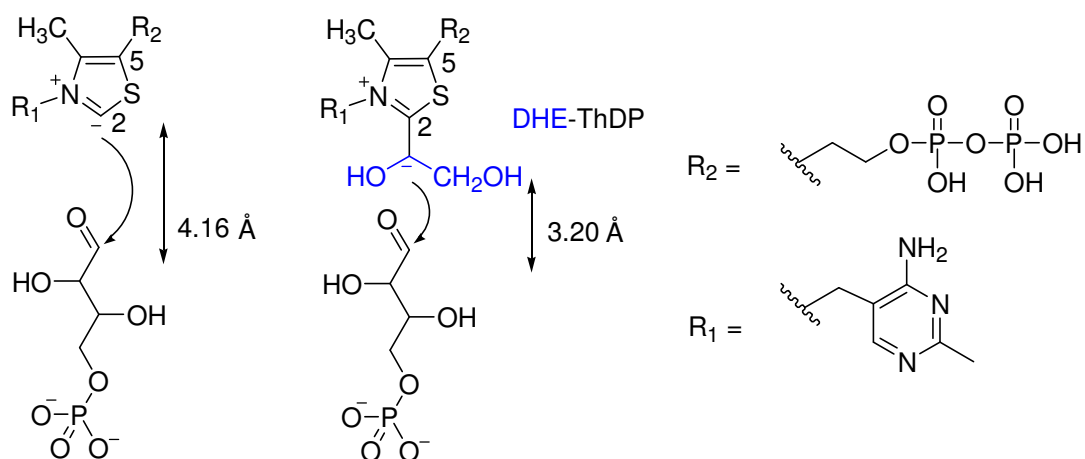


Figure 5: Schematic interaction of ThDP with E4P

Despite the successes of Schneider's preliminary X-ray crystal studies on substrate binding, important key features of the catalytic cycle remained elusive. Most importantly, what is the driving force for the C2-C3 cleavage of the substrate donor molecule upon formation of the DHE-ThDP carbanion intermediate? Recent studies by Schneider attempt to address the issue with a non-phosphorylated donor substrate, hydroxypyruvic acid and its isolated DHE-ThDP carbanion crystal structure³⁰ in the active site of TK. However the study does not take into account the natural TK sugar phosphates which behave differently in the active site. Recently in the literature, Tittman's group have reported the first crystal structure of the ketose-cofactor adducts trapped in the active site of *E. coli* TK, shedding more light on the mechanism of TK.³¹

The X-ray crystal structure revealed xylulose-5-phosphate (Xu5P) is covalently bonded to C2 carbon of the thiazolium ring (ThDP), as determined by the (i) tetrahedral shape of Xu5P C2' carbon that is sp³ hybridised. (ii) The distance between the C2' carbon of the sugar and C2 carbon of ThDP is 1.5 Å, suggesting the carbonyl addition of the sugar to the ThDP's C2 had indeed taken place. The structure itself reveals key features of the Xu5P-ThDP intermediate: the C2'-C2 bond was not coplanar to the thiazolium ring, there is an out-of-plane distortional angle of (25-30°) implying conformational strain on the intermediate. The glyceraldehyde-3-phosphate (G3P) generated relieves the bond tension with the formation of a planar unrestrained DHE-ThDP enamine intermediate an important driving force for the elimination of product (Fig. 6).

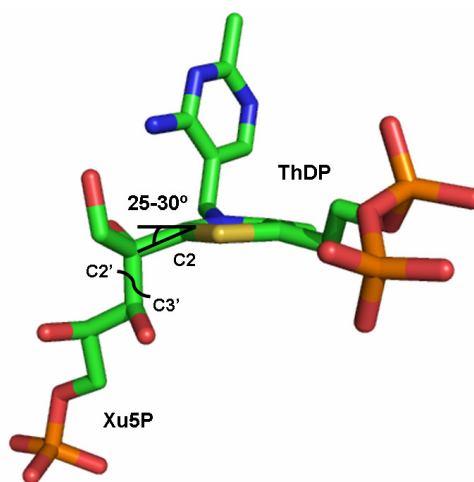


Figure 6 Crystal structure of Xu5P-ThDP adduct with an out-of-plane distortional angle (25-30°) (2R80.pdb)_from www.rcsb.org/pdb

Similar findings have also been reported in ThDP-dependant enzymes involving pyruvate as the substrate, such as pyruvate oxidase³² (POX) and pyruvate dehydrogenase³³ (PDH). These form a pyruvate-ThDP adduct with varying degrees of out-of-plane distortions from 5 -7° (POX) to 11° (PDH). The cleaved C2'-C3' bond of the Xu5P is perpendicular to the positively charged thiazolium ring of ThDP to act as

an optimal electron sink for the electron pair of the DHE-ThDP intermediate upon elimination of G3P. The facile conjugation with the electron pair of thiazolium π -electrons makes the cleavage possible, effectively maximising the overlap to give a more stable conformation. This has been predicted and considered from theoretical based ThDP-based enzymes^{34,35} and has experimentally been shown to operate in enzymes catalyzing decarboxylation reactions.^{32, 33}

1.2.3 Site directed mutagenesis on selected amino acid residues with catalytic activity

Non-phosphorylated donor substrates such as fructose and ribose sugars can be used in the TK reaction. However previous research conducted had shown poor substrate affinity indicative from the large K_M values compared with its phosphorylated counterparts.³⁶ The importance of hydrogen bonding and tight ionic interactions with the phosphate moiety and the amino acid residues at the entrance of the cleft to the active site is believed to contribute to the enzyme's catalytic activity. This was further demonstrated by selective mutations at the phosphate binding site: the polar amino acid residues were substituted with a non polar alanine residue, which resulted in high K_M (μM) values for mutants R359A, R528A, and H469A (Table 1). It is important to note the larger K_M value for ribose-5-phosphate (R5P) in comparison to its counterpart xylulose-5-phosphate (Xu5P). The rational basis for the large difference in K_M values can be attributed to the closeness of the C2 carbon of the thiazolium ring and the carbonyl centre from the acceptor molecule. Xylulose binds deeper into the channel weakening the important interaction between the phosphate group and arginine residues. The mutant H469A is enclosed in the interior of the substrate channel which can effectively hydrogen bond to the phosphate group of xylulose. This was rationalised by noting the effect this residue on the K_M value for the xylulose substrate compared to K_M values of mutants R359A and R528A (Fig. 7).

Enzyme	Activity	Xu5P (K_M) μM	R5P (K_M) μM
Wild type	100	73	146
D477A	1.7	595	1750
H469A	77	829	5970
R359A	31	163	5650
R528A	17	318	7000

Table 1: The kinetic data of several TK mutants with Xu5P and R5P as acceptor substrates

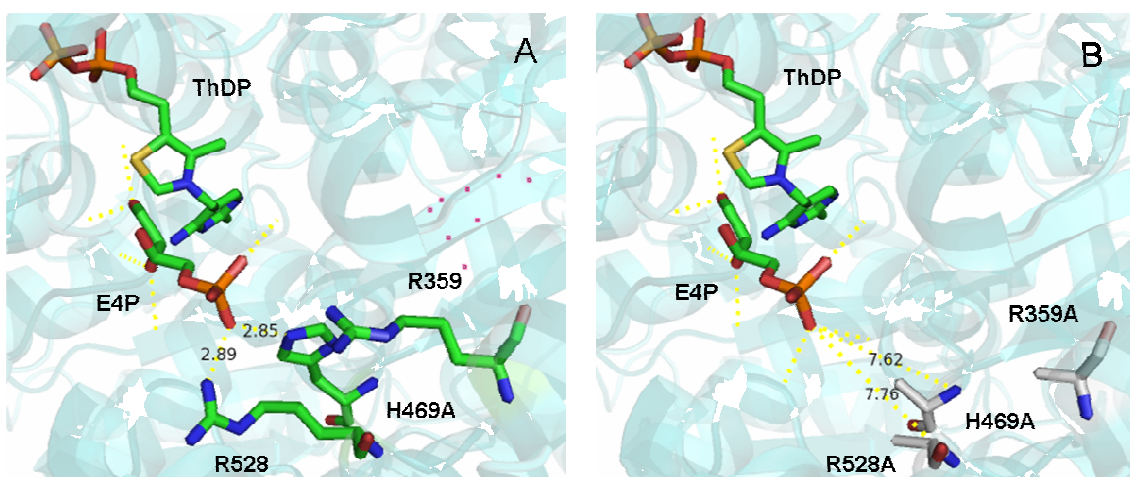


Figure 7: (A) WT amino acid residues hydrogen bond to E4P (B) Mutant amino acid residues hydrogen bonding to E4P (mutagenesis performed by pyMOL)

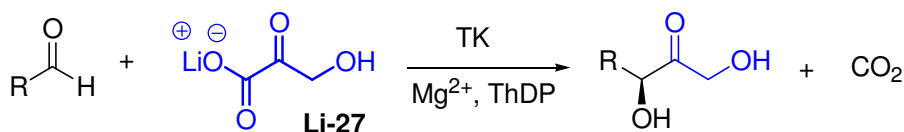
1.2.4 Amino acid residue Asp477 responsible for enantioselectivity

Previous work conducted by Whitesides³⁷ and Kochetov³⁶ noted that sugar phosphates with *D-threo* configurations at the C3 and C4 carbon atoms can act as efficient donors in the TK reaction. The high stereoselectivity of the enzyme can be recognised from C3 and C4 hydroxyl groups forming hydrogen bonds to the side chains of Asp477, His30, and His263. The C3 and C4 carbon atoms correspond to the C1 and C2 carbon atoms of the aldose acceptor molecule. On a structural hypothesis, the removal of the hydroxyl group, or the inversion of the stereocenter disrupts the hydrogen bonding and lowers the substrate affinity of the acceptor molecule.³⁸

Schneider investigated the stereospecificity of wild type and mutant TK D477A.³⁸ A series of acceptor aldehydes were screened with/without the hydroxyl group present at the C2 carbon position and kinetic K_{cat}/K_M values were compared. The K_{cat}/K_M results indicated that α -hydroxyaldehydes with specific *D*-configurations (e.g. ribose-5-phosphate) are required for high catalytic activity compared with α -deoxyaldehydes. This strongly suggested that the hydroxyl group at C2 in the acceptor substrate was highly important for catalytic activity. Further evidence was provided with the screening of TK mutant D477A with various acceptor molecules, which revealed a considerable decrease in catalytic activity, when Asp was replaced with the non-polar residue, Ala. The studies conducted by Schneider's group provided a strong case for determining that Asp477 was involved in acceptor substrate specificity, but it failed to address the issue of the stereoselectivity of the ketodiol products generated. The kinetic parameters alone provided evidence that Asp477 was involved in the increase in product yield; however increased kinetic activity does not also lead to high selectivities in the products formed.

1.2.5 Protocols for the transketolase reaction

It is known that the transketolase-catalysed interconversion of carbohydrates is a reversible reaction. To drive the equilibrium to completion, Srere *et al.*³⁹ demonstrated that β -hydroxypyruvic acid (HPA) could be used as a substrate for TK. The decarboxylation of HPA and the subsequent removal of CO₂ from the reaction mixture render it an irreversible condensation reaction (Scheme 15). The Lithium HPA salt (**Li-27**) has since been used as a substrate in many experimental TK reactions instead of ketose sugars.



Scheme 15: Irreversible Condensation reaction of Li-27

The pH of the reaction will exceed 7.5, the optimum pH for TK,⁴⁰ due to the consumption of one proton per molecule of product formed. This pH can be easily maintained by using buffer or adding acid slowly over the course of the reaction.

Current biological studies involve the isolation of transketolase and this can be isolated from three main sources:

- Baker's yeast, *Saccharomyces cerevisiae*, commercially available (Fluka) at moderate cost. Stable for several months in its lyophilized powdered form, and at pH 7.5 in gly-gly buffer solution.
- Spinach leaves, which can be used immediately after isolation. The activity of the enzyme can be greatly improved if purified to homogeneity; however activity is lost after a few days.⁴¹

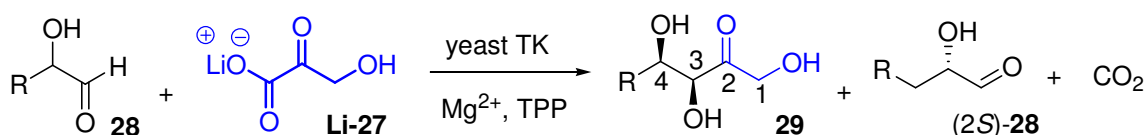
Unfortunately neither of these sources yields considerable quantities of the enzyme, however catalytic findings have been demonstrated on a small scale.⁴² The drawbacks have been surmounted by introducing the TK gene into a high copy plasmid leading to an over-expression of the protein in *E. coli*.⁴³

1.2.6 Transketolase: A biocatalyst for asymmetric carbon-carbon bond synthesis and applications in organic syntheses using yeast, spinach and *E.coli* TK.

In the oxidative pentose phosphate pathway, it is known that ribose 5-phosphate (α -hydroxyaldehyde) is a donor molecule in the TK-catalysed reaction. In the early 1990s,

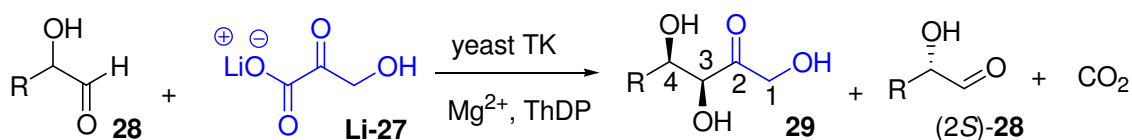
research focused on a wide variety of non-phosphorylated α -hydroxyaldehydes as substrate acceptor molecules; for yeast, spinach and *E.coli* TK.

Whitesides *et al.* conducted experiments using α -hydroxyaldehydes, HPA and commercially available yeast TK whilst maintaining the pH of the reaction mixture at pH 7.5 by controlled slow addition of an HPA solution (*ca* pH 4.0).⁴² When using α -hydroxyaldehydes and HPA, the hydroxyketone group was transferred with the formation of a (3*S*,4*R*) chiral triol **29**, in decent yields (30-60%). Most significant of these findings was the kinetic resolution of racemic α -hydroxyaldehydes **28** with TK. The recognition of chirality in the aldehydic moiety afforded (2*S*)-**28** with *ees* >95%, although the isolated yields were modest (9-23%) (Scheme 16). Effenberger *et al.* later significantly improved the yields of these optically pure (2*S*)-aldehydes (50-78%) by using different R (*e.g* PhCH₂OCH₂, CH₃OCH₂, SHCH₂, FCH₂) side chains.⁴⁴



Scheme 16: The yeast TK biotransformation reaction using Li-27 and 28

On inspection of the chiral triols isolated; the relative rates for the formation of **29b-29d** suggested that the branching of the aldehyde leads to lower reaction rates, aldehydes **29h-29i** containing an extra hydroxyl group revealed a slight preference for the dihydroxyl aldehydes compared to the mono hydroxyl aldehydes. However comparisons in yields proposed by Effenberger *et al.* ranging from 72-80% suggested otherwise. Both research groups, used CH₃CH₂- (**29c**, **29n**), and MeOCH₂- (**29e**, **29k**) aldehydic groups with varying product yields, but this could be attributed to the different reaction conditions used in the biocatalysis. Effenberger *et al.* uses stoichiometric amounts of substrates whilst maintaining the temperature at 30 °C, in comparison to Whitesides' variable substrate concentrations (Table 2).



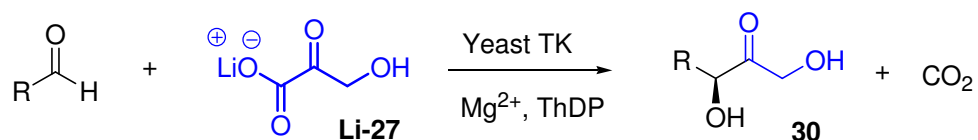
R	29	V _{rel}	Yields %	(2S)-28 (ee%)
H	a	100	60	n/a
CH ₃	b	20	44	>95
CH ₃ CH ₂	c	33	45	95
CH ₃ (CH ₂) ₂	d	22	39	77
MeOCH ₂	e	27	38	94
H ₂ C=CH	f	56	30	-
H ₂ C=CHCH ₂	g	28	45	95
(S)-H ₂ C=CHCHOH	h	49	60	-
(R)-H ₂ C=CHCHOH	i	50	63	-
PhCH ₂ OCH ₂	j	-	79	98
MeOCH ₂	k	-	72	99
SHCH ₂	l	-	80	99
EtSCH ₂	m	-	74	99
CH ₃ CH ₂	n	-	50	99

Table 2: Reported results of α -hydroxyaldehydes as acceptor molecules with yeast TK. Whitesides *et al.* (pink), biotransformation conditions; Li-27 (10 mM), aldehyde (50-130 mM), pH maintained by addition of Li-27, 10-30U TK added. Effenberger *et al.* (blue), biotransformation conditions: 25-50 mM scale, equimolar reagents, Tris.HCl buffer (0.5 M, pH 7.6) incubated at 30 °C, unspecified amount of enzyme used.^{42,44}

The stereochemistries of **29f-29i** were determined from the optical rotations of known carbohydrates, however no attempts were made to accurately determine the ees of the carbohydrates isolated.⁴² The stereochemistries of the compounds were not discussed but were inferred to possess high ees from the determination of the known absolute stereochemistry of **29c**. The ees of compounds **29j-29m** were determined by gas chromatography on a β -cyclodextrine phase; however the absolute stereochemistry was presumed to possess the (2*R*,3*S*)-configuration.

The Dumuyck began preliminary investigations on the tolerance of a greater variety of substrate acceptor molecules, more specifically non- α -hydroxyaldehydes (Scheme 17).⁴⁵ This investigation reported initial relative velocities of the substrates expressed as a percentage compared to the initial velocity of glycolaldehyde, a highly reactive acceptor. The initial velocities were monitored by the consumption of hydroxypyruvate by using an enzymatic assay.⁴⁶ Some general conclusions were made on the nature of the aldehyde acceptor molecule; the presence of a hydroxyl group or an oxygen atom

at an α -carbon or/and β -carbon **30c-30d** enhanced relative rates. Steric hindrance near the aldehyde group reduced the reactivity **30f**. An α,β -Unsaturated aldehyde **30e** is accepted as TK substrate, benzaldehyde **30g** is a poor substrate but the presence of hydroxy-groups on C2 **30h** leads to higher activities. Heterocyclic aldehydes **30i-30k** were better substrates than benzaldehyde but overall low initial velocities were observed (Table 3).⁴⁵



Scheme 17: The yeast TK reaction using a non- α -hydroxyaldehyde with Li-27

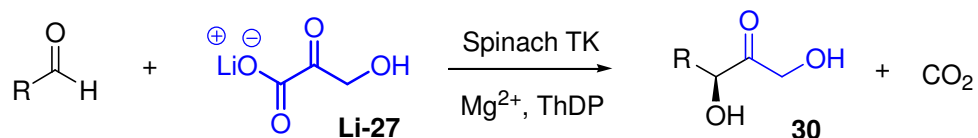
R	30	V_{rel}
HOCH ₂ -	a	1
CH ₃ -	b	0.25
CH ₃ OCH ₂ -	c	0.32
(<i>R,S</i>) CH ₃ CHOHCH ₂	d	0.29
(CH ₃) ₂ CH=CH	e	0.11
(<i>R,S</i>) CH ₃ CH(OBz)-CH ₂ ⁷ -	f	0.14
Phenyl-	g	<0.1
2-hydroxyphenyl-	h	0.28
2-Furanyl-	i	0.11
2-Thiophenyl-	j	0.32
2-Pyridyl	k	0.13

Table 3: V_{rels} of non- α -hydroxyaldehydes using yeast TK. Demuynck *et al.* biotransformation conditions; TK (1 U ml⁻¹), gly-gly buffer 0.1 M at pH 7.5, aldehyde (60-200 mM), and Li-27 (7.5 mM).

Isolated yields were not reported in this publication. The assay used to determine the V_{rels} depended heavily on the depletion of Li-**27**. No controls were mentioned in their studies to ensure the degradation of Li-**27** was not influenced by the decarboxylation of the α -keto acid⁴⁷ or the possible aldol condensation of substrates in aqueous solution.⁴⁸ In conclusion, the V_{rels} calculated may not be an adequate description for the initial relative velocities and substrate affinities of acceptor aldehydes used.

Dumuynck's group later addressed these issues by investigating the stability of Li-**27** in various buffers as well as the biocatalytic potential of spinach TK.⁴⁹ The stability of Li-**27** was monitored over a period of time with four different buffered solutions; gly-gly, triethanolamine, HEPES and Tris. All buffers showed 20-80% depletion of Li-**27** in 24 hours but Tris was found to be the most Li-**27** stable and was then selected for biocatalysis. The results obtained from the biotransformation of spinach TK confirmed

previous results from yeast TK, that the presence of an α -hydroxyl group in the aldehyde leads to higher reaction rates. The replacement of the hydroxyl group with a methylthiol **30p**, or methoxy- group **30n** revealed a decrease in the V_{rels} of reactions (Table 4).

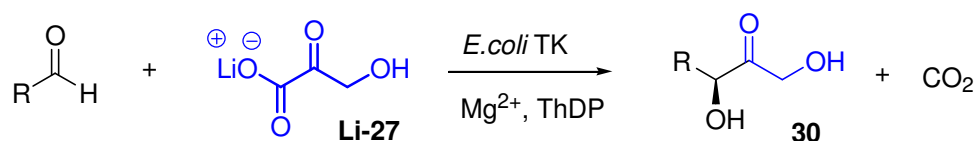


R	30	V_{rel}	Yield %	ee%
H-	l	0.12	30	70
OH-	m	1	70	64
CH ₃ O-	n	0.32	45	60
ClCH ₂ -	o	0.23	-	-
CH ₃ S-	p	0.35	46	64
CH ₃ SCH ₂ -	q	0.24	20	76

Table 4: The Spinach TK reaction with various acceptor aldehydes. Demuyneck *et al.* biotransformation conditions; Spinach TK (250 U), Tris buffer 0.1 M at pH 7.5, Li-27 (100 mM), aldehyde (100 mM)

The *ees* of **30l-30q** were determined by preparing the trifluoroacetate derivatives of these sugars and analysis by GC and the (*S*)-configuration of the new stereogenic carbon center was inferred from previous studies on ketose sugars with L-erythrulose.⁵⁰ and 4-deoxy-L-erythrulose.⁴⁶

TK from *E. coli* has several added benefits over spinach and yeast TK, such as the greater acceptance of the donor molecule Li-**27** with a conversion rate which is 30 times and 6 times higher than the rates for spinach and yeast TK respectively.⁵¹ TK from *E. coli* was determined to be relatively non-specific for the aldehyde acceptor, similar to that for the aldehyde specificity profile reported for yeast. In general, the condensation of α -hydroxyaldehydes **28** with Li-**27** using *E.coli* TK was similar to that of yeast TK and was specific for aldehyde acceptor molecules bearing the α -hydroxyl group in the D (i.e. 2*R*)-configuration (Scheme 18).



Scheme 18 TK-catalysed reaction with Li-27 and (*R*)- α -hydroxyaldehyde

An experiment measuring Li-**27** depletion at different time intervals when using enantiomers of glyceraldehyde demonstrated that D-glyceraldehyde reacts at

approximately the same rate as the achiral substrate glycolaldehyde, however, no reaction with L-glycolaldehyde was observed (Fig. 8).⁵²

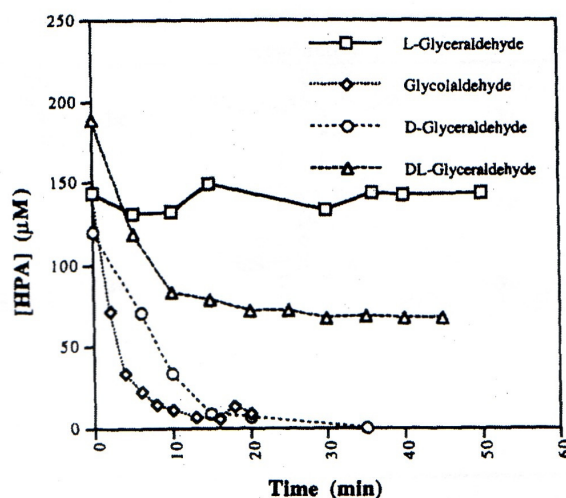


Figure 8 Depletion of HPA towards D-, L- and DL-glyceraldehyde. Reprinted from “Transketolase from *Escherichia coli*: A practical procedure for using the biocatalyst for asymmetric carbon-carbon bond synthesis” with permission from Elsevier⁵²

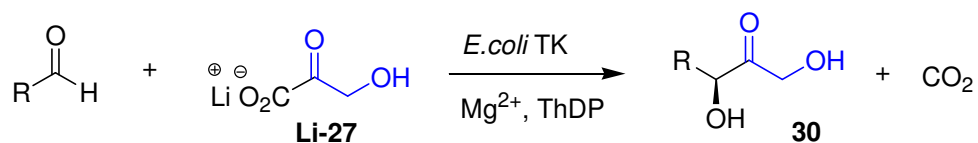
Previous investigations⁵⁰ had concluded that yeast TK enzyme has a kinetic preference for α -hydroxyaldehydes having a $2R$ -configuration as evidenced by the relative rates of D-glyceraldehyde (78%) and L-glyceraldehyde (<0.01) relative to that of glycolaldehyde (Table 5).

Substrates	V_{rel}
D-glyceraldehyde 3-phosphate	44
D-erythrose 4-phosphate	33
D-arabinose 5-phosphate	24
D-glucose 6-phosphate	9
D-glyceraldehyde	78
L-glyceraldehyde	<0.01
DL-glyceraldehyde	56
D-erythrose	56
D-glucose	4

Table 5: The relative rates of various substrates for the TK reaction

Preliminary relative rates studies by Turner *et al.* also monitored the depletion of Li-27 in bioconversions using non α -hydroxyaldehyde acceptor molecules, with cell free *E. coli* TK lysates.⁵¹

This demonstrated low activity for simple aliphatic aldehydes, **30r-30t**, however it was still possible to obtain product on a preparative scale. The cyclic acceptor molecules revealed to have the poorest activity, presumably due to the unfavourable electrostatic and steric interactions in the enzyme's binding site (Table 6).



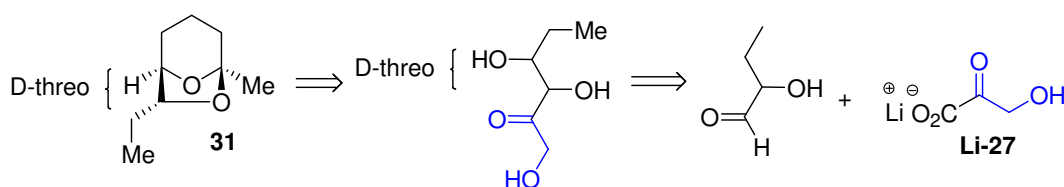
R	30	V _{rel}
	r	1
	s	0.2
	t	0.18
	u	0.05
	v	0.04
	w	0.03

Table 6: *E. coli* TK with various acceptor molecules. Turner *et al.*⁵¹ biotransformation reaction; Li-27 (7.5 mM), gly-gly buffer (70 mM at pH 7.6), aldehyde (100 mM) TK (3U) in 1 ml.

Isolated yields were omitted from this publication, with no further discussion on stereochemistries of the generated analogues **30**. The substrate specificity profile of *E. coli* TK appears to show a similar trend to that reported for yeast TK. Characterisation of the substrate specificity profile will be discussed later.

1.2.7 Transketolase in synthesis

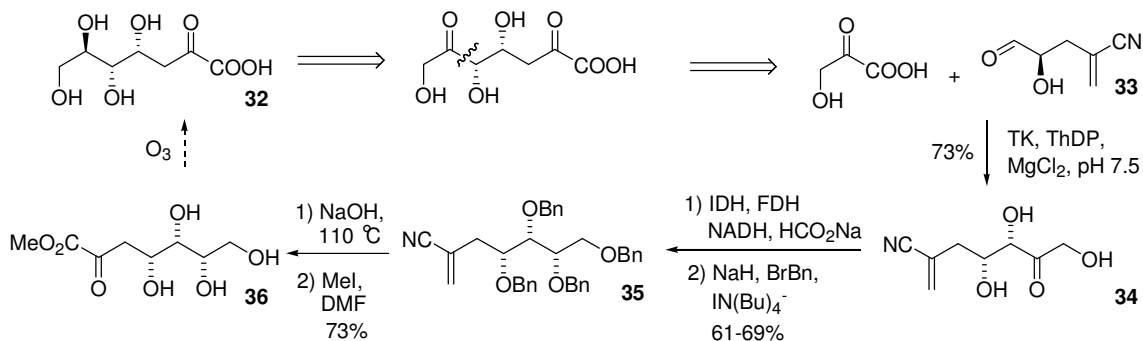
The use of TK has been employed in complex syntheses of biologically important molecules, for instance TK from baker's yeast was utilised for the stereospecific synthesis of the naturally occurring beetle pheromone (+)-*exo*-brevicomin **31** (Scheme 19).³⁷



Scheme 19: Retrosynthesis of (+)-exo-Brevicomine

The process involved the transfer of the ketol unit to a 2-hydroxy butyraldehyde acceptor substrate molecule. A vicinal diol possessing the D-threo isomer of the product (45% yield) with *ees* >95% was generated. Then a short sequence of reactions involving conversion the protected ketose to an aldose, a Wittig extension of the aldehyde, and subsequent hydrogenation and ketal hydrolysis afforded the title compound.

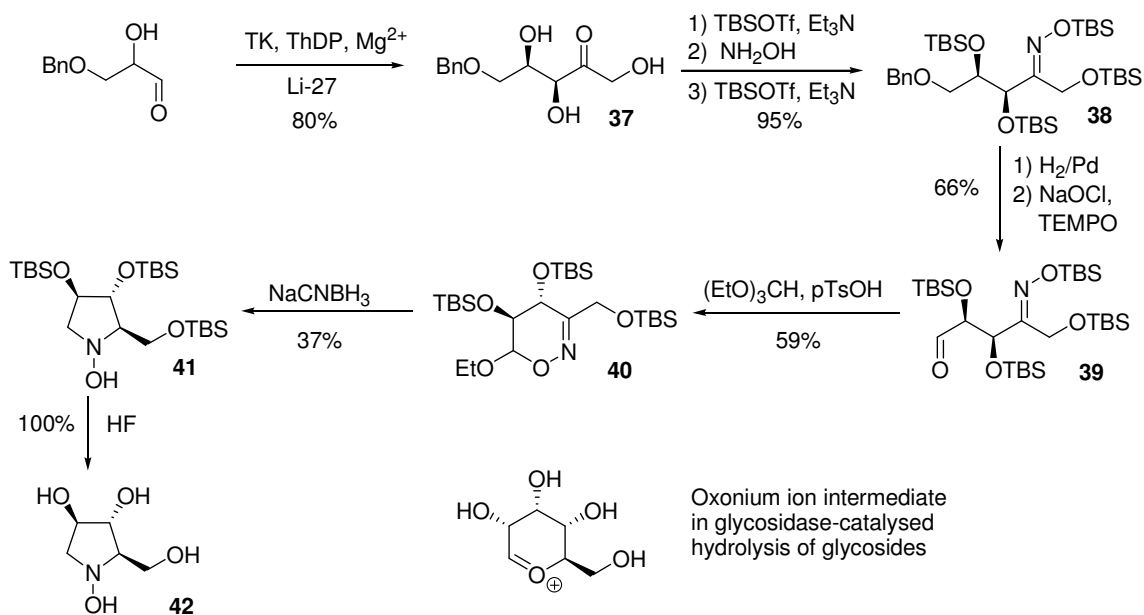
Transketolase has also recently been used to synthesize ulosonic acids, 3-deoxy-D-manno-2-ulosonic acid (KDO) and 3-deoxy-D-glycero-D-galacto-2-nonulosonic acid (KDN). These are integral components of lipopolysaccharides of Gram-negative bacteria. The new synthetic analogues (e.g **32**) generated may be useful in developing new antibacterial agents.⁵³ Currently in the literature most enzymatic approaches to these compounds involve aldol condensations with pyruvate or phosphoenolpyruvate (PEP) with aldoses.⁵⁴ A versatile method was investigated using an (*S*)- α -hydroxyaldehyde containing a terminal nitrile **33**. The D-threo isomer **34** was isolated in a 73% yield.⁵⁵ Subsequent enzymatic reduction proceeded using iditol dehydrogenase (IDH) with formate dehydrogenase (FDH) and sodium formate to regenerate NADH *in situ*. The hydroxyl groups of the compound were then protected as benzyl ethers **35**. Hydrolysis of the nitrile group **36**, final ozonolysis of the methylene esters and deprotection by hydrogenation completes the formation of ulonic acid analogue **32** (Scheme 20).



Scheme 20: Retrosynthesis and synthesis of an ulosonic acid analogue

Many types of imino sugars have been reported in recent years containing a different spectrum of activity against a range of glycosidases, such as with the synthesis of

fagomine using yeast TK (such as 1,1-dideoxyiminoalditols).^{56a} Most recently the *E. coli* TK-mediated coupling of racemic 3-*O*-benzylglyceraldehyde with **Li-27**, has been carried out on a multigram scale to provide triol **37** as an important precursor of a novel *N*-hydroxypyrrolidine. The synthesis proceeded via the protected oxime **38** (83%), which converts to the aldehyde **39** (66%), and is cyclised to the 1,2-oxazine **40**. The oxazine undergoes a rearrangement followed by a reduction to yield the protected *N*-hydroxypyrrolidine **41** (37% over two steps). Finally the deprotection with HF generated the active product **42** in quantitative yield (Scheme 21).^{56b}



Scheme 21: Synthesis of novel *N*-hydroxypyrrolidine

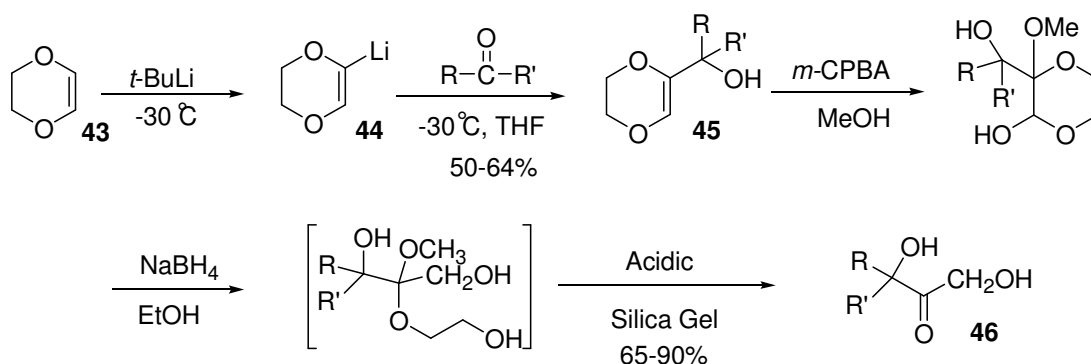
1.3 Synthesis of acyclic α,α' -dihydroxyketones

The biocatalytic transketolase reaction is well documented for the formation of α,α' -dihydroxyketones. However there is a lack of methodologies for the chemical synthesis of α,α' -dihydroxyketones in the literature and until recently no one-pot chemical synthesis of these was available. Multistep chemical strategies to α,α' -dihydroxyketones are reviewed below.

1.3.1 Addition of 2-lithio-1,4-dioxane to aldehydes/ketones followed by peracid oxidation

Research conducted by Fetizon *et al.*⁵⁷ formulated a five-step synthetic approach. This involved the synthesis of dihydro-1,4-dioxin-2-yl lithium **44**, prepared by the lithiation of dihydro-1,4-dioxin **43** with *t*-butyllithium, and reaction with aldehydes or ketones, to give the intermediate adduct **45** in moderate yields ranging from 52 to 64%.

Methanolic peracid epoxidation and subsequent reduction and acid hydrolysis yielded the α,α' -dihydroxyketone **46** (Scheme 22).

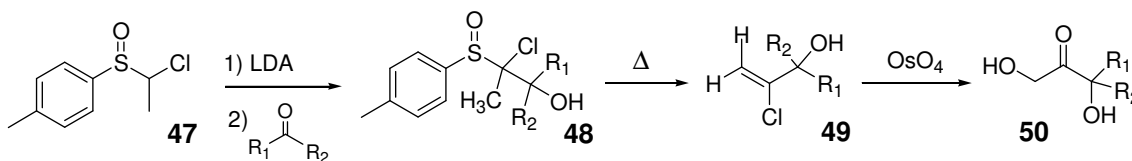


Scheme 22: Multi-step synthesis of ketodiol 46

The difficulties in this strategy are that it relies on the synthesis of **45**, synthesised from a high cost starting material **43**, as a prerequisite for the eventual α,α' -dihydroxyketone reaction. Whilst affording a racemate, it is noteworthy for its production of α,α' -dihydroxyketones in the final synthetic step with yields ranging from moderate to excellent yields (65 to 95%).

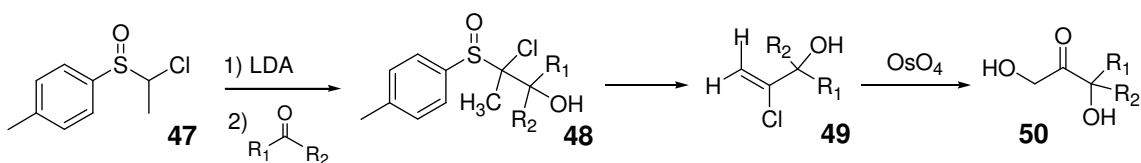
1.3. 2-Chloroalkyl *p*-tolyl sulfoxides as hydroxycarbonyl anion equivalents

The difficulties associated with creating a stable hydroxyketol anion equivalent stems from the subsequent β -elimination of hydroxide or alkoxide upon generation of the anion via umpolung approaches (using diathianes or hydrazones). In 1991 Satoh *et al* described a strategy involving the conversion of carbonyl compounds to α -hydroxy acids, esters, and amides and α,α' -dihydroxy ketones. As in the transketolase reaction involving the donation of a two-carbon nucleophilic moiety, Satoh used a donor substrate of 1-chloroalkyl *p*-tolyl sulfoxide⁵⁸ as the hydroxycarbonyl anion equivalent. The carbon bearing the sulfinyl group and a chlorine atom requires one oxidation state higher than its present state to be used as a hydroxyl anion equivalent. Thus, the three step conversion of **47** to α,α' -dihydroxyketones **50** proceeds via an oxidation with OsO_4 of the vinyl chloride intermediate **49** (Scheme 23).



Scheme 23: Chloroalkyl *p*-tolyl sulfoxides used in the synthesis of ketodiol 50

The oxidation reaction with various ketones via vinyl chloride intermediate **49** was performed cleanly, to afford products **50a** (67%), **50b** (68%), **50c** (79%) (Table 7).

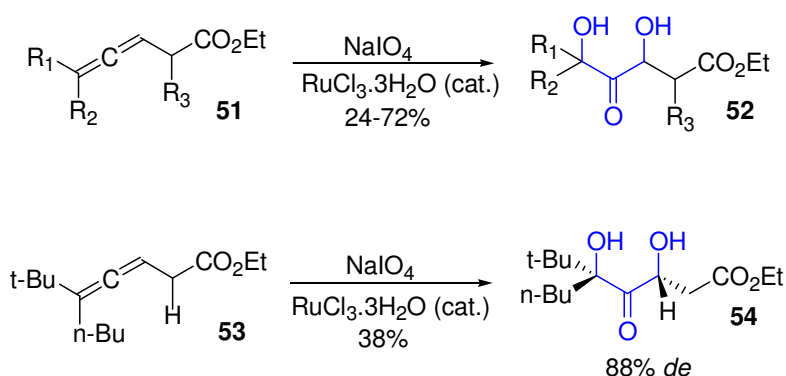


Ketone (R ₁ R ₂)	Chloro Alcohol 48 %	Vinyl Chloride 49 %	α,α' -dihydroxyketones 50 %
 a	81	97	67
 b	93	97	68
 c	94	98	79

Table 7: Examples of the synthesis of ketodiols using chloroalkyl *p*-tolyl sulfoxides

1.3.3 The ruthenium-catalysed oxidation of allenes

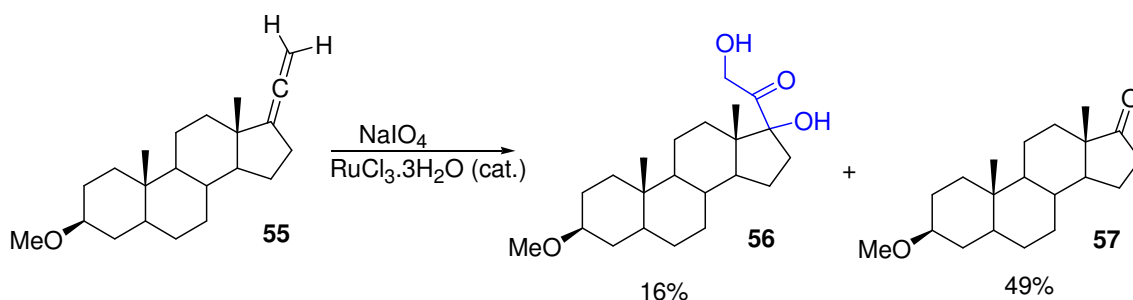
A recently developed oxidation method known for the *cis*-dihydroxylation of alkenes dubbed as the 'flash dihydroxylation' due to its efficiency and short reaction times⁵⁹ was used to catalyse the oxidation of β -allenic esters **51** and **53**. The ruthenium-catalysed oxidation⁶⁰ of β -allenic esters afforded α,α' -dihydroxyketones **52** in 24-72% yields with good levels of chiral transfer of one particular chiral allene **54** in 88% *de* (Scheme 24).



Scheme 24: Ruthenium catalysed oxidation of allenes to ketodiols **52** and **53**

Most significant, is the application of this method to the synthesis of corticosteroids exemplified by the conversion of allenic steroid⁶¹ **55** into dihydroxyketone **56** (16% yield) and ketone side product **57** (49% yield), demonstrating the application of ruthenium catalysed flash oxidation of allenes to target molecules possessing biological activity (Scheme 25). Further improvements of the method by using non-aqueous

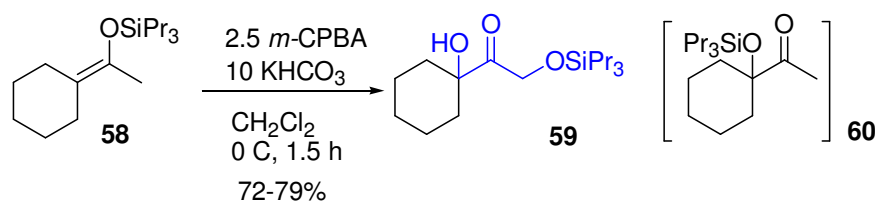
conditions and lower temperatures were reported to be currently under development to increase its efficiency.



Scheme 25 The synthesis of corticosteroids

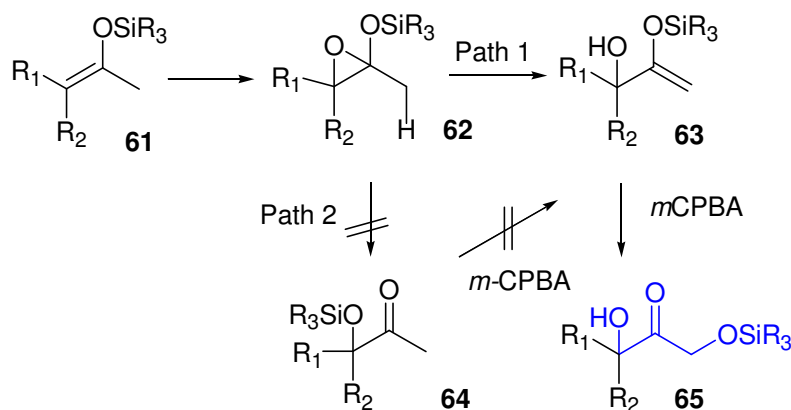
1.3.4 A double hydroxylation of enol silyl ethers

In 1975, Hassner initially reported the oxidation of enol silyl ether with peracid as a reliable method for the preparation of α -hydroxyketones.^{62a} Thereafter, research conducted by Horiguchi *et al*,^{62b} reported that if the enol silyl ester **58** possessed certain structural features, the reaction afforded hydroxyl siloxy ketone **59** and could be converted to the corresponding dihydroxyketone. Significantly there was no trace of the 'normal oxidation' product **60** found (Scheme 26).



Scheme 26 Preparation of α -silyoxy and α -hydroxy ketones

Mechanistic studies have shown an interesting pathway differing from the normal reaction (path 2) proceeding via the migration of the silyl group from the enol oxygen **61** to the epoxide oxygen **64**. Product **63** was isolated by using only one molar equivalent of the oxidant determined through reaction path 1 involving the rearrangement of intermediate epoxide to the allylic alcohol (loss of hydrogen). Subsequent oxidation afforded the desired dihydroxyketone **65** (Scheme 27).

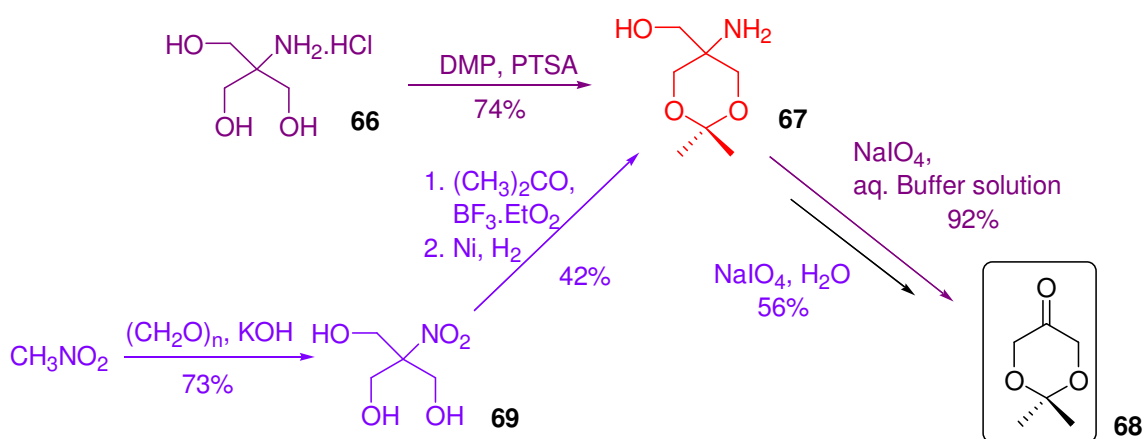


Scheme 27: Mechanistic pathway for the generation of α -silyoxy and α -hydroxy ketones **65**

The 'non-Hassner' reaction pathway is preferred by the silyl enol ether of methyl alkyl ketones and steric hindrance at the site of the initial oxidation favours the pathway. Taking into account these contributing factors, yields ranging from 72-79% for the double hydroxylation of enol silyl ethers have been achieved.^{62b}

1.3.5 The SAMP/RAMP-Hydrazone Methodology

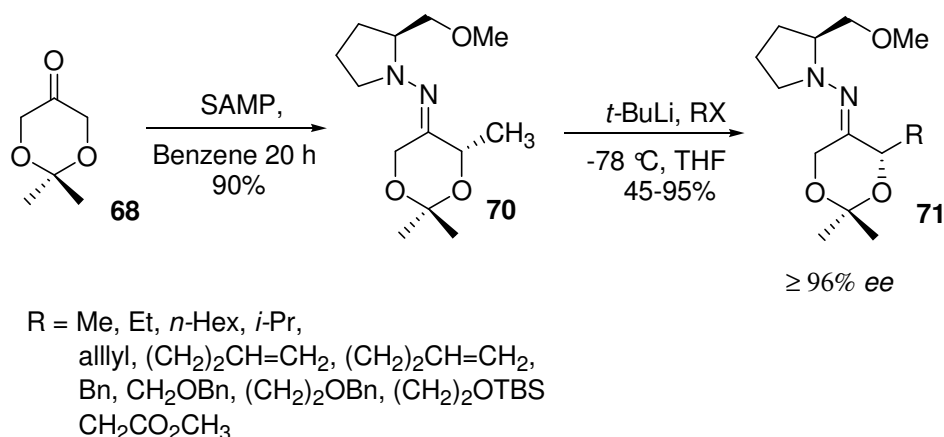
There are two closely related syntheses of the dihydroxyacetone equivalent, 2,2-dimethyl-1,3-dioxan-5-one. The first approach was developed by Hoppe *et al.*⁶³ Starting from commercially available 2-amino-2-(hydroxymethyl)propane-1,3-diol hydrochloride salt (Tris.HCl) **66**, the diol was protected in acid-catalysed conditions by the formation of the acetal **67** in the presence of 2,2-dimethoxypropane. Subsequent oxidation with the treatment of sodium periodate generated a formaldehyde by-product and 2,2-dimethyl-1,3-dioxan-5-imine which was subjected to hydrolysis *in situ*, affording 2,2-dimethyl-1,3-dioxan-5-one **68** in 68% yield over two steps. The other approach to dioxanone **68** is a four-step procedure, starting from nitromethane.⁶⁴ A base-catalysed nitroaldol reaction in the presence of paraformaldehyde gave 2-(hydroxymethyl)-2-nitropropane-1,3-diol **69**. Then sub-sequent Lewis-Acid catalysed acetal formation was followed by a hydrogenation. The β -aminoalcohol was obtained, and subjected to sodium periodate cleavage, with a significantly lower 17% yield (Scheme 28).



Scheme 28: Two approaches for the synthesis of 2,2-dimethyl-1,3-dioxan-5-one. DMP=2,2-dimethoxypropane, PTSA = *p*-toluenesulfonic acid.

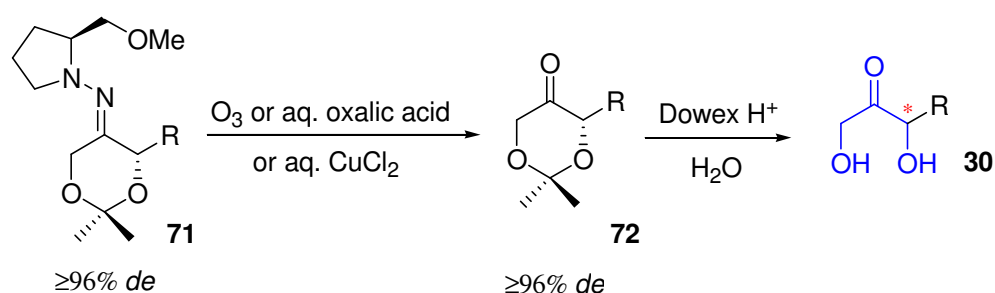
The dioxanone provides a useful tool in asymmetric synthesis, when coupled with the chiral auxiliary (*S*)-1-amino-2-methoxy-methylpyrrolidine (SAMP) or its enantiomer RAMP, to give the SAMP hydrazone **70**.⁶⁵ Treatment with *tert*-butyl lithium to form the lithium azaenolate at low temperatures, and then subsequent reaction with electrophiles such as Michael acceptors, alkyl halides, and aziridines have been used

to afford α -alkylated hydrazones **71** with high diastereoselectivities ($\geq 96\%$ *de*) (Scheme 29).



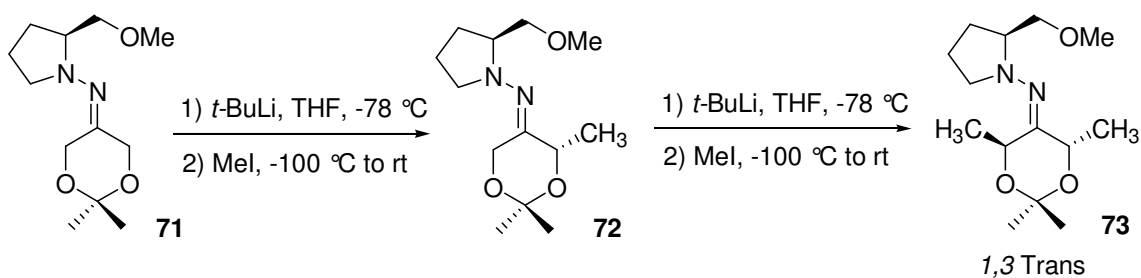
Scheme 29: The asymmetric synthesis of 4-substituted 2,2-dimethyl-1,3-dioxane-5-ones

Cleavage of the chiral auxiliary can be carried out oxidatively with ozone,⁶⁶ or under biphasic conditions (solutions of aqueous copper (II) chloride⁶⁷ or oxalic acid⁶⁸ with hexane or ether). Ozonolysis does not affect the acetal protecting group, and the chiral auxiliary can be recycled by reduction of the nitrosamine cleavage product. However substrates containing other unsaturated carbon bonds are more likely to form large amounts of byproducts. Oxalic acid cleavage is more amenable as no carcinogenic nitrosamine by-product is formed as in the case in ozonolysis and a simple extraction is used to recover the chiral auxiliary from the aqueous phase after basification. Copper (II) chloride cleavage is advantageous as the substrate substituents containing acid-labile or unsaturated carbon groups are not affected in this hydrolytic procedure (Scheme 30).⁷⁰



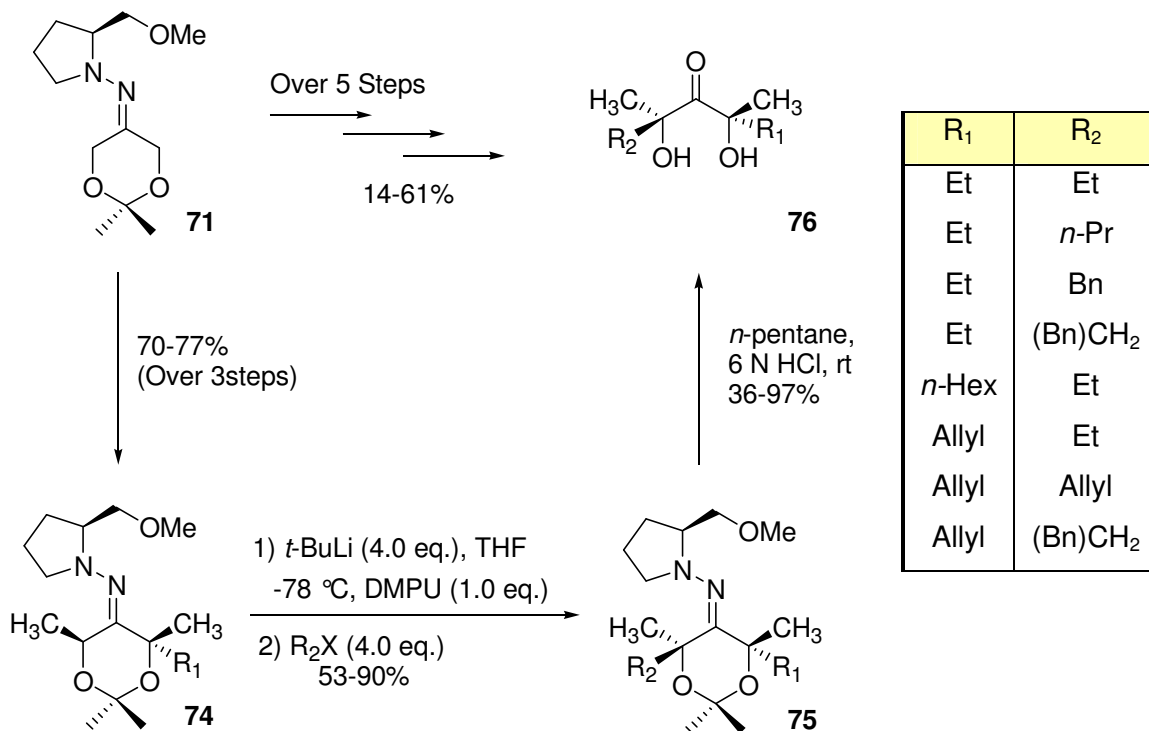
Scheme 30: Cleavage of chiral auxiliary and acetal protecting group to afford ketodiol product

The monoalkylation concept was further extended to α,α' -bisalkylations.⁶⁹ The monoalkylated hydrazone products can be further reacted following the monoalkylation procedure again. 1,3-*Trans* substituted products were exclusively isolated in 58-83% yield and ees $>96\%$ (Scheme 31).



Scheme 31: Formation of Disubstituted 2,2-Dimethyl-1,3-dioxane-5-ones.

Most recently, the Ender's group has extended the highly stereoselective alkylation technique towards the asymmetric synthesis of α,α' -quaternary 2-keto-1,3-diols **76**.⁷⁰ This was achieved by sequential alkylations of the SAMP-hydrazone and the yields over three consecutive alkylations ranged from 70% ($R_1 = \text{Et}$) to 77% ($R_1 = n\text{-Hex}$) **74**. However attachment of the secondary α' -quaternary carbon center in the substrate molecule without the presence of complexing agent afforded low yields. Introducing one equivalent of 1,3-dimethyl-2-oxo-hexahydropyrimidine (DMPU) to the reaction mixture increased the nucleophilicity of the azaenolate. This was evident from the moderate to very good yields **75** (53-90%), and high diastereoselectivities (91-97%).⁷⁰ The removal of the chiral auxiliary was not straight forward as there was too much steric demand to generate the Criegee intermediates by ozonolysis ($\approx 25\%$). An alternative acid-catalysed cleavage protocol of both the acetal and the chiral auxiliary was performed, providing moderate to excellent yields (36-97%) of ketodiol products formed **76** (Scheme 32).



Scheme 32: Symmetric synthesis of α,α' -quaternary 2-keto-1,3-diols

1.3.6 Aims of Research

The aim of this research was principally two-fold; (i) pursue the potential of a library of *E.coli* TK mutants through directed evolution processes to accept a variety of substrates, (ii) organocatalytic approaches to enantiopure ketodiol. Both comparative methods allow the synthesis of valuable intermediates for contemporary industrial production of enantiomerically pure pharmaceuticals, agrochemicals or fine chemicals.

In vivo the enzyme transketolase (TK) reversibly transfers a two carbon ketol unit from a ketose donor to an aldose phosphate acceptor. The use of hydroxypyruvate (HPA) **Li-27** as a ketol donor yields an irreversible reaction with the evolution of carbon dioxide generating the desired ketodiol product. The condensation of HPA with glycolaldehyde and propanal as acceptor substrates has well been described in the literature.⁹⁰⁻⁹² The nature of the aldehydic acceptor tolerance of TK to generate chiral synthons for use in synthetic applications is further investigated. Furthermore a chiral assay for successful characterization of these structural ketodiol motifs is also explored.

The development of the enzyme TK as a practical biocatalyst for enzyme-catalysed asymmetric carbon-carbon bond synthesis on a small scale has since led to the discovery of the first biomimetic TK reaction at UCL. Optimisation studies and preliminary mechanistic studies will be performed and an eventual organocatalytic approach to enantiopure dihydroxyketones will also be pursued.

Chapter 2.0

The modified Mosher's method

2.1 Determination of the absolute stereochemistry of chiral carbinol carbons

Determining the absolute stereochemistry of natural compounds and synthetic compounds is an essential task for organic chemists. The infamous history of thalidomide,⁷¹ an effective sedative against morning sickness **78**, and a potent teratogen **77** that may cause severe birth defects if the drug is taken during pregnancy serves as a crucial model for identifying compounds of correct configuration and *ee* (Fig. 9).

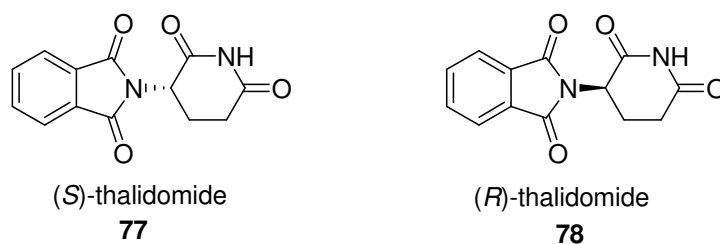
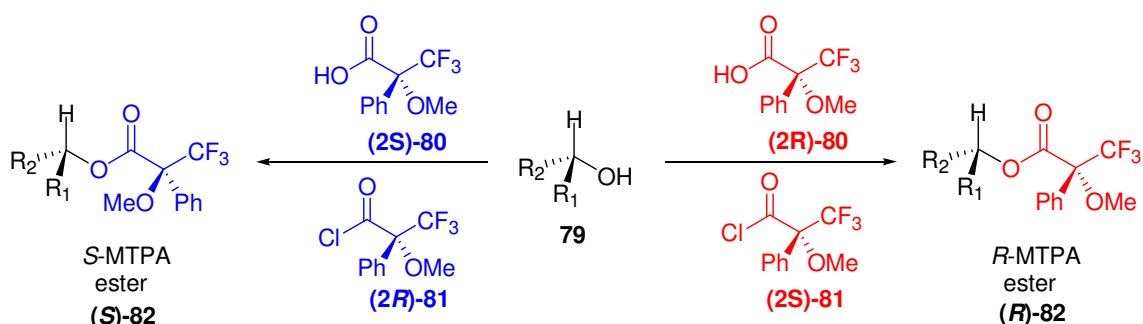


Figure 9: The two enantiomers of thalidomide

Such useful methods for identifying substances of unknown structural ‘scaffolds’ include (i) comparisons of optical rotations via polarimetric methods to those of known literature values (ii) X-ray Crystallography and various exciton chirality methods⁷² (iii) and NMR spectroscopy via the use of lanthanide shift reagents and chiral derivatising agents⁷³ of which the Mosher’s method using 2-methoxy-2-(trifluoromethyl)phenylacetic acid (MTPA) **80** or chloride (MTPA-Cl) **81** to form the Mosher’s ester **82** is most prevalently used (Scheme 33).⁷⁴



Scheme 33: The synthesis of (*R*)- and (*S*)- Mosher’s ester from the stereogenic carbinol centre

2.2 Determining the absolute stereochemistry of chiral carbinols using Mosher’s ester analysis

The Mosher’s Method is a reliable method for determining the absolute configuration of stereogenic carbon centers with secondary alcohols **79** (i.e R_1R_2CCHOH , wherein $R_1 \neq R_2$), primary amines ($R_1R_2CCHNH_2$, or $R_1R_2CCHNHR_3$ wherein $R_1 \neq R_2 \neq R_3$) and amino acids. The determination of the carbinol carbons involves the coupling of the hydroxyl group in two separate but analogous experiments of each enantiomer of the Mosher’s acid. (i.e **2R** and **2S**) to afford the corresponding MTPA esters (Scheme 33).

Each of the diastereoisomers possesses different physical and most notably spectroscopic properties; differential in chemical shifts of resonances in ^1H NMR spectra, or the ^{19}F atom in the CF_3 group in the MTPA moiety.⁷⁵

Mosher proposed that predicting the absolute configuration of the secondary alcohol depended upon the configuration of the ester carbonyl, the methine proton of the stereogenic carbon, and the trifluoromethyl (CF_3) groups of the MTPA moiety lie on the same plane (0° dihedral angle) **82**. Although this is not the only conformation populated by rapid interconverting rotamers, another stable conformation calculated by perturbative configuration interaction using localized orbitals (PCILO)⁷⁶ predicted the close proximity of the methoxy group (0° dihedral) to the ester carbonyl. However, in light of empirical evidence such as X-ray studies and IR adsorption⁷⁶ (in CCl_4) on (*R*)-MTPA esters of various cyclohexanols *i.e* 4-*trans-tert*-butylcyclohexanol⁷⁷ validates that Mosher's original proposal is preferred. Mosher and coworker state that these conformations 'are intended to represent a model which successfully correlates known results...they may in fact measure the effective average of many conformations' (Fig. 10).⁷⁵

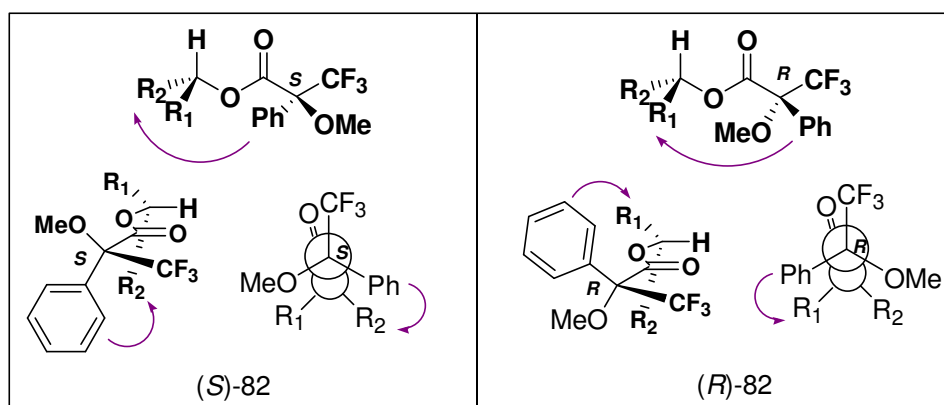


Figure 10: Common conformational representations of the MTPA-esters. The diamagnetic shielding effect is indicated by the arrow.

When the aryl group of the MTPA esters is in the Mosher's hypothesized conformation, it is known to impose a diamagnetic shielding effect on the proton environments residing above or below the plane of aryl ring (Fig. 10). Thus, the protons with spatial proximity of the aryl ring will exhibit an upfield chemical shift in the ^1H NMR spectrum. On inspection of the two conformations exhibited by both diastereoisomers key characteristic features are revealed. Protons residing on the R_2 substructure of (*S*)-**82** are more shielded and upfield relative to that of (*R*)-**82**, conversely protons residing on R_1 substructure of the (*R*)-**82** are more shielded (upfield) relative to that of the (*S*)-**82**, and this is the basic concept of the Mosher's method.

The ^1H chemical shift differences are calculated ($\Delta\delta = \delta_{\text{S-MTPA}} - \delta_{\text{R-MTPA}}$)⁷⁸ and the protons residing in R_1 will be positive ($\Delta\delta > 0$) while protons of the R_2 environment will be negative ($\Delta\delta < 0$). Thus, by assigning the values of the chemical shift differences ($\Delta\delta$) one can deduce the (sub)structures of R_1/R_2 indicating the correct absolute stereochemistry of the secondary alcohol of the carbinol center. In addition to the absolute configuration of the Mosher's esters, the derivatives can deduce the enantiomeric excess ($\text{ee \%} = \text{major isomer} - \text{minor isomer}$) of the sample of interest, by measuring the relative intensities of ^1H or ^{19}F NMR spectroscopy signals with similar environments in each diastereoisomer.⁷⁹ However, further justification by complementary measurement by gas or liquid chromatographic analysis is also normally provided.

2.2.1 ^{19}F Chemical Shifts of α -Methoxy- α -trifluoromethylphenylacetate (MTPA) Derivatives⁷⁵

At the time of Mosher's publication, NMR machines normally available were 60-100 MHz instruments and the complete assignment of protons of complex organic molecules was not feasible. Instead, Mosher and coworkers developed modifications of this model, providing a rationale to correlate the absolute configuration and ^{19}F NMR chemical shifts of MTPA-esters. This method had an inherent advantage over proton chemical shift differences ($\Delta\delta$) of the same compound; generally the ^{19}F NMR chemical shift differences for the $\alpha\text{-CF}_3$ of diastereomeric derivatives are greater and are unobstructed in this spectral region. Studies had also shown that the presence of TFA had a significant effect on $\alpha\text{-CF}_3$ resonances, and on the chemical shift differences between diastereomeric MTPA esters.⁷⁹

In light of these findings, configuration correlation models (Fig. 11) has been proposed for rationalizing the nonequivalent $\alpha\text{-CF}_3$ chemical shift differences. The diamagnetic deshielding of the $\alpha\text{-CF}_3$ of the MTPA substituent by the carbonyl ester is believed to be responsible for the observed phenomena. The magnitude of nonequivalence of each ^{19}F diastereomer is up to 0.73 ppm, and the model predicts the $\alpha\text{-CF}_3$ environment to be deshielded (downfield) or more shielded (upfield). The deshielding of $\alpha\text{-CF}_3$ group is dependant upon the electronic or steric bulkiness of R_1 or R_2 carbon substituents and its effect to force the $\alpha\text{-CF}_3$ group out of coplanarity ($\theta \neq 0^\circ$).

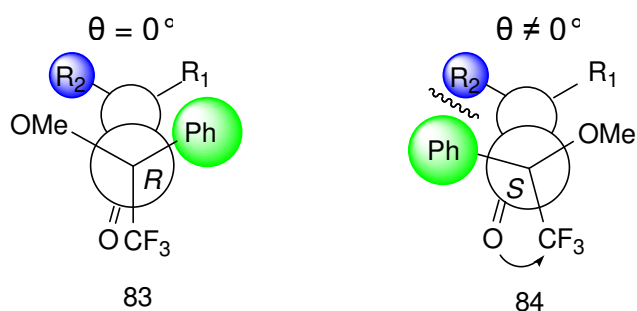


Figure 11: Configuration-correlation models where (*R*)-MTPA diastereomer is downfield relative to alternate diastereomer

If we assume the model was based solely on sterics; then phenyl is larger than the methoxy group and R_2 bulkier than R_1 then under these conditions the sterics are minimized and the α - CF_3 is coplanar with the carbonyl of the diastereomer **83**. Conversely if the bulkier R_2 substituent is juxtaposing the equally bulky phenyl group, an imposing steric interaction incurs resulting into the displacement of α - CF_3 out of coplanarity with the carbonyl of the MTPA ester **84** in a less deshielded (upfield) environment. Predicting the absolute stereochemistry based on the ^{19}F NMR nonequivalence of MTPA diastereomers follows this configuration-correlation model. Hence if the diastereomer was prepared from (*R*)-(+)-MTPA with a downfield α - CF_3 signal ($\delta < 0$) in comparison to the other α - CF_3 resonance of the alternate diastereomer, it will adopt the configuration shown in **84** where R_1 is smaller than R_2 . If (*S*)-(-)-MTPA was used to prepare a diastereomer, then the diastereomer **85** with the relatively downfield α - CF_3 signal will adopt conformation **86** an enantiomer of **84**. The absolute stereochemistry of the molecule with subsequent assignment of the Cahn-Ingold-Prelog nomenclature rules then follows (Fig. 12).

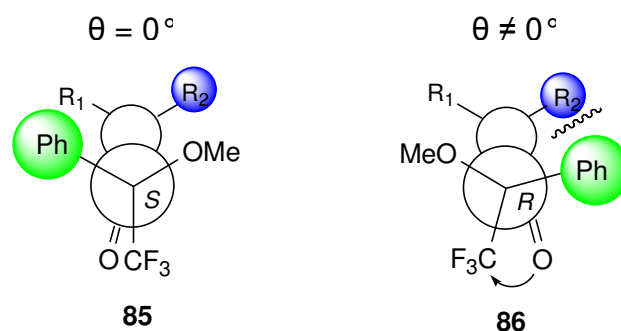


Figure 12: Configuration-correlation models where *S*-MTPA diastereomer is downfield relative to alternate diastereomer

The main setback towards this modified Mosher's approach stems from organic compounds with increased complexity. The ^{19}F NMR method relies upon the substituents of β - and the β' - carbons responsible for eliciting a chemical shift difference of the CF_3 (^{19}F) group. However other substituents (on the γ , δ , ϵ position),

may have a greater steric interaction with the phenyl group of the MTPA moiety entirely.⁸⁰ In such cases a simple comparison between the bulkiness of β -substituents can be considered futile *i.e* Borneol **87** (Fig. 13).

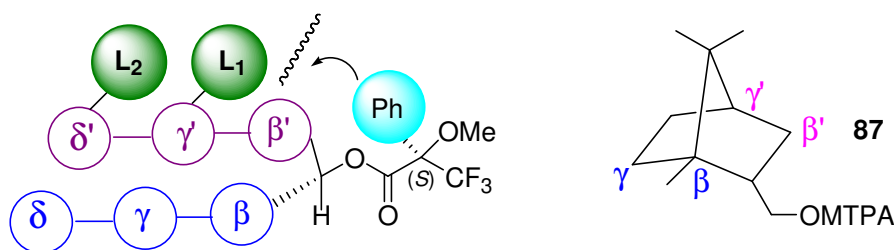


Figure 13: Conformational representation of the interaction between γ , δ substituents and the aryl group of MTPA, an example of borneol an exception to this model

2.2 Modified Mosher's method on the absolute stereochemistry of β -chiral primary alcohols.

Currently in the literature there are few examples for determining the absolute configurations of β -chiral primary alcohols due to the irregularities of $\Delta\delta$ (chemical shift differences).⁸¹ However, attempts to determine the absolute stereochemistry of natural products possessing a branched methyl group at C2 (β) relative to primary alcohols were first described by Minale *et al.*⁸² A modified Mosher's method was used to elucidate the absolute stereochemistry of steroids containing a chiral methyl group at C25 with a primary hydroxyl group at C26 **88** (Fig. 14). Once the samples were derivatised to the MTPA diastereomers, a unique splitting pattern was observed with the oxymethylene protons. The ¹H NMR spectra of (*R*)-(+)-MTPA esters, gave a smaller chemical shift difference ($\Delta\delta = \delta_{\text{Low}} - \delta_{\text{High}}$, *ca.* 0.04 ppm) for the methylene protons of the 25*S* isomer, than those of the 25*R* isomer ($\Delta\delta \approx 0.14$). However, the relationship was reversed when (*S*)-(-)-MTPA esters were used.

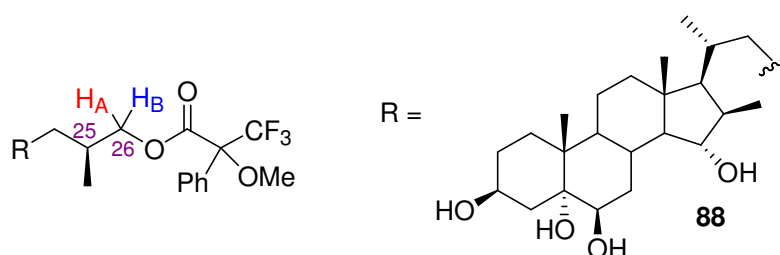


Figure 14: Investigating the stereochemistry steroid **88**

Kobayashi's⁸³ group further substantiated Minale's proposal with a series of known primary alcohol stereochemistries with a methyl group at the C2 (β) position. Thus, the absolute configurations were determined by calculating the chemical shift difference of the lower field protons (δ_{Low}) and higher field (δ_{High}) oxymethylene protons. It was observed that the (*S*)-MTPA esters of compounds **89-92** possessing the 2*S*-

configuration had the largest chemical shift difference ($\Delta\delta$ ca. 0.20-0.14) compared to those of the (*R*)-MTPA esters ($\Delta\delta$ ca. 0.00-0.05). A typical splitting pattern is shown in (Fig. 15, spectra **A** and **B**) and these results corresponded well to Minale's proposal of predicting the chiral C2 centre.

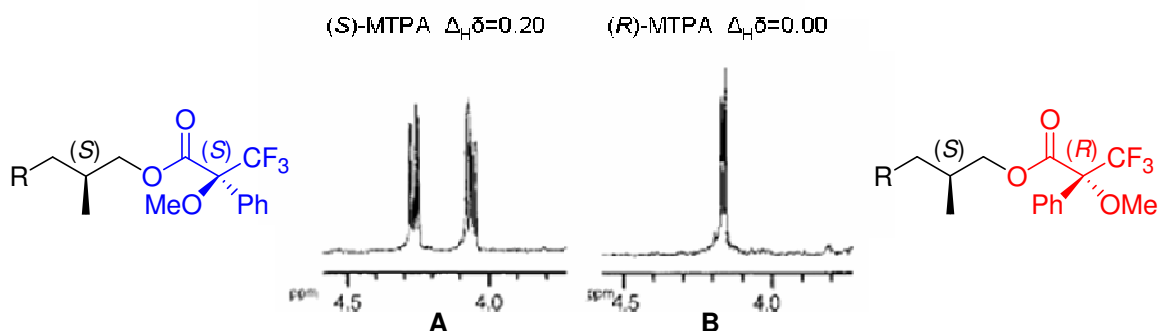


Figure 15: ABX splitting pattern of diastereotopic protons. Reprinted from "Application of Modified Mosher's Method for Primary Alcohols with a Methyl Group at C2 Position", with permission from Chemical and Pharmaceutical Bulletin.⁸³

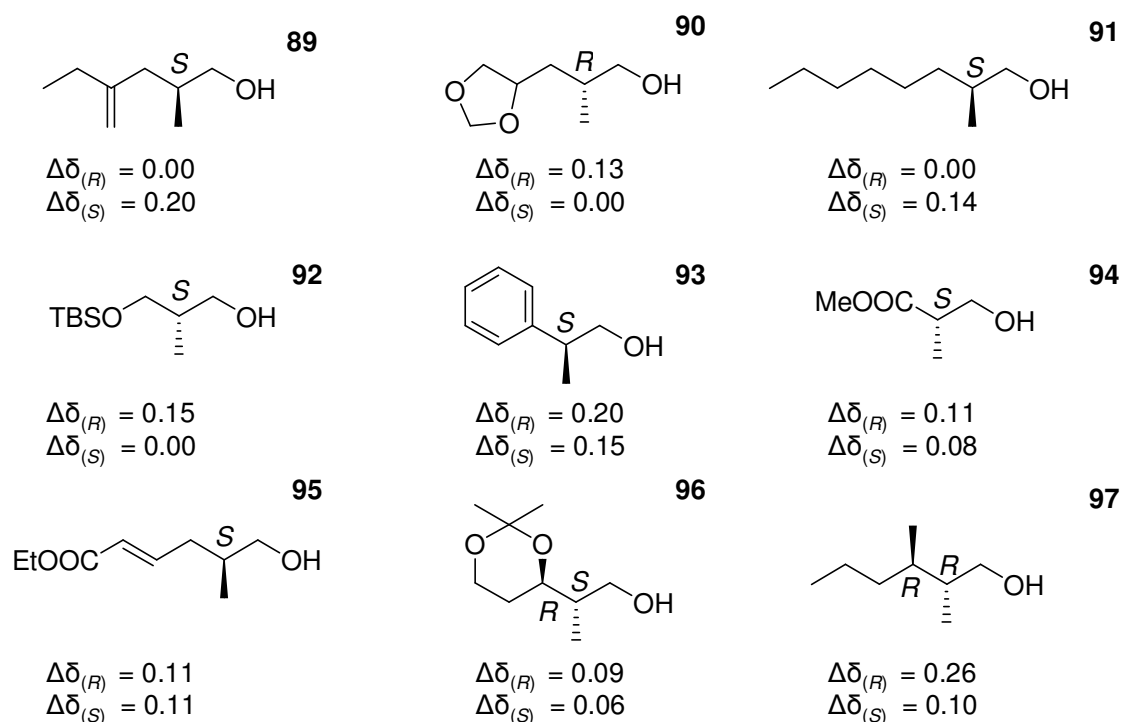


Figure 16: Chemical shift differences $\Delta\delta$ of oxymethylene protons of MTPA esters of primary alcohols with a Methyl group at C2-position.

For compounds **93-95** containing a level of unsaturation, such as a carbonyl, a conjugate ester, or a phenyl group the chemical shift difference ($\Delta\delta$) was small. This is due to the deshielding effect of the aryl ring of the MTPA ester and the unsaturated moiety. Compounds **96-97** containing consecutive stereocenters at C2 and C3 varied on chemical shift differences ($\Delta\delta$), due to the restricted rotation around the C2-C3 bond. The study suggested that the level of unsaturation increased in the molecule the splitting pattern of the oxymethylene protons were less resolved with chemical shift

differences (<0.05 ppm), so it may be difficult to predict the absolute stereochemistry at the C2 position. Likewise, molecules containing a consecutive chiral center at C3 could not be used with this model.

Simultaneously, another research group has conducted experiments assigning naturally occurring 2,3- epoxy-2-methylbutanoate esters.⁸⁴ In this case, the esters were reduced to form a diol with C2 (β) position branched with a methyl and a hydroxyl substituent compound **98** (Fig. 17).

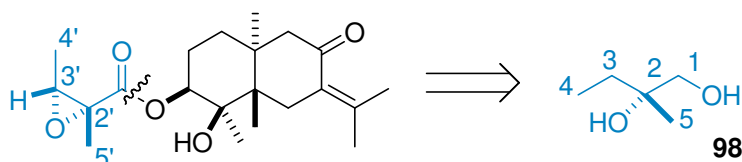


Figure 17: Retrosynthesis of bioactive natural product from 2-methyl-1, 2-butanediol

The primary alcohol of **98** was MTPA-derivatised to form the Mosher's ester and the ^1H NMR spectra indicated an AB system of diastereotopic oxymethylene protons with a distinct chemical difference between the pairs of diastereomers. The $(2R,2'R)$ and $(2S,2'S)$ configurations gave rise to the ^1H NMR spectrum **A** (Fig.18) with small chemical shift differences, in comparison with the $(2R,2'S)$ and $(2S,2'R)$ configurations spectrum **B** (Fig. 18). No explanation is given in the paper, however it may be due to the anisotropic effect from the aryl ring of the MTPA substituent that may have an electrostatic or steric interaction with the hydroxyl group residing on the same face. A large chemical shift difference in the oxymethylene protons was observed compared to the smaller chemical shift differences when the aryl and hydroxyl substituents were on opposite faces (Fig 18).

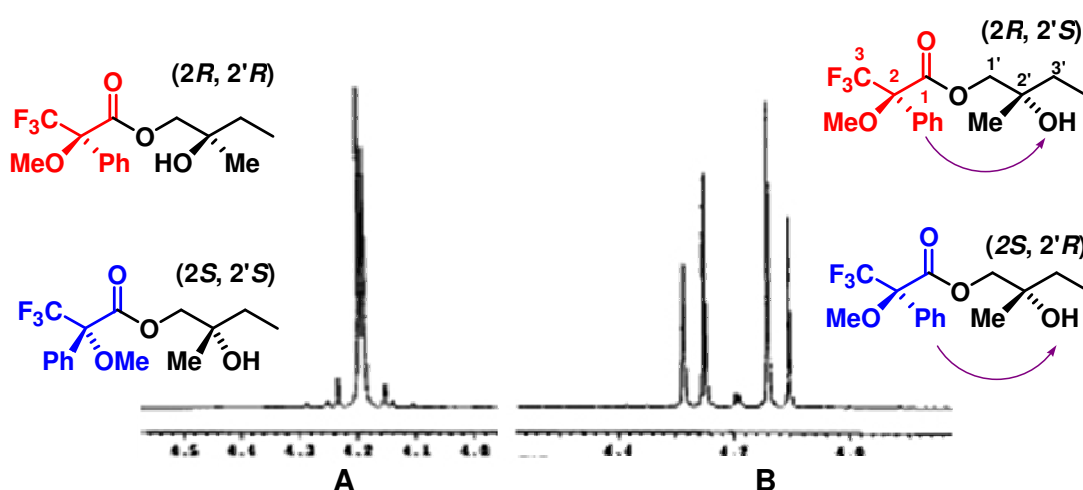
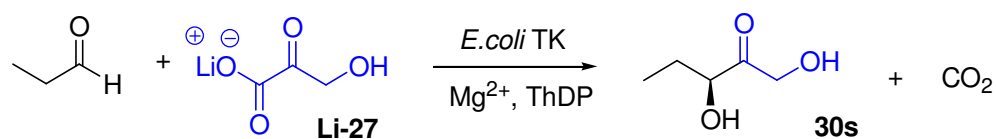


Figure 18: The ^1H NMR AB-spectra of diastereotopic oxymethylene protons, the arrows represent the anisotropic interaction of the aryl ring and the hydroxyl group. Reprinted from "Stereochemical assignment of naturally occurring 2,3-epoxy-2-methylbutanoate esters", with permission from John Wiley and Sons.⁸⁴

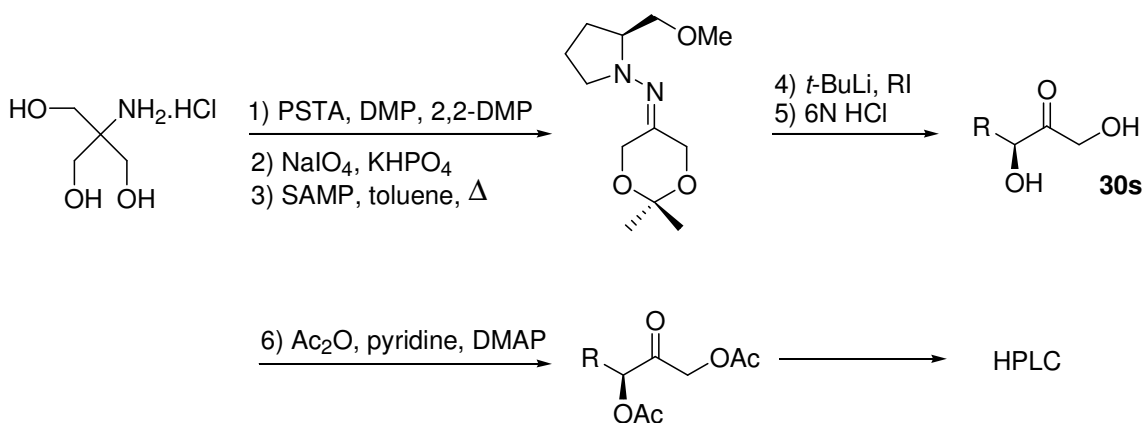
2.3 Application of a modified Mosher's method for the determination of chiral 1,3-dihydroxyketones

α,α' -Dihydroxyketone functionalities are present in several biologically important compounds and can further be used as synthons for further structural elaborations to a range of compounds involving ketosugars. The enzyme transketolase (TK) has been shown to successfully generate the dihydroketone product **30s** *in vitro* via the condensation of hydroxypyruvate (HPA, Li-27) with propanal as previously described (Scheme 34).^{42,46, 51,52, 85}



Scheme 34: TK-catalysed reaction with propanal and HPA

Chiral assays for the determination of the absolute stereochemistry of these structural motifs have been one of the focuses when using TKs. Currently Ender's chiral auxiliary methodology⁵⁹ generating α,α' -dihydroxyketones in high enantioselectivities with subsequent HPLC/GC analysis for comparative purposes has been used to confirm absolute stereochemistries. This six step procedure tolerates a broad range of electrophilic acceptors (Scheme 35); however the reaction fails to accommodate derivatives when R = Ar and is a time consuming method for determining the absolute stereochemistry.



Scheme 35: Ender's chiral auxiliary methodology

A reliable and convenient method via a Mosher's ester would be a useful and effective tool for determining the carbinol stereocenter of the α,α' -dihydroxyketone motif. Currently in the literature the modified Mosher's method has been applied to 1,3-diols via synthesis of the mono-MTPA and di-MTPA esters,⁸⁶ however the irregularities of chemical shift difference ($\Delta\delta$) of acyclic anti-1,3-diols made this method not useful in most cases. The potential of a modified Mosher's method prompted us to examine it

as a method for determining the enantiomeric purities and absolute stereochemistry of stereochemically defined α,α' -dihydroxyketones (Fig.16).

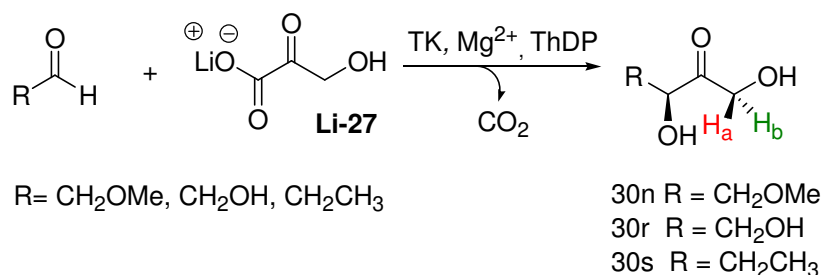


Figure 16: TK- catalysed reactions forming α,α' -dihydroxy ketones 30

The absolute stereochemistry and optical purity of (3*S*)-1,3-dihydroxypentan-2-one has previously been established (Figure 16).⁸⁷ Preliminary investigations involved the coupling of the MTPA moiety, to the primary hydroxyl group of **30s**, generated after biotransformation with WT-TK. The diastereotopic protons H_a and H_b in **30s** are observed as doublets at 4.59 ppm and 4.70 ppm, with a large geminal coupling constant of 19.0 Hz. Attachment of the MTPA moiety to a hydroxyl group deshields the CH_2 protons by about 0.5 ppm.⁸³

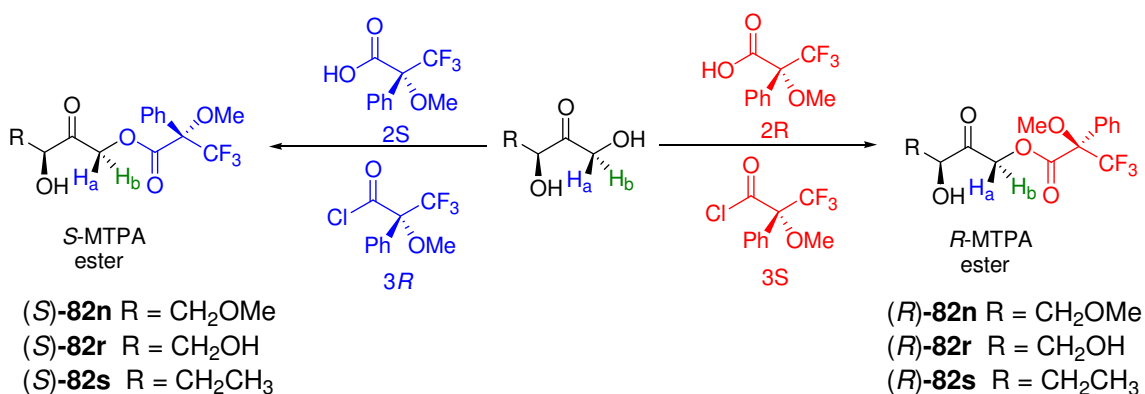


Figure 17: Formation of MTPA ester

The esterification of **30s** with (*R*)- or (*S*)- MTPA was performed under standard procedures using the MTPA-Cl/triethylamine or MTPA/DCC coupling method. After removal of starting materials and urea side products the MTPA esters were analysed by ^1H NMR spectroscopy in CDCl_3 . The ^1H NMR spectra of the (*R*)- and the (*S*)- MTPA esters (*R*)-**82s** and (*S*)-**82s** differ only in the chemical shifts of the diastereotopic protons H_a and H_b ; in the (*S*)-MTPA ester the major isomer (2*S*,3*S*) resonated at δ_{H} 4.93 ppm and 5.17 ppm with a 0.24 chemical shift difference ($\Delta\delta_{\text{H}}^{2\text{S},3\text{S}}$) and the minor isomer resonated at δ_{H} 5.05 ppm ($\Delta\delta_{\text{H}}^{2\text{S},3\text{R}}$ is 0). For the (*R*)-MTPA ester the major isomer (2*R*,3*S'*) resonates at δ_{H} 5.05 ppm ($\Delta\delta_{\text{H}}^{2\text{S},3\text{R}}$ is 0), and the minor isomer at δ_{H} 4.93 and 5.17 ppm ($\Delta\delta_{\text{H}}^{2\text{R},3\text{R}}$ is 0.24) (Fig. 18). The average of the two *ee* values

calculated from the integration of H_aH_b gave comparable results (55%) to the literature value of 58% ee determined by GC methods.⁸⁶

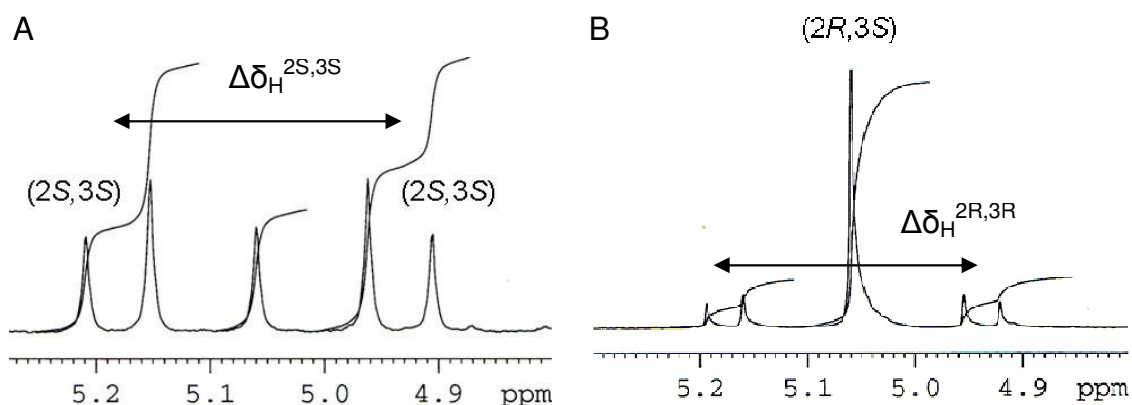


Figure 18: (A) *S*-MTPA ester (*S*)-82s and (B) *R*-MTPA ester (*R*)-82s

Other dihydroxyketones with reported absolute configurations were then investigated to validate the method further. Firstly commercially available L-erythrulose was prepared from glycoaldehyde **30r** and **Li-27** using TK. The corresponding (*R*)- and (*S*)-MTPA esters were prepared using MTPA acid chlorides, obtaining product yields of 51% and 63% respectively. There are three hydroxyl groups present in L-erythrulose and only approximately 1.0 eq (*S*)-MTPA-Cl was used in the esterification process to avoid multiple esterification. The only isolatable compound observed was with the MTPA substituent attached to the primary α -ketoalcohol. The ^1H NMR spectra revealed H_a and H_b in the (*S*)-MTPA ester (2*S*,3*S*) were observed at δ_H 5.05 and 5.23 ppm ($\Delta\delta_H^{2S,3S}$ is 0.18) and no minor isomer (2*R*,3*S*) was detected. For the (*R*)-MTPA ester (2*R*,3*S*) the diastereotopic protons were at $\Delta\delta_H$ 5.11 and 5.19 ppm ($\Delta\delta_H^{2S,3S}$ is 0.18) and negligible signals for the minor isomer were observed. The average integrations of the signals for H_a and H_b indicated L-erythrulose was formed in >95% ee. This confirms the original observation that $\Delta\delta_H^{2S,3S'} > \Delta\delta_H^{2S,3R'}$.

2-Methoxyethanal was prepared from acid deprotection of commercially available methoxyacetaldehyde dimethyl acetal,⁴² and was then used directly as an aldehyde acceptor with wild type *E. coli* TK to further validate the Mosher's ester method. Previous studies involving spinach TK using 2-methoxyethanal as the aldehyde acceptor have been reported, with a 60% ee observed (*S*-major isomer).⁴⁹ Compound **30n** was obtained in 30% yield from the biotransformation using WT-TK, and coupling to MTPA-Cl gave compounds (*R*)-**82n** and (*S*)-**82n** with H_a and H_b for the major isomers at 5.13 and 5.17 ppm (2*R*,3*S*) and 5.02 and 5.29 ppm (2*S*,3*S*) respectively. Again, this demonstrated $\Delta\delta_H^{2S,3S}$ (0.27) > $\Delta\delta_H^{2S,3R}$ (0.04), with the average integrations of the H_a and H_b protons of both MTPA esters giving an ee of 57%, comparable to WT-spinach TK.⁴⁹ The stereoselectivity of *E. coli* WT-TK was comparable to that of

spinach TK with 2-methoxyethanal. This data indicated that the Mosher's method is applicable to aliphatic α,α' -ketodiols and *ee* measurements can be determined within 5% of the values given by GC or HPLC methods, as well as determining the absolute stereochemistries.

Although the proton coupling system differs to that of Kobayashi *et al.* on chiral primary alcohols with methyl groups at the C2 position (ABX),⁸³ the chemical shift differences of the diastereotopic protons are in agreement with his preliminary findings, where $\Delta\delta_{\text{H}}^{2\text{R},3\text{R}}$ and $\Delta\delta_{\text{H}}^{2\text{S},3\text{S}} > \Delta\delta_{\text{H}}^{2\text{S},3\text{R}}$ and $\Delta\delta_{\text{H}}^{2\text{R},3\text{S}}$. However the reverse is true for Torres-Valencia *et al* on chiral primary alcohols with a methyl and a hydroxyl group at the C2 position (AB).⁸⁴ This can be accounted for by the diamagnetic effect of the aryl ring of the MTPA substituent on the hydroxyl group affecting the chemical shift differences of the vicinal diastereotopic protons (Fig. 19). The differences in the chemical shift patterns of α,α' -dihydroxyketones and its analogues compared with previous work conducted on chiral primary alcohols, is that there is a ketone on C2.

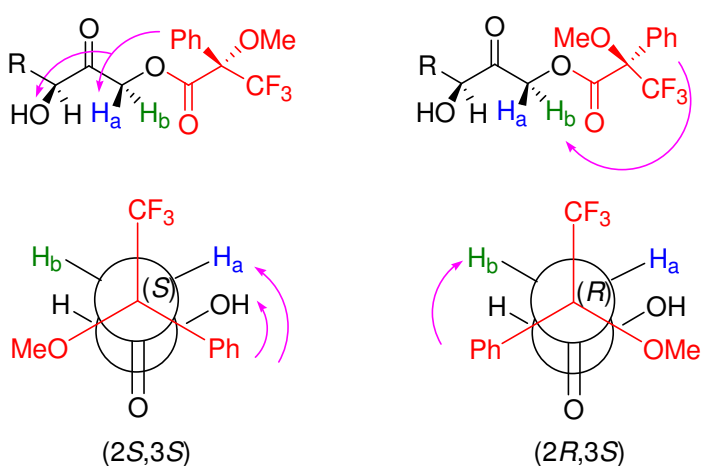


Figure 19: A conformational model proposed for the analysis of the diastereomeric MTPA ester

The conformational restriction of the C2-C3 bond may confer a larger observed chemical shift difference of the diastereotopic protons. The diamagnetic effect of the aryl group of the MTPA substituent can affect the protons residing above or below the plane of the aryl ring; it is also possible that the spatial position of the hydroxyl group at the stereogenic centre C3 may impose an added electronic effect on the diastereotopic proton closest to the hydroxyl group on rapid rotation. As a result there is a greater chemical inequivalency between the diastereotopic protons which is observed from the large chemical shift differences of the spectral data.

The anisotropic shielding effect can 'reach' a considerable distance within a molecule, even the most remote protons can be differentially deshielded in two diastereomers.⁷⁵ However, of all examples investigated there are no other significant proton chemical

shifts that are uniquely identifiable in the (*R*)-MTPA and (*S*)-MTPA esters, other than the diastereotopic protons to which the MTPA substituent is attached.

The ^{19}F NMR chemical shifts of α -methoxy- α -trifluoromethylphenylacetate derivatives of both diastereomers of the molecules studied have the same chemical resonances at δ -72.2. The α -CF₃ chemical shifts in both MTPA esters were identical and can be accounted for by the insignificant electronic or small steric bulkiness of the R₁ or R₂ carbon substituents to displace the α -CF₃ group out of coplanarity ($\theta \neq 0^\circ$) with the carbonyl of the MTPA ester to a less deshielded (upfield) environment (Fig. 20).

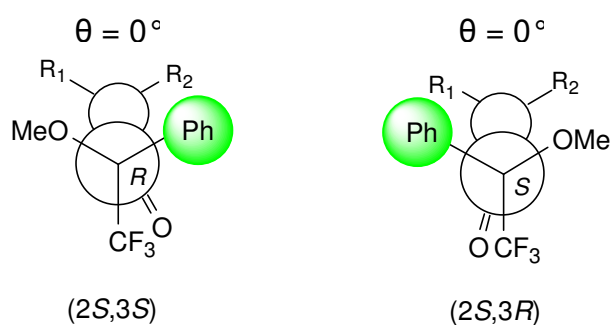


Figure 20: Configuration correlation models of MTPA esters where R is small $R_1 \approx R_2$

This method was then used on a range of analogues of aliphatic α,α' -dihydroxyketones with lipophilic R group substituents and is described in later chapters. It was also tentatively applied to aromatic substrates as described in Chapter 4. Overall this method has the potential for applications with a range of ketodiols.

Summary

The Mosher's method is a useful tool for identifying the absolute stereochemistry of stereogenic carbon centres with secondary alcohols, or primary amines. Recently a modified Mosher's method was applied to determine the absolute stereochemistry of commercially available β -chiral primary alcohols. We have utilized the modified Mosher's method to determine the reliability of this method to confirm the absolute stereochemistry of readily available chiral 1,3-dihydroxyketones such as L-erythrose. The attachment of an (*S*)- or (*R*)-MTPA ester to the primary alcohol of a 1,3-dihydroxyketone reveal a large chemical shift difference $\Delta\delta$ with the diastereotopic protons H_a and H_b. This led to the general agreement with Kobayashi's preliminary finding where $\Delta\delta_{\text{H}}^{2\text{R},3\text{R}}$ and $\Delta\delta_{\text{H}}^{2\text{S},3\text{S}} > \Delta\delta_{\text{H}}^{2\text{S},3\text{R}}$ and $\Delta\delta_{\text{H}}^{2\text{R},3\text{S}}$. The Mosher's method can be used as a tool to determine the absolute stereochemistry and the ees of 1,3-dihydroxyketone analogues.

Chapter 3.0
Aliphatic aldehydes used in the TK
reaction

3.1 UCL developments prior to thesis research

Research conducted by Lilly *et al.* involved excision of a fragment of DNA encoding for the TK gene from the plasmid of *E.coli* (BJ502/pKD112A) back into a high copy plasmid, and overexpression of the protein in *E.coli*. The new transformants JM107/pQR183 and JM107/pQR183 gave TK with approximately four fold greater activity when grown on glycerol than BJ502/pKD113A.⁵¹ *E.coli* TK accepts HPA better than yeast or spinach TK, with 6 times and 30 times higher specific enzyme activity, respectively.^{46,50,88} Initial rate velocities when using simple aldehydes showed low specificity for aldehyde substrates other than glycolaldehyde and α -(*R*)-hydroxyaldehydes.⁵¹

To achieve industrial viability, an important requirement is for greater specific enzyme activity on a broader range of non-phosphorylated substrates. Therefore variants of TK are desired, with improved enzyme activity and one method of achieving this is using directed evolution. In the literature there have been a number of X ray crystallographic studies of yeast,²⁶⁻²⁸ and *E.coli* TK,⁸⁹ with/without its naturally occurring substrate in the enzyme binding site and this provided data for designing a directed evolutionary strategy. One systematic approach used for the directed evolution of TK was site-targeted saturation mutagenesis of amino acid residues chosen firstly on structural grounds, selecting 10 amino acid residues which lie within 4 Å of the bound substrates in the TK active site. The second approach was the selection of amino acids for mutation on phylogenetic grounds: 9 amino acid residues within 10 Å of the binding site of ThDP cofactor that have varied during the course of bacterial and yeast TK evolution (Fig. 21).⁹⁰ Single point mutations were applied using the Quikchange kit (Stratagene, Netherlands) with the plasmid (pQR711) transformed into electrocompetent XL10 (Stratagene) *E.coli* cells.⁹⁰⁻⁹¹

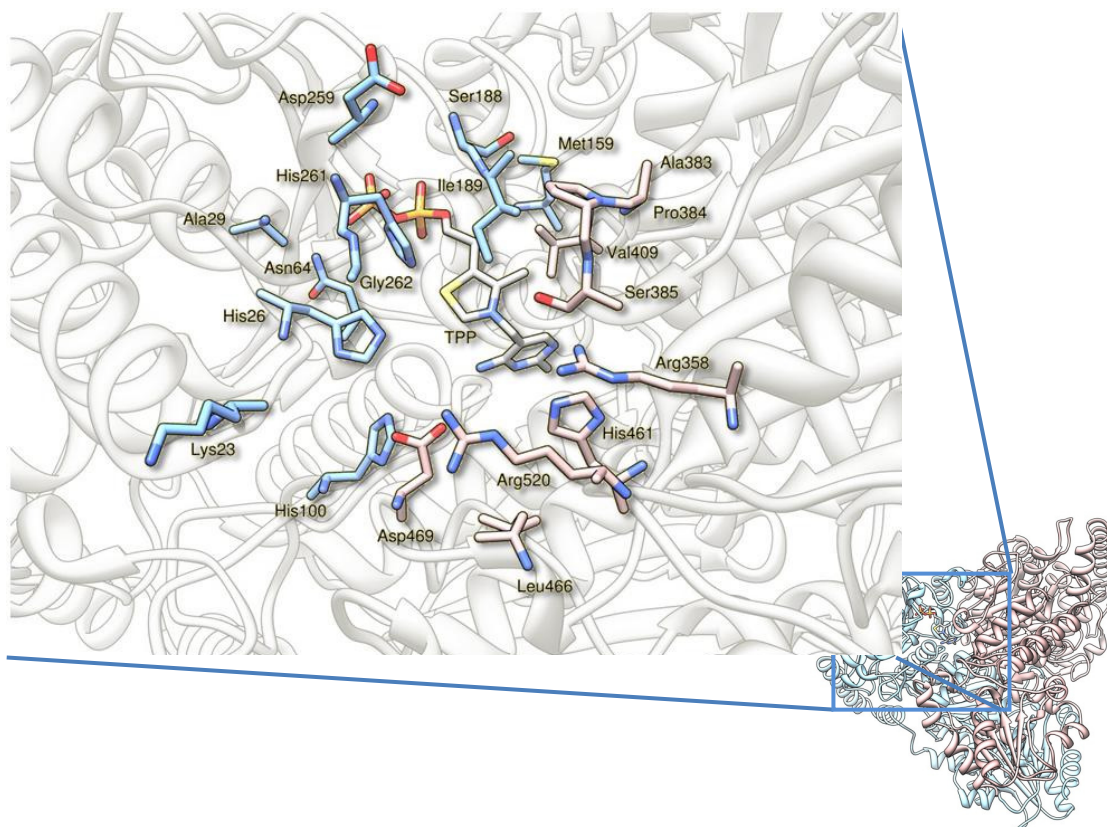
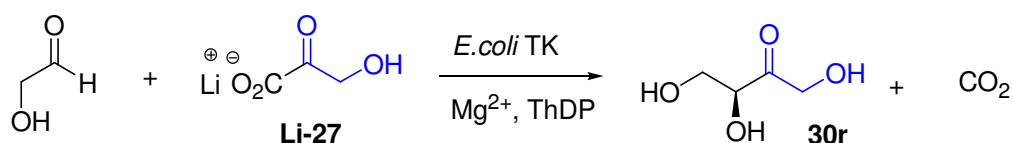


Figure 21: Location of structurally defined and phylogenetic sites relative to the ThDP cofactor in the *E.coli* TK active site.

3.1.1 Directed evolution of TK substrate specificity towards the non-phosphorylated substrate, glycolaldehyde

The structural and phylogenetic libraries were subjected to TK biocatalytic conditions with **Li-27** and glycolaldehyde to generate L-erythrulose **30r** (Scheme 36).⁹⁰ High throughput HPLC screening of the reaction products from these libraries was used initially for the determination of specific TK activities (Table 8). The highest performing TK mutants using glycolaldehyde as a substrate in activity were A29E, H461S, R520V, and R520Stop relative to the specific activity of WT-TK.



Scheme 36: Biotransformation of glycolaldehyde with Li-27 as substrate using mutant *E.coli* TK

Enzyme	[30r]/TK ($\mu\text{mol mg}^{-1}\text{min}^{-1}$)	[30r]/TK Rel. WT	Rate (mM min^{-1})	[TK] (g ml^{-1})
WT	0.65	1	0.29	0.44
A29E	1.95	3.0	0.66	0.34
H461S	3.14	4.8	0.60	0.19
R520V	2.3	3.6	2.16	0.92
R520Stop	2.3	3.6	0.054	0.023

Table 8: The performance of selected TK mutants

X-ray crystallographic data is currently not available for these mutants, however the altered activities can be rationalised. Residue H461 and R520 mutations both interact with the phosphate moiety of naturally occurring TK substrates. Mutant H461S removes a positively charged histidine which usually interacts with a phosphate group. The effect of the R520V mutation reduces the amino acid chain length permitting greater accessibility to the TK binding site. The increased TK specificity for R520Stop is surprising as the mutation caused a deletion of residues from the C-terminal domain (540-680) and 20 residues from the Pyr (pyridinium binding) domain. The function of the C-terminal domain is still relatively unclear as it does not participate in cofactor binding or recruitment of substrates into active site.

A thorough kinetic analysis for the TK mutant A29E was explored as it was the highest performing phylogenetic variant located in contact with the terminal phosphate of ThDP. As a result A29E, was considered most likely to directly affect the catalytic activity of TK. The precise interactions made between glycolaldehyde, HPA and the amino acid residues, are not yet known. However, presumably the A29E mutant could inadvertently affect the pK_a of the ThDP cofactor, potentially through electrostatic interactions; it may also anchor the orientation of the cofactor permitting the reactive enamine intermediate (DHE) to sufficiently couple with glycolaldehyde (Fig. 22).

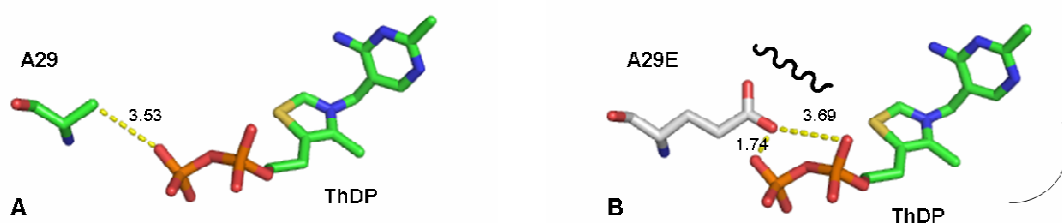
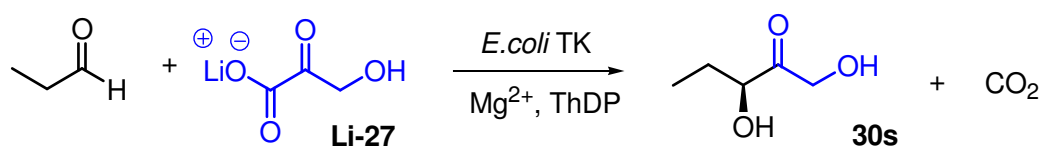


Figure 22: The interaction with A29 (A) and the postulated interaction with A29E (B) crude mutagenesis performed using pyMol (1NGS.pdb, from www.rcsb.org/pdb)

3.1.2 Directed evolution of TK substrate specificity towards an aliphatic aldehyde propanal

WT spinach TK can tolerate a range of non-hydroxylated aliphatic aldehydes with activities ranging from 5 to 35% in comparison to glycolaldehyde.⁴⁹ *E.coli* TK has been shown to accept propanal at approximately 20% of the level with glycolaldehyde whilst cyclic aldehydes **30u** and **30v** (page 37) have shown lesser activities <5%.⁵¹ To achieve industrial viability for larger scale processes, the substrate specificity and enzyme activity has to be improved for biocatalytic usage. Thus a simple aliphatic aldehyde, propanal was investigated as a bench mark for further investigation (Scheme 34). The libraries of TK variants responsible for enhancing TK activity of α -hydroxylaldehydes were screened against non-hydroxylated acceptor substrate propanal, to identify novel *E.coli* TK variants which have improved substrate activity for the generation of the ketodiol product, 1,3,-dihydroxypentan-2-one (**30s**). The screening involved a high throughput colorimetric assay as discussed below.



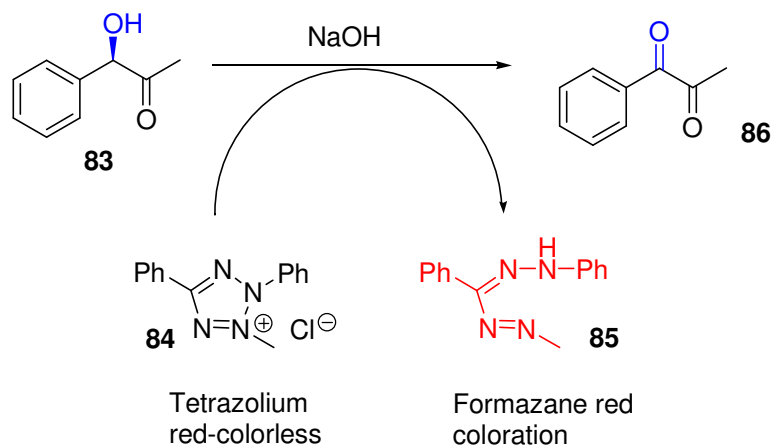
Scheme 34: TK-catalysed reaction with propanal and Li-27

3.1.3 The colorimetric assay for screening transketolase activity⁹²

Research at UCL focused on the preparation of ketodiols by screening libraries of TK mutants. In particular mutants were generated with the aim of increasing the rate of reaction with a range of aldehyde substrates compared to those used by the wild type enzyme. The use of a rapid, sensitive and a readily available assay is crucial for the facile identification of active mutants. In the literature, TK activity has been monitored using a spectrophotometric method involving the use of an NADH dependant enzyme measuring residual **Li-27**,⁹³ and an HPLC assay for erythulose production and **Li-27** depletion.⁹⁴ A fluorogenic assay which measures the production of the fluorescent umbelliferone catalysed by TK⁹⁵ has been reported and most recently a coupled assay using xylulokinase (XK) to monitor TK activity, based on the *in vitro* synthesis of xylulose-5-phosphate, a natural substrate for TK.⁹⁶ However these methods suffer from poor sensitivities restricted substrate structure or low throughput.

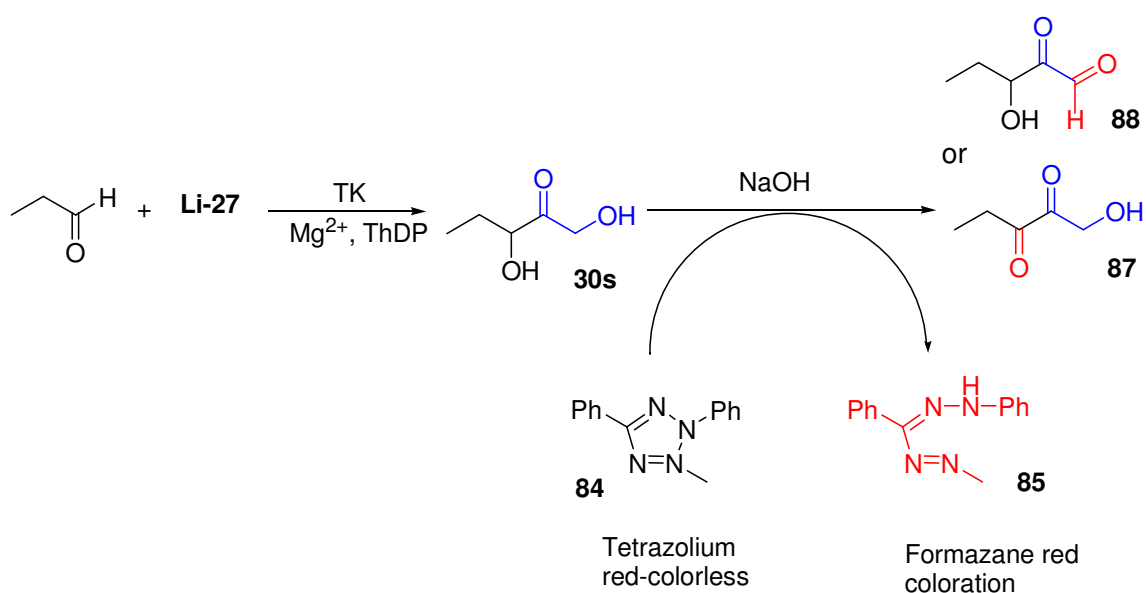
A more generalised method for detecting TK variant activity was identified for use with non-hydroxylated aldehydes. A recent pyruvate decarboxylase (PDC) assay for the detection of aromatic acyloins **83** used 2,3,5-triphenyltetrazolium chloride **84**

(tetrazolium red). Tetrazolium red is colourless and oxidises a phenylacetylcarbinol 2-hydroxyketone **83** motif to the diketone whilst the tetrazolium red is reduced to the corresponding formazane **85** which has an intense red coloration $\lambda_{\text{max}} \approx 485 \text{ nm}$ (Scheme 37).⁹⁷



Scheme 37: The oxidation of **83 to the diketone **86** generating red coloration**

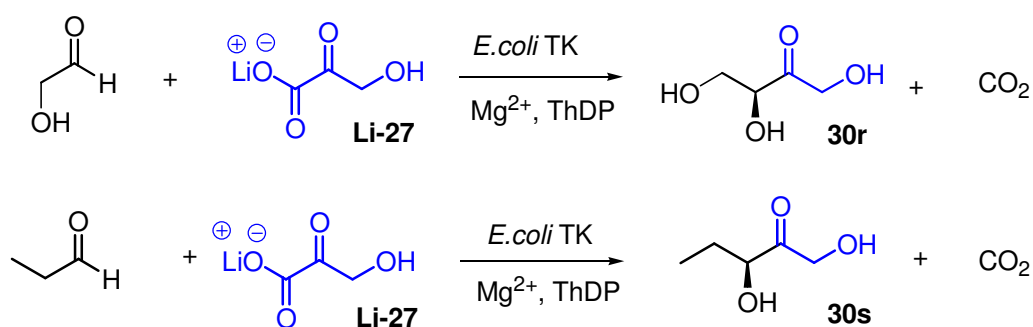
A ketol moiety exists in the starting material **Li-27** as well as the ketodiol product and it was considered whether this colorimetric assay could be modified for use with TK and non- α -hydroxylated aldehyde acceptors. A model system used **Li-27** and *E. coli* TK (XL10/pQR711), and initial experiments used 1,3-dihydroxy-pentan-2-one **30s** at concentrations typical of those to be used in TK assays (gly-gly buffer at pH 7.0). A calibration assay for the reduction of formazene using concentrations of **30s** established a protocol that avoided optical density (OD) saturation. It was determined that the bioconversion was detectable even at concentrations as low as 2.5 mM. An alternative substrate 1, 3-dihydroxypropiophenone was used in the assay and results were comparable (Scheme 38).



Scheme 38: The oxidation of the ketodiol to the diketone **87 or ketone-aldehyde **88** Forming the reduced formazane red**

Once the sensitivity of the assay was established, it was necessary to investigate the effects of the tetrazolium red after a TK reaction with aldehyde, cofactors and other components of the lysate which may mask the assay. Control experiments readily established that ThDP, Mg^{2+} and TK lysate gave no coloration in the well plate. Some reaction occurred between the **Li-27** and the tetrazolium red due to the presence of the hydroxyketone moiety present in **Li-27**. A quarternary amine ionic exchange resin was successful in removing unreacted **Li-27** secondary amine resins were avoided in case a chemical coupling of **Li-27** and propanal were observed.⁹⁸ Overall the assay was found to be suitable to detect bioconversions >8% and enable TK variants to be identified that couple **Li-27** to aldehyde acceptors.

Previous studies involving the substrate activity of TK variants towards the non-phosphorylated substrate glycolaldehyde, revealed catalytic activity among a set of mutants at phylogenetic and conserved residues lying within 10 Å of the ThDP cofactor. Several residues interacted with the phosphate group of ThDP and the natural phosphorylated substrates. Further studies revealed a distinct cluster of residues found to improve the substrate activity towards propanal and glycolaldehyde. High throughput screening by the colorimetric assay when using propanal and TLC analysis identified 8 libraries containing variants with enhanced relative activities for the formation of **30s** compared to WT-TK, D469T, D469Y, R520V, A29E, D259A, H26A, R358I, and H61S. The greatest improvements in TK specificity towards propanal were in libraries D469 (4.9-fold) and R520 (4.7-fold). The results also revealed the specific activities of the TK variants towards the formation of **30r** and **30s** which can be expressed as a ratio (Table 9). In this case D469T and D469Y had an 8.5-fold and 64-fold improvement compared to WT-TK (Scheme 39).



Scheme 39: Biotransformations using *E. coli* TK to generate **30r** and **30s**

Enzyme	[30s]/TK ($\mu\text{mol mg}^{-1}\text{min}^{-1}$)	[30s]/TK Rel. WT	[30s]/[30r]	[30r]/TK ($\mu\text{mol mg}^{-1}\text{min}^{-1}$)
WT	0.029	1	0.045	0.65
D469T	0.14	4.9	0.38	0.37
D469Y	0.127	4.4	2.9	0.04
R520V	0.14	4.7	0.059	2.3
A29E	0.10	3.4	0.050	1.95
D259A	0.066	2.3	0.044	1.5
H26A	0.066	2.3	0.25	0.26
R358I	0.055	1.9	0.037	1.37
H461S	0.040	1.4	0.013	3.1

Table 9: The specific substrate activities of the formation of 30s and 30r

The mutated residues containing the highest activities were clustered together in groups. Residues D469, H100, and H26 are clustered around the binding site, which interacts with the C2 hydroxyl group of erythrulose-4-phosphate (E4P). However in propanal the hydroxyl group at the C2 position is replaced by a methyl group removing any potential of hydrogen bonding. Residues R520, R358, and H461 are located at the entrance of the enzyme cleft interacting with the phosphate group of E4P. Mutations at these points will most likely improve catalytic activity by removal of the charge at the entrance of the enzyme cleft, thereby increasing accessibility to the binding site. The phylogenetic residues identified, A29 and D259, belong in the active site of second shell, the methyl group of A29 interacts with the terminal phosphate group of ThDP, and the mutation to A29E may increase catalytic turnover but not the substrate specificity (Fig. 23).

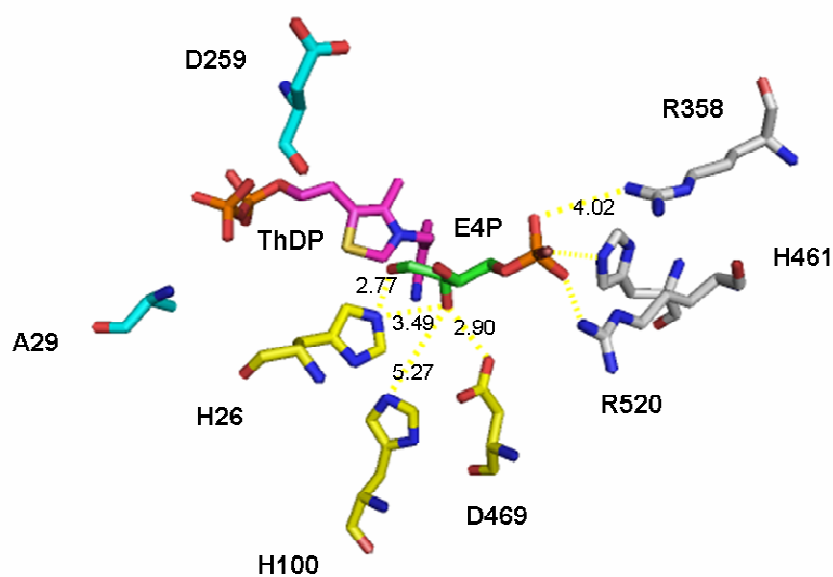
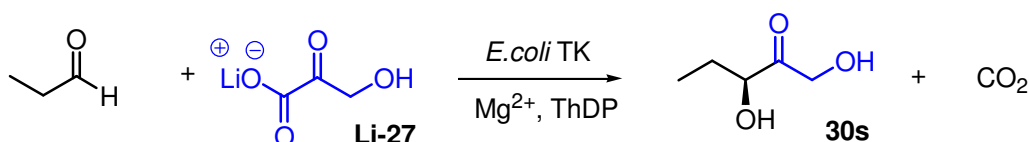


Figure 23: Clustered enzyme mutants responsible for catalysis in the active site of TK using pyMOL (1NGS.pdb, from www.rcsb.org/pdb)

Mutant D469T was selected for further kinetic experiments using purified enzyme, since it showed high activity and gave a significant increase in specificity towards propanal. The kinetics of purified WT and D469T were determined at a 50mM **Li-27** concentration over a range of propanal concentrations, and revealed an 8.9-fold increase in V_m , but a decreased K_M of 2.5-fold for propanal compared to WT-TK (Table 10). This suggests the methyl group on propanal has created specific interactions with the mutated residue that has replaced Asp, which interacts with an α -hydroxyated aldehyde (e.g glycolaldehyde). This was evident by no improvement in activity with D469T towards glycolaldehyde. It was concluded that the variants in the D469 library were most likely to have specific interactions with non- α -hydroxyated aldehydes, favouring side chains with non-polar groups.



Enzyme	V_m (mM min ⁻¹)	K_M (mM)
WT	0.037	140
D469T	0.33	55

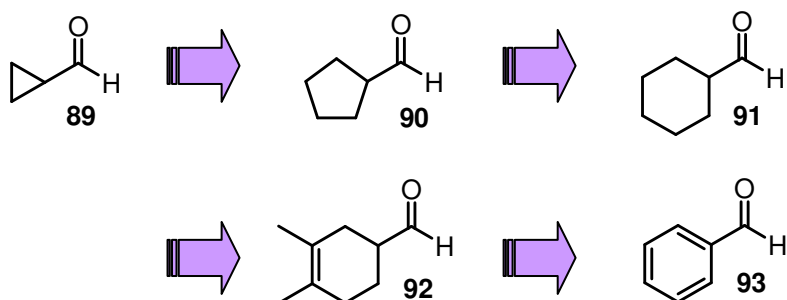
Table 10: Kinetic parameters for WT and D469T-TK

3.1.4 Investigating cyclic aldehydes with evolved TK enzymes

It is of great interest to explore a broad substrate repertoire beyond that currently used with TK. This would lead to the formation of complex α,α' -dihydroxyketones for conversion into other synthons for further structural elaborations including ketosugars and 2-amino-1,3-diols.^{85,99} However, to achieve industrial viability, an important requirement is greater specific enzyme activities and high stereoselectivities on a broad substrate range beyond the current biocatalytic conversion of α -hydroxyaldehydes and aliphatic aldehyde propanal.

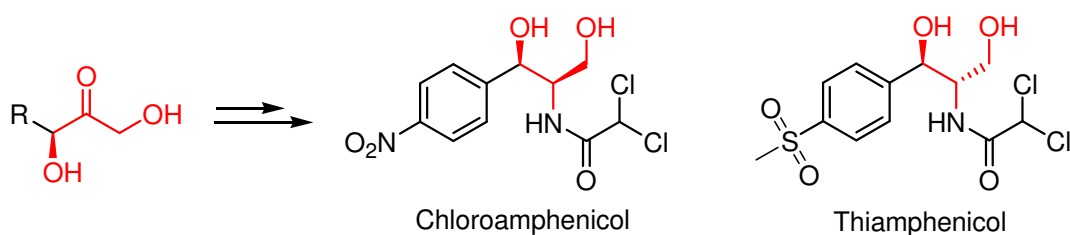
In the literature, there have been few studies using cyclic aliphatic aldehydes as an acceptor molecule with TK. However cyclic aldehydes have been shown to be very poor acceptor substrate molecules. For *E.coli* WT-TK, Turner *et al.* noted the poor relative velocity of cyclohexanecarboxaldehyde C_6 (0.04) in comparison with glycolaldehyde.⁵¹ A systematic study was now carried out with the aim of understanding the tolerance of TK mutants towards cyclic aldehydes, from

cyclopropanecarboxaldehyde **89** to cyclohexanecarboxaldehyde **91**, and then an increase in complexity with 3,4-dimethylcyclohex-3-ene-1-carboxaldehyde **92** and finally an aromatic acceptor substrate **93** (Scheme 40).



Scheme 40: The objectives

Such compounds including aromatic analogues, can be further modified with transaminase enzymes (EC 2.6.1.57) for the direct synthesis of aminodiol antibiotic motifs such as those in the chloramphenicol and thiamphenicol antibiotics (Scheme 41).



Scheme 41: Potential routes to biologically active compounds

3.2 Active mutant Identification with cyclic substrates

The reaction plates of *E.coli* TK mutant library D469 (Fig. 24) obtained by saturation mutagenesis were incubated with **Li-27**, cofactor stock solution (ThDP and magnesium chloride) and cyclopentanecarboxyaldehyde **90** for two days prior to the treatment with the tetrazolium-based colorimetric assay. In analogous, but separate experiments the reaction plates of D469 *E.coli* TK were incubated with cyclopropanecarboxyaldehyde **89** and cyclohexanecarboxyaldehyde **91** as acceptor molecules.

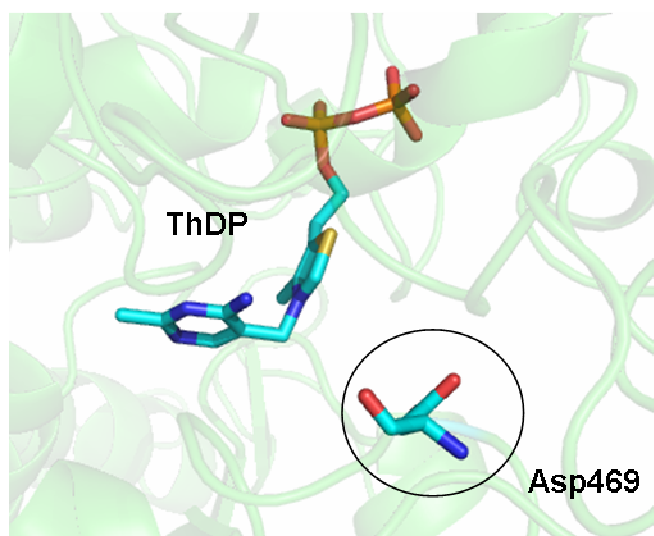


Figure 24: Enzyme active site to *E.coli* TK highlighting position of D469

Each of the 96 well plates was subjected to an MP-Carbonate scavenger resin (Biotage) and was left standing for 3 hours to remove unreacted HPA. The colorimetric assay involved the oxidation of the ketodiol product formed from the biocatalysis, while the colorless tetrazolium salt was reduced resulting in an intense red coloration. The optical densities (OD_{485nm}) from the D469 libraries displayed good activities with no inactive mutants generated (Fig. 26). The variants selected were based on the consistent high performing wells towards **89**, **90**, and **91** aldehydes (Fig. 25). The wells B6, B7, D5, E3, F12, G6, and H4 were investigated further on a preparative scale.

The bioconversion of cyclic aliphatic substrates with TK mutants

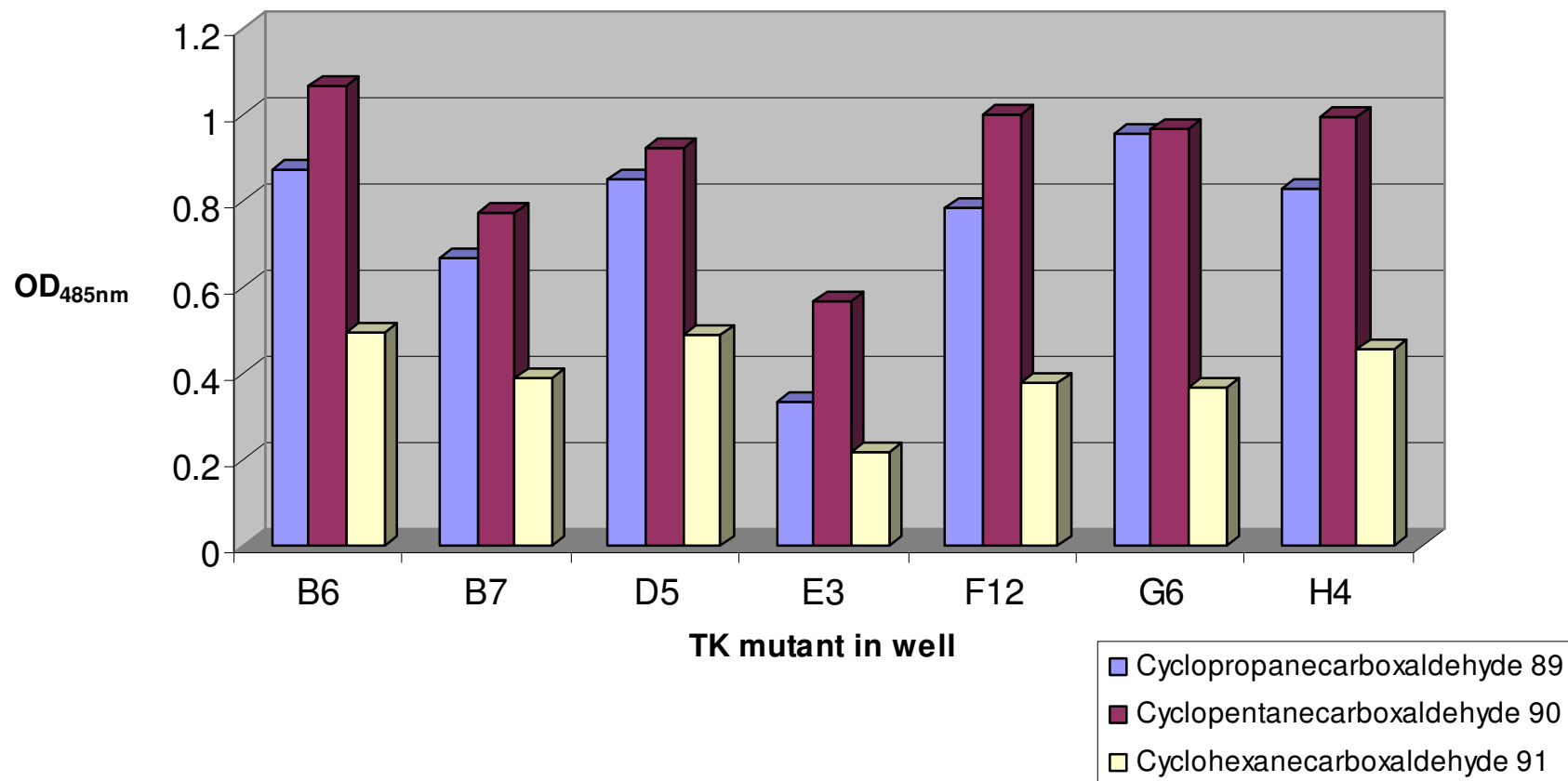


Figure 25: ODs of selected D469 *E.coli* TK with substrates 89, 90, 91

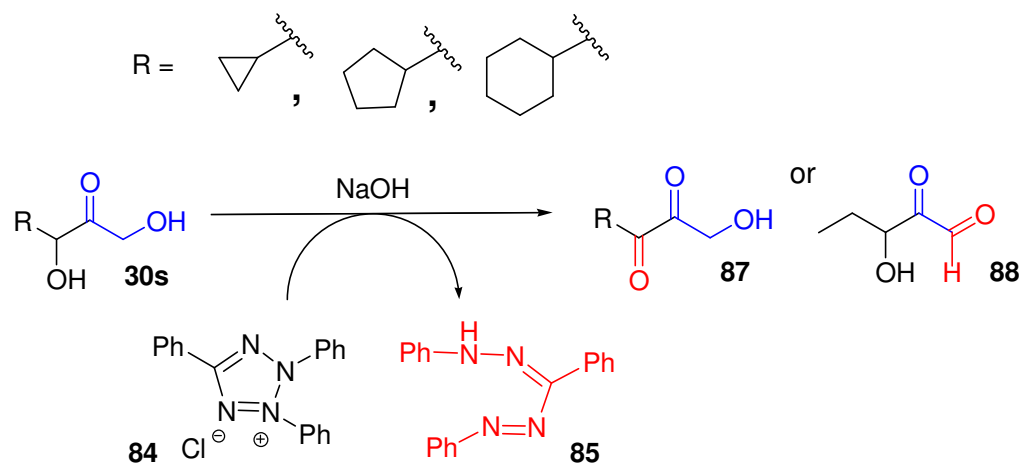
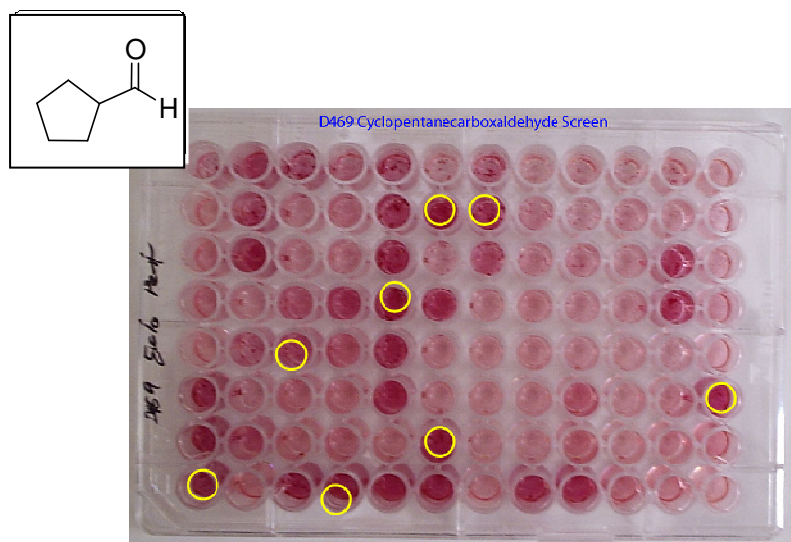
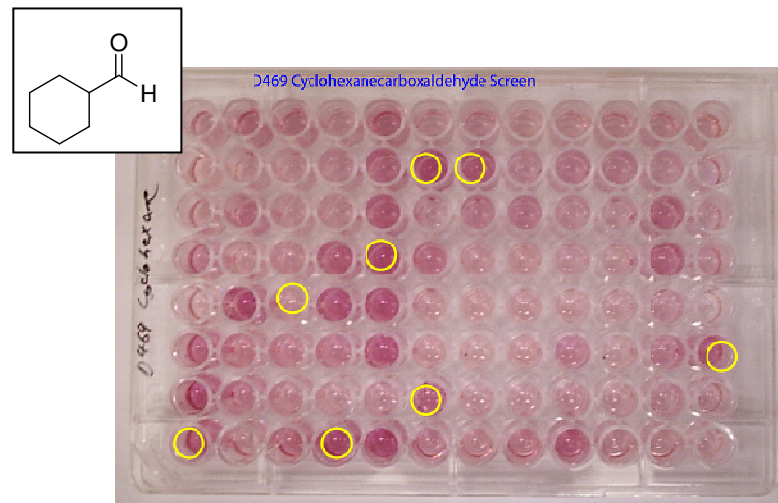
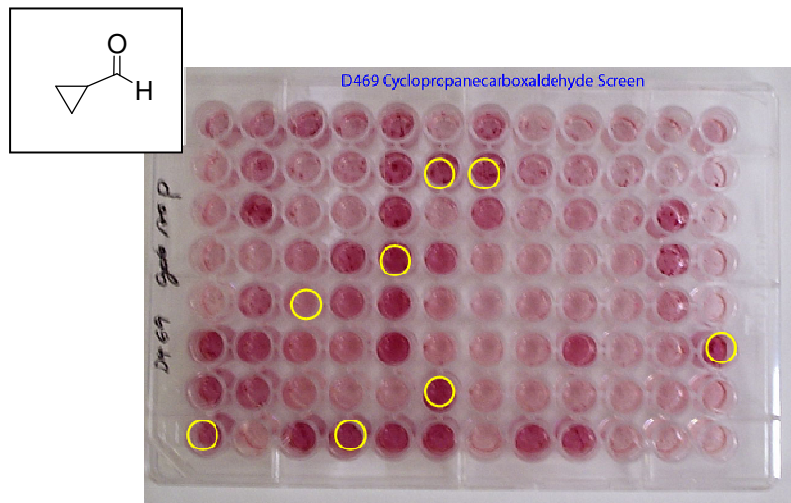


Figure 26: Colorimetric plates screened against the cyclic aldehydes

3.3 Obtaining *E. coli* TK cell-free lysates

Some of the D469 wells described above showing good conversions to products contained mutants that had previously been sequenced (Hibbert *et al.*)⁹⁰ including the mutants identified with improved activity towards propanal; D469T and D469E. Biocatalytic reactions using the D469T and D469E were explored further at a 50 mM concentration, obtaining preparative quantities to determine the stereochemistry of the ketodiol product generated. Colonies were therefore picked from wells of the master plate and were streaked onto Luria-Bertani (LB) agar plates. The individual colonies were selected and grown in LB for 12 hours and then the 50 ml innoculum was transferred to further LB broth, and was incubated for 8 hours. Some culture was left aside for glycerol stocks. The supernatant was discarded and approximately 0.1 g of cell pellet was afforded from 50 ml of innoculum. The cell pellet was resuspended in sodium phosphate buffer (10 ml for 1 g), the suspension was sonicated on ice and the crude lysate centrifuged, then the clarified lysate was pipetted into Eppendorf flasks and was stored at -20°C. The TK protein concentration in lysates was determined using SDS-PAGE (fraction of the total protein which is TK) and the Bradford assay (total protein concentration) performed by Phattaraporn Morris (Fig. 27, Table 11).

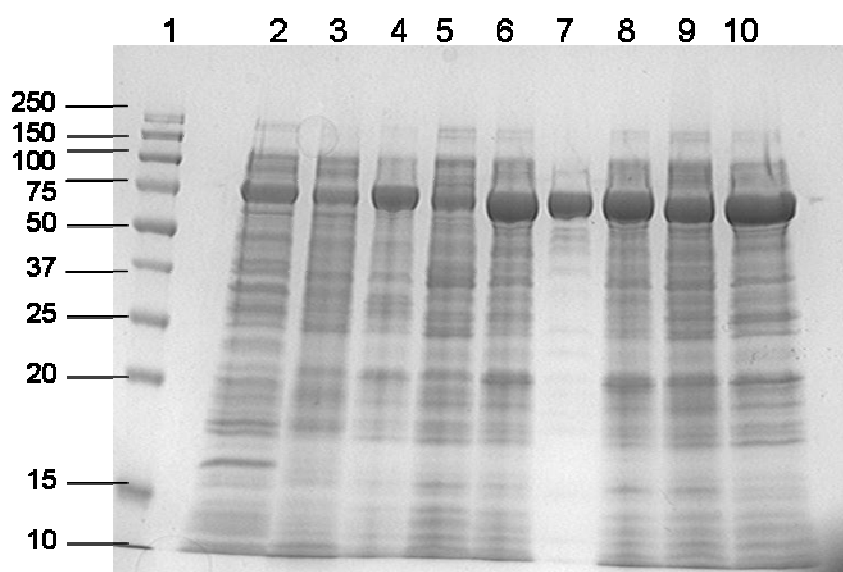


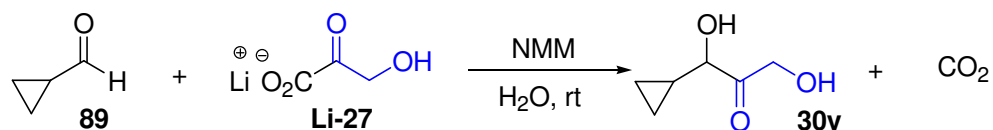
Figure 27: Top view of a 7.5% SDS-page gel of TK variants, WT-TK, and purified TK. The enzyme was purified using a XK 16/20 chromatographic column. The dark band represents the denatured TK protein monomer at 75kDa. The samples are as follows: (1) Protein standard marker; (2) WT; (3) D469L; (4) H4; (5) H26Y; (6) D469T; (7) Purified TK; (8) D469E; (9) D469S; (10) G6

Enzyme	TK [mg ml ⁻¹]
WT	0.24
D468L	0.20
H4	0.32
H26Y	0.22
D469T	0.30
D469E	0.30
D469S	0.30
G6	0.32

Table 11: The calculated TK protein concentration in lysates

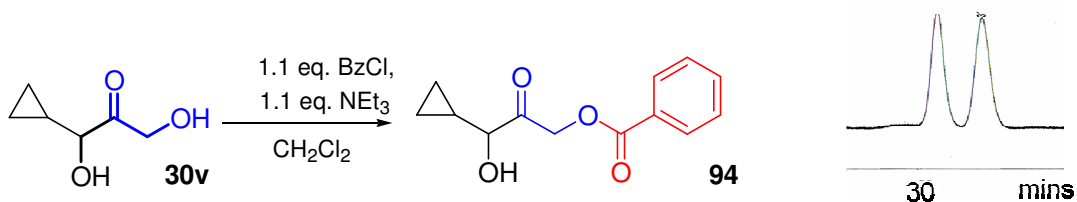
3.4 Cyclopropanecarboxaldehyde as an acceptor substrate for the TK reaction

The biomimetic TK reaction with cyclopropanecarboxaldehyde **89** was conducted in a THF:H₂O (1:1) solution in the presence of **Li-27** and *N*-methylmorpholine (NMM) used as a catalyst to afford the ketodiol product **30v** in 12% yield. The isolated racemic ketodiol was purified using silica gel chromatography and **30v** was used as a standard reference in reactions to assess the stereoselectivity of the biotransformations using HPLC.



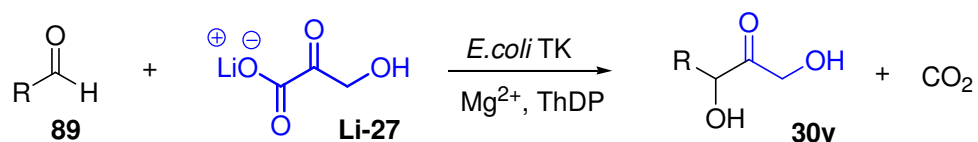
Scheme 42: The biomimetic formation of **30v**

The ketodiol product was derivatised to the UV active monobenzoate, using triethylamine and benzoyl chloride, to generate **94** with 87% yield (Scheme 43). A 10 μ l benzoylated ketodiol sample was injected in a chiralpak-AD column at varying flow rates from 0.8-1.2 ml min⁻¹ and eluting at different isochratic solvent systems using hexane (95-99%): isopropanol (5-1%) concentrations. The sample was detected but not separable using the chiralpak-AD column. However, successful separation of the racemic products was discovered using a chiralpak-OD column eluting at hexane:isopropanol (97:3) and a concentration of 1 ml min⁻¹ with peaks detected at 33.2 mins and 34.9 mins with equal integrations (Scheme 43).



Scheme 43: Benzoylation of 30v and HPLC data of 94

In separate, but comparable biotransformations, the selected TK mutants from the D469 library exhibiting high enzyme activity from the colorimetric assay were all used at a 50 mM reaction mixture with **89**, stated to pH 7.0 and left to stir for 48 hours. The ketodiols products **30v** were purified via silica gel chromatography. The TK variants D469L, D469K and G6 used in the bioconversions afforded poor yields 1-10% comparable to WT-TK. The TK mutant H26Y exhibited no activity against this substrate. However TK mutants D469T, D469E and H4 revealed some substrate activity with better yields in comparison to other TK variants under investigation.



R	D469E %	D469T %	D469K %	D469L %	G6 %	H4 %	H26Y %	WT-TK %
	10	10	2	2	1	10	nr	2

Table 12: The percentage yields obtained from acceptor substrate 89

The products from the TK mutant biotransformations were monobenzoylated **94** and the ees were determined from the established HPLC procedure compared to WT-TK (Fig. 28).

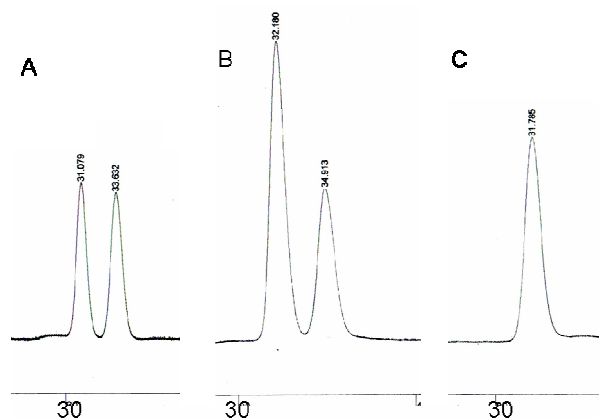


Figure 28: (A) racemate 94; (B) D469T product with added racemate; (C) D469T product

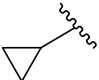
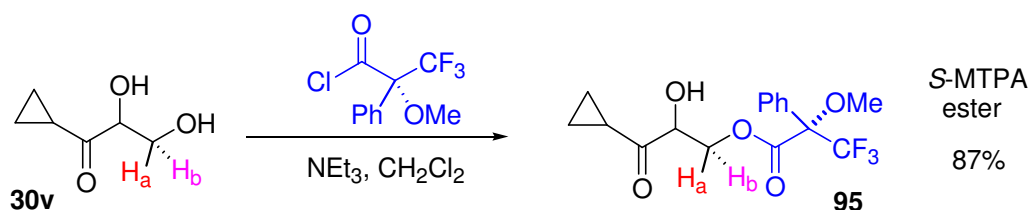
R	D469E	D469T	D469K	D469L	G6	H4	H26Y	WT-TK
	ee%	ee%	ee%	ee%	ee%	ee%	ee%	ee%
	>99	99	99	99	99	99	nr	72

Table 13: The *ees* obtained from selected D469 mutants of **30v**

The absolute stereochemistry of the product **30v** was determined by coupling the terminal hydroxyl group of **30v** with an (*R*)-MTPA-Cl generating the (*S*)-MTPA ester **95** (Scheme 44).



Scheme 44: Formation of the (*S*)-MTPA ester **95**

The AB splitting pattern is observed from diastereotopic protons H_a and H_b of the (*S*)-MTPA ester **95**. The major isomer (*2S,3S*) resonated at δ_H 5.37 ppm and 4.95 ppm with a chemical shift difference $\Delta\delta_H^{2S,3S}$ of 0.42 with trace amounts of the minor isomer at δ_H 5.17 ppm and 5.05 ppm ($\Delta\delta_H^{2S,3R}$ is 0.12). A recent procedure to assign the absolute stereochemistry at C3 of α,α' -dihydroxyketones (see previous chapter),¹⁰⁰ established that the chemical shift patterns of the diastereotopic protons, derivatised as Mosher's esters, varied such that $\Delta\delta_H^{2S,3S} > \Delta\delta_H^{2S,3R}$. This indicated that the stereochemistry at C3, formed by D469T, had the (*3S*)-configuration (Fig. 29).

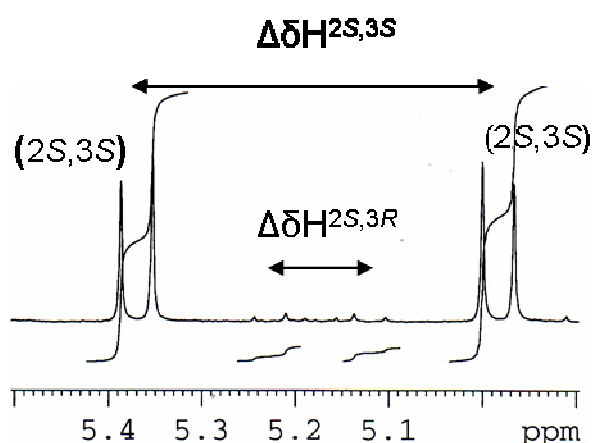


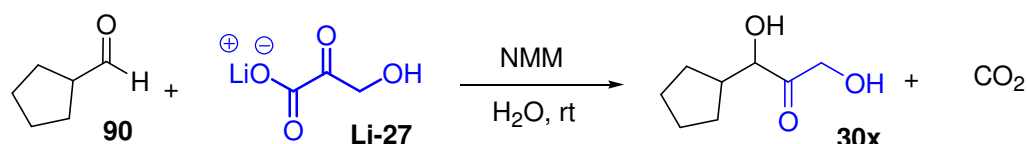
Figure 29: ¹H NMR region 5.0 to 5.5 ppm of (*S*)-MTPA ester **95**

The D469E TK mutant was selected for biocatalysis with cyclopropanecarboxaldehyde **89**, due to the high yielding (70%) and excellent *ees* (88%) obtained using propanal as substrate.⁸⁷ The structural differences between propanal and cyclopropane-

carboxyaldehyde affect the substrate activity of TK. The non-cyclic aldehyde, can freely move between side chains and enter the active site for catalysis. However the cyclopropane structure may have more limited access to the acceptor binding site and conformational restrictions which could account for the low yield with high ees are obtained.

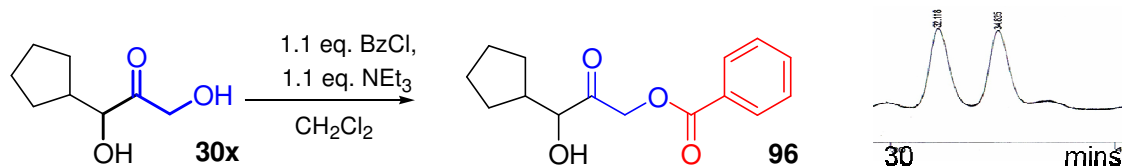
3.5 Cyclopentanecarboxaldehyde as an acceptor substrate for the TK reaction

The biomimetic reaction with cyclopentanecarboxaldehyde **90** was performed in water in the presence of **Li-27** and *N*-methylmorpholine used as a catalyst and adjusted to pH 8.0 to afford the ketodiol product **30x** in 20% yield. However, the reaction became slower when adjusted to pH 7.0 with less isolated product (5%) after 48 hours (Scheme 45).



Scheme 45: Biomimetic formation of **30x**

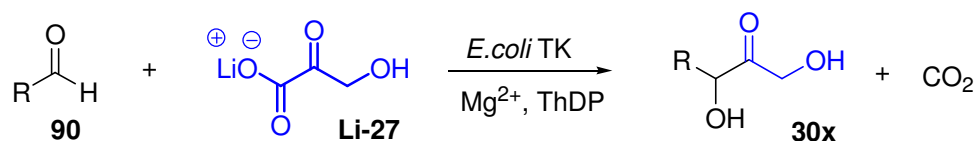
The ketodiol was then derivatised to the UV active benzoate, using benzoyl chloride and triethylamine as before. Only the monobenzoylated product **96** was obtained, probably due to steric hindrance preventing the benzylation at the secondary alcohol (Scheme 46). A 10 μ l benzoylated ketodiol sample analysed as with **94** using a chiralpak-AD column at varying flow rates from 0.8-1.2 ml min⁻¹ and eluting at different isochratic solvent system using hexane (95-99%): isopropanol (5-1%) concentrations. The sample was detected, but not separable using the chiralpak-AD column. However, the racemic mixture was detected and successfully separated using a chiralpak-OD column eluting at hexane:isopropanol (97:3) concentration at 1 ml min⁻¹ with peaks detected at 32.1 mins and 34.8 mins with equal integrations (Scheme 46).



Scheme 46: Benzoylation of **30x** and HPLC data of **96**

The selected TK mutants (D469E, D469T, D469K, D469L, G6, H4 and H26Y) were prepared as before and the biotransformations performed with **90** at pH 7.0 for 48 hours. The biotransformation reaction was monitored by TLC analysis and the product purified using silica gel chromatography. TK mutants D469E and D469T when used

with **90** have obtained **30x** in isolated yields of 40% and 30% respectively. Poor substrate activity was revealed for WT-TK and H26Y, whilst D469L afforded no product after 48 hours (Table 14).



R	D469E	D469T	D469K	D469L	G6	H4	H26Y	WT-TK
	%	%	%	%	%	%	%	%
	40	30	10	nr	10	10	2	2

Table 14: The percentage yields obtained from acceptor substrate **90**

Products from the TK mutant biotransformations were monobenzoylated and the *ees* were determined from the established HPLC procedure described above. The D469 TK mutants selected for biotransformations exhibited excellent *ees* compared to the racemic mixture obtained from WT-TK (Fig. 30). Mutant H26Y afforded the opposite isomer than the mutants from the D469 TK library.

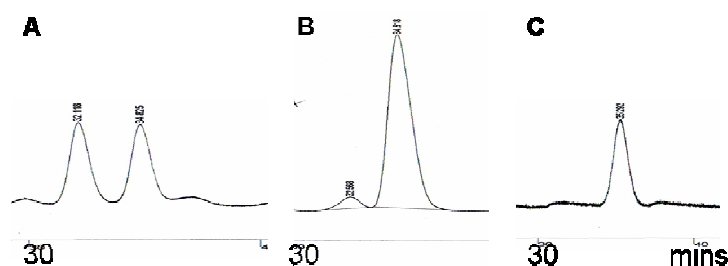
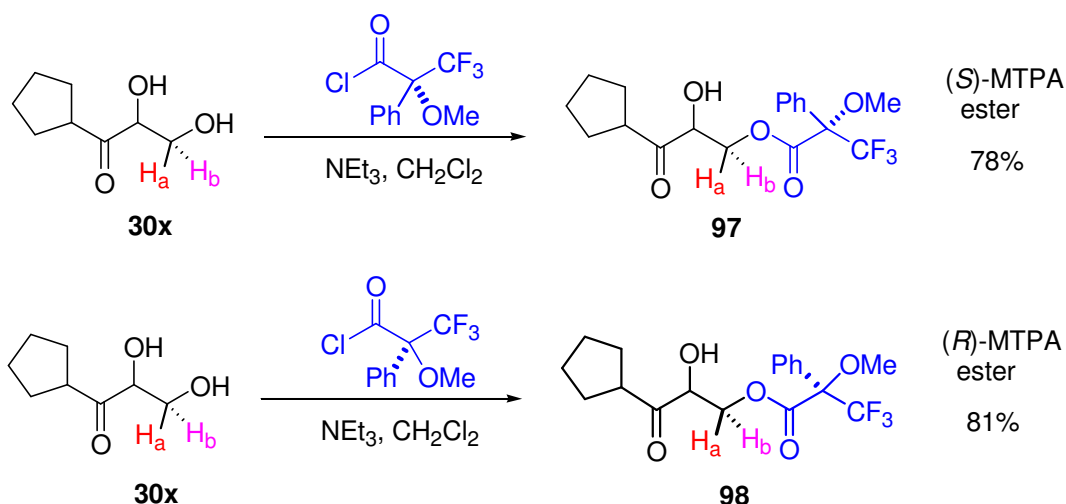


Figure 30: (A) racemate of **96**; (B) D469T product with added racemate **96**; (C) D469T product

R	D469E	D469T	D469K	D469L	G6	H4	H26Y	D469WT
	<i>ee</i> %	<i>ee</i> %	<i>ee</i> %	<i>ee</i> %	<i>ee</i> %	<i>ee</i> %	<i>ee</i> %	<i>ee</i> %
	>99	99	25	nr	99	99	30	0

Table 15: The *ees* obtained from selected D469 mutants of **30x**

The absolute stereochemistry of **30x** was examined, in separate but comparable reactions coupling the terminal hydroxyl group of **30x** with (*R*)-MTPA-Cl and (*S*)-MTPA-Cl in presence of triethylamine generating an (*S*)-MTPA ester **97** and (*R*)-MTPA ester **98** respectively (Scheme 47).



Scheme 47: Formation of (*S*)-MTPA and (*R*)-MTPA ester, **97** and **98**

In racemic ketodiol **30x**, the (*S*)- and (*R*)-MTPA esters exhibited comparable splitting patterns (Fig. 31, B). In the (*S*)-MTPA ester **97**, the major isomer (*2S,3S*) resonated at δ_{H} 5.21 ppm and 4.93 ppm with a chemical shift difference $\Delta\delta_{\text{H}}^{2\text{S},3\text{S}}$ of 0.28 with no (*2R,3S*) isomer present (Fig. 31, A). In the (*R*)-MTPA ester **98**, the major isomer (*2S,3R*) resonates at δ_{H} 5.08 ppm and 5.05 ppm with a chemical shift difference $\Delta\delta_{\text{H}}^{2\text{S},3\text{S}}$ of 0.03 with no (*2R,3R*) isomer present (Fig. 31,C). The assignment of the absolute stereochemistry at C3 of α,α' -dihydroxyketones (see previous chapter),¹⁰⁰ established that the chemical shift patterns of the diastereotopic protons, derivatised as Mosher's esters, varied such that $\Delta\delta_{\text{H}}^{2\text{R},3\text{R}}$ and $\Delta\delta_{\text{H}}^{2\text{S},3\text{S}} > \Delta\delta_{\text{H}}^{2\text{S},3\text{R}}$ and $\Delta\delta_{\text{H}}^{2\text{R},3\text{S}}$. This indicated that the stereochemistry at C3 in **97**, formed by D469T, had the (*3S*)-configuration (Fig. 31).

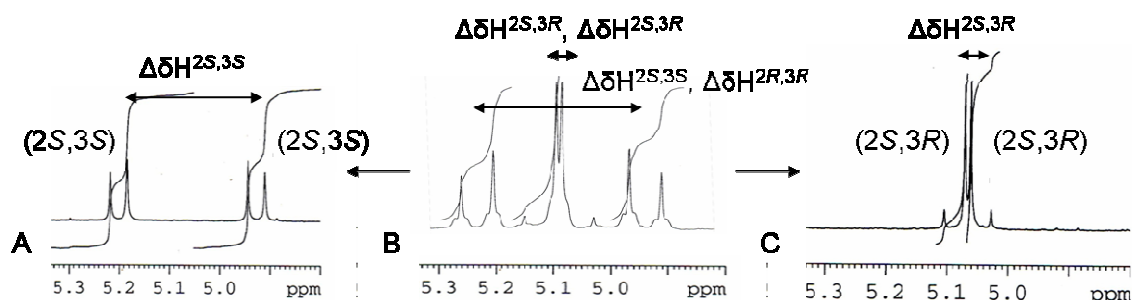


Figure 31: (A) SMTPA ester of D469T (B) racemic (*S*)-, (*R*)-MTPA esters, (C) (*R*)-MTPA ester D469T

The modified Mosher's method also revealed from the ^1H NMR integration of H_a and H_b of the D469T mutant product the ee was >99% which was comparable to the data via HPLC. Hence the D469 TK mutants assessed were stereoselective for the (*S*)-configuration.

The rationale for the generally higher yields (30-40%) for D469T and D469E mutants with cyclopentanecarboxaldehyde **30x** in comparison to cyclopropane **30v** (10%) is

presumably due to the ring size. The cyclopentane ring bears a resemblance to the natural substrate ribose-5-phosphate **RP5** (furanose form) which enters deep in the enzyme cleft that lies in close proximity to ThDP and Asp469 for catalysis to occur (Fig.32).

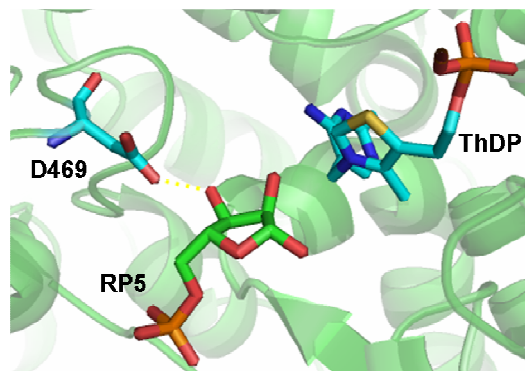
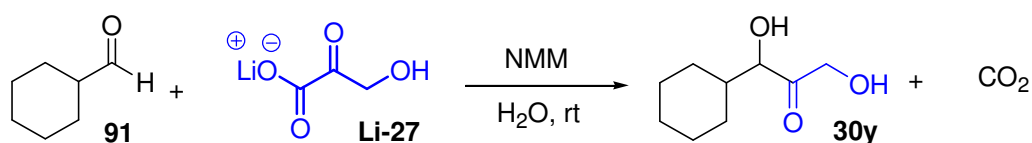


Figure 32: RP5 furanose form in enzyme active site with ThDP

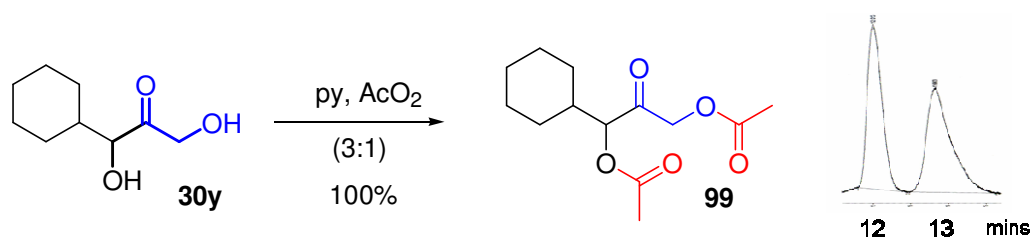
3.6 Cyclohexanecarboxaldehyde as an acceptor substrate for the TK reaction

Preliminary investigations on the TK biomimetic reaction involved reactions with stoichiometric amounts of cyclohexanecarboxaldehyde **91**, *N*-methylmorpholine and **Li-27** in aqueous media at room temperature to afford ketodiol product in 25% yield. The reaction has since improved in yield (50%) with cases of stereoselectivity introduced in ketodiol product formation (Chapter 5). The racemic ketodiol was purified from the reaction mixture using silica gel eluted with 1:1 EtOAc:hexane. The readily generated **30y** was used as a standard reference for product identification on TLC and stereoselectivity of the biotransformations using HPLC (Scheme 48).



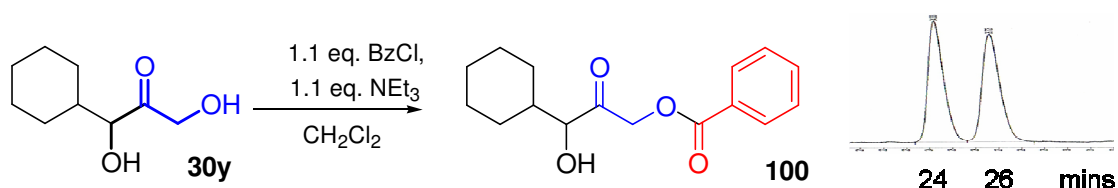
Scheme 48: Biomimetic formation of ketodiol **30y**

Initially the hydroxyl groups were acetylated using a pyridine: acetic anhydride (3:1) mixture followed by an acid/base work up to afford quantitative yields of **99** (Scheme 49). A 20 μl acetylated ketodiol sample was analysed using a chiralpak-AD column at a 1 ml min^{-1} flow rate eluting with a hexane:isopropanol (98:2) isochratic solvent system. The isomers were detected and separated at 12.0 mins and 13.6 mins with equal integrations. However, separation of the isomers was not consistent and the acetylated esters were not readily detected with diluted samples.



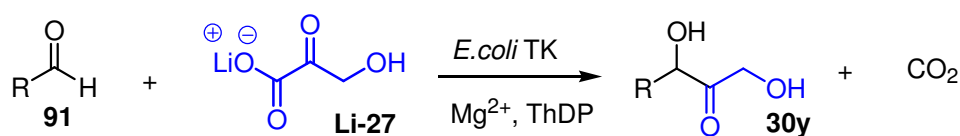
Scheme 49: Acetylation of ketodiol 30y

The ketodiol, was then derivatised as the monobenzoate for better detection under UV. The benzoylated product was purified and analysed by HPLC using a chirapak-OD column. The mono- benzoylated product **100** exhibited clear separations of the isomers; using an isochratic solvent system; hexane: isopropanol (97:3) concentration, at a flow rate of 1.0 ml min⁻¹ (Scheme 50).



Scheme 50: Benzoylation of ketodiol 30y

The TK mutants selected were used with **91** as previously described for **89** and **90** and the product **30y** was isolated in each case by silica chromatography. The D469 TK mutants all revealed some substrate activity with D469E exhibiting the highest conversion yields. Poor substrate activity was revealed for WT-TK and mutants D469K, and D469T, whilst D469L and H26Y afforded no product after 48 hours (Table 16).



R	D469E	D469T	D469K	D469L	G6	H4	H26Y	D469WT
	%	%	%	%	%	%	%	%
	10	3	3	nr	4	4	nr	1

Table 16: The percentage yields of ketodiol product 30y

The products from the TK mutant biotransformations, were monobenzoated and the ees were determined from the established HPLC procedure previously mentioned (Fig. 33). Excellent ees were observed compared to the racemic mixture formed with WT-TK (Table 17).

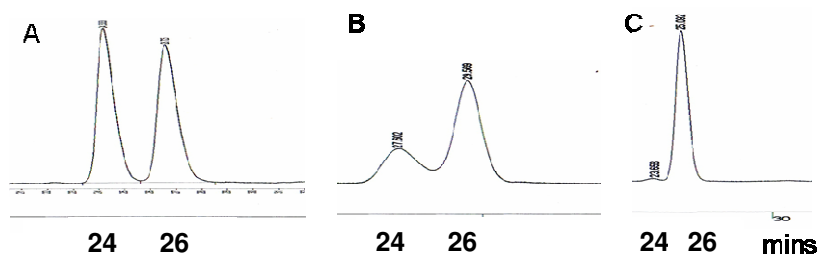
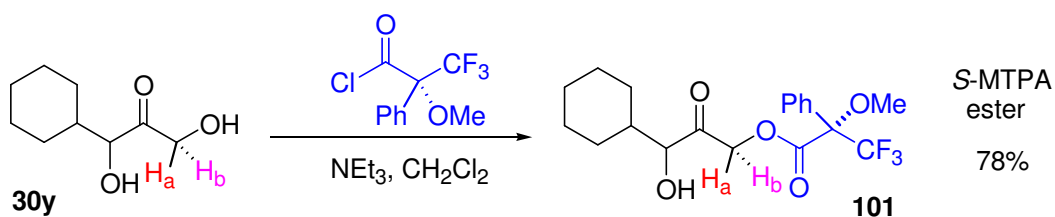


Figure 33: (A) racemate **30y**; (B) D469T product with added racemate **30y**; (C) D469T product

R	D469E <i>ee</i> %	D469T <i>ee</i> %	D469K <i>ee</i> %	D469L <i>ee</i> %	G6 <i>ee</i> %	H4 <i>ee</i> %	H26Y <i>ee</i> %	D469WT <i>ee</i> %
	97	99	25	nr	99	99	nr	0

Table 17: The *ees* obtained from selected D469 mutants of **30y**

The absolute stereochemistry of the biosynthesised product **30y** from D469E was determined by coupling the terminal hydroxyl group of **30y** with an (*R*)-MTPA-Cl generating an (*S*)-MTPA ester (Scheme 51).



Scheme 51 Formation of the (*S*)-MTPA ester **101**

As previously, the major isomer (*2S,3S*) resonated at δ_{H} 5.19 ppm and 4.90 ppm with a chemical shift difference $\Delta\delta_{\text{H}}^{2\text{S},3\text{S}}$ of 0.29 with trace amounts of minor isomer. This indicated stereochemistry at C3, formed by D469T, was the (*3S*)-configuration (Fig. 34).

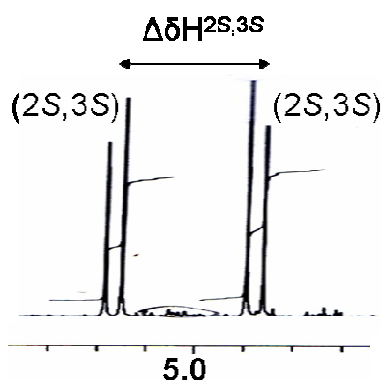


Figure 34: ^1H NMR of H_a H_b from **101**

The rationale behind the low yields exhibited using cyclohexanecarboxaldehyde as a substrate is presumably due to the large cyclohexane ring which does not readily enter the narrow enzyme cleft to reach the enzyme active site. The generally high *k_{es}* revealed by the TK mutants in comparison to WT-TK is presumably due to the restricted conformations and orientations of the cyclohexane ring in the TK mutant active sites.

3.7 Initial relative rates of D469T

Due to the high stereoselectivity of D469T with the cyclic aldehydes, the initial relative rates were determined and relative velocities were compared to the comparable data for propanal (Table 18). The D469T-TK mutant has previously been shown to have an 8.5-fold specificity towards propanal over that of glycolaldehyde when compared to WT-TK. However D469T with cyclic aldehydes gave lower specific substrate activities in relation to propanal. Furthermore, as the ring size increased the substrate specific activity decreased. This may be a result of restricted orientation exhibited by the cyclic rings which increases with ring size. The D469T TK mutant was shown to have an 0.4 fold relative activity towards cyclopentanecarboxaldehyde **90** as substrate with a higher yield obtained in comparison to lower yielding cyclopropane-carboxaldehyde **89** exhibiting a 0.6 fold relative activity. The differences in substrate activity are possibly due to product inhibition.

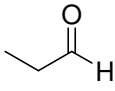
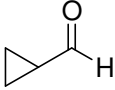
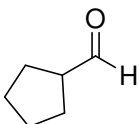
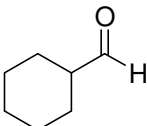
Aldehyde	Mutant	Initial rate [mM h ⁻¹]	TK (mg ml ⁻¹)	Spec. activity (mmol mg ⁻¹ min ⁻¹)	Initial rel. rate
	D469T	12.52	0.3	0.70	1
	D469T	7.45	0.3	0.41	0.6
	D469T	4.47	0.3	0.25	0.4
	D469T	3.46	0.3	0.19	0.3

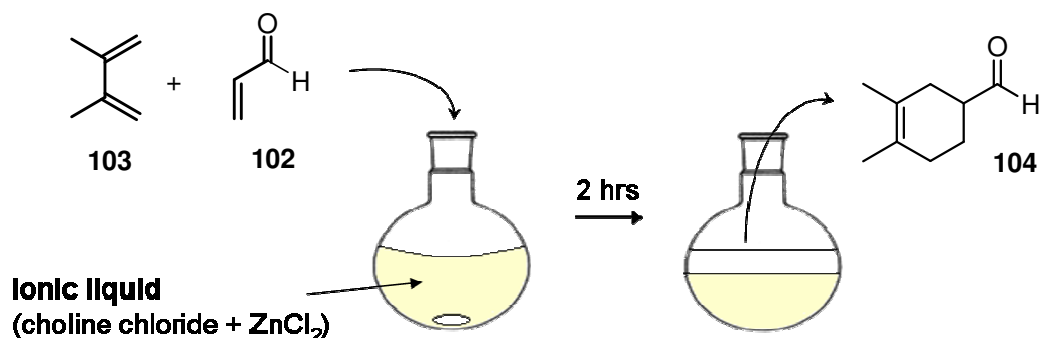
Table 18: The kinetic kinetic data obtained for D469T on various acceptor substrates obtained by the colorimetric assay

3.8 Synthesis of 3,4-dimethyl-3-cyclohexene-1-carboxaldehyde and the formation of the ketodiol product

The use of novel substrates, including bulky, and hydrophobic moieties with diverse functional groups for further chemical modification would enhance the synthetic applications of TK. This rationale led to the use of a Diels-Alder cyclic adduct 3,4-dimethyl-3-cyclohexene-1-carboxaldehyde, that differs slightly from previous cyclic aliphatic aldehydes investigated due to the presence of an unsaturated bond and two methyl groups on the cyclohexene ring. This aldehyde was selected as a representative cycloaddition precursor.

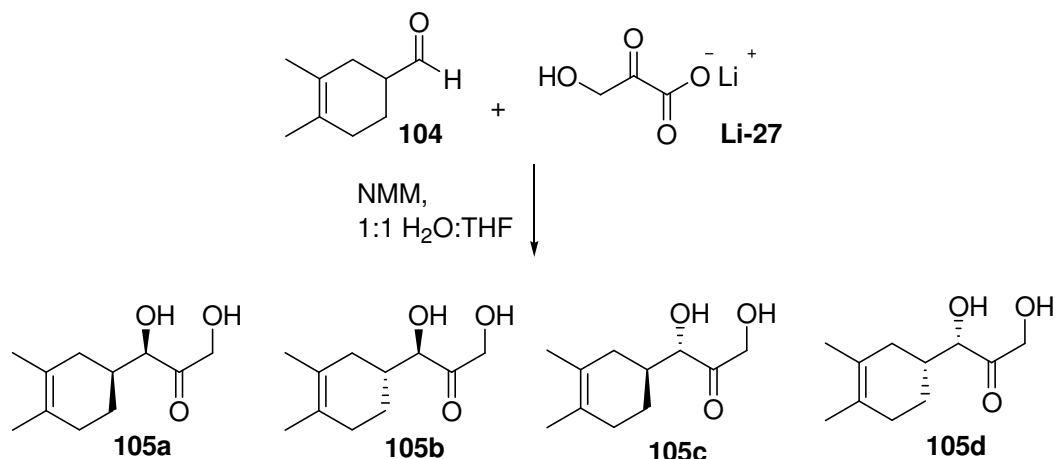
The aldehyde 3,4-dimethyl-3-cyclohexene-1-carboxaldehyde **104** was synthesized from a Diels-Alder reaction in a Lewis acid ionic liquid containing choline chloride and zinc chloride (1:2). The added benefits of this reaction are; the ionic liquid is not moisture sensitive and the reaction has a short reaction time at an ambient temperature.¹⁰¹ The ionic liquid was formed by heating the choline chloride and Zinc Chloride to approximately 150 °C and was left to stir until a colourless melt was obtained which was then cooled to a viscous liquid. The addition of water was essential to reduce the viscosity of the ionic liquid, so the reaction can be stirred magnetically. It also highlighted that the ionic liquid has not declined in catalytic efficacy with traces of water present.

Acrolein **102** and 2,3-dimethylbutadiene **103** were then added to the magnetically stirred ionic liquid at 26 °C for 2 h. The reaction mixture was left to stand, then product decanted off and the ionic liquid washed with hexane which was evaporated. This afforded aldehyde **104** in an 85% yield (Scheme 52).¹⁰² The recyclability of the viscous ionic liquid was also explored by the addition of water (≈ 0.5 ml) and the reactions were repeated generating comparable yields of **104** (82%).



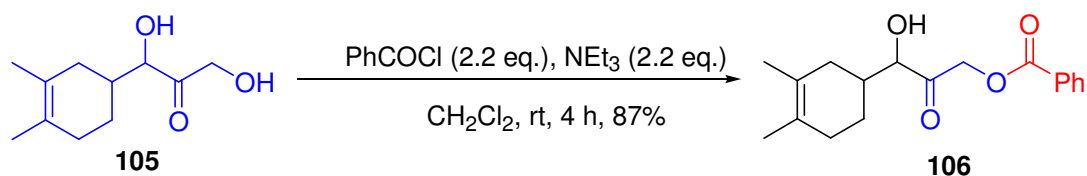
Scheme 52: Formation of aldehyde **104** via ionic liquid

The biomimetic TK reaction was performed using a THF:H₂O (1:1) reaction mixture adjusted to pH 7.0, and stoichiometric amounts of aldehyde **104**, *N*-methylmorpholine (NMM) and **Li-27** to prepare ketodiol product **105(a-d)** as a four diastereomeric mixture in 10% yield. The yield marginally increased to 15% when the THF:H₂O reaction mixture was not adjusted to pH 7.0 during the course of the reaction (Scheme 53).



Scheme 53: Biomimetic reaction of aldehyde 104

The ketodiol mixture was derivatised, to form the UV detectable benzoates, using benzoyl chloride and triethylamine again, only the mono-benzoylated product **106** at the primary alcohol position was obtained (Scheme 54).



Scheme 54: Benzoylation of ketodiol 105

A 10 μ l benzoylated ketodiol sample was analysed using a chiralpak-AD column at varying flow rates from 0.8-1.2 ml min⁻¹ and eluting at different isocratic solvent system using hexane (90-99%): isopropanol (10-1%) concentrations. The four isomers were detected at 28.6 min, 30.8 min, 34.0 min, and 43.1 min with equal integrations under isocratic conditions using isopropanol (3%) as the polar stationary phase and hexane (97%) as the non-polar mobile phase with a 0.8 ml min⁻¹ flow rate (Fig. 35).

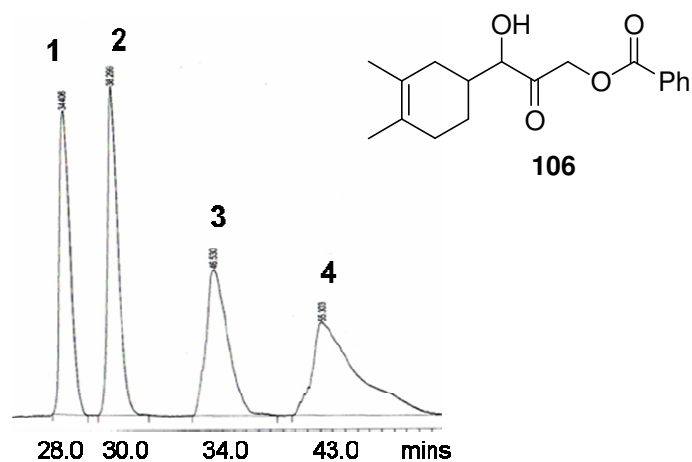


Figure 35: HPLC trace of 4 isomers of 106

3.9 The colorimetric screening of library D469 with aldehyde 104

A high-throughput colorimetric screening using tetrazolium red was used to detect formation of the product in the bioconversion. Lydia Crago (UCL Biochemical Engineering) performed the colorimetric assay, screening the D469 library with acceptor substrate **104** (Fig. 36).

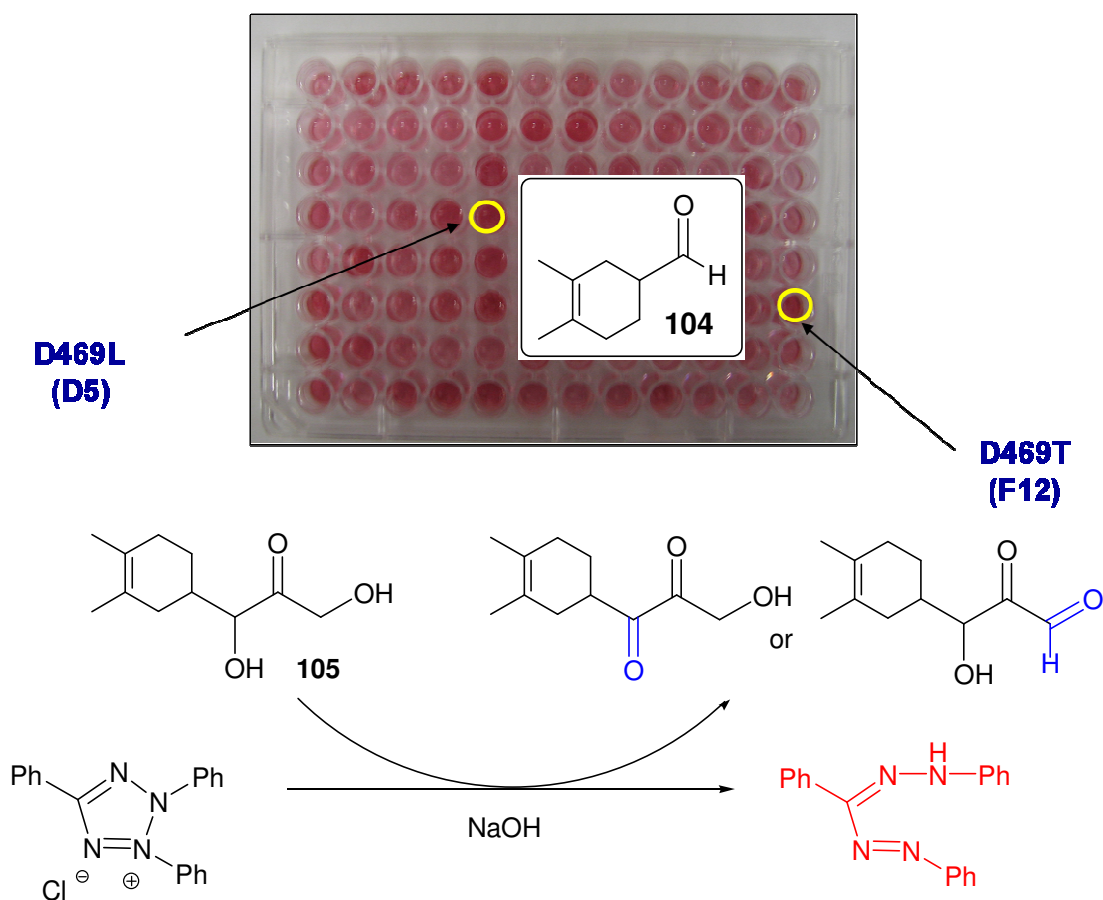


Figure 36: Colorimetric assay on D469 library with aldehyde 104

The investigation led to 5 mutants (wells B6, B7, D5, F1 and F12) that were identified with good activities against **104**. These mutants were sequenced and further examined for accurate expression levels of the protein (Table 19).¹⁰³

Well Number	Mutant	Relative Activity ^{a,b} (D469T = 1)	TK expressed (% total protein)
WT	D469	0	31
F12	D469T	1	33
B6	D469K	0.82	35
B7	D469S	0.81	32
F1	D469T	0.79	19
D5	D469L	0.76	25

Table 19: The relative activities and total expressed protein of D469 TK mutants

Two strains of D469T were identified from wells F12 and F1, however the greater overall expression, cell growth and activity in well F12 was selected for further work. A TLC plate was taken to visualise the ketodiol product formation using D469T TK in comparison to the poor substrate accepting WT-TK enzyme (Fig. 37). The TLC analysis was also used to confirm product conversion with the mutant demonstrating activity against **104**.

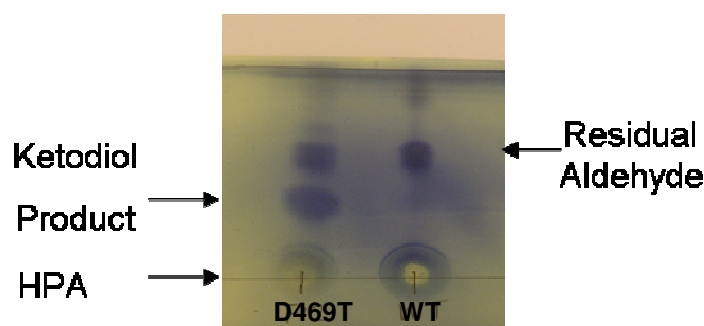
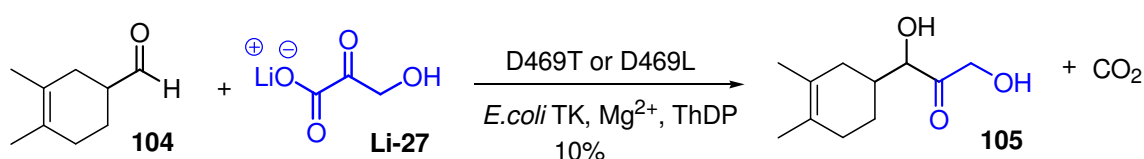


Figure 37: Comparison of WT-TK and D469T-TK mutant by TLC

3.10 Aldehyde acceptor **104** as acceptor substrate for the TK reaction

In separate, but analogous biotransformations, D469T and D469L were used in 50 mM reaction mixtures with aldehyde **104**, at pH 7.0 and 48 hours, affording 10% yields of **105** in both cases (Scheme 55).



Scheme 55: The biotransformation of **104 and Li-27 to generate ketodiol **105****

The products from the TK mutant biotransformations, were monobenzoylelated and the absolute stereochemistry was determined from the established HPLC procedure previously mentioned. The D469T and D469L TK mutants selected were highly diastereoselective in nature, for the same major diastereomer with traces of the remaining 3 isomers formed (Fig. 38, peak 3). Preparative-scale biotransformation using mutants D469T⁹¹ and D469L proved to have the most interesting enantioselective and were further explored, however since D469T was more active than D469L, the determination of absolute stereochemistry and kinetic analyses was carried out with D469T (Fig. 38).

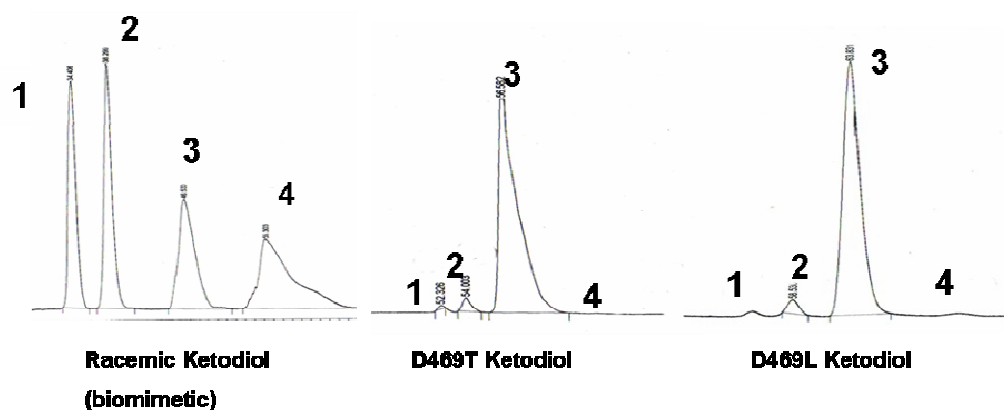
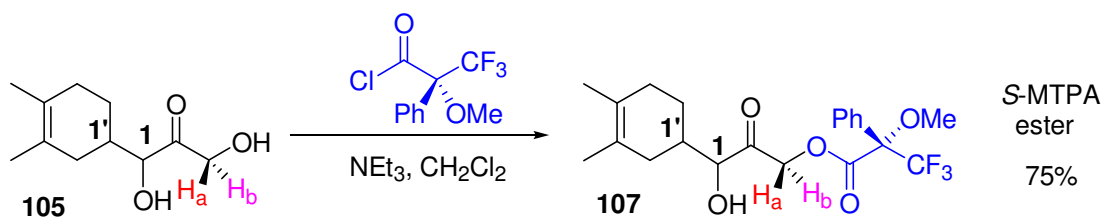


Figure 38: HPLC traces of monobenzoylelated products 105

The absolute configuration and enantioselectivity of D469T TK was determined *via* preparation of the 1'*R*-aldehyde (*R*)-**104** and the recently developed modified Mosher's acid method. To determine the stereochemistry at the C1 position, the biotransformation product **105** from the reaction using the D469T was reacted with (*R*)-MTPA-Cl to form the (*S*)-MTPA ester **107** at the primary alcohol (Scheme 56).



Scheme 56: Formation of (*S*)-MTPA ester 107

Following the modified Mosher's method the stereochemistry at C1, formed by D469T, was assigned the *S*-configuration (1*S*) (Fig. 39).

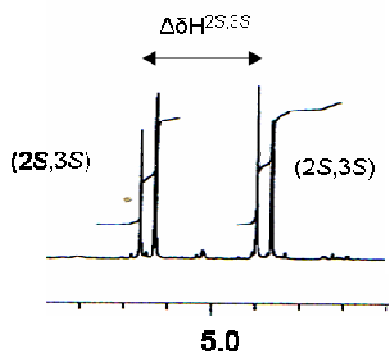


Figure 39: ^1H NMR spectra of H_a and H_b of **107**

The $\text{C}1'$ stereocenter was determined by generating a stereodefined ($1'R$)-ketodiol from a ($1R$)-aldehyde (R)-**104** precursor (Fig. 40).

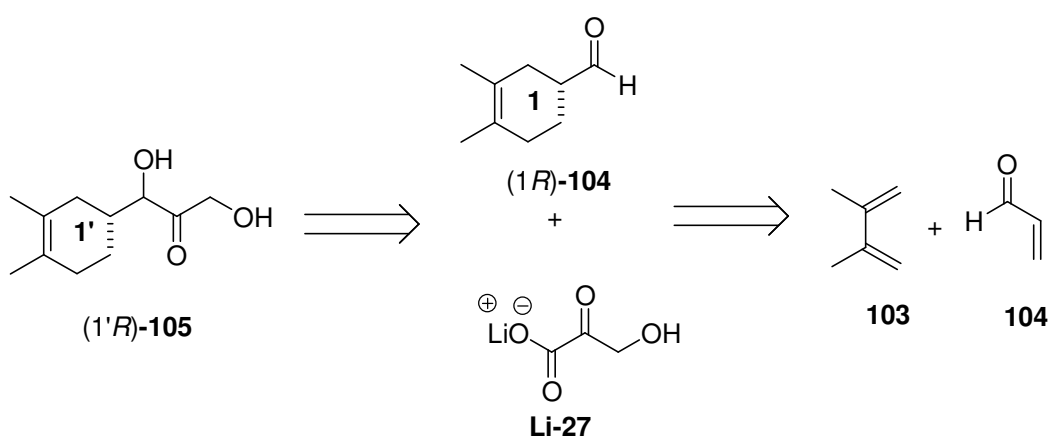
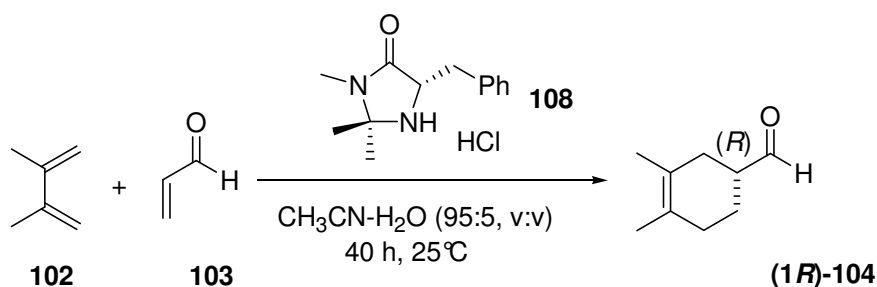


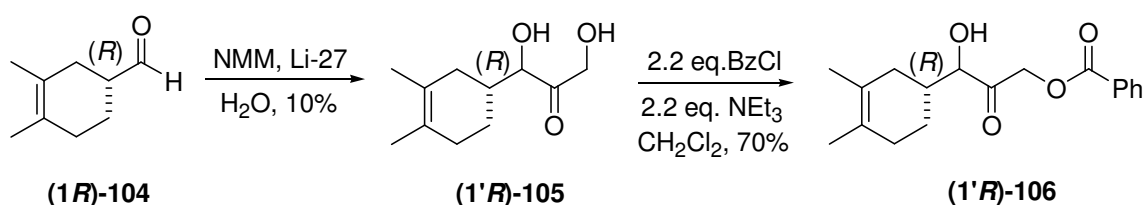
Figure 40: Retrosynthesis of ($1'R$)-**105**

Macmillan catalyst, ($5S$)-2,2,3-trimethyl-5-phenylmethyl-4-imidazolidinone **108**, was used to generate the ($1'R$)-aldehyde ($1R$)-**104** and was reacted with **102** and **103** in a $\text{CH}_3\text{CN}-\text{H}_2\text{O}$ (95:5,v:v) solvent mixture, to generate ($1R$)-**104** in an 83% yield (Scheme 59).¹¹²



Scheme 57: Diels-Alder formation of ($1R$)-**104**

The aldehyde was directly used in the biomimetic reaction in the presence of *N*-methylmorpholine, and **Li-27** to generate ($1'R$)-**105** (10% yield). The ketodiol ($1'R$)-**105** was then monobenzoylated to afford ($1'R$)-**106** (70% yield).



Scheme 58: The formation of the benzoylated product 106

The HPLC spectra of (1'R)-106 was compared to the HPLC traces of the D469T-TK product (1S)-106 and the biomimetic four isomer product 106 (Fig. 41).

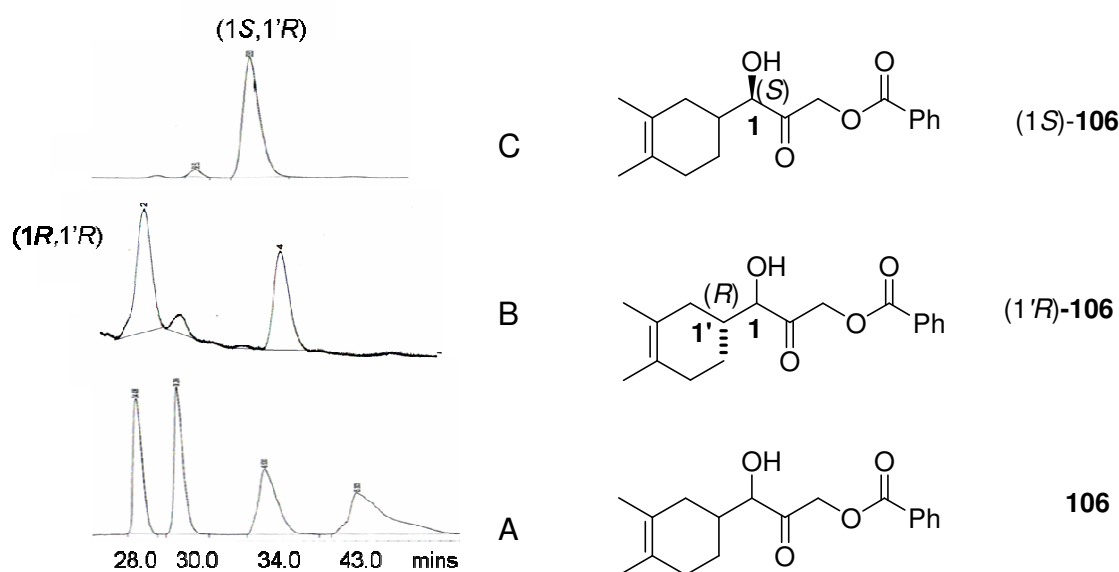
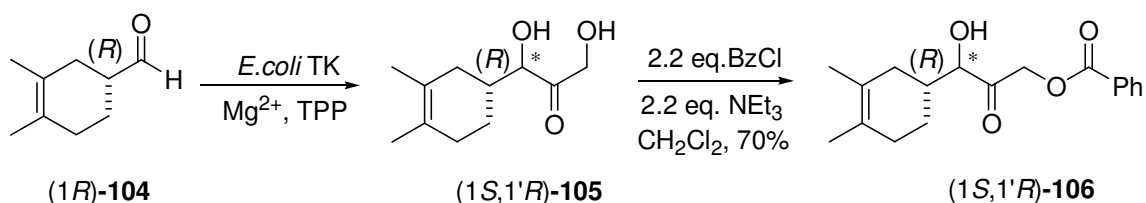


Figure 41: Spectra (A) Biomimetic, (B) 2 major peaks and (c) D469T product, 1 major peak

These experiments helped elucidate the absolute stereochemistry of the major isomer of the D469T-TK product as (1S,1'R) (Fig. 41). Closer inspection of the D469T-TK ketodiol HPLC spectra (Fig. 41) indicated that a 93:7 (*anti:syn*) product was formed.

Additional experiments were conducted using (1R)-104 in the biotransformation with D469T-TK. This yielded the same major diastereoisomer 105 (as determined by HPLC analysis) was afforded as with racemic 104 in the same yield (10%). The major isomer (1S,1'R)-105 was formed in 97% ee (minor isomer (1R,1'R)-105) and no (1S,1'S) or (1R,1'S)-105 isomers were detected (Scheme 59). This confirmed the biotransformation using racemic 104 with D469T-TK is highly enantioselective for (1R)-104. Since the ketodiol product 105 is formed in the same yield regardless of whether racemic or optically pure 104 is used, this suggested that the reaction was not inhibited by (1S)-104 and that the rationale for the low yield of the reaction is most likely due to product inhibition which can be tackled by process engineering techniques *in situ*.¹⁰⁴



Scheme 59: Formation of (1S, 1'R)-106

The only current X-ray crystal structure of *E. coli* TK, in a non covalent complex with with acceptor aldose ribose-5-phosphate (R5P) can shed light on the alleged stereoselective nature of the mutant enzyme. The replacement of the aspartate residue (D469) involved in the catalytic activity disrupts the important hydrogen bonding (2.74 Å) to the C2 hydroxyl group of acceptor substrate (R5P) molecule (A, Fig. 42). The mutation to a threonine residue, containing a neutral side chain, may result in a steric clash between neighbouring side chains (B, Fig. 42) and may require a side chain rearrangement to accommodate a new side chain. However the mutation may be favorable due to weakened hydrogen bonding (5.69 Å) capacity with the D469T residue allowing a larger substrate such as **104** to bind (C, Fig. 42).

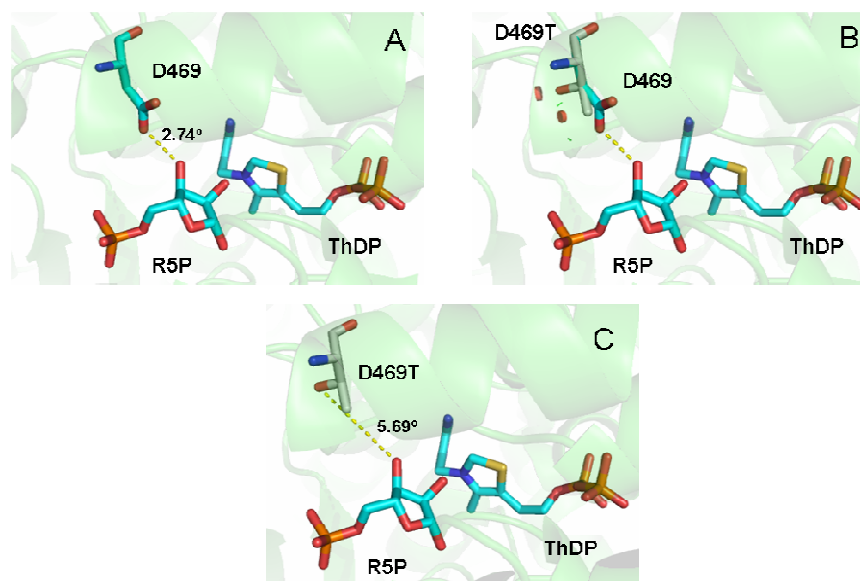


Figure 42 (A) D469 hydrogen bonding to R5P (B) D469/D469T steric clash to neighbouring side chains (C) D469T hydrogen bonding to R5P (a crude pyMOL mutagenesis (1NGS.pdb, taken from www.rcsb.org/pdb))

The D469T mutant has previously been shown to have 8.5-fold improved specificity towards propanal relative to glycolaldehyde when compared to WT, highlighting that the conversion of an acidic residue to threonine may favour conversions with more lipophilic substrates.^{87,91} It is surprising nevertheless, that a single point mutation of an enzyme shows high catalytic activity with bulkier substrates in comparison to WT, as usually an accumulation of multiple mutations is required.¹⁰⁵

The colorimetric assay was also used to obtain kinetic data (performed by Lydia Crago) using purified His-tagged D469T TK with **104** at a various concentrations (0–50 mM) and 50 mM Li-**27**.⁹¹ A V_{\max} of 0.07 mM min⁻¹, an apparent K_M of 69.9 mM, and a k_{cat} of 17.5 s⁻¹ was observed. This resulted in a 18,000-fold improvement in substrate specificity (k_{cat}/K_M) for D469T compared to WT-TK.

3.11 Summary

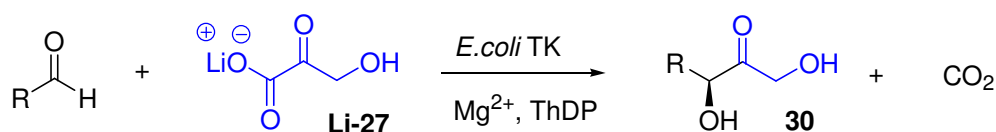
We have identified and demonstrated TK mutants with improved substrate activity towards cyclic aliphatic aldehyde substrates with increasing ring size in comparison to WT-TK. The TK mutants, are highly enantioselective with cyclic substrates **89**, **90** and **91** generating (*S*)-ketodiol products with >99% *ees*. Further kinetic experiments revealed that the high yielding mutant D469T has poorer substrate specificity with the cyclic aldehydes in comparison to propanal as substrate due to the increasing lipophilicity and steric bulk of the cyclic aldehydes investigated. The mutant D469T-TK has shown an 18,000-fold increase in reaction rate for cyclic aldehyde **92** in comparison to WT-TK. The biotransformation revealed D469T to be highly diastereoselective for the (1*S*,1'*R*)-**105** isomer, affording a (97:3) *anti:syn* product. Further experiments indicated that the (1*S*)-**104** aldehyde is not accountable for enzyme inhibition and suggests that product inhibition is presumably responsible for the low yielding ketodiol product generated. The high activity and high stereospecificity demonstrated by D469T highlights the importance of exploring the promiscuity of this mutant in the future using an even broader range of complex cyclic substrates.

Chapter 4.0
Aromatic aldehydes used in the TK
reaction

4.1 Aromatic aldehydes used as novel substrates in the TK reaction

As previously described in the introduction (Chapter 1), Dumunyck first reported relative reaction rates of several aromatic aldehydes used as acceptor molecules with **Li-27** as the donor substrate in the yeast TK reaction.⁴⁶ The relative rates were determined by monitoring **Li-27** depletion by HPLC; with no attempts made to isolate the ketodiol products. The relative velocities calculated revealed that the aromatic aldehydes are in general poor substrates with yeast TK reaction in comparison to glycoaldehyde.

Turner *et al.* performed preliminary investigations with several aromatic aldehydes as acceptor molecules and **Li-27** as the donor substrate for the *E. coli* TK reaction. Furfural showed poor substrate affinity with *E. coli* TK, assessed via the depletion of **Li-27** but no apparent product was isolated.⁵¹ Enantiomerically pure aromatic α -hydroxyaldehydes were synthesized and also used as substrates leading to novel optically pure triols **30iv** and **30v** with moderate to good yields 44% and 54% respectively.⁴³ A non α -hydroxyaldehyde, phenylacetaldehyde was also used as an acceptor substrate and gave the product **30ii** in 33% yield (Table 20).⁵²



R (Aldehyde)	30	Yield%	V _{rel}
	i	-	0.3
	ii	33	-
	iii	76	-
	iv	44	-
	v	54	-

Table 20: Other aromatic substrates used as substrates

Our aim was now to investigate in detail the feasibility of using aromatic aldehydes to give ketodiols with potential for conversion to aminodiols.

4.2 The colorimetric screening of library D469 with benzaldehyde

The reaction plate of the *E. coli* D469 library obtained by saturation mutagenesis was incubated with benzaldehyde and **Li-27** and then the tetrazolium-red colorimetric assay was used to detect the ketodiol product **30Ar1** (Fig. 43). The colorimetric assay of the 96-well plate highlighted the overall poor optical densities for the variants in comparison to the colorimetric assay with the cyclic aliphatic aldehydes, suggesting poor substrate affinity of *E. coli* TK for benzaldehyde. The screening revealed, however that the percentage well containing mutant D469K had the highest optical density. Selected mutants were then grown to prepare cell-free lysates for biocatalysis. TK mutants D469E, D469K, D469S, and D469T were chosen for their relatively high optical densities on the assay read-out or for exhibiting high enantioselectivities and substrate activity with cyclic aliphatic aldehydes.¹⁰⁶ Mutant H26Y TK was also selected for exhibiting good activity with long chain aliphatics and affording (3*R*)-ketodiols.⁸⁷ The preparative biotransformations were conducted at a 50 mM scale and monitored by TLC analysis.

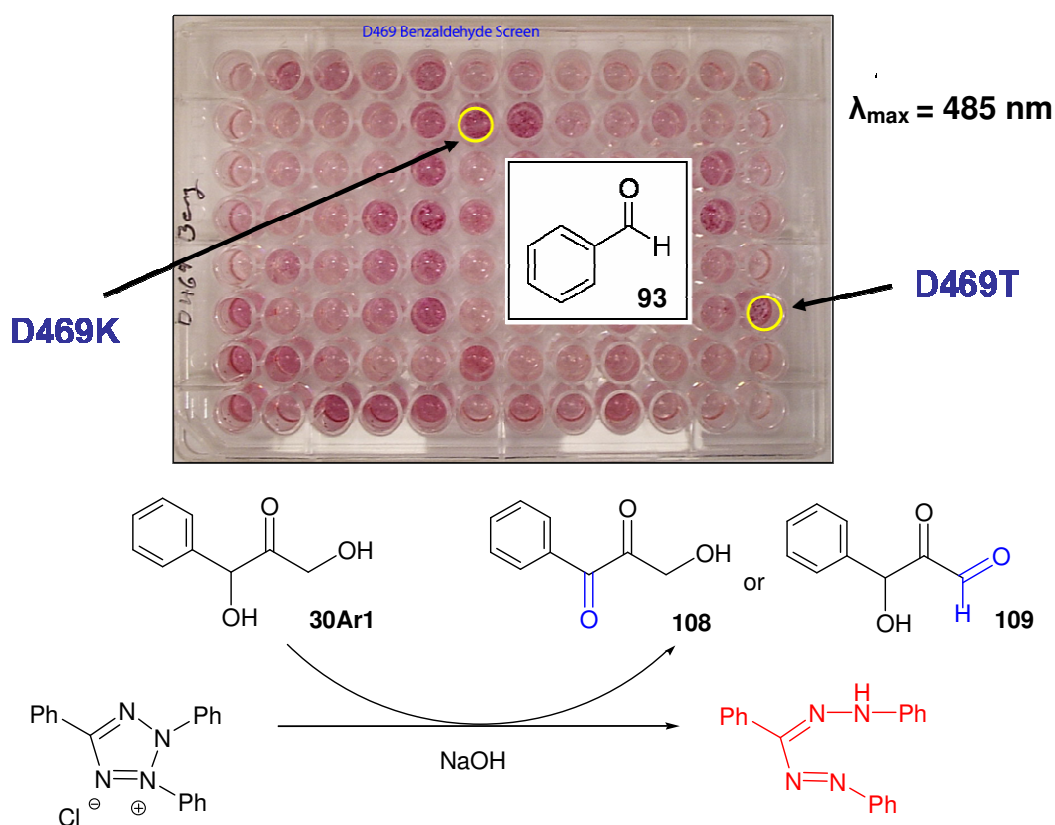
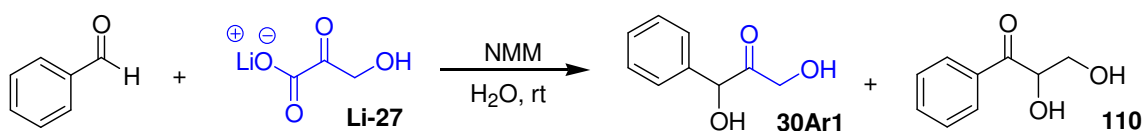


Figure 43: The colorimetric assay screening library D469 for active TK mutants with benzaldehyde

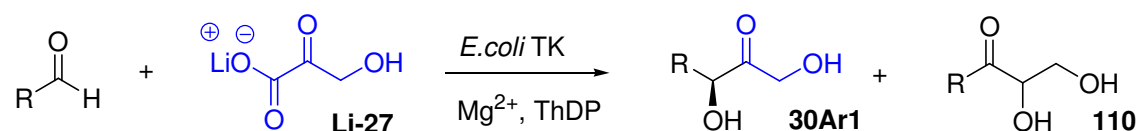
4.3 Benzaldehyde as an acceptor substrate for the TK reaction

Initially racemic **30Ar1** was prepared using the biomimetic reaction in aqueous media with stoichiometric amounts of benzaldehyde, *N*-methylmorpholine and **Li-27** (see Chapter 5). The reaction mixture was adjusted to pH 7.0, to reduce the formation of the by-product **110** which had been observed when storing **30Ar1** in solution (Scheme 60).



Scheme 60: Formation of **30Ar1** and **110** in water

The racemic **30Ar1** isolated had an R_f value of 0.45 in (1:1) ethyl acetate: hexane and this was used together with NMR analysis to determine the outcome of the reaction. The biotransformations performed exhibited no catalytic activity with WT-TK or the mutant H26Y to generate **30Ar1** or **110**. The D469 variants assessed generated **30Ar1** in low product yields < 5% (Table 21).



R	D469E (%)	D469T (%)	D469K (%)	G6 (%)	H26Y (%)	WT-TK (%)
	30Ar1 (3) 110 (0)	30Ar1 (3) 110 (0)	30Ar1 (2) 110 (0)	30Ar1 (2) 110 (0)	nr	nr

Table 21: The yields of the biotransformation product **30Ar1** and **110** using several TK mutants

Increasing the polarity of the eluent to 100% ethyl acetate for D469E, D469T, D469K, and G6 revealed the formation of a side product with an R_f of 0.4. The product isolated has a parent ion m/z $[M+Na]^+ = 249.21$, and with further NMR analysis the following structure **111** has been proposed (Fig. 44).

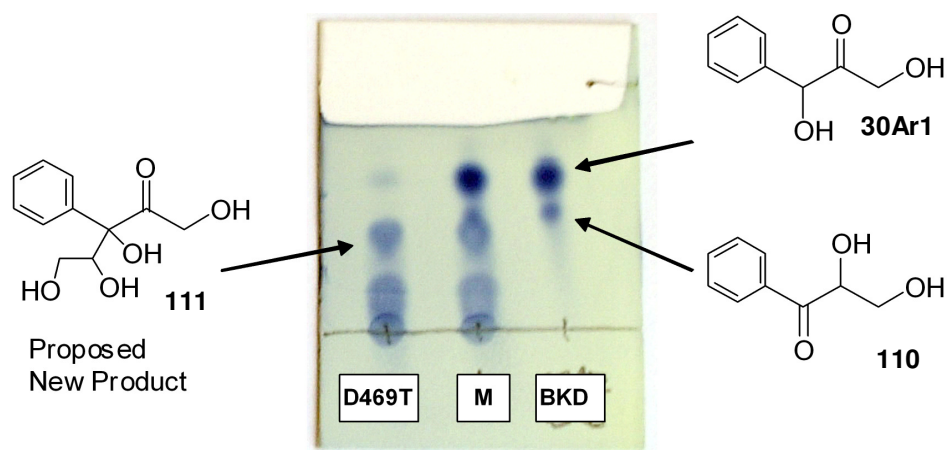
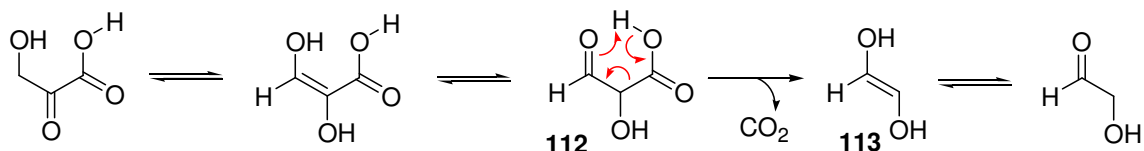


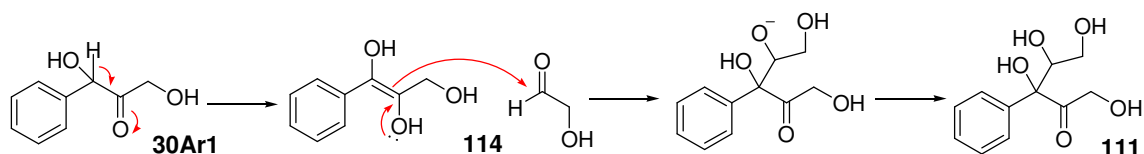
Figure 44: TLC plate showing the biotransformation products of D469T, in comparison to the biomimetic products

A mechanism for the ‘double-addition’ product has been proposed involving the tautomerisation of **Li-27** *in situ* to form the tartronate semialdehyde **112**, a β -ketocarboxylic acid which undergoes decarboxylation in a concerted process. The ease of decarboxylation depends on the stability of the stable 6-membered transition state, which lowers the activation energy for decarboxylation to occur at mild conditions.¹⁰⁷ Decarboxylation of β -ketocarboxylic acids leads initially to the formation of the enediol **113** then tautomerises to the corresponding carbonyl to generate glycolaldehyde *in situ* (Scheme 61).



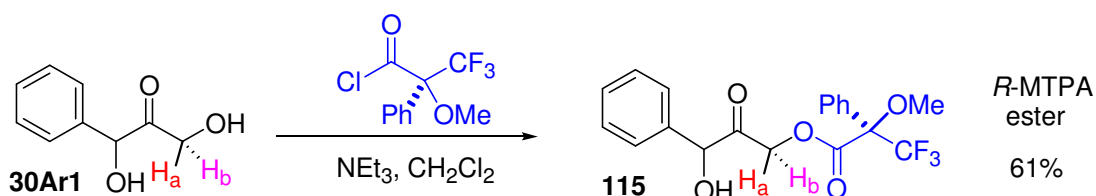
Scheme 61: The generation of glycolaldehyde *in situ* via decarboxylation of a β -ketocarboxylic acid

The acidity of the α -H in **30Ar1** generated in the biotransformation leads to formation of the electron rich enediol **114** which attacks the carbonyl of glycolaldehyde, with subsequent proton transfer, affording the ‘double addition’ product **111** (Scheme 62).



Scheme 62: Mechanism for the generation of the proposed structure of the by-product formed

To determine the absolute stereochemistry of **30Ar1** the Mosher’s derivatisation method (Chapter 2) was used. Compound **30Ar1** produced by mutant D469T was coupled to (*S*)-MTPA-Cl at the terminal hydroxyl group to generate the (*R*)-MTPA ester **115** (yield 61%) (Scheme 63).



Scheme 63: Formation of (*R*)-MTPA ester **115**

The calculated chemical shift difference of the major isomer ($\Delta\delta_{\text{H}}$ 0.31) was larger than for the minor isomer ($\Delta\delta_{\text{H}}$ 0.02) of the (*R*)-MTPA ester **115** (Fig. 45). This indicated the stereochemistry at C3, formed by D469T, was assigned as having (*3R*)-configuration, with an approximate 90% *ee* (Fig. 45).

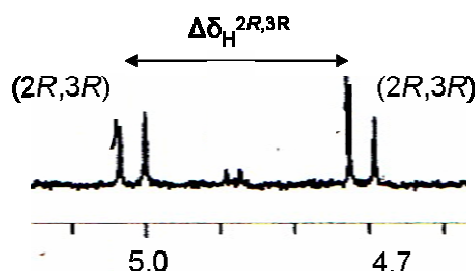
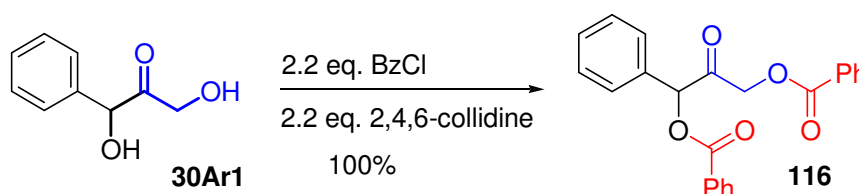


Figure 45: NMR spectra of (*R*)-MTPA ester of **115**

The HPLC assay to determine the *ees* of **30Ar1** involved the dibenzoylation of the ketodiol products. The hydroxyl groups of racemic **30Ar1** were benzoylated using a benzoyl chloride and 2,4,6-collidine to afford quantitative yields of the dbenzoylates (Scheme 64). The dibenzoylated product **116** isomers were readily separated by chiral HPLC, using a chiralpak-AD column, with a hexane:isopropanol (82:18) concentration, at a flow rate of 1.0 ml min⁻¹ and gave the retention times of 10.5 min (*R*-isomer) and 13.4 min (*S*-isomer). Using this assay, the *ees* of the ketodiols from other D469 TK variants were determined with the majority (*R*)-isomer obtained (Table 22).



Scheme 64: Acetylation of **30Ar1** and a spectrum of the separated isomers **116**

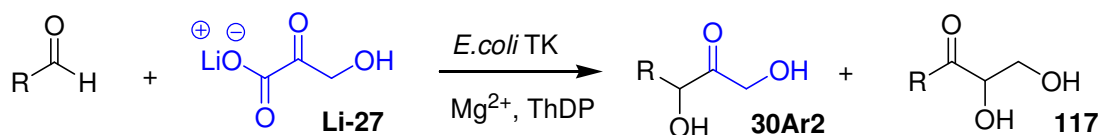
Aldehyde	D469E <i>ee</i> %	D469T <i>ee</i> %	D469K <i>ee</i> %	G6 <i>ee</i> %	H26Y <i>ee</i> %	WT-TK <i>ee</i> %
	0	70	82	72	-	-

Table 22 The percentage *ees* of ketodiol **30Ar1** upon formation of **116**

A variety of aromatic aldehydes were screened on a preparative scale and several examples are given below:

4.4 Furfural as an acceptor substrate for the TK reaction

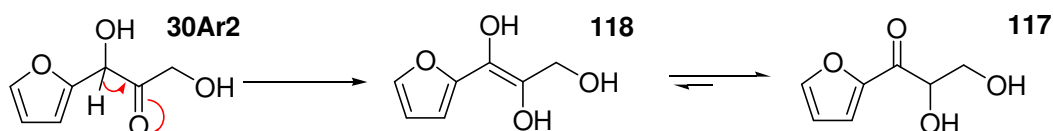
The selected mutants used in biocatalytic conversions with benzaldehyde were also screened with furfural. In separate but analogous biotransformations, the TK mutants selected were conducted at a 50 mM reaction mixture, at pH 7.0 and for 48 hours. The biotransformation reaction was monitored by TLC analysis and revealed that two products were formed in several experiments. The compounds isolated were ketodiol **30Ar2** and rearranged ketodiol **117**. The results revealed that WT-TK and H26Y mutants had poor activity with furfural exhibiting no product formation after 48 hours (Table 23).



R	D469E (%)	D469T (%)	D469K (%)	G6 (%)	H26Y (%)	WT-TK (%)
	30Ar2 (5) 117 (1)	30Ar2 (3) 117 (1)	30Ar2 (3) 117 (1)	30Ar2 (4) 117 (1)	nr	nr

Table 23: Isolated biotransformation yields of 30Ar2 and by-product 117 using several TK mutants

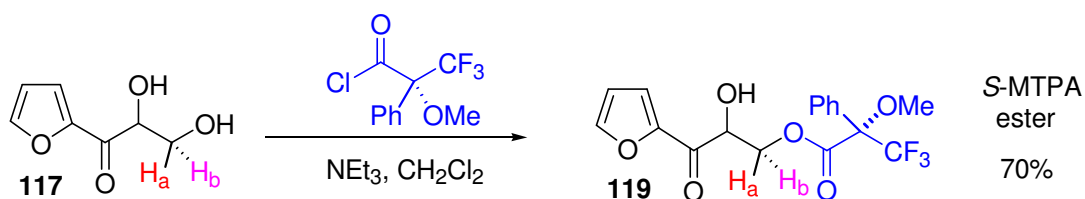
The thermodynamically favoured rearranged product is formed from the deprotonation of the acidic α -H of the ketodiol to generate the enediol **118** which tautomerises to form the preferred oxo tautomer **117** in conjugation with the furan ring (Scheme 65).



Scheme 65: Mechanism of ketodiol 30Ar2 rearranged to 117

To determine whether the rearranged ketodiol product was enzymatically generated, **117** was derivatised to the Mosher's ester by coupling the terminal hydroxyl group with an (*R*)-MTPA-Cl generating an (*S*)-MTPA ester **119** (Scheme 66). A unique splitting pattern was observed from the diastereotopic protons H_a and H_b of the (*S*)-MTPA ester. The two outer multiplet signals at δ 3.06 and δ 3.45 ppm represented one isomer while the inner multiplet δ 3.30 represents another (Fig. 46). The equal ^1H NMR integrations

of H_a and H_b revealed the rearranged ketodiol as a racemate. This suggests **117** was formed *in situ* from **30Ar2** by conversion to the favoured thermodynamic product.



Scheme 66: Formation of (S)-MTPA ester **119**

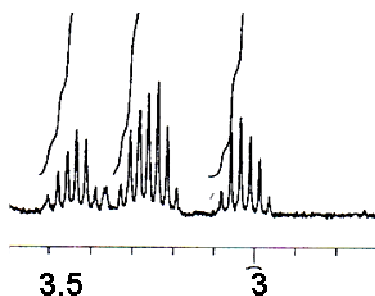
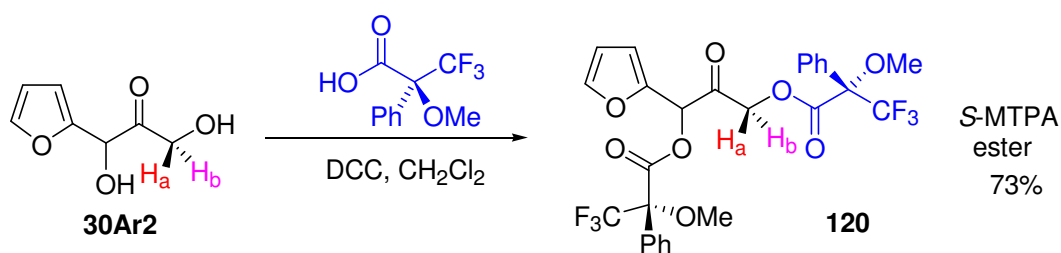


Figure 46: ^1H NMR representing H_A and H_B of **119**

The absolute stereochemistry of **30Ar2** resulting from the D469T mutant was investigated by coupling to (*R*)-MTPA-Cl. However, when the reaction was performed in the presence of base triethylamine this resulted in the formation of the thermodynamically more stable **119**. A DCC coupling reaction was carried out which formed the diMTPA ester under neutral conditions (Scheme 67). The calculated chemical shift difference of the major isomer ($\Delta\delta_H$ 0.19) was larger than minor isomer ($\Delta\delta_H$ 0.00) of the (*S*)-MTPA ester. This suggested the stereochemistry at C3, formed using D469T, was the (*3S*)-configuration, and was generated in approximately 80% ee (Fig. 47).



Scheme 67: DCC coupling forming (S)-MTPA ester of **30Ar2**

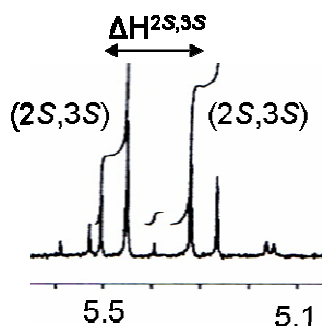
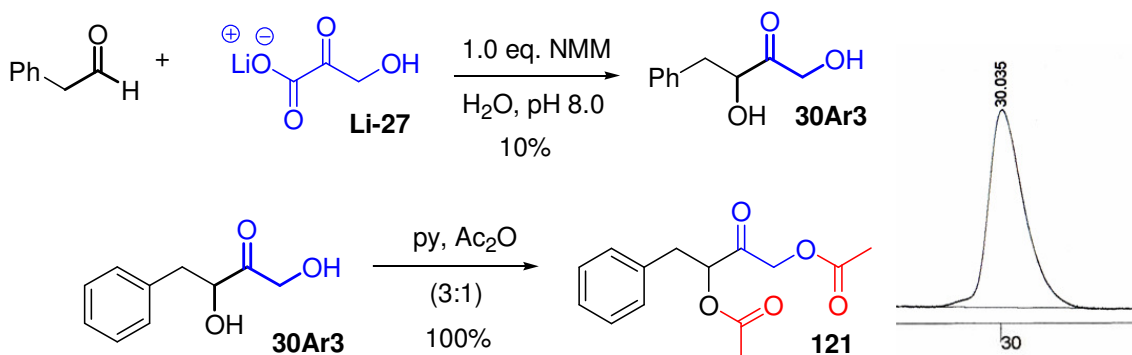


Figure 47: ^1H NMR of H_a and H_b of **120**

The *ees* of the ketodiols obtained from the other mutant TKs are pending identification. Nevertheless, ester formation using triethylamine as base was avoided. Derivatisation using benzoic or acetic acid will be carried out using DCC coupling reagent to avoid racemisation and analysis of the *ees* can be achieved using chiral HPLC.

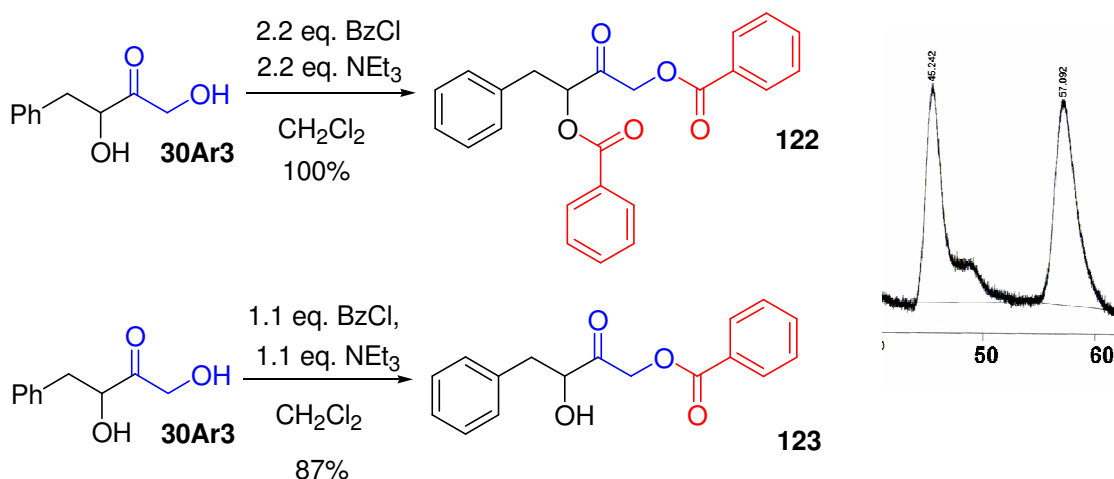
4.5 Phenylacetaldehyde as an acceptor substrate for the TK reaction

The biomimetic reaction with phenylacetaldehyde was conducted using THF:H₂O (1:1) solution at pH 7.0 in the presence of **Li-27** and *N*-methylmorpholine as a catalyst, to afford the ketodiol product **30Ar3** in 5% yield. The yield increased two-fold, when the THF:H₂O (1:1) reaction mixture was not adjusted at pH 7.0, but performed at pH 9.0. Unlike the other aromatic aldehydes, phenylacetaldehyde is not in conjugation with the aromatic ring and is less likely to generate the ‘rearranged product’. The ketodiol contains an aromatic chromophore that can be detected by UV absorption. Initially the hydroxyl groups in **30Ar3** were acetylated using a pyridine:acetic anhydride (3:1) mixture for 4 hours followed by an acid/base work up to afford quantitative yields of **121**. The acetylated product **121** was detected by normal phase chiral HPLC columns available, however various manipulations in the protocol and the use of different chiralpak columns (AD, OD, OJ) established that the isomers were inseparable. (Scheme 68)



Scheme 68: Formation of **30Ar3** and acetylated product **121** (spectra of inseparable isomers)

The ketodiols, was therefore derivatised to the mono-, and dibenzoylated products, **122** and **123** respectively using benzoyl chloride and triethylamine for 12 hours at room temperature. The benzoyated products were purified by silica gel chromatography before analyzing **122** and **123** using the chirapak-OD column. The dibenzoylated product was detected but the isomers appeared inseparable under different isopropanol and hexane concentrations and protocols. The mono-benzoylated product **123** exhibited clear separation of the isomers; using an chirapak-OD column, with a hexane:isopropanol (97:3) concentration, at a flow rate of 0.8 ml min⁻¹ (Scheme 69).



Scheme 69: Generation of a Mono-, dibenzoylated products (spectra of separated isomers of 123)

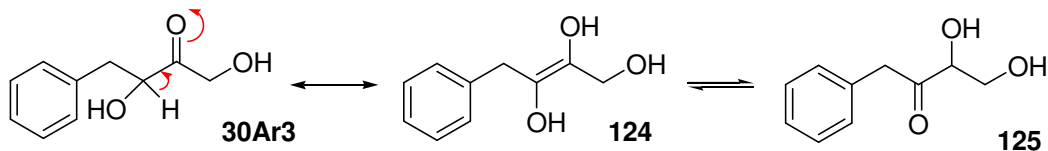
In separate, but analogous biotransformations, the TK mutant reactions were all conducted at 50 mM concentrations at pH 7.0 for 48 hours and monitored by TLC. The ketodiols were purified using silica gel chromatography (R_f 0.45, Hexane:EtOAc; 4:1). WT-TK variant and H26Y gave **30Ar3** in low yields (5%) compared to the D469 TK mutant which gave **30Ar3** in 43-50% yields (Table 24).

R	D469E	D469T	D469K	G6	H26Y	WT-TK
	%	%	%	%	%	%
	43	50	45	50	5	5

Table 24: Yields of ketodiols 30Ar3 generated

Previous work conducted by Turner *et al.* gave **30Ar3** in 33% when using unbuffered medium at pH 7.0 (pH Stat). In comparison, the corresponding TK reaction in 0.1 M

glycylglycine buffer at pH 7.0 gave **30Ar3** in 26% yield. When they repeated the TK reaction in unbuffered media a 'rearranged ketodiol' by-product **125** (18% yield) was obtained. However the biotransformations conducted in this work with TK variants gave negligible amounts of the 'rearranged ketodiol' product. This can be rationalised by the different reaction conditions used in the biotransformation which were not specified in detail by Turner and coworkers (Scheme 12).⁵²



Scheme 70: Rearrangement mechanism of **30Ar3**

The absolute stereochemistry or the enantiopurity of the ketodiol product has not been reported in the literature. Following the HPLC assay, by monobenzoyleating the ketodiol products from the TK mutant biotransformations, the *ees* were determined. Both H26Y and WT-TK were low yielding, but high *ees* were observed. Most importantly H26Y generated the same (*S*)-isomer as all the other D469 TK mutants in a direct contrast to the (*R*)-ketodiol products observed for H26Y with linear aliphatic aldehydes (Table 25).⁸⁷

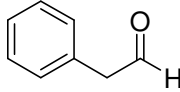
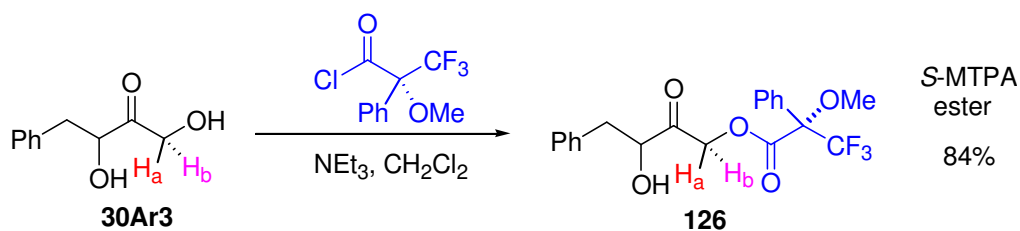
Aldehyde	D469E <i>ee</i> %	D469T <i>ee</i> %	D469K <i>ee</i> %	G6 <i>ee</i> %	H26Y <i>ee</i> %	WT-TK <i>ee</i> %
	90	96	95	92	88	93

Table 25: The percentage *ees* of ketodiol **30Ar3** generated

The absolute stereochemistry of the D469T ketodiol product **30Ar3** was determined by coupling the terminal hydroxyl group with an (*R*)-MTPA-Cl generating an (*S*)-MTPA ester as previously described (Scheme 71).



Scheme 71: Formation of the (*S*)-MTPA ester **126**

An interesting splitting pattern was observed for methylene protons H_a and H_b of the (*S*)-MTPA ester **126**. The major isomer (*2S,3S*) resonates at δ_H 5.16 ppm and 4.95 ppm with a 0.21 chemical shift difference ($\Delta\delta_H^{2S,3S}$ is 0.21) and the minor isomer resonates at δ_H 5.07 ppm and 5.04 ppm ($\Delta\delta_H^{2S,3R}$ is 0.03). This suggested that the stereochemistry at C3, for **30Ar3** formed by D469T had the (*3S*)-configuration. An

approximation of the *ee* was determined from the NMR integration of H_a and H_b giving a 90% *ee*, compared to the 96% *ee* measured via HPLC. Overall the D469 TK mutants assessed were stereoselective for the (*S*)-configured product (Fig. 48).

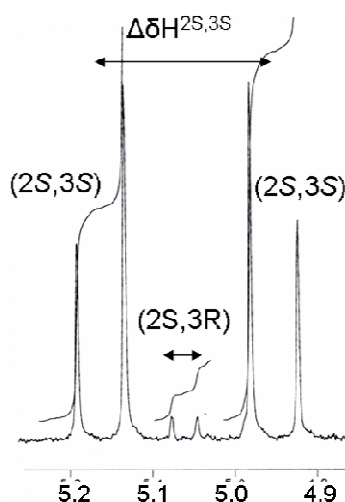


Figure 48: ¹H NMR spectrum of H_A and H_B of 126

4.6 2-Phenylpropionaldehyde as an acceptor substrate

The biomimetic reaction was performed using 2-phenylpropionaldehyde as the acceptor aldehyde in a THF:H₂O (1:1) solvent system to prepare the ketodiol product as a four diastereomeric mixture in 20% yield. The *de* of the diastereomers was determined by ¹H NMR spectra, wherein the relative integrations of the separable protons were compared. For instance, the ¹H NMR spectrum of ketodiol **30Ar4** (Fig. 49, Spectrum A), revealed H_A at δ 1.28 as a doublet (*J* 7.1 Hz) for the major isomer, while the same proton resonated at δ 1.43 as a doublet (*J* 7.1 Hz) for the minor isomer with relative integrations of 4:1 (*de* 60%). In comparison with D469T TK mutant affording ketodiol **30Ar4** exhibited separable doublets; with the major doublet at δ 1.28 ppm, and the minor doublet resonating at δ 1.43 ppm revealed higher relative integrations 11:1 (*de* 83%) (Fig. 49, Spectrum B).

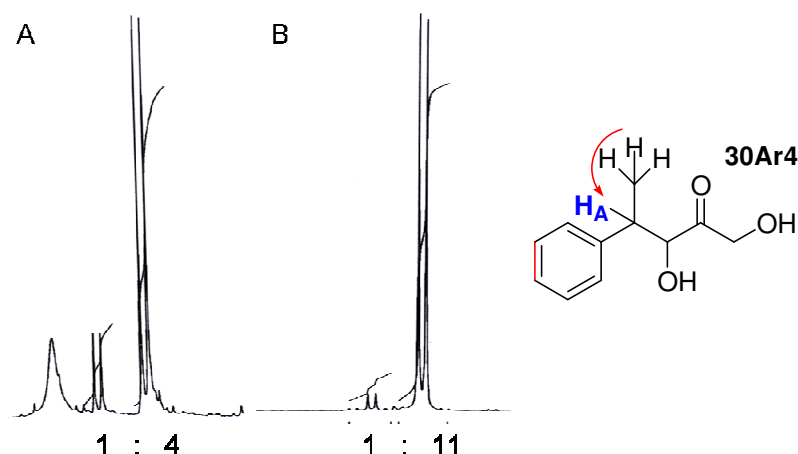


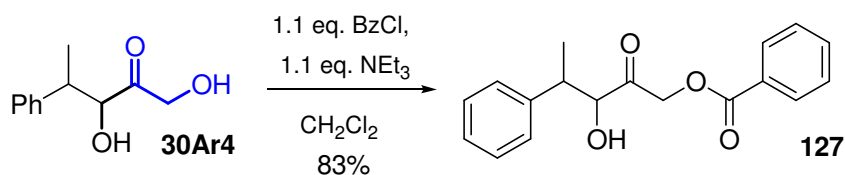
Figure 49: ¹H NMR spectra of biomimetic (A) and ¹H NMR of D469T (B)

In separate, but analogous biotransformations, the TK mutants using D469E, D469T, D469K, G6, H26Y and WT-TK were all conducted at 50 mM concentrations at pH 7.0 (pH Stat) for 48 hours and monitored by TLC analysis. The ketodiols were purified under silica gel chromatography (R_f of 0.40, Hexane:EtOAc; 1:1). The TK variant H26Y when used in the biotransformation afforded no product. The WT-TK gave rise to comparable yields as with the D469 TK mutants which exhibited moderate yields (Table 26).

R	D469E	D469T	D469K	G6	H26Y	WT-TK
	%	%	%	%	%	%
	30	40	38	38	nr	35

Table 26: The yields of the biotransformation product 30Ar4

The isomeric mixture of **30Ar4** from the biomimetic reaction was then benzoylated using benzoyl chloride and triethylamine. Only the monobenzoylated product **127** was obtained, highlighting the steric hindrance by the aryl ring preventing the benzoylation from occurring at the secondary alcohol (Scheme 72).



Scheme: 72 Benzoylation of 30Ar4

The monobenzoylated product was detected via HPLC at a wavelength of 214 nm using a chiralpak-OD column. The isomers from the biomimetic reaction were detected with two different sets of isomers with equal integration under isocratic conditions using isopropanol (3%) as the polar stationary phase and hexane (97%) as the non mobile phase with a 0.8 ml min⁻¹ flow rate (Fig. 50, **A**). The HPLC traces corresponded to the NMR data where a 1:4 diastereomeric ratio was noted. The ketodiol products from D469T-TK mutant were monobenzoylated and subjected to the same HPLC procedure. This revealed that D469T was highly diastereoselective with a preference

for the formation of the same major isomer peak 1 with traces of a smaller isomer peak 3 present (Fig. 50, **B**).

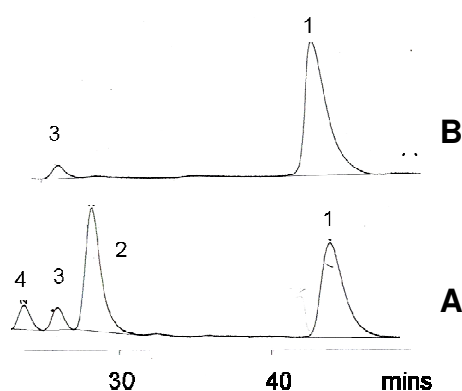
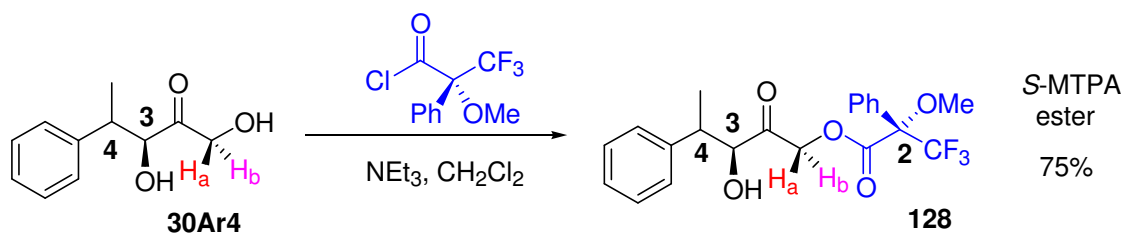


Figure 50: Spectrum A (127 obtained from D469T) Spectrum B (127 Racemate from biomimetic)

The absolute configuration and diastereoselectivity of D469T was determined via the preparation of the *R*-aldehyde and the developed Mosher's method. To determine the stereochemistry at the C3 position, **30Ar4** was reacted with (*R*)-MTPA-Cl to attach the Mosher's ester **128** at the primary alcohol (Scheme 73).



Scheme 73: Formation of (*S*)-MTPA ester 128

The calculated chemical shift difference of the major isomer ($\Delta\delta_{\text{H}}$ 0.16) was larger than the minor isomer ($\Delta\delta_{\text{H}}$ 0.00) of the (*S*)-MTPA ester. This indicated the stereochemistry at C3, formed by D469T, had the (*3S*)-configuration, and an approximate 91% ee at the *3S* position was observed via integration of H_a and H_b protons (Fig. 51).

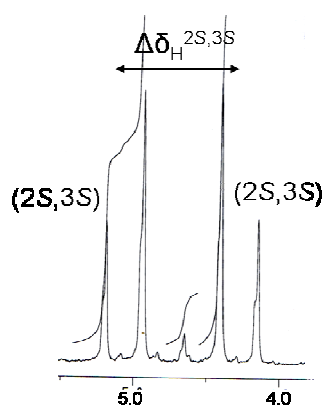
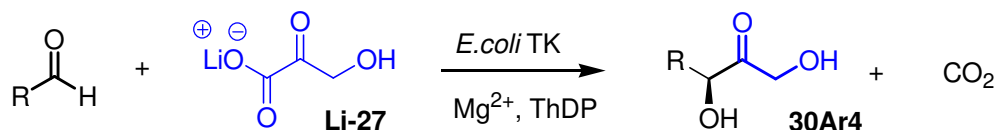


Figure 51: ^1H NMR of H_a and H_b of 128

The ketodiol products from the remaining TK mutants D469E, D469K, G6, H26Y and WT-TK were benzoylated and the C3 absolute configurations were determined via

HPLC. All contained the (3*S*) configuration with *ee* at 3*S* shown below with the minor isomer presumed 3*R* product (Table 27).

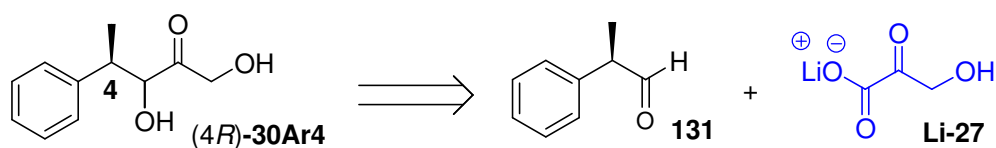


Ketodiol	D469E <i>ee</i> %	D469T <i>ee</i> %	D469K <i>ee</i> %	G6 <i>ee</i> %	H26Y <i>ee</i> %	WT-TK <i>ee</i> %
	90	91	89	88	nr	76

Table 27: The percentage *ees* of **30Ar4**

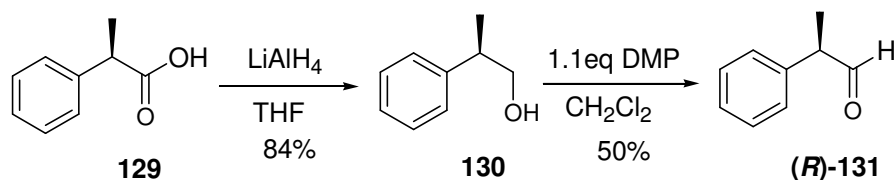
The results indicate a continued stereoselective preference for the (3*S*)-isomer across most aryl aldehydes explored with the D469 TK library. This also suggested that the interactions with the α -methyl group from the acceptor aldehyde contributed a pivotal role in directing the diastereoselectivity of the ketodiol product formed. The TK mutant H26Y revealed no activity with 2-phenylpropionaldehyde as the substrate acceptor molecule. In general H26Y appeared to have poor substrate activity with aromatic substrates, possibly due to access of the substrate in entering the substrate cleft of the TK enzyme.

The C4 stereocentre in the major isomer of **30Ar4** formed using D469 variants was determined by generating a stereodefined (4*R*)-ketodiol from an (*R*)-aldehyde **131** precursor (Scheme 74).



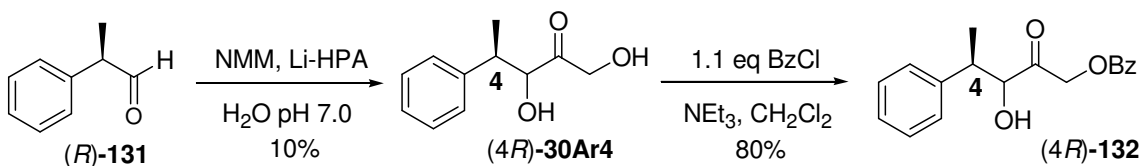
Scheme 74: Retrosynthesis of (4*R*)-**30Ar4**

Commercially available (*R*)-carboxylic acid **129** was reduced to the (*R*)-alcohol **130** using LiAlH_4 in 84% yield. Oxidation to the aldehyde (*R*)-**131** using Swern conditions has been reported to generate racemic mixtures.¹⁰⁸ Therefore Dess-Martin periodinane (1.2 eq.) was used and added in one portion to **130** and the reaction was stirred for 3 hours after which TLC analysis indicated the reaction was complete (Scheme 75).



Scheme 75: Formation of (*R*)-aldehyde **131**

The aldehyde (*R*)-**131** was directly used in a 1:1 THF:H₂O biomimetic reaction in the presence of *N*-methylmorpholine at pH 7.0 generating (*4R*)-**30Ar4** in a 10% yield. The ketodiol was then monobenzoyleated to generate product (*4R*)-**132** in 80% yield (Scheme 76).



Scheme 76: Formation of benzoyleated (*4R*)-**132**

The HPLC trace of (*4R*)-**132** was compared to the HPLC traces biomimetic product of the non-chiral aldehyde **127**. These experiments helped elucidate the absolute stereochemistry of the major isomer of the D469T-TK product as (*3S,4R*) and the minor product (*3S,4S*) in a 91:9 *anti:syn* ratio.

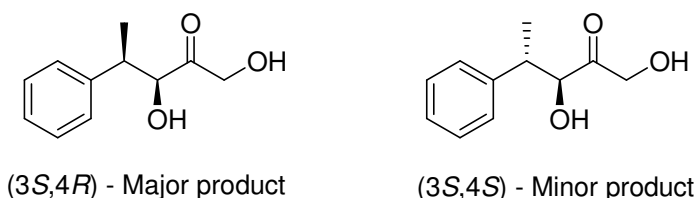


Figure 52: HPLC traces of **30Ar4**

The results suggested that the TK catalysed reaction of 2-phenylpropanal **131** containing the C2 methyl group is enantioselective for the (*4R*)-configuration. The TK mutant biotransformations revealed that they are diastereoselective for the *anti* products generating (*3S,4R*)-**30Ar4** as the major isomer (Table 28).

Ketodiol (<i>3S,4R</i>)- 30Ar4	D469E <i>anti:syn</i>	D469T <i>anti:syn</i>	D469K <i>anti:syn</i>	G6 <i>anti:syn</i>	H26Y <i>anti:syn</i>	WT-TK <i>anti:syn</i>
	90:10	91:9	89:11	88:12	nr	76:24

Table 28: The diastereoselectivities generated from WT and D469 TK mutants

This is in direct contrast to a similar aromatic substrate containing a C2 hydroxyl group that was substrate selective for the (*R*)-configuration as determined by Turner *et al.* by the failed enzyme catalysed coupling reaction of the (*S*)-aldehyde **131-OH** (Fig. 53).⁴³



Figure 53: Acceptor substrates

Further experiments are now required to confirm the *E.coli* TK selectivity for **30Ar4** by conducting a biotransformation using (*R*)-**131** as the acceptor substrate. The moderate yields from the mutant TK biotransformations suggests the (*R*)-**129** may have an inhibitory effect on TK but for further evidence the TK inhibition studies are required (Fig. 54).

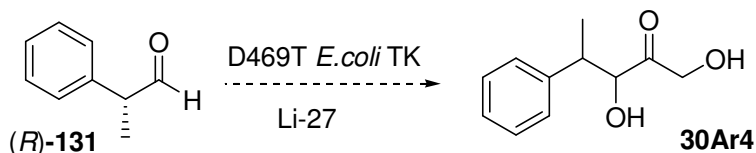


Figure 54: Further biotransformations

4.7 Substrate specific activity, Initial rates of reaction of Phenylacetaldehyde and 2-Phenylpropionaldehyde

The substrate specific activity for D469T and acceptor molecules **131** and **133** was calculated to reveal the performance of the enzyme in biocatalytic conditions. D469T with propanal revealed a 4-fold and 5-fold greater activity over substrates **133** and **131** respectively. This suggested the D469T TK mutant exhibited some substrate activity towards aryl substituents but they were less readily accepted than propanal. However further research is required for the substrate specific activities for WT-TK with acceptor molecule **131** and **123** to rationalise the effects of mutation, if any, on these substrates. In particular the biotransformations using WT-TK and D469T-TK with aldehyde **131** afforded the product **30Ar4** in comparable yields (Table 29).

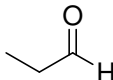
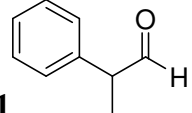
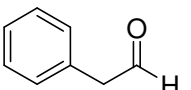
Mutant	Aldehyde	Initial rate [mM h ⁻¹]	TK (mg ml ⁻¹)	Spec. activity (mmol mg ⁻¹ min ⁻¹)	Initial rel. rate
D469T		12.52	0.3	0.70	1
D469T	131 	2.81	0.3	0.16	0.2
D469T	133 	3.15	0.3	0.18	0.4

Table 29: The D469T kinetic and specific activity data on substrates 93 and 133

4.8 Other aromatic aldehydes used as acceptor substrate molecules

A diverse range of aromatic aldehydes were screened on a preparative 50 mM scale with **Li-27** and cofactors in a non-buffered medium at pH 7.0 (pH Stat) with a variety of novel TK variants. The poorly soluble aromatic aldehydes containing electron donating/withdrawing substituents **134-137**, **140**, **141**, **145** at varying positions of the aryl ring gave no ketodiol product as determined by TLC analysis after 48 hours. The reaction mixture was stirred for further 5-7 days with no ketodiol product generated. Biotransformations were also conducted on water soluble pyrrol- **142-144**, pyridine-carboxaldehydes **138** and **139** monitored for 7 days with no ketodiol products formed. However, erythrulose was isolated as a side product generated by the self-condensation of **Li-27**, which indicated the poor substrate affinity of the nitrogen-containing aromatic rings (Fig. 55).

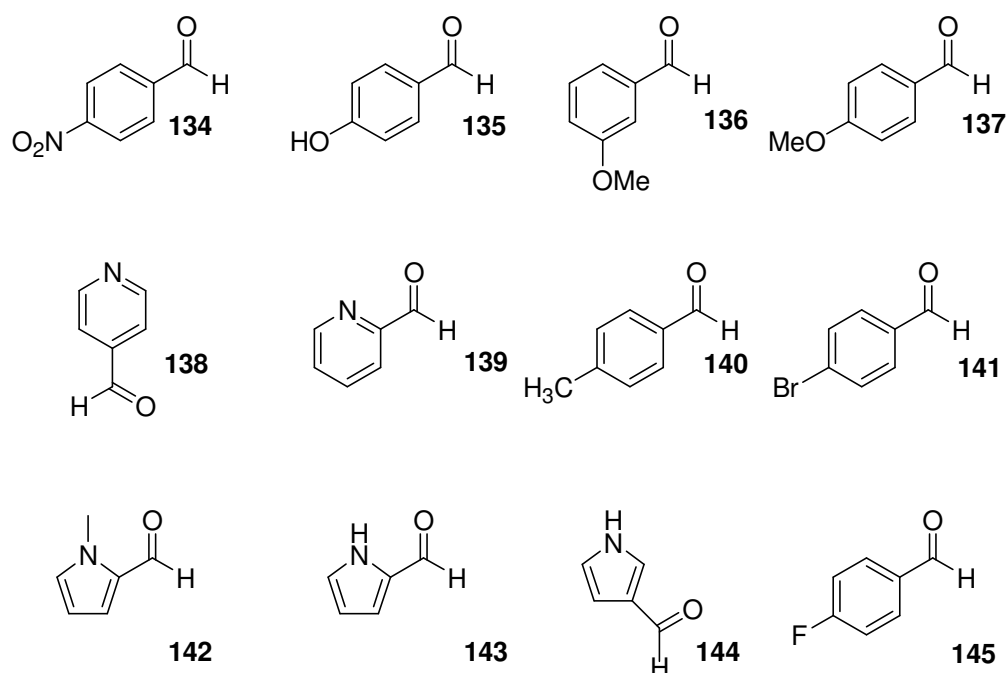


Figure 55: Various aldehyde acceptors used in the TK reaction

The rationale behind the poor substrate affinity of aromatic aldehydes is principally two fold; the solubility, and the inflexibility of the planar aromatic aldehyde to enter the narrow, deep enzyme cleft. Further work requires important X ray crystallographic data to shed light on aromatic acceptor substrates in the enzyme active site. Increased aromatic substrate activity may also be achieved by selecting mutants from another library or begin a 'second cycle' of saturation mutagenesis with existing TK mutants.

4.9 Summary

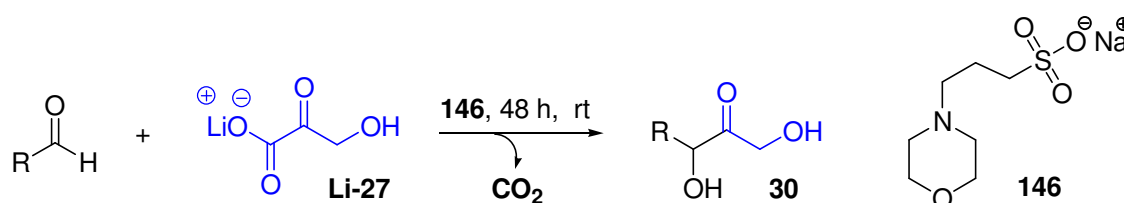
We have identified and demonstrated TK mutants with improved substrate activity towards aromatic aldehyde substrates in comparison to WT-TK. The biotransformations with TK mutants D469E, D469K and D469T and G6 with benzaldehyde and furfural afforded ketodiols in poor yields in (1-4%) with the generation of byproducts (1-4%). However the biotransformation with D469T-TK with phenylacetaldehyde and 2-phenylpropionaldehyde as substrates generated moderate yields of 50% and 40% respectively. The ees obtained for **30Ar3** was 88-96% generating the (*S*)-isomer. The TK mutants were diastereoselective for the (3*S*,4*S*)-**30Ar4** isomer with *des* ranging from 88 to 96%. The initial rate experiments with D469T revealed poor substrate specificity with aromatic aldehydes **131** and **133** in comparison to propanal as substrate due to the poor solubility of the aromatic aldehydes. Further screening of TK mutants is required for aldehydes with a nitrogen containing ring or begin a second round of mutagenesis with existing TK mutants.

Chapter 5.0

The biomimetic TK reaction

5.1 Reporting the first pioneering biomimetic transketolase reaction

The UCL Department of Chemistry and the UCL Department of biochemical engineering have a research programme to develop TK-catalysed carbon-carbon bond formation. Experiments were carried out using the enzyme TK and its cofactor ThDP in various buffered and non buffered media. Several reactions involved the use of enzyme and buffer in the reaction mixture with the omission of ThDP, or simply ThDP and buffer only. Ironically this led to the discovery that using the buffer 4-morpholine propane sulfonic acid **146** (MOPS) with no enzyme or ThDP still led to the formation of racemic α,α' -dihydroxyketones (Scheme 77). The omission of ThDP rules out the mechanistic involvement of ThDP via the thiazolium ylid, and indicates that **146** was promoting the carbon-carbon bond forming reaction.⁹⁸ Initial results involving **146** were promising, although the problems encountered were the presence of unreacted aldehyde after the course of the reaction monitored by TLC and the sluggish nature of the reaction requiring at least 72 hr at rt.



Scheme 77: Biomimetic reaction using **146** as catalyst

In light of these recent findings the aim of this part of the project was to investigate this novel one pot synthesis of racemic ketodiols, in terms of the substrate scope of the reaction. A variety of aldehyde acceptors were used: aromatic and aliphatic aldehydes. Optimisation studies and preliminary mechanistic studies were performed. Novel catalysts were synthesized and investigated for asymmetric induction in the biomimetic TK reaction.

5.1.1 Biomimetic TK research performed prior to PhD studies

To date a variety of acceptor aldehydes have been screened for biomimetic activity using MOPS and *N*-methylmorpholine (NMM). The aliphatic aldehydes in particular afforded moderate yields from 20-40%, however, aromatic aldehydes with electron donating and withdrawing substituents have been shown to be poor acceptors and gave products in poor yields <10%. The effect of pH was found to be crucial for ketodiol synthesis and the reaction proceeded at pH 7.0-9.0, however, pH 8.0 is preferential for greater yields. The reaction can be performed at room temperature and requires approximately 24-48 hours for completion. For reduced reaction times to <12 hours the temperature was increased to 30 °C to 40 °C. Several co-solvents have

shown a marginal increase ($\approx 4\%$) in ketodiol production using a 1:1 THF:H₂O or 1:1 CH₃OH:H₂O mix, but most importantly it provided miscibility between the catalyst that is often insoluble in water and the water-soluble hydroxypyruvate substrate donor.

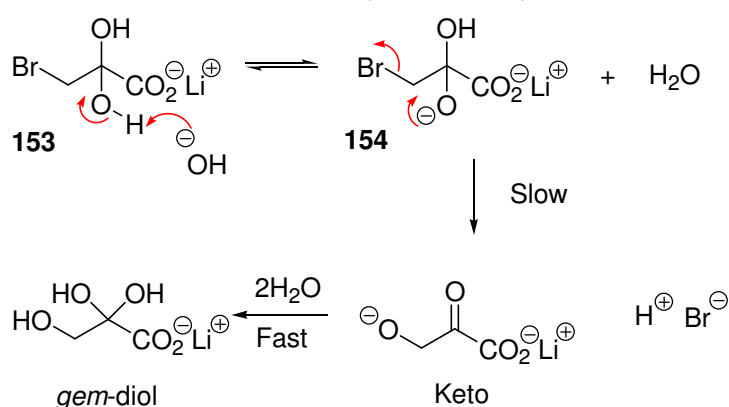
Thus far several organocatalysts were screened in preliminary investigations. DABCO **147**, DBU **148**, 3-hydroxyquinuclidine¹⁰⁹ **149** and (*R*)-(-)-2-pyrrolidinemethanol **151** were chosen for their catalytic properties in the Baylis-Hillman reaction¹¹⁰. L-Proline **150** was selected as it is known chiral organocatalyst in the aldol condensation reaction.¹¹¹ An imidazolidinone (Macmillian) catalyst **152** used in asymmetric Diels-Alder reaction was also screened.¹¹² The results suggested catalysts containing a secondary amine motif were less successful in generating ketodiol products than the tertiary amine catalysts (Table 30).

Catalyst	Structure	Yield %
147		17%
148		0%
149		27%
150		1%
151		1%
152		0%

Table 30: Catalysts used for the biomimetic TK reaction

5.2 Preparation of lithium hydroxypyruvate as a ketol donor from bromopyruvic acid

Srere *et al*, demonstrated that β -hydroxypyruvic acid is a useful donor with potential to drive the equilibrium to completion in the TK reaction. The relatively high cost involved in the preparation of β -hydroxypyruvic acid is one limitation in a large scale synthesis using this reaction. An alternative is synthesis of the lithium salt which has been reported¹¹³ but poor overall yields are typically observed (23% on a 2.5 g scale) and the salt has a low concentration in water (2.5 g from 235 ml of water). The reaction procedure has been modified to omit the recrystallisation step to generate lithium hydroxypyruvate **Li-27** with a two fold increase in yield (51 %).⁵² Thus, to 10.0 g of β -bromopyruvic acid dissolved in 100 ml of water, 1 M lithium hydroxide solution was added at such a rate the pH did not exceed pH 9.5. Studies suggested that within the pH range 7-10, a hydroxyl group is deprotonated from the *gem*-diol **153** which then initiates the elimination of the bromine **154** (Scheme 78).⁴⁷



Scheme 78: Mechanistic investigation of the formation of Li-27

Subsequent reported attempts to produce **Li-27** led to comparatively low yields and in some instances the precipitation of by-products from the reaction mixture, such as lithium bromopyruvate.⁵² It was found to be essential that the pH level remained in the critical region of pH 7-10 as increasing the basicity of the reaction mixture further by a small amount lead to the onset of a slow aldol condensation reaction.⁴⁷ Conversely if the reaction mixture was too acidic, the intramolecular nucleophilic substitution $\text{S}_{\text{N}}2$ reaction does not occur (Scheme 79).

Following the literature procedure for the preparation of **Li-27** from Turner *et al*.⁵² was carried out by stirring β -bromopyruvic in the presence of 1 M lithium hydroxide solution for an hour at pH 9.3 and then adjusted to pH 5.0 using glacial acetic acid. The lithium hydroxypyruvate present in solution was concentrated *in vacuo* and left to crystallise overnight. **Li-27** is practically insoluble in ethanol, thus by washing the crude product isolated with ethanol any starting material was removed from product. The white solid

was filtered and dried *in vacuo* to generate >95% pure **Li-27** (46 %) as a white powder **Li-27** was characterised by ^1H NMR and appeared to be hydrated in D_2O . However ^{13}C NMR spectroscopy revealed there to be six different ^{13}C environments present in solution. Three quaternary peaks were indicative of carbonyl groups at 203.0, 177.0 and 167.9 ppm. This implied that the **Li-27** salt exists in solution with the keto- **156** and the *gem*-diol **155** form (Fig. 56).

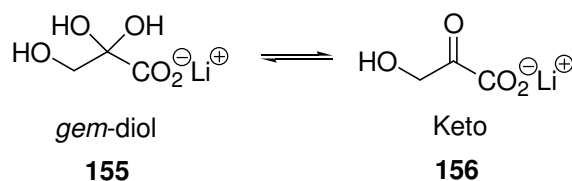


Figure 56: **Li-27** existing in *gem*-diol and keto form

The presence of a *gem*-diol had also been acknowledged by earlier research conducted by Bellamy and Williams¹¹⁴ on a similar system which showed that pyruvic acid existed in the keto form **158**, whilst the lithium monohydrate salt was in the *gem*-diol form **157** (Fig. 57).

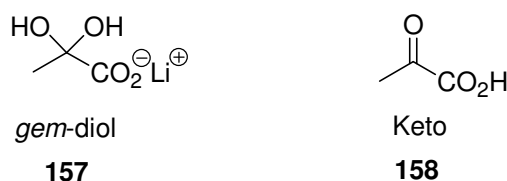
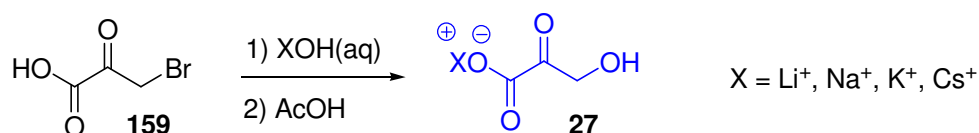


Figure 57: Pyruvic acid and lithium monohydrate salt in different forms

Fortunately the formation of the *gem*-diol **155** is in equilibrium in solution with its keto-tautomer **156** and there is no mention in the literature of any problems in using the lithium-salt substrate **Li-27** in biotransformations.

5.2.1 Other alkaline metal hydroxypyruvates and their reactivity in ketodiol synthesis

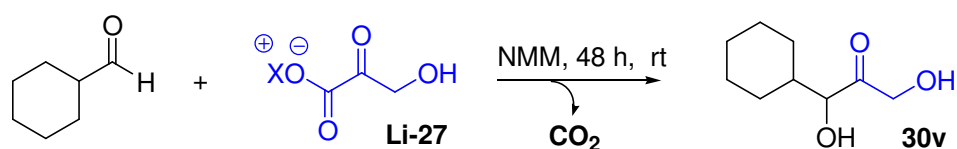
Other alkaline metal hydroxypyruvates were synthesized from the corresponding metal hydroxides using a similar procedure to that used for **Li-27** preparation (Scheme 79).



Scheme 79: The formation of hydroxypyruvate salt

The percentage conversion from the bromopyruvate **159** to the desired hydroxypyruvate increased down the alkaline metal series and the colour of the crystals changed from white with **Li-27** to brown cesium hydroxypyruvate **Cs-27**. This may possibly due the

small traces of impurities. All alkaline hydroxypyruvate salts displayed the same ^1H NMR resonances in D_2O as the lithium salt; an approximate 55: 45 ratio in favour of the 'keto' form over the 'gem-diol' form. The hydroxypyruvate salts were investigated separately by reacting the substrates with cyclohexanecarboxaldehyde (1.0 equiv) in the presence of *N*-methylmorpholine (1.0 equiv) dissolved in water (50 mM concentration) for 48 h. The ketodiol yields from the various hydroxypyruvate salts implied the varying degrees of reactivity in aqueous solution (Table 31). Thus, the cation must serve an important function to facilitate the carbon-carbon bond forming reaction. The **Cs-27** salt was reacted with cyclohexanecarboxaldehyde in the presence of NMM in water, and the product **30v** was formed in 50% yield. A significant 30% increase in comparison with the lithium salt. This could be a result of counterion effects; the lithium ion is smaller and has a greater charge density than cesium and has the ability to polarise anions and induce a more covalent character. Cesium with its low charge density and its large polarisability differs with other alkali metal salts; with the lowest degree of solvation properties and ion pairing.

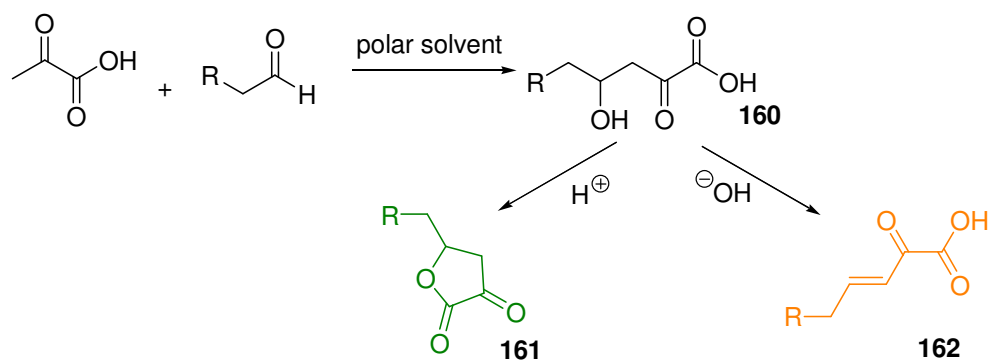


X	Formation of HPA salt	30v
	%	%
Lithium	46	25
Sodium	20	29
Potassium	72	38
Cesium	100	50

Table 31: The formation of HPA salt and the ketodiol product 30v

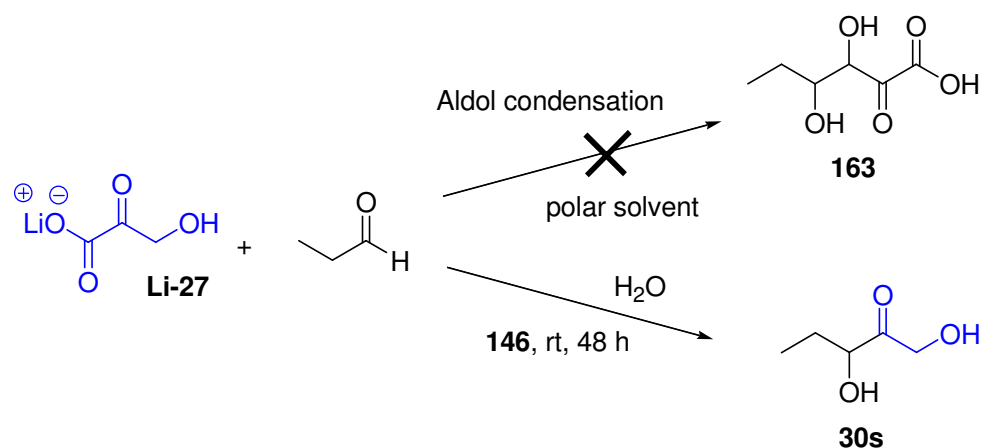
5.3 Aliphatic aldehydes as acceptor molecules for the biomimetic TK reaction

There have been few reactions reported between aliphatic aldehydes and α -keto acids in the literature.¹¹⁵ One example is the reaction between pyruvic acid and aliphatic aldehydes to yield α -keto- γ -hydroxy acid **160** in a polar solvent⁴⁸ via a direct aldol condensation reaction (Scheme 80). In acidic conditions **160** cyclizes to a lactone **161**, and in basic conditions to an α -keto- β,γ -unsaturated acid **162** (Scheme 80).^{48,116,117}



Scheme 80: The direct aldol condensation of pyruvate and an aliphatic aldehyde in polar solvent

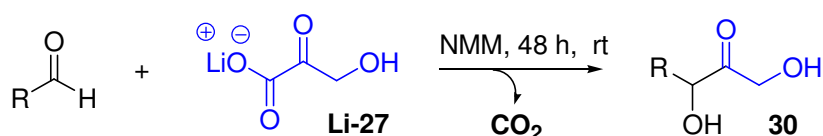
However when **Li-27** was used in the reaction with propanal in the presence of **146** (MOPS) the formation of the α - α' dihydroxyketone was observed (**30s**, 18%). The addition occurred at the α -keto carbon of the acid evolving carbon dioxide during the reaction (Scheme 81). The requirement for a tertiary amine such as **146** suggested that the mechanism mimics the transketolase reaction (See Chapter 3 and 4).



Scheme 81: Reactions of α -keto acids

The reaction between **Li-27**, propanal with MOPS **146** in a non-buffered media was a slow reaction requiring at least 48 h to generate **30s** in a low yield. It had been found after screening amines containing similar heterocyclic rings that *N*-methylmorpholine (NMM) also promoted the carbon-carbon bond forming reaction with better yields. Therefore both MOPS **146** and predominantly NMM were used as the catalysts in this investigation.

Other aliphatic aldehydes were used to synthesize racemic ketodiols as useful tools for chiral assay development and as acceptor substrates for the TK reaction. The reaction mixture was stirred using stoichiometric amounts of catalyst NMM, **Li-27** and aldehyde to generate ketodiol products in low yields ranging from 10-25% (Table 32).



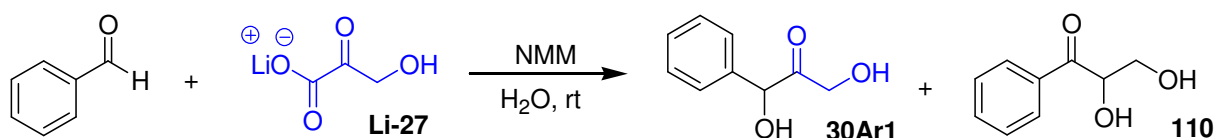
R	30	Yield %
	s	22
	w	25
	v	10
	x	25
	y	25

Table 32: The TK biomimetic reaction of ketodiol 30

In all cases with aliphatic aldehydes traces of by-products under non-adjusted pH conditions were observed which were easily removed by purification using column chromatography. Cyclohexanecarboxaldehyde was the aliphatic aldehyde of choice for further mechanistic studies, biotransformations and the investigations into asymmetric biomimetic reactions.

5.4 Aromatic aldehydes as acceptor molecules for the biomimetic TK reaction

The reaction was also carried out using benzaldehyde with **Li-27** in non-pH adjusted reaction mixtures involving NMM, and was left to stir for 48 h. The ketodiol was not produced instead an isomer was isolated (**110** rearranged, 5%).



Scheme 82: The formation of ketodiol product 30Ar1 and the rearranged product 110

Spectrum A (Fig. 58) shows the expected ^1H NMR spectra of the ketodiol product **30Ar1** with the distinctive AB system diastereotopic protons H_A and H_B at 4.30 and 4.38 ppm. A singlet at 5.36 ppm is the α -H. Spectrum B (Fig. 58) shows the ABX system, indicating the rearrangement of **30Ar1** to form **110**. The methylene protons H_A and H_B are still diastereotopic but the coupling pattern has changed due to the coupling with the α -H on the adjacent carbon.

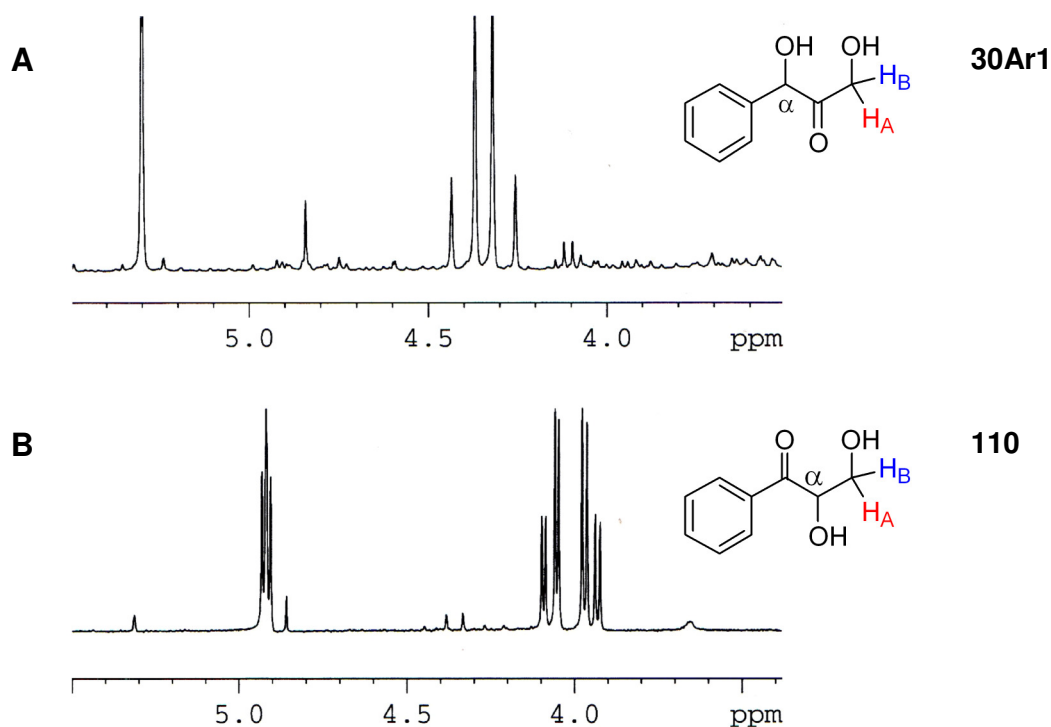
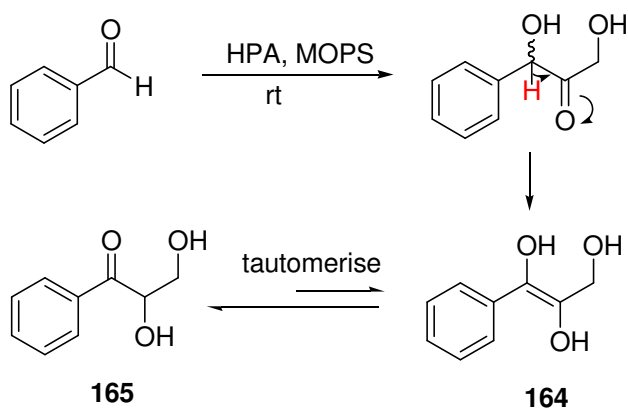


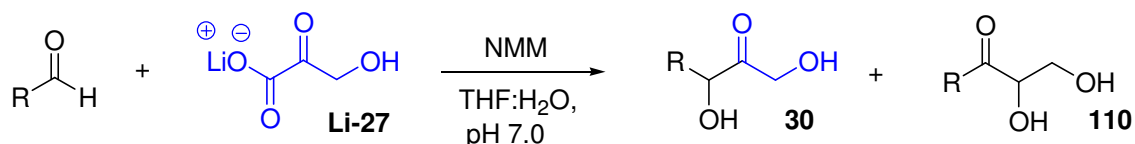
Figure 58: ^1H NMR of **30Ar1 and **110****

The desired ketodiol was however synthesized using NMM at an adjusted pH 7.0 for over 48 hours (**30Ar1**, 5%). The **Cs-27** donor substrate was also investigated in the presence of benzaldehyde (1.0 equiv.) and NMM (1.0 equiv.) and reaction was maintained at pH 7.0 obtaining **30Ar1** in 10% yield. The rearranged product **110** could be formed via the desired ketodiol **30Ar1** due to the acidity of the α -H and formation of the enediol **164** which tautomerises to form the preferred oxo tautomer **165** in conjugation with the benzene ring (Scheme 83). Most important of these initial findings was the rearrangement of the isolated ketodiol after one week in water rearranging to the more stable constitutional isomer **165**. Further investigations involved the use of benzaldehyde as the aromatic aldehyde of choice for use in biocatalytic ketodiol synthesis.



Scheme 83: Mechanism for the rearrangement of ketodiol to generate 165

Other aromatic aldehydes were used as substrates for the biomimetic TK reaction (Table 33). The aromatic ketodiols generated were further used as tools for the development of an HPLC assay. The biomimetic reaction with 2-phenylpropion-aldehyde as the acceptor substrate to generate ketodiol **30Ar4** was determined to be *anti*-diastereoselective (4:1) at pH 7.0 (Chapter 4). The yields varied in range from 4-20% with small amounts of isolated 'rearranged products' **110a** and **110d**.

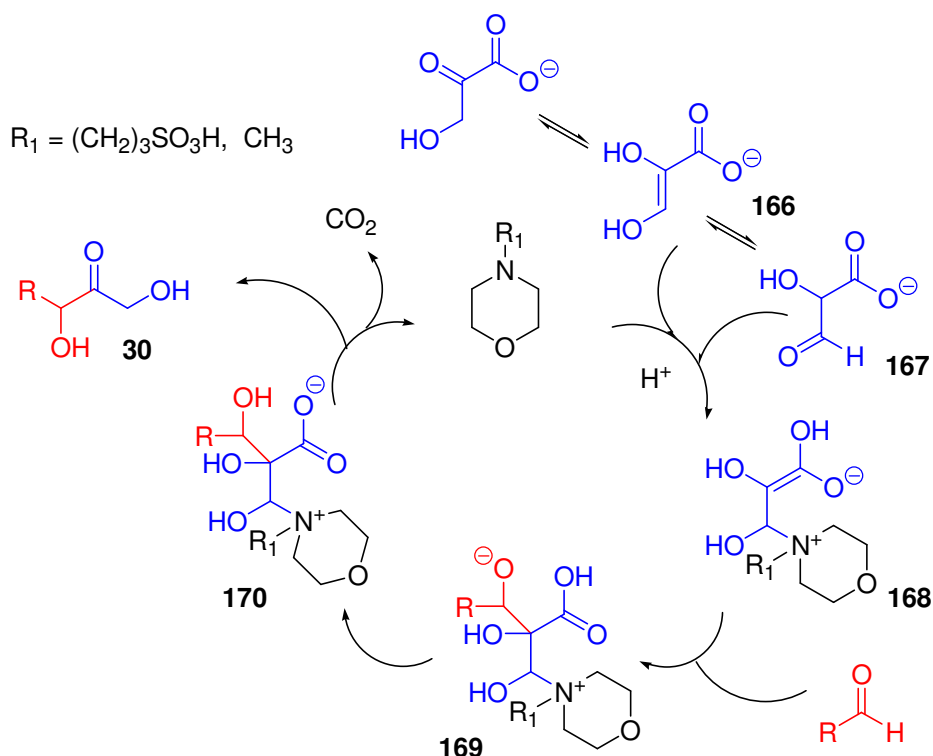


R	Yield (%)
	30Ar2 (4) 110a (2)
	30Ar3 (15) 110b (0)
	30Ar4 (20) 110c (0)
	30Ar5 (4) 110d (1)
	30Ar6 (5) 110e (0)
	30Ar7 (5) 110f (0)

Table 33 Aromatic aldehydes used in the biomimetic TK reaction conducted pH 7.0
5.5 Mechanistic implications

5.5.1 Postulated reaction mechanism

To date, a reaction mechanism has been proposed to be reminiscent of the Baylis-Hillman reaction.¹¹⁸ The catalyst used is a tertiary amine and what is proposed is the formation of the quaternary ammonium enolate **168** which has been described in cyclopropanation reactions.¹¹⁹ Thus the carbanion enolate **166** or tartronic acid semi aldehyde **167** is formed leading to the conjugate addition of the amine. The presence of another heteroatom or an alcohol side chain in the tertiary amine may through hydrogen bonding stabilize enolate. Addition of the aldehyde **169**, proton transfer to yield **170**, subsequent elimination of the tertiary amine and decarboxylation at the end of the reaction releases the racemic ketodiols (Scheme 84).



Scheme 84 Postulated biomimetic reaction mechanism

5.5.2 NMR investigations using bromopyruvate and hydroxypyruvate

In order to understand why these substituted pyruvates, hydroxy- and bromopyruvate react differently *in situ*, the nature of the anions was monitored under aqueous conditions. Fisher et al. (1982)¹²⁰ have reported the predominant structure for 3-bromopyruvate in D_2O is the hydrated *gem*-diol form. The evidence was based upon UV spectroscopy and reported an equilibrium constant of 1.84.¹²¹ This equilibrium can also be observed via a number of ^1H NMR observations taken in D_2O . Rather than a single resonance of the methylene protons, two resonances are observed for **Li-27**; a large signal at δ 3.71 ppm and a smaller signal at δ 4.61 ppm. The two methylene

protons are chemical shift equivalent and these two resonances must derive from different 'forms' of bromopyruvate, most likely the 'keto' and the hydrated *gem*-diol form. Thus, the methylene protons of the keto form are at δ 3.71 ppm and those of the *gem*-diol at δ 4.61 ppm, a ratio 1:21 in favour of the *gem*-diol at pH 2.61 (Fig. 59, spectrum B). At a higher pH the relative intensities of the keto form only slightly increased to 15% at pH 7.35.

Fischer concluded that nucleophilic attack of H₂O or ⁻OH on the 3-halogen position in comparison with hydration was slow in all cases. All the α -hydroxypyruvate alkaline metal salts synthesised, yielded two resonances, singlets at δ 4.60 ppm (keto) and δ 3.54 ppm (*gem*-diol). In comparison with 3-bromopyruvate, the ratio of these two peaks were at approximately 1:1, in slight favour of the keto form at pH 7.50 (Fig. 59, spectrum B). The differences between the 3-bromopyruvate and the α -hydroxypyruvate, is not unexpected, however the electron withdrawing halide in bromopyruvate will facilitate attack by water on the keto carbon. Reports have conducted that the *gem*-diol species is the predominant form in fluoropyruvate at pH 6.3 (*gem*-diol:keto ratio, 6:1), but not evident in pyruvate itself.

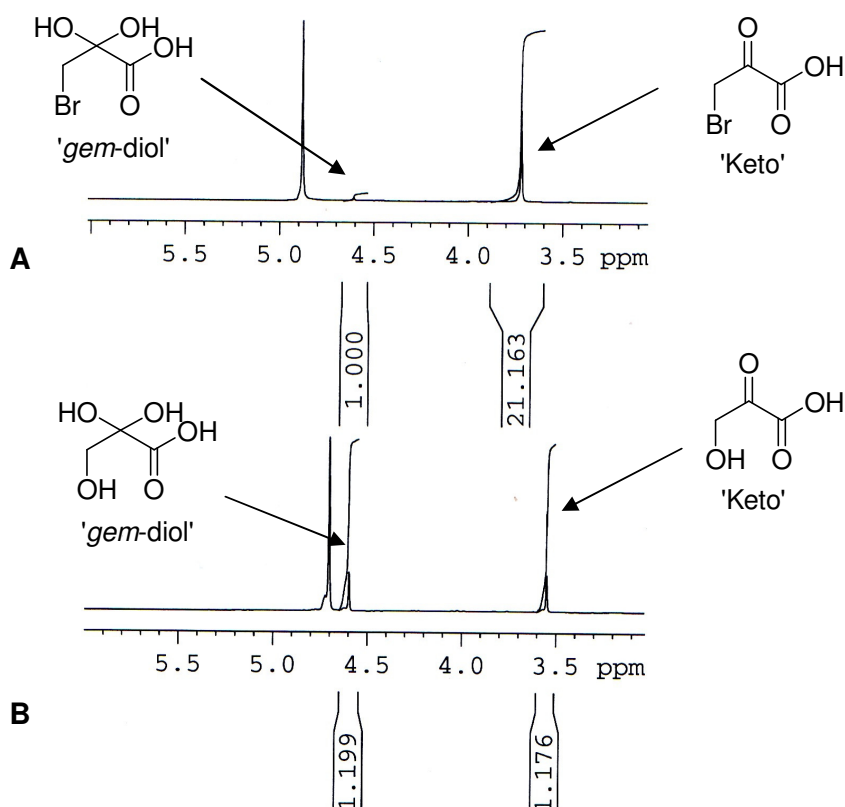


Figure 59: (A) bromopyruvate, pH 2.61; (B) alkaline metal- HPA salt, pH 7.50

The degree of *gem*-diol formation by the respective anions at the 3-carbon position can be viewed as a measure of the reactivity on the carbonyl carbon, since the *gem*-diol is formed from the attack of a weakly nucleophilic water molecule as a result of the electron-withdrawing effect of the substituents on the third position. The order $F > Br > OH > H$ is in fact observed (Fig. 60). This ordering of substituent electronegativities and *gem*-diol formation by the respective anions can be used to explain the apparent limitations of **Li-27** as donor affording moderate ketodiols yield and also predict whether fluoropyruvate and pyruvate could be potential donors. The electron withdrawing substituents determine the reactivity of the carbonyl carbon towards nucleophilic attack by both an amine and water present *in situ*. Thus the keto-moiety in 3-bromopyruvate is too reactive and predominantly hydrating, effectively removing most of the reactive keto form from solution by preventing the formation of the postulated quaternary carbanion enolate **168** (Scheme 84), leading to the conjugate addition of the tertiary amine catalyst. In comparison, approximately 55% of **Li-HPA** exists as the 'keto' form and is less readily hydrated than 3-bromopyruvate affording low to moderate ketodiols yield dependent on the alkaline metal HPA salt synthesised.

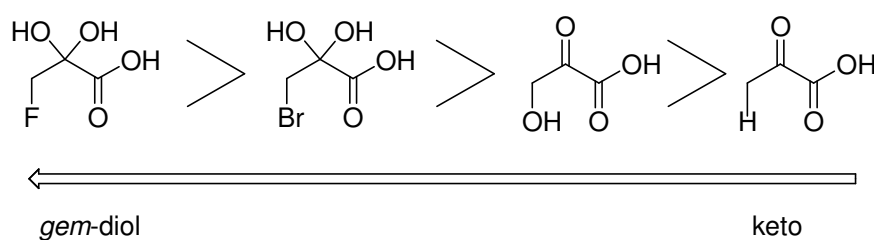


Figure 60: The major forms of pyruvates existing in water

However a preliminary investigation, has recently reported pyruvate (the free acid) and the sodium salt failed to give any reaction under these biomimetic conditions.¹⁶ In light of these findings, there is a need to reassess the model by further consideration of different α -keto acid substrates; notably on the free acid or the salt equivalent. It appears the hydroxyl- group and the availability of the keto group is an essential requirement on the 3-position and must stabilise the quaternary carbanion enolate **168**, similar substituted pyruvates with similar electron withdrawing properties could be considered as well as the effect of the hydroxyl-group on a longer carbon chain analogue (Fig. 61).

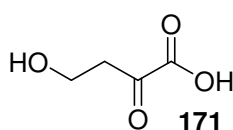
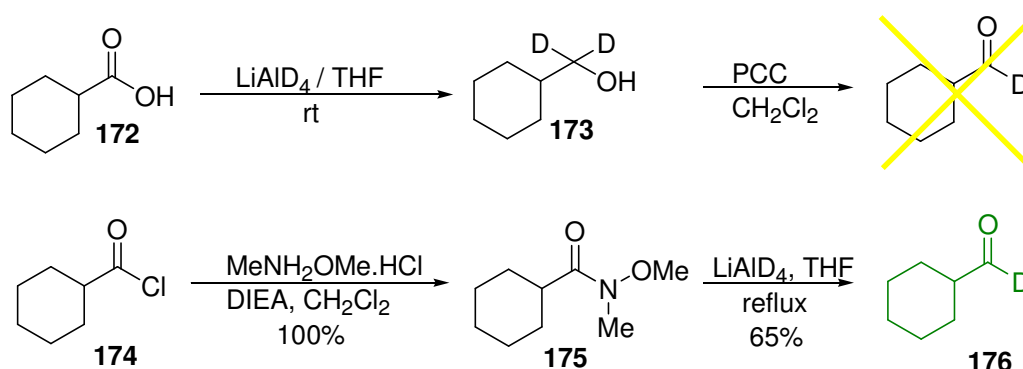


Figure 61 A donor acceptor substrate

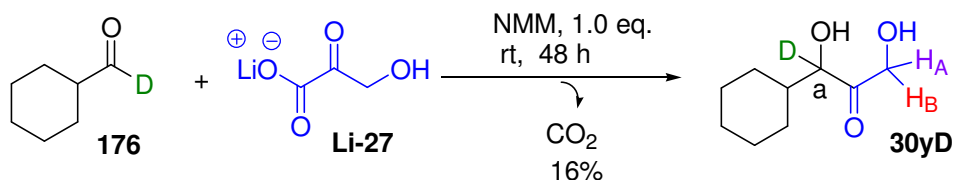
5.5.3 Synthesis of [1-²H]-cyclohexancarboxyaldehyde and its use in ketodiol synthesis

To further elucidate our understanding of the proposed mechanism, a deuterated aldehyde was synthesized to investigate any deuterium exchange after coupling of the aldehyde (Scheme 85). The initial methodology for synthesizing the deuterated aldehyde for mechanistic studies required a two step synthesis, involving the reduction of the commercially available cyclohexanecarboxylic acid with lithium aluminium deuteride (LiAlD₄) to obtain the deuterated alcohol **173** in 70% yield. The alcohol was subjected to mild oxidative conditions using pyridinium chlorochromate (PCC). Several difficulties ensued with the separation of the unreacted alcohol, the deuterated aldehyde product **176**, and traces of the over-oxidised carboxylic acid. To rectify this problem, an alternative route via the Weinreb amide¹²² was investigated avoiding the problem of over-reduction to the alcohol due to a highly stable metal-chelated intermediate. Benzotriazol-1-yloxy)tris(dimethylamino)-phosphonium hexafluorophosphate (BOP) was used as a coupling reagent with cyclohexanecarboxylic acid to synthesize the Weinreb amide product **56**, in 75% yield. However to scale up the reaction the high cost of BOP led to the use of an alternative method. Instead, cyclohexanecarbonyl chloride **174** was reacted directly with the *N,O*-dimethylhydroxylamine hydrochloride in the presence of *N,N*-diisopropyl-ethylamine (DIEA) to obtain the Weinreb amide **175** in quantitative yield. This was then reduced using lithium aluminium deuteride (LiAlD₄) to the aldehyde **176**. Some unreacted starting material was readily removed by an acidic workup to give the pure aldehyde in 65% yield.



Scheme 85: Formation of deuterated aldehyde **176**

The biomimetic reaction using the newly synthesised deuterated aldehyde **176** with **Li-27** in the presence of NMM as catalyst (Scheme 86) was investigated at two different pHs; at pH 8.0 (maintained using a pH stat autotitrator), and an unadjusted pH which was monitored after 48 hours was pH 9.7.



Scheme 86: Biomimetic reaction involving deuterated aldehyde

The ^1H NMR spectral data of product **30y** at different conditions were collated and revealed an AB system with diastereotopic protons at δ 4.75 ppm (H_A) and δ 4.35 ppm (H_B) as usual, with α -H proton at **a** was observed at δ 4.15 ppm (Fig. 62, spectrum A). When using **176** at pH 8.0 (Fig. 62, spectrum B) the α -H absorption was absent from the ^1H NMR at δ 4.15 ppm of **30yD**. This implied there was no apparent deuterium exchange after coupling

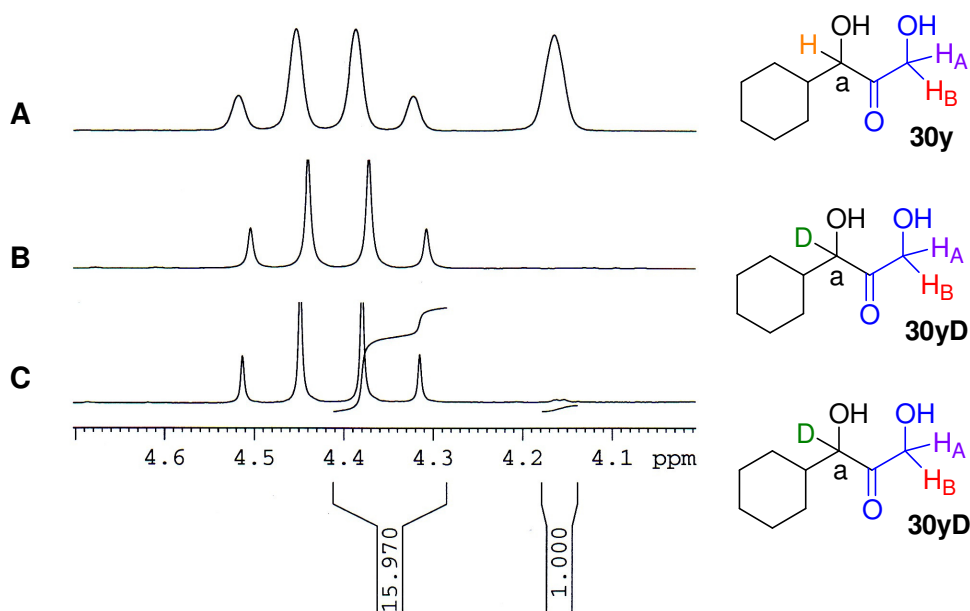


Figure 62: ^1H NMR spectra of ketodiol production with aldehyde (A); generated ketodiol product at pH 8.0 with **176 (B); and at pH 9.7 with **176** (C)**

This was further verified by the ^{13}C NMR data and splitting by the deuterium nucleus of the single at δ 80.8 ppm into a triplet (J 25.0 Hz). At pH 9.7 notable deuterium exchange at the α -H with a small amount 1:16 (D:H) deuterium transfer occurring implying a slow epimerisation. Also that tautomerisation at **a** is not involved in the biomimetic mechanism. This highlighted that although the C-H bond is weaker than C-D, at pH <9 epimerisation is unlikely to occur and application in a biomimetic asymmetric reaction is worthwhile exploring.

5.5.4 Deuterium oxide experiments used in ketodiol synthesis

In the biomimetic reaction, metal-hydroxypyruvate salts are soluble in aqueous solution and the reaction can proceed successfully if the catalyst and aldehyde are homogenous in solution. Continuing with our on-going mechanistic investigations, the reaction was conducted in D₂O to investigate the nature of the carbanion or enol intermediate **166** upon conjugate addition of the tertiary amine. The D₂O reactions investigated were at pH 7.0 and pH 8.0 adjusted by a pH stat autotitrator, injecting small amounts of 1 M hydrochloric acid if the reaction became slightly basic. Therefore some residual H₂O would be present in the reaction (Fig. 63).

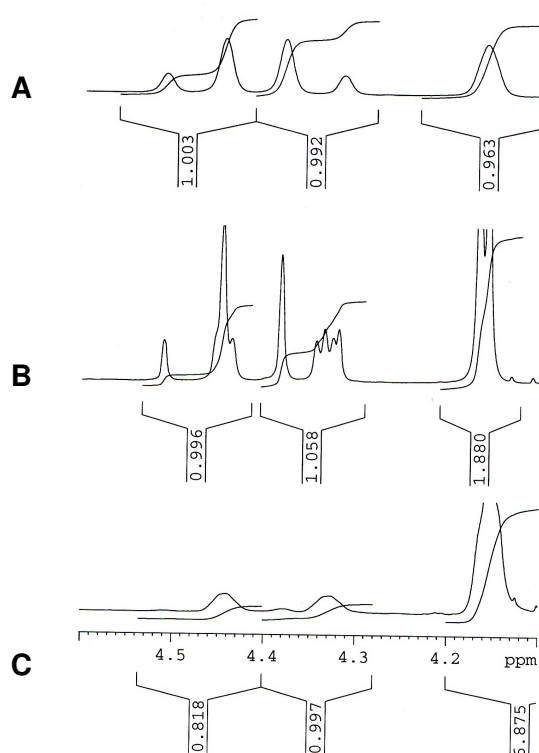


Figure 63: NMR spectra of ketodiol production (A) H₂O solution at pH 8.00; (B) D₂O solution at pH 7.00; (C) D₂O solution at pH 8.00

The spectral data of the control reaction conducted in water at pH 8.0 demonstrates a clear symmetrical integration of the diastereotopic protons H_A and H_B in due to the (Fig. 63, spectrum A). The product isolated from the D₂O reaction mixture at pH 7.0 revealed the introduction of deuterium due to the reduced integration of the diastereotopic protons compared to α' -H proton at **a** and the unsymmetrical broadening of these absorption peaks due to geminal coupling CH-D. The increase of pH led to an increase in rate of deuterium exchange of the diastereotopic protons as expected, as indicated by the severe broadening of the peaks and further reduced peak integrations.

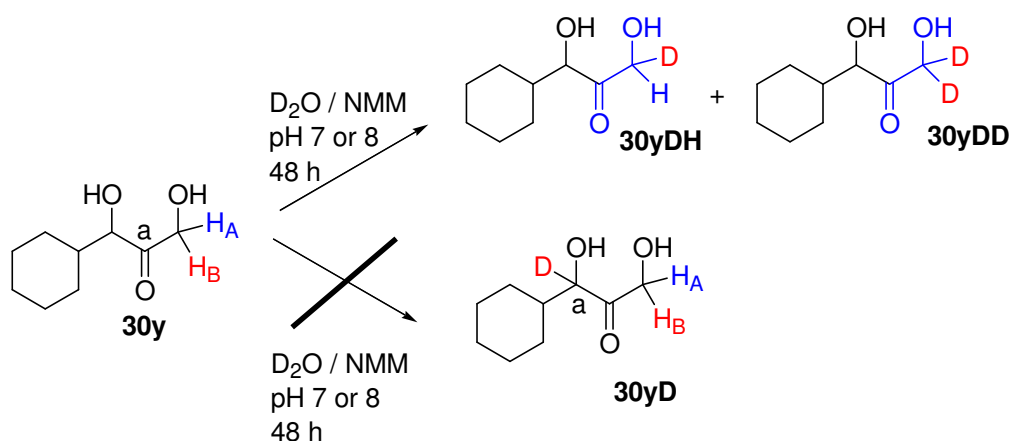
The products determined by mass spectrometry reveal the presence of compounds **30yDH**, **30yDD** and **30y** (Fig. 64).



Figure 64: Deuterated containing compounds **30yDH** and **30yDD**

So, by increasing the pH between the values 9-10 will complete the deuterium exchange at the diastereotopic protons. The D_2O experiments would be in agreement with the formation of the carbanion enolate or enol intermediate **166** prior to the addition of the tertiary catalyst. However deuteriums exchange could also occur after **30y** is formed in D_2O media. Another experiment in D_2O was carried out using **30y** in the presence of NMM (1.0 eq.) only to assess tautomerisation at **166**. These separate D_2O solutions were maintained at pH 7.0 and pH 8.0 and were left to stir for 2 days.

There is a possibility that deuterium exchange can occur at either the α -H or the diastereotopic protons as two enolates can be formed. It was expected (*c.f.* 1, 3-dihydroxypropiofenone) that the α -H is the more acidic, and would lead to enolate formation under thermodynamic control. However, formation of the kinetic enolate was observed due to the less sterically crowded α -protons generating **30yDH** and **30yDD** (Scheme 87). The resulting spectra obtained were comparable to that of spectra B and C (Fig. 63), and no enolization of the α' -H at **a** was observed leading to **30yD**. More deuterium labelled experiments maybe required to elucidate the mechanism further.



Scheme 87: Pathway favoring kinetic enolate **30yDH** and **30yDD**

5.6 Cinchona alkaloid catalysts for ketodiol synthesis

Cinchonine **177**, cinchonidine **178**, quinidine **179** and quinine **180** are members of the cinchona alkaloid family that are commercially available at low costs (Fig. 65).¹²³ They are comprised of two ring structures, quinoline and the nucleophilic quinuclidine core, comparable in nucleophilicity to that of piperidine, pyridine and morpholine towards carbonyl containing molecules.¹²⁴ The β -hydroxyamine part of the molecule is responsible for inducing stereoselectivity, in theory if cinchonine affords one enantiomer via catalysis, cinchonidine generates the opposite enantiomer with comparable enantioselectivities. The structure of the cinchona alkaloids and its shelf-life chemical stability makes it a suitable molecule for use in asymmetric synthesis, and they were selected for use in the biomimetic reaction.

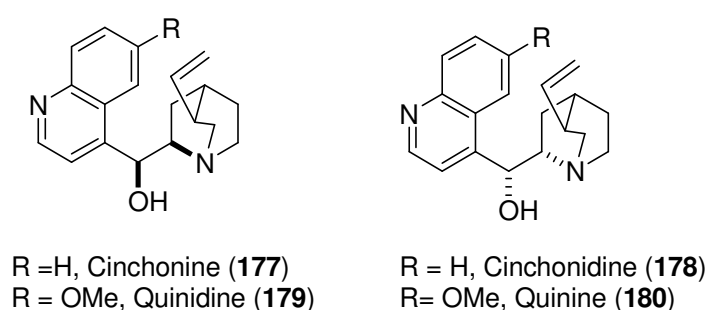
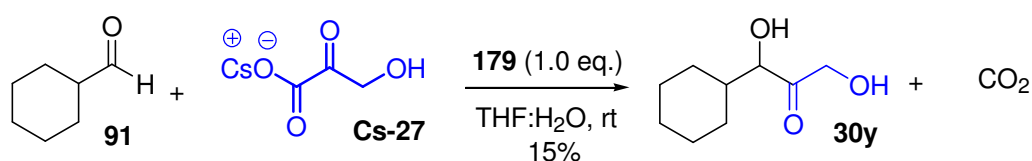


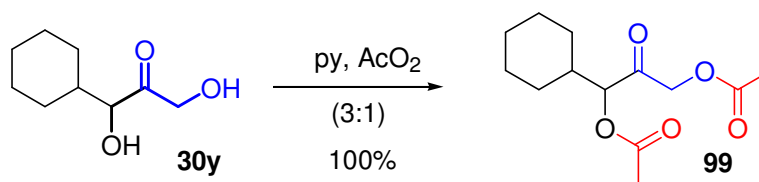
Figure 65: The cinchona alkaloids

The first cinchona alkaloid screened as a 'catalyst' was quinidine **179** (1.0 mol equiv), together with **Cs-27** (1.0 mol equiv) and cyclohexanecarboxaldehyde (1.0 mol equiv.) in aqueous media. The poor solubility of quinidine led to the reaction being stirred vigorously for 72 hours. However, only a trace amount of ketodiol product was detected by TLC analysis. This problem was circumvented by the introduction of a co-solvent capable of dissolving the catalyst that was also miscible with water. The reaction mixture was comprised of a THF:water (1:1) solution which provided an overall homogeneous system for ketodiol synthesis. The ketodiol product was detected by TLC after 6 hours and was isolated after 24 hours, affording ketodiol product **30y** in 15% yield.



Scheme 88: Using quinidine as a catalyst for biomimetic TK reaction

Ketodiol **30y** formed using quinidine (1.0 equiv.) was acetylated under standard conditions using pyridine, with the presence of acetic anhydride with catalytic amounts of DMAP. The acetylated ketodiol **99** analysed using chiralpak-AD column at a 1 ml min⁻¹ flow rate, eluting with a hexane:isopropanol (98:2) isochratic solvent system. The isomers were detected and successfully separated at 12.0 mins and 13.6 mins with equal integrations (Fig. 66, spectrum A). The ketodiol product resulting from the quinidine **179** reaction was subjected to acetylation and analysed via HPLC. A racemic mixture was detected with two peaks at 12.0 min and 13.9 min of equal integration (Fig. 66).



Scheme 49: Acetylation of **30y** to generate **99**

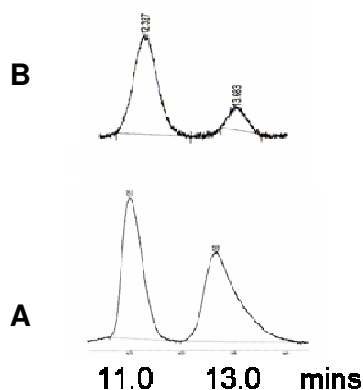
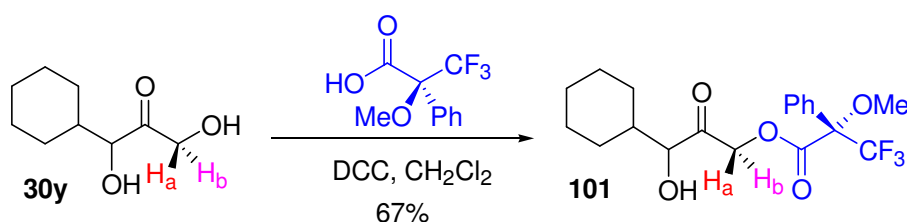


Figure 66: Diacetylated racemic ketodiol product (A) and quinidine catalysed product (B)

Initially, the cinchonine-catalysed ketodiol product formed using the same reaction conditions as for quinine **180** showed some degree of enantioselectivity (Fig. 65, spectrum B), in favour of the isomer with the faster eluting time. It was calculated that approximately 70-75% ee of the major isomer was apparently achieved.

Another analytical tool for elucidating the presence of enantiomeric excess is via the use of a chiral derivatising agent as previously described; (*S*)-(-)- α -methoxy- α -(trifluoromethyl)-phenylacetic acid (*S*)-MTPA was used to form the Mosher's ester (**101**).⁷⁴



Scheme 89: Formation of the Mosher's ester **101**

The enantiomeric excess can be determined approximately by the differing chemical shifts of H_a and H_b and integrations of these signals in the ¹H NMR spectra. The cinchonine- catalysed ketodiol product was reacted with *N,N'*-dicyclohexylcarbodiimide (DCC) and (*S*)-MTPA to form the Mosher's ester at the primary alcohol position **101** in 67% yield. Surprisingly the integration from the coupling pattern of the diastereotopic protons revealed the presence of a racemic product (Fig. 67). A further sample of the ketodiol generated from quinindine **177** was acetylated again and analyzed via HPLC which verified the cinchonine ketodiol product **30y** was indeed racemic.

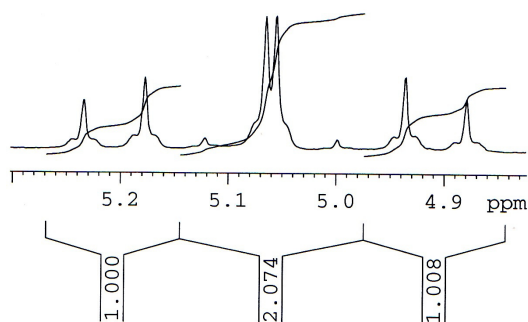


Figure 67: Racemic mixture of Mosher's ester 30y

Various attempts have been made to reproduce the initial results indicating high ees, solutions containing, 5 mol%, 10 mol%, and 50 mol% of the cinchonine catalyst were screened but racemic ketodiol products **30y** were again detected via HPLC and upon formation of the Mosher's ester. The concentration of the reaction mixture was also investigated, including the standard 50 mM solution to 100 mM, 200 mM and 500 mM concentrations, each affording racemic products of **30y**, via acetylation and HPLC analysis.

It was concluded that a contaminant may have masked the true HPLC data. The acetylated ketodiol products were measured at a wavelength of 214 nm, using a 10 μ l injection sample, and one problem associated with acetylated ketodiol products was the low sensitivity when detecting the signals. A larger experimental error may therefore ensue and the peaks were sometimes difficult to resolve. This was circumvented by benzoylating the ketodiol product with a more readily detectable chromophore (See chapter 3). The mono-benzoylated ketodiol product **100**, gave a better detection sensitivity and resolution between the enantiomers increased, but with longer eluting times at 12.0 and 13.6 mins under isocratic conditions (hexane:isopropanol; 97:3).

The biomimetic TK reaction using stoichiometric amounts of quinine **180** catalyst in a 1:1 THF:H₂O reaction solution was performed resulting in a 17% product yield. Other

reaction condition, involved reducing the catalyst loading to 20 mol%. The reaction became sluggish, but ketodiol was obtained after 48 hours in 5% yield. The ketodiol was benzoylated and the 10 μl sample was analysed by HPLC which revealed a 5% ee (*R*-isomer) for the reaction conditions using 20 mol% quinine as catalyst compared to the racemic ketodiol product generated when 1.0 equiv of quinine was used (Fig. 68).

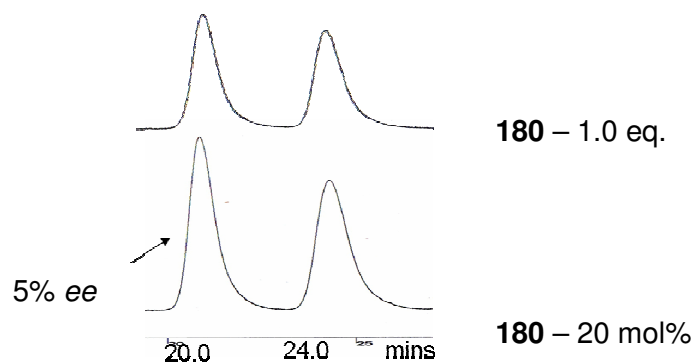
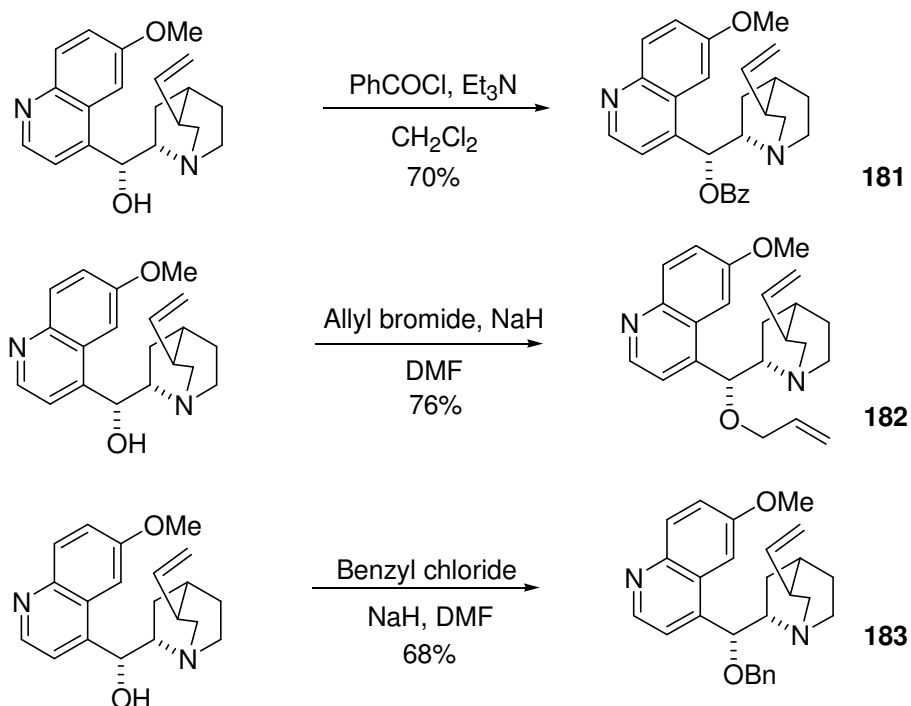


Figure 68: The HPLC trace of quinine catalysed biomimetic reaction

5.6.1 Synthesis of cinchona alkaloid catalysts

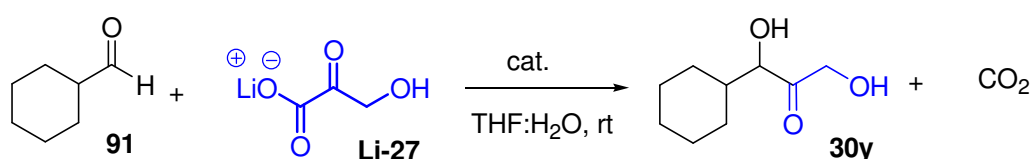
The preliminary findings, prompted us to investigate other cinchona alkaloid analogues previously used in asymmetric catalytic reactions. Thus compounds **181-183** were synthesized from quinine by modification of the hydroxyl group to the ether **182**, **183** or to the formation of the ester **181**, as previously described (Scheme 90).¹²⁵



Scheme 90: Formation of quinine analogues

5.6.2 Organocatalytic TK reaction using the cinchona alkaloid catalysts

The biomimetic reactions were performed with the synthesized cinchona alkaloids using 1.0 equiv. or 20 mol% of catalyst in a 1:1 THF:H₂O solution. The reactions were stirred for 48 hours and purified as before by silica chromatography using a 1:1 EtOAc:hexane solvent system. The isolated ketodiols were benzoylated and inspected under HPLC conditions previously described. The results reveal the products were formed in low yield with poor ees obtained. Reducing the catalyst loading lowered the yield approximately two-fold. The addition of a bulky side group on the hydroxyl moiety increased the ees (Table 34, **183**, 20 mol%).



Catalyst	Conversion (%)	ee (%)	Major isomer
181 , 1.0 eq.	18	8	(<i>R</i>)
181 , 20 mol%	7	4	(<i>S</i>)
182 , 1.0 eq.	15	4	(<i>R</i>)
182 , 20 mol%	4	3	(<i>S</i>)
183 , 1.0 eq.	14	0	-
183 , 20 mol%	5	19	(<i>R</i>)-

Table 34: Biomimetic reaction with acceptor aldehyde **91** with various catalysts

The absolute stereochemistry of **30y**, was determined by comparing the HPLC analysis from the biotransformation product of mutant D469T TK (Fig. 69) (see previous chapter 3).

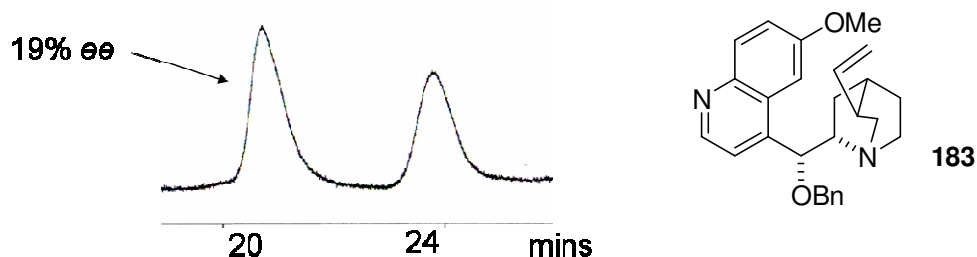


Figure 69: The HPLC trace of the biomimetic reaction using catalyst **183**, 20 mol%

Following the proposed mechanism and formation of the zwitterionic species, the approach of the aldehyde leads to two diastereomeric transition states that can predict the isomer formed. The model suggests the role of the hydroxyl groups in HPA is to lock the conformation of the complex by hydrogen bonding to one of the lone pairs of

the aldehyde carbonyl, but also lowers the energy of the transition state by stabilising the negative charge developing on the oxygen atom during the addition. The function of the benzyl group which gave the 19% ee is not clearly understood, but presumably due to steric interaction may interfere with the addition of the aldehyde to the zwitterionic complex (Fig. 70).

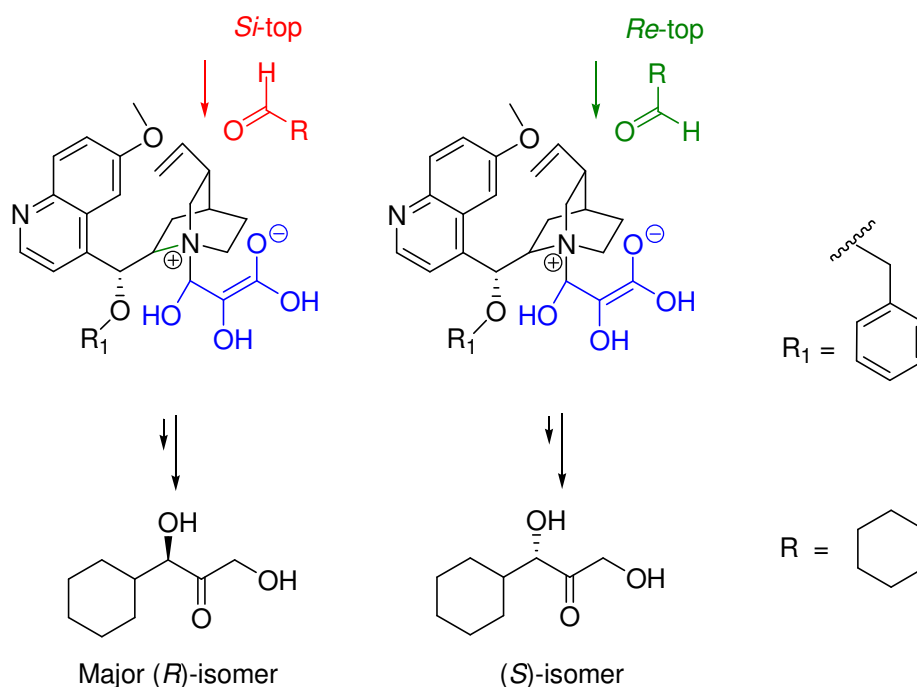


Figure 70: A postulated intermediate for the generation of ketodiol using 183

Preliminary investigations involving commercially available cinchona phase transfer catalyst *N*-benzylcinchoninium chloride was also investigated, however no product was generated. This is presumably due to problems with quaternisation of the nucleophilic tertiary amine moiety. Other commercially available cinchona ligands; (DHQD)₂PHAL and (DHQD)₂AQN were screened, both affording poor yields of **30y** (1%) and ees (3%) (Fig. 71).

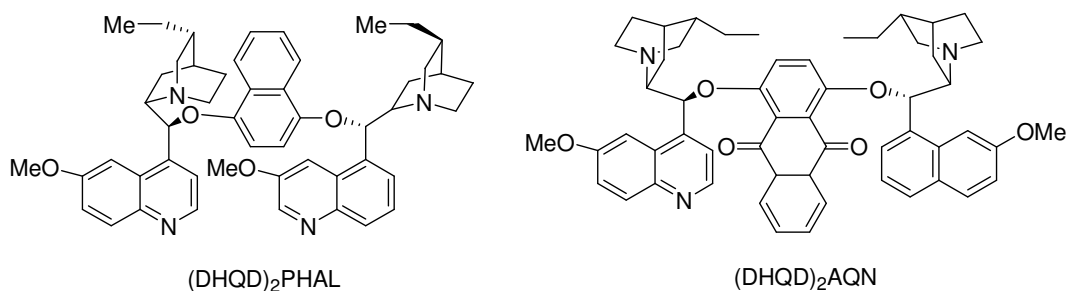


Figure 71: Screening of commercially available cinchona alkaloids

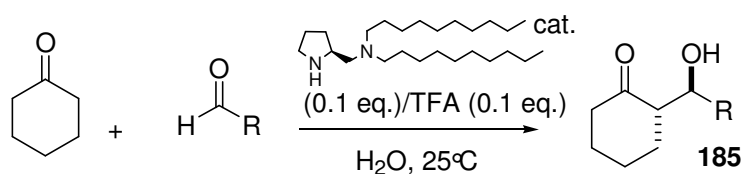
5.7 Chiral diamine catalysts for ketodiol synthesis

Further screening of catalysts for the biomimetic reaction, highlighted the importance of a tertiary nucleophilic moiety. A class of catalysts investigated were chiral diamines as they have been developed by Mukaiyama *et al.* as effective chiral ligands and effective catalysts;¹²⁶ these can also be used for kinetic optical resolutions as developed by Oriyama *et al.*¹²⁷ Most recently chiral diamines have been shown to promote the Baylis-Hillman reaction enantioselectively, giving good yields and moderate to good ees of up to 75% (Table 35, **184a-c**).

R	184	Time (d)	Yield %	Optical Yield %
	a	2	70	65
	b	3	72	75
	c	4	67	69

Table 35: The reactions were conducted with 30 mol% of the diamine, 1.0 eq. of aldehyde and 5.0 eq. of methyl vinyl ketone in EtOH at 0 °C

Chiral diamine catalysts have also been used in direct asymmetric aldol reactions in water.¹²⁸ The catalysts have been designed with appropriate hydrophobic alkyl chains, to assemble hydrophobic reactants in water and sequester the transition state from water in the presence or absence of additives. A newly discovered diamine/TFA bifunctional catalyst system (Scheme 91) has demonstrated excellent reactivity, diastereoselectivity and enantioselectivity in water (Table 36, **185a-c**).



Scheme 91: Catalyst used in direct aldol condensation

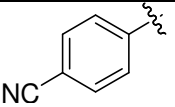
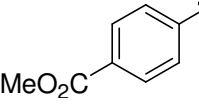
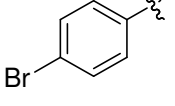
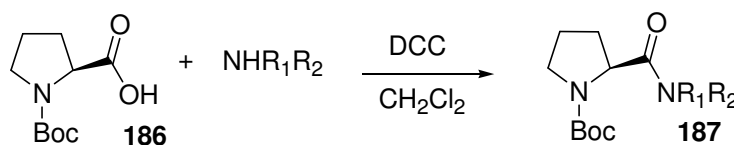
R	185	time (h)	yield %	anti:syn	ee %
	a	48	99	86:14	87
	b	48	89	90:10	91
	c	72	43	91:9	97

Table 36: Diamine/TFA-catalysed aldol reaction with various arylaldehydes in water

5.7.1 Synthesis of chiral diamine catalysts for the biomimetic TK reaction

The effective use of chiral diamine catalysts in water reported by Barbas III *et al.* prompted investigations with variety of catalysts containing the pyrrolidine ring motif. The diamine catalysts were synthesized from (*S*)-Boc-proline using DCC in the presence of a primary/secondary amine. After 24 hours the insoluble urea by-product was removed by filtration followed by an acid/base wash before purifying the product by silica gel chromatography to form the amide **187a-f** in yields ranging from 75 to 88% (Table 37).



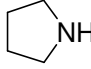
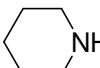
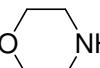
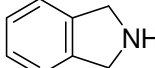
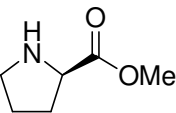
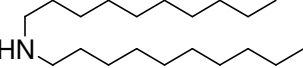
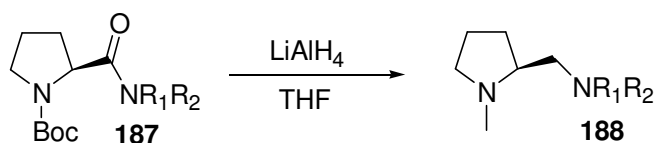
NHR ₁ R ₂	187	yield %
	a	85
	b	89
	c	83
	d	90
	e	76
	f	85

Table 37: Formation of (*S*)-Boc-proline

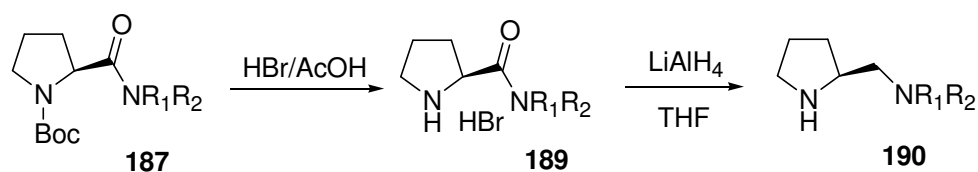
The amides were then reduced, by heating under reflux with lithium aluminium hydride (LiAlH₄) to generate the *N*-methyldiamine catalysts **188a-f** in good yields 50-75% (Table 38).^{129,130}



NHR ₁ R ₂	188	yield %
	a	60
	b	70
	c	63
	d	50
	e	68
	f	75

Table 38: The reduction of the amide **187** to the diamine catalyst **188**.

Two *N*-H diamine catalysts were also synthesized by cleaving the Boc-protecting group using 33% HBr in acetic acid and forming the pyrrolidinium bromide **189**.¹³¹ This was subsequently heated under reflux lithium aluminium hydride (LiAlH₄) to reduce the amide functionality and generate the *N*-H diamines **190a-b** in 55-60% yields (Table 39).^{132,133}

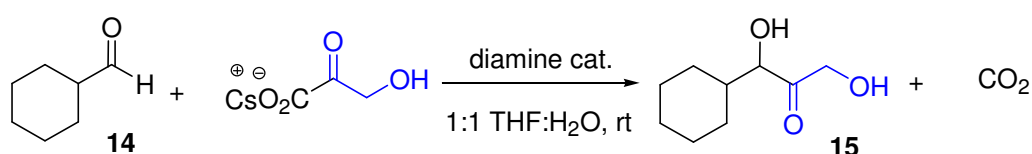


NHR ₁ R ₂	190	yield %
	a	55
	b	60

Table 39: Generation of diamine **190**

5.7.2 Organocatalytic reaction using the diamine catalyst for the TK reaction

Initially the biomimetic TK reaction was conducted in the presence of diamine catalyst (1.0 mol eq.), **Cs-27** (1.0 mol eq.) and cyclohexanecarboxaldehyde (1.0 mol eq.) in 1:1 THF:H₂O solution. The reaction was stirred for 48 hours and product was detected by TLC analyses and subsequently purified generating 20-30% of the ketodiol product **30y**. The biomimetic reactions were also performed at reduced catalytic loading (5-20 mol%), the reactions appeared sluggish after 48 hours with lower yields (4-10%). The reactions with *N*-H diamine catalysts **190a** and **190b** (5 mol%) were performed in aqueous media in the presence/absence of water stable lewis acid triflates (scandium and ytterbium)¹³⁴ affording low ketodiol yields (1-4%). The ketodiol products were then derivatised and the *ees* were determined (Table 40).



Entry	catalyst	yield %	ee%
1	188a	30	2
2	188b	26	5
3	188c	27	5
4	188d	20	4
5	188e	21	4
6	188f	24	5
7	188a	7	4
8	188b	10	5
9	188c	6	4
10	188d	6	3
11	188e	4	5
12	188f	8	4
13	190a	4	20
14	190b	3	4
15	190a/Sc(OTf)₃	1	5
16	190a/Yb(OTf)₃	1	4
17	190b/Yb(OTf)₃	1	2
18	190b/Sc(OTf)₃	1	3

Table 40: Entries 1-6; diamine cat. (1 eq.), aldehyde (1 eq.), **Cs-27** (1 eq.), Entries: 7-12; diamine cat. 20 mol%, Entries 13-14; diamine cat. 5 mol%, H₂O solvent, Entries 15-18; diamine cat 5 mol%, Lewis acid (1 mol%)

The results revealed that stoichiometric amounts of *N*-methyldiamines with reactants generate product with low *ees* (<5%). The increase in the lipophilicity of the diamine did not increase product yield. A reduction in the catalyst loading decreased the product yield 2-fold (entries 7-12), which had no effect on the overall *ees* obtained (<5%). The *N*-H diamine (entry 13) was found to be the best catalyst with low catalyst loading in water affording ketodiols with 20% *ee*. The presence of a Lewis acid with the chiral diamine ligand, had an adverse effect on product yield, with no *ee*.

The absolute chemistry of the major enantiomer obtained (entry 13) was determined to be the (*S*)-isomer. Consideration of the zwitterionic species gave an amine conjugate intermediate stabilised by the hydrogen bonding of the secondary amine. A *Re* stereofacial approach of the prochiral aldehyde would lead to the generation of the major (*S*)-isomer **30y** (Fig. 72).

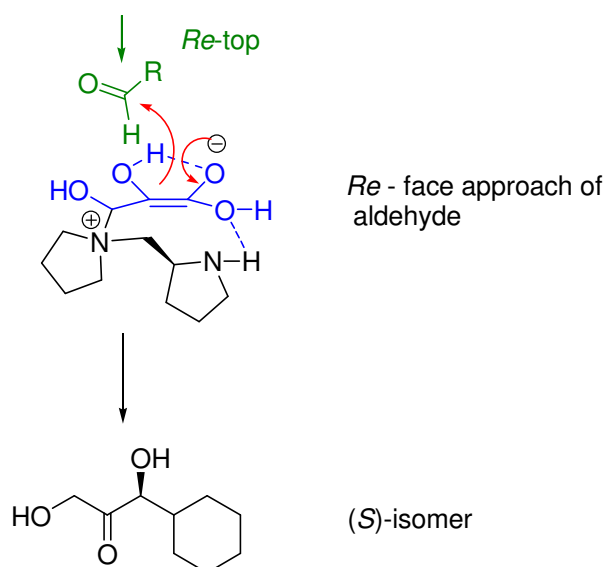


Figure 72: The proposed reaction intermediate for the generation of (*S*)-**30y**

5.7.3 Summary

We have investigated and assessed the substrate tolerance of this novel one pot chemical synthesis of racemic ketodiols in aqueous media. The biomimetic reaction with aliphatic aldehydes afforded ketodiols in yields of 10-25% and with aromatic aldehyde acceptors generating low ketodiols yields of 4-20% with minor 'rearranged' byproduct in conjugation with the aromatic ring (4-15%). The biomimetic reaction with 2-phenylpropionaldehyde as an acceptor molecule generated *syn*-stereoselective (4:1) ketodiols at pH 7.0. The use of **Cs-27** as an alternative donor to **Li-27** revealed a 2-fold increase in ketodiols production with cyclohexanecarboxaldehyde as substrate in comparison to a 2-fold increase with benzaldehyde used as substrate. Preliminary

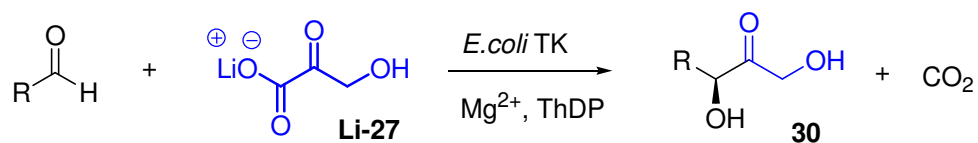
mechanistic investigations were performed enhancing our understanding of the reaction mechanism. Newly synthesized cinchona alkaloid catalysts and diamine chiral catalysts in low catalyst loading were screened with cyclohexanecarboxaldehyde in the biomimetic reaction obtaining 20% *ee*. Designing further chiral tertiary catalysts to improve *ee* is desirable.

Chapter 6.0

Conclusion and Future Work

Future work

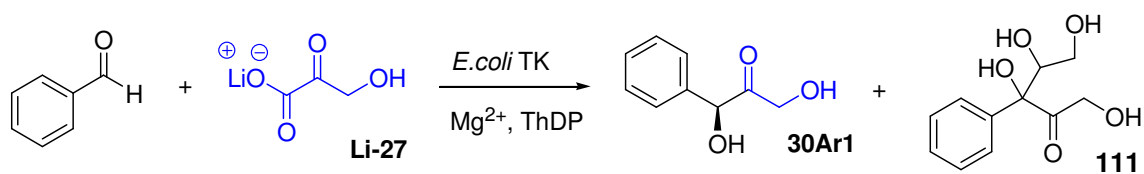
We have shown mutant transketolases obtained by directed evolution, with improved substrate specificity towards non-natural aliphatic and aromatic aldehydes. The use of a novel, rapid, colorimetric assay for screening biological active mutants in a 96 well plate format has successfully identified a number of active mutants, principally D469T and D469E with enhanced substrate specificity towards non-hydroxylated aldehyde acceptors. The course of our studies revealed the high enantioselective nature of the reaction for cyclic substrates generating (*S*)-ketodiol products with >99% *ees* obtained.



Scheme 92: Biotransformations using *E. coli* TK.

However it would be also desirable to locate TK mutants generating (*R*)-ketodiol products. The H26Y mutant has been shown to generate the (*R*)-isomer with propanal and other linear aliphatic aldehydes, in comparison to the poor substrate affinity with cyclic aliphatic aldehydes. Further evaluation of the H26 library or other phylogenetic TK libraries is required to isolate a mutant or mutants with high substrate affinity for cyclic aldehydes generating the (*R*)-ketodiol product.

We have also reported the first novel aromatic aldehyde substrates accepted by *E. coli* TK mutants D469E, D469K, D469T and G6 with benzaldehyde and furfural affording ketodiol products in poor yields (1-4%) with the generation of byproducts. On closer inspection it was revealed the byproduct generated from the TK biotransformation with benzaldehyde was a 'double addition product' **111**. Further investigation into the generation of **111** can provide insight into the differences between the mechanistic action of aromatic aldehydes in comparison to aliphatic aldehydes as substrates in the enzyme's active site. Performing different reaction conditions to circumvent the generation of **111** to obtain the desired ketodiol product **30Ar1** is also worth pursuing.



Scheme 93: Generation of 'double addition product 111'

The TK biocatalytic synthesis of aromatic ketodiols is currently in its infancy, expanding the substrate scope further to accept nitrogen containing aromatic and other heterocyclic aldehydes is desirable. The insolubility of some aromatic aldehydes containing electron withdrawing/donating substituents on various positions on the aryl ring is a hindrance to ketodiol synthesis. Investigations in catalytic activity, stability and the interactions of solvent with protein structure in a mixed water-organic solvent system are certain factors that need to be addressed.

To elucidate our understanding of the highly stereospecific nature of TK mutants on aliphatic and aromatic aldehyde acceptor molecules, further work would involve important X-ray crystallographic data on the D469 TK mutants. Most recently Tittmann *et al.* have provided an X-ray structure of *E.coli* TK with acceptor aldose ribose-5-phosphate noncovalently bound in the active site.³¹ Ideally an X-ray crystal structure of mutant *E.coli* TK in the presence of a non-phosphorylated acceptor molecule trapped in the enzyme's active site would provide us with a 'snapshot' of the reactive intermediate accountable for the catalytic activity and the high stereospecificity of the D469 TK mutants.

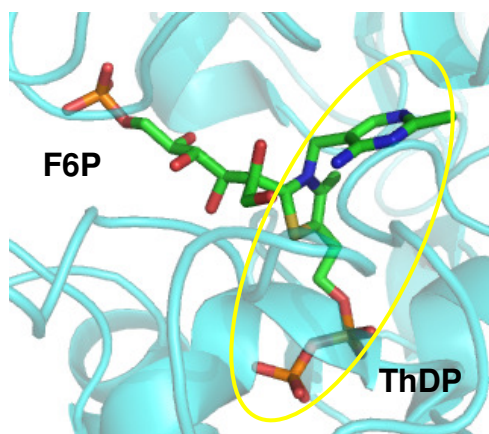


Figure 73: An X-ray crystal structure of a trapped F6P-ThDP intermediate

Further investigations of this novel one pot synthesis of racemic dihydroxyketones; in terms of substrate scope of the reaction is required. Such as the use of a variety of aldehyde acceptors: aromatic, aliphatic hydrophobic and hydrophilic aldehydes to generate useful 'carbon scaffolds' for pharmaceutical and agrochemical purposes. Alternative donors other than hydroxypyruvate (HPA) will be investigated to assess the general synthetic utility of the reaction. Do other α -keto acids; such as 3-mercaptopyruvic acid and 3-phenylpyruvic acid work in a similar manner to that of hydroxypyruvate? (Fig. 74).

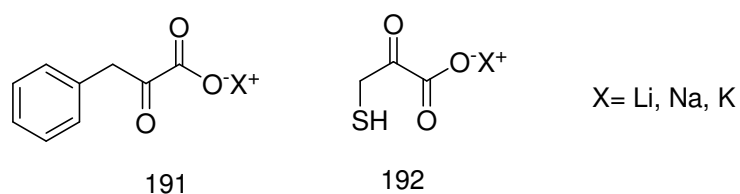


Figure 74 Phenylpyruvate 191 and Mercaptopyruvate 192

The newly synthesized cinchona alkaloid catalysts and diamine chiral catalysts in low catalyst loading has shown enantioselectivities with cyclohexanecarboxaldehyde in the biomimetic reaction obtaining 20% *ee*. Further screening of the catalysts with commercially available chiral aldehydes is worth pursuing. Other available catalysts such as chiral phosphorus ligands was overlooked in these studies. A screening of several phosphorus ligands is worth considering with a systematic approach to the development of designing chiral tertiary catalysts to improve the *ees* currently obtained.

Chapter 7.0

Experimental

General Experimental

¹H NMR and **¹³C NMR** were recorded using Bruker AMX 300 MHz, Avance-500 MHz and Avance-600 MHz machines. **¹⁹F NMR** were recorded using a Bruker AMX 300 MHz machine. NMR spectra were recorded at 298 K unless otherwise indicated. Splitting patterns are abbreviated as singlet (s), doublet (d), triplet (t), double doublets (dd), quartet (q) multiplet (m). The chemical shifts are given in ppm (δ), relative to tetramethylsilane (TMS) as reference and coupling constants (J) are given in Hertz. When necessary, assignments were aided by DEPT-135 and decoupling experiments. **IR Spectra** were obtained from a Nicolet FT-IR machine and Shamadzu FTIR-8700 are reported in wavenumbers (cm^{-1}) and the characteristic bands are abbreviated by (s) strong absorption, (m) medium absorption, (w) weak absorption. **ES⁺ mass spectra** were acquired using Thermo Finnegan MAT 900XP and Micro Mass Quattro LC. **CI spectra** and **HRMS** were obtained using, Fisons VG70-SE and LTQ Orbitrap XL (courtesy of EPSRC National Mass Spectrometry Service Centre, Swansea University). **Normal Phase High-Performance liquid Chromatography (HPLC)** was measured using a U.V detector prostar/dynamic system24 (2 Volts) absorbance with 214 nm. The analytes were separated and *ees* determined by using a Chirapak AD/OD columns (Daicel; Chiral Technologies Europe, France) 25 cm \times 0.46 cm. The polar stationary phase (isopropanol) and nonpolar mobile phase (hexane) were used as indicated. **Thin Layer Chromatography (TLC)** was carried out on pre-coated aluminium backed silica plates (Merck 60 F254 normal phase) and examined under UV fluorescence at 254 nm or 297 nm, or using phosphomolybdic acid (PMA) [PMA hydrate (12 g) and ethanol (250 ml)] as a general stain. **Flash silica chromatography** was carried out on silica gel using BDH silica 40 (63 μm). All chemicals were used as received from Aldrich Chemical Co., BDH laboratory supplies, Fischer Chemical Co. and Lancaster Chemical Co. without further purification unless where stated. Solvents used were of the analytical and HPLC grade. Dry solvents were obtained using anhydrous alumina columns.¹³⁵ **Optical rotations** were recorded on a Perkin Elmer model 343 polarimeter at 589 nm, quoted in $\text{deg cm}^2 \text{g}^{-1}$ and conc (c) in g/100 ml. **Melting points (M.p.)** were established using a Gallenkamp apparatus and measured in $^{\circ}\text{C}$. **The Colorimetric assay** used FLUOstar Optima plate reader (BMG Labtechnologies, Aylesbury, UK), and was measured at $\text{OD}_{485\text{nm}}$.

TK Cell-free lysate preparation.

Luria Bertani-agar plates with ampicillin (150 $\mu\text{g/ml}$) for growth selection were streaked with *Escherichia coli* XL10 transformed with the plasmid containing the appropriate TK mutant gene from glycerol stocks (25% v/v glycerol stored at -80°C) and incubated for

16 h at 37 °C. A single colony was picked and used to inoculate 250 ml shake flasks containing 25 mL LB-glycerol (containing ampicillin 150 µg/ml) and incubated overnight at 37 °C and 200 rpm using an SI 50 orbital shaker (Stuart Scientific, Redhill, UK). The overnight culture was used to inoculate a 1 L shake flask containing 100 ml LB-glycerol Amp media (10% v/v), and incubated at 37 °C and 200 rpm. The fermentation was monitored by OD₆₀₀ until the absorbance was no greater than 4. The culture was pelleted by centrifugation at 4000 rpm for 20 minutes at 4 °C and approximately 2 g of cell paste was obtained and then resuspended in cold sodium phosphate buffer (5 mM, pH 7) to a final suspension of 1 g cell paste per 10 ml buffer. The cells were then disrupted by sonication for 3 minutes at 4 °C using a Soniprep 150 sonicator (MSE, Sanyo, Japan), and centrifuged at 4500 rpm for 20 minutes at 4 °C. The supernatant cell-free lysate (approximately 20 ml) was aliquoted and stored at -20 °C until needed. The TK protein concentration of cell-free lysate was determined to contain approximately 0.3 mg ml⁻¹

TK conversions.

The biotransformations were conducted in 50 mM reaction concentrations. ThDP (22 mg, 48 µmol) and MgCl₂·6H₂O (39 mg, 180 µmol) were dissolved in H₂O (10 ml) and the pH adjusted to 7 using 0.1 M NaOH. To this stirred solution, at 25 °C, was added TK clarified lysate (2 ml, containing approximately 0.3 mg ml⁻¹) and the mixture stirred for 20 min. In another flask, Li-1 (110 mg, 1.00 mmol) and the aldehyde (1.00 mmol) were dissolved in H₂O (8 ml) and the pH adjusted to 7 with 0.1 M NaOH. Following the 20 min enzyme/cofactor pre-incubation, the 1/aldehyde mixture was added to the enzyme solution and the mixture stirred at rt for 24 h. During this time, the pH was maintained at 7.0 by addition of 1 M HCl using a pH stat (Stat Titrino, Metrohm) and the reactions were followed by TLC analysis. Silica was added and the reaction mixture concentrated to dryness, dry loaded onto a flash silica gel column, and purified as indicated.



Screening of libraries for activity

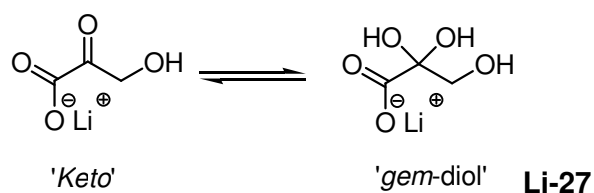
Preparation of cell samples: The 96-well reaction plates were thawed from -80 °C resulting in the freeze-thaw lysis of the 100 µl cell cultures. A 12x cofactor stock solution (28.8 mM ThDP, 108 mM MgCl₂, 50 mM Tris, pH 7.0; 25 µl) was added to each well and the plate was then incubated at 25 °C for 20 min. A 4 x **Li-27** stock solution (200 mM in 50 mM Tris, pH 7.0; 75 µl) and an aldehyde stock solution (150 mM in 50 mM Tris, pH 7.0; 100 µl) were then added to each well and the plate incubated at 25 °C for a further 2 h.

Assaying reaction plates for production of ketodiol: 50 µl of reaction mixture were transferred from each well to a fresh 96-well plate containing 50 µl of 50 mM Tris, pH 7.0 and 20 mg of MP-Carbonate Scavenger Resin (Biotage), which was added to each well using a resin loader (Radleys). After 2 h, Tris (100 µl, 50 mM, pH 7.0) was added to each well, with mixing, and 50 µl from each well transferred to a fresh 96-well plate. A plate reader (Fluostar, BMG-labtech) fitted with an autoinjector was then used to add 2,3,5-triphenyltetrazolium chloride (20 µl, 0.2% solution in methanol) then 3M NaOH (10 µl). The plate was shaken for 10 s, left for 1 min and an absorbance reading taken of each well at 485 nm.

Colorimetric assay to determine the initial rate velocity

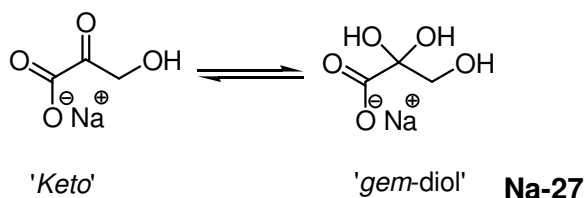
D469T TK lysate, 60 µl was incubated with 100 µl cofactor solution (TPP (2.4 mM), and MgCl₂ (9 mM)) for 20 mins at 20 °C. **Li-27** (7.4 mg, 50 mmol) and aldehyde (50 mmol) was added to the reaction mixture. Aliquots (50 µl) were taken at hourly intervals and the reaction was quenched with 50 µl methanol. The aliquots were transferred onto a microwell plate containing 10 mg MP-Carbonate resin (Biotage AB) and incubated at 20 °C for 3 h.⁹² 50 µl of the quenched reaction sample was transferred without resin into a microwell plate. 50 µl of each concentration was diluted with 100 µl of water. Automated injection of 20 µl of tetrazolium red solution (0.2% of 2,3,5 triphenyltetrazolium chloride in methanol) and 10 µl 3 M NaOH (aq) with shaking by FLUOstar Optima plate reader, was followed by immediate measurement at OD_{485nm}.⁹²

Lithium hydroxypyruvate⁵²



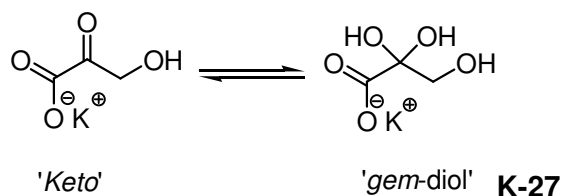
Bromopyruvic acid (10.05 g, 0.06 mol) was dissolved in water (100 ml) and 1 M LiOH solution was added at such a rate that the pH did not exceed 9.5 whilst stirring. Glacial acetic acid was added dropwise into the solution to adjust it to pH 5.0. The mixture was concentrated *in vacuo* to approximately a 20 ml final volume and the concentrate was left to crystallise overnight. The crude product was washed with ethanol and collected by filtration then suspended in ethanol (50 ml) at 40 °C for 30 min. The product was collected by filtration and washed with ethanol (50 ml) affording a white powder (2.977 g, 46%). **M.p.** 115-125; **IR (KBr)** 3462-2619 (br, O-H), 1708 (s, C=O); **¹H NMR (300 MHz; D₂O)** δ 3.60 (2H, s, CH₂, keto), 4.64 (2H, s, CH₂, gem-diol); **¹³C NMR (75 MHz; D₂O)** δ 65.8 (CH₂), 66.5 (CH₂), 94.8 (gem-diol), 167.9 (C=O) (keto), 177.0 (C=O) (gem-diol), 203.0 (C=O) (keto); **m/z (ES⁺)** 220 (2M⁺, 100%), 152 (MNa⁺, 20).

Sodium -hydroxypyruvate



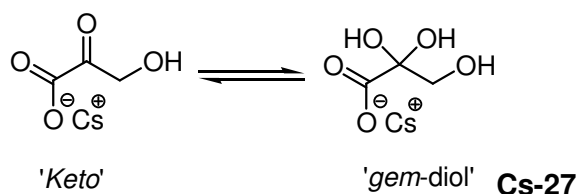
Bromopyruvic acid (10.06 g, 0.06 mol) was dissolved in water (100 ml) and 1 M NaOH solution was added at such a rate that the pH did not exceed 9.5 whilst stirring. Glacial acetic acid was added dropwise into the solution to adjust it to pH 5. The mixture was concentrated *in vacuo* to approximately a 20 ml final volume and the concentrate was left to crystallise overnight. The crude product was washed with ethanol and collected by filtration then suspended in ethanol (50 ml) at 40 °C for 30 min. The product was collected by filtration and washed with ethanol (50 ml) affording a white powder (1.517 g, 20%). **M.p.** 120-130; **IR (KBr)** 3462-2619 (br, O-H), 1708 (s, C=O); **¹H NMR (300 MHz; D₂O)** δ 3.60 (2H, s, CH₂, keto), 4.64 (2H, s, CH₂, gem-diol); **¹³C NMR (75 MHz; D₂O)** δ 65.8 (CH₂), 66.5 (CH₂), 94.8 (gem-diol), 167.9 (C=O) (keto), 177.0 (C=O) (gem-diol), 203.0 (C=O) (keto); **m/z (ES⁺)** 103 (M-Na⁺ 100%).

Potassium hydroxypyruvate⁵²



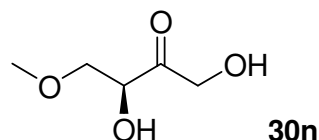
Bromopyruvic acid (10.01 g, 0.06 mol) was dissolved in water (100 ml) and 3 M KOH solution was added at such a rate that the pH did not exceed 9.5 whilst stirring. Glacial acetic acid was added dropwise into the solution to adjust it to pH 5. The mixture was concentrated *in vacuo* to approximately a 20 ml final volume and the concentrate was left to crystallise overnight. The crude product was washed with ethanol and collected by filtration then suspended in ethanol (50 ml) at 40 °C for 30 min. The product was collected by filtration and washed with ethanol (50 ml) affording an orange powder (6.123g, 72%). **M.p.** 125-135; **IR (KBr)** 3462-2619 (br, O-H), 1708 (s, C=O); **¹H NMR (300 MHz; D₂O)** δ 3.60 (2H, s, CH₂, keto), 4.64 (2H, s, CH₂, gem-diol); **¹³C NMR (75 MHz; D₂O)** δ 65.8 (CH₂), 66.5 (CH₂), 94.8 (gem-diol), 167.9 (C=O) (keto), 177.0 (C=O) (gem-diol), 203.0 (C=O) (keto); **m/z (ES⁺)** 103 (M-K⁺, 100%).

Cesium hydroxypyruvate



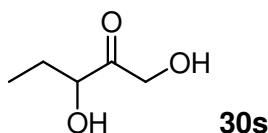
Bromopyruvic acid (10.15 g, 0.06 mol) was dissolved in water (100 ml) and 4 M cesium hydroxide solution was added at such a rate that the pH did not exceed 9.5 whilst stirring. Glacial acetic acid was added dropwise into the solution to adjust it to pH 5. The mixture was concentrated *in vacuo* to approximately a 20 ml final volume and the concentrate was left to crystallise overnight. The crude product was washed with ethanol and collected by filtration then suspended in ethanol (50 ml) at 40 °C for 30 min. The product was collected by filtration and washed with ethanol (50 ml) affording an orange-brown powder (14.012g, >99%). **M.p.** 135-145; **IR (KBr)** 3462-2619 (br, O-H), 1708 (s, C=O); **¹H NMR (300 MHz; D₂O)** δ 3.60 (2H, s, CH₂, keto), 4.64 (2H, s, CH₂, gem-diol); **¹³C NMR (75 MHz; D₂O)** δ 65.8 (CH₂), 66.5 (CH₂), 94.8 (gem-diol), 167.9 (C=O) (keto), 177.0 (C=O) (gem-diol), 203.0 (C=O) (keto); **m/z (ES⁺)** 103 (M-Cs⁺, 100%).

1, 3-Dihydroxy-4-methoxy-butan-2-one¹⁰⁰



Following the TK conversion protocol, WT-TK gave **30n** as an oil (40 mg, 30%). $[\alpha]_{\text{D}}^{20} = +2.0$ (*c* 2.0, CHCl_3), lit. $[\alpha]_{\text{D}}^{25} = +3.0$ (*C* 0.017, MeOH); **IR (Neat)**: 3415br s, 2923s, 1727s; **¹H NMR (300 MHz; CDCl_3)** δ 3.36 (3H, s, OCH_3), 3.61 (1H, dd, *J* 9.9 and 4.4, CHHOMe), 3.70 (1H, dd, *J* 9.9 and 4.4, CHHOMe), 4.38 (1H, t, *J* 4.4 and 4.4, CHOH), 4.43 (1H, d, *J* 19.7, CHHOH), 4.53 (1H, d, *J* 19.7, CHHOH); **¹³C NMR (75 MHz; CDCl_3)** δ 59.5 (OCH_3), 66.7 (CH_2), 73.4 (CH_2), 74.8 (CHOH) 210.8 ($\text{C}=\text{O}$); ***m/z* (FTMS)** $[\text{M}+\text{NH}_4]^+$ calcd for $\text{C}_5\text{H}_{14}\text{O}_4\text{N}$ requires 152.0917, found 152.0919.

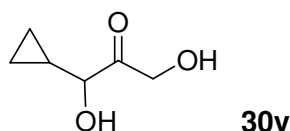
1,3-Dihydroxypentan-2-one⁵²



To a stirred solution of **Li-27** (0.33 g, 3.00 mmol) in water (60 ml) at rt, was added propanal (217 μl , 3.00 mmol) and *N*-methylmorpholine (364 μl , 3.00 mmol). The reaction mixture was stirred at rt for 48 h, and monitored by TLC. The solvent was removed *in vacuo* and the crude product dry loaded onto a flash silica chromatography column (EtOAc: 40-60% petroleum ether, 2:1) affording **30s** (0.0789 g, 22%) as a white solid. **R_f** 0.29 (EtOAc: petroleum ether, 2:1); **M.p.** 102-106; **IR (KBr)** 3407 (br, O-H), 2925-2855 (C-H); 1720 (s, C=O); **¹H NMR (300 MHz; MeOD)** δ 0.95 (3H, m, CH_3), 1.59 (1H, m, $\text{CH}_3\text{-CHH}$) 1.79 (1H, m, CH_3CHH), 4.11 (1H, m, CHOH), 4.39 (1H, d, *J* 19.3, $\text{O}=\text{C-CHH}$), 4.47 (1H, d, *J* 19.3, $\text{O}=\text{C-CHH}$); **¹³C NMR (75 MHz; MeOD)** δ 9.7 (CH_3), 28.0, 66.6 (CH_2OH), 77.5 (CHOH) 214.1 ($\text{C}=\text{O}$); ***m/z* (ES⁺)** 118 (M^+ , 20%), 136 ($[\text{M}+\text{H}_2\text{O}]^+$, 45%), 60 ($[\text{M}-\text{C}_4\text{H}_2\text{O}_2]^+$, 47%).

Biotransformation Product; The 50 mM TK reaction using WT-TK generated white solid (*S*)-**30s** (0.360 g, 77%), 59% *ee* (*S*-isomer); $[\alpha]_{\text{D}}^{20} = +13.3$ (*c* 0.15, CHCl_3), spectra assignments same as above.

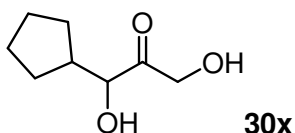
1-Cyclopropyl -1,3-dihydroxy-2-propanone¹⁰⁶



To a stirred solution of **Li-27** (0.33 g, 3.00 mmol) in water (60 ml) at rt, was added cyclopropanecarboxaldehyde (224 μ l, 3.00 mmol) and *N*-methylmorpholine (364 μ l, 3.00 mmol). The reaction mixture was stirred at rt for 48 h, and monitored by TLC. The solvent was removed *in vacuo* and the crude product dry loaded onto a flash silica chromatography column (neat EtOAc) affording product **30v** (0.039 g, 10%) as a colourless oil. R_f 0.50; IR (KBr) 3380 (b, O-H), 3007-2923 (C-H) 1723 (s, C=O); ^1H NMR (300 MHz; CDCl_3) δ 1.24-1.76 (4H, m), 2.19 (1H, m), 2.69 (2H, s, OH), 4.30 (1H, d, J 3.0), 4.37 (1H, d, J 21.0, CHHOH), 4.50 (1H, d, J 21.0, CHHOH); ^{13}C NMR (75 MHz; CDCl_3) δ 25.8, 29.1, 43.0, 65.9 (CH_2OH), 77.0 (CHOH), 211.4 (C=O); m/z (GC-CIP) calcd $[\text{M}+\text{NH}_4]^+$ for $\text{C}_6\text{H}_{14}\text{NO}_3$ requires 148.0968 found 148.0969.

Biotransformation product (S)-30v: The *ees* was determined from the HPLC benzoylated method (See **94**). The 50 mM TK reaction using WT-TK gave **30v** (3 mg, 2%) in 72% *ee* (1*S*-isomer), H26Y-TK gave no reaction, D469T-TK, gave **33v** (3 mg, 2%) in 99% *ee* (1*S*-isomer), and D469L-TK gave **30v** (14 mg, 10%) in 99% *ee* (1*S*-isomer), D469K-TK, 15 **30v** (2 mg, 2%) in 99% *ee* (1*S*-isomer) and D469E-TK generated (S)-**30v** a colourless oil (13 mg, 10%) in 99% *ee* (1*S*-isomer), $[\alpha]_{\text{D}}^{20} = +70.0$ (c 0.3, CHCl_3). The absolute stereochemistry of **30v** generated using D469E-TK was determined using the Mosher's derivatisation method (See **95**).

1-Cyclopentyl -1,3-dihydroxy-2-propanone¹⁰⁶

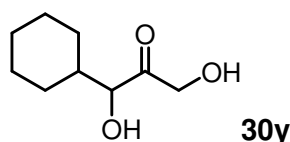


To a stirred solution of **Li-27** (0.33 g, 3.00 mmol) in water (60 ml) at rt, was added cyclopentanecarboxaldehyde (320 μ l, 3.00 mmol) and *N*-methylmorpholine (364 μ l, 3.00 mmol). The reaction mixture was stirred at rt for 48 h, and monitored by TLC. The solvent was removed *in vacuo* and the crude product dry loaded onto a flash silica chromatography column (EtOAc:hexane, 1:1) affording product **30x** (0.119 g, 25%) as a white solid. R_f 0.21 (EtOAc:hexane, 1:1); **M.p.** 115-125; IR (KBr) 3411 (br, O-H), 2952-2868 (C-H); 1718 (s, C=O); ^1H NMR (300 MHz; CDCl_3) δ 1.31-1.75 (8H, m), 2.18

(1H, m) 3.04 (2H, s, OH), 4.30 (1H, m, CHOH), 4.36 (1H, d, J 21.0, CHHOH), 4.50 (1H, d, J 21.0, CHHOH); ^{13}C NMR (75 MHz; CDCl_3) δ 25.6, 29.0, 42.9, 65.8 (CH_2OH), 76.9 (CHOH), 211.4 ($\text{C}=\text{O}$); m/z (GC-CIP) found $[\text{M}+\text{NH}_4]^+$ 176.1281 for $\text{C}_8\text{H}_{18}\text{NO}_3$ requires 176.1281.

Biotransformation Product (S)-30x: The *ees* was determined from the HPLC benzoylated method (See 96). The 50 mM TK reaction using WT-TK gave **30x** (2 mg, 1%) as a racemate, H26Y-TK gave **30x** (3 mg, 2%) in 30% *ee* (1*R*-isomer), D469T-TK gave **30x** (47mg, 30%) in 99% *ee* (1*S*-isomer) and D469K-TK gave **30x** (16mg, 10%) in 25% *ee* (1*S*-isomer), and D469E-TK gave **30x** (63 mg, 40%) in 99% *ee* (*S*-isomer), $[\alpha]_{\text{D}}^{20} = +33.0$ (c 0.5, CHCl_3). The absolute stereochemistry of **30x** was determined using the Mosher's derivatisation method (See 98).

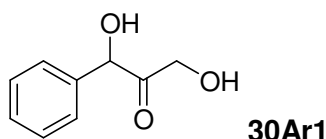
1-Cyclohexyl -1,3-dihydroxy-2-propanone⁵¹



To a stirred solution of **Cs-27** (0.71 g, 3.00 mmol) in water (60 ml) at rt, was added cyclohexanecarboxaldehyde (363 μl , 3.00 mmol) and *N*-methylmorpholine (364 μl , 3.00 mmol). The reaction mixture was stirred at rt for 48 h, and monitored by TLC. The solvent was removed *in vacuo* and the crude product dry loaded onto a flash silica chromatography column (EtOAc:hexane, 1:1) affording **30y** (0.24 g, 47%) as a white solid. R_f 0.21; **M.p.** 110-120; **IR (KBr)** 3429 (b, O-H), 1712 (s, $\text{C}=\text{O}$), 2925-2855 (C-H); ^1H NMR (300 MHz; CDCl_3) δ 0.89 -1.30 (11H, m), 2.96 (2H, s, OH), 3.96 (1H, d, J 6.0, CHOH), 4.34 (1H, d, J 19.5, CHHOH), 4.45 (1H, d, J 19.5, CHHOH); ^{13}C NMR (75 MHz; CDCl_3) δ 27.4, 27.7, 30.4, 42.9, 67.4 (CH_2OH), 80.7 (CHOH), 214.3 ($\text{C}=\text{O}$); m/z (ES^+) 172.8 ($[\text{M}]^+$, 10), 343.2 ($[\text{2M}]^+$, 100); m/z (HRMS) calcd $[\text{M}+\text{H}]^+$ for $\text{C}_9\text{H}_{17}\text{O}_3$ requires 173.11722, found 173.11736.

Biotransformation Product (S)-30y: The *ees* was determined from the HPLC benzoylated method (See 100). The 50 mM TK reaction using WT-TK gave **30y** (1 mg, 1%) as a racemate, D469T-TK gave **30y** (5 mg, 3%) in 99% *ee* (1*S*-isomer); D469K-TK gave **30y** (5 mg, 3%) in 25% *ee* (1*S*-isomer), and D469E-TK generated **30y** gave (17 mg, 30%) in 97% *ee* (1*S*-isomer), $[\alpha]_{\text{D}}^{20} = +33.0$ (c 0.5, CHCl_3). in 97% *ee* (1*S*-isomer). The absolute stereochemistry with D469E-TK was determined using the Mosher's derivatisation method (See 101).

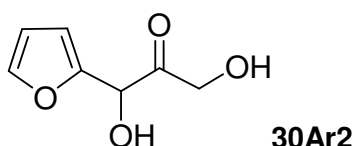
1, 3-Dihydroxypropiophenone¹³⁶



To a stirred solution of **Cs-27** (0.71 g, 3.00 mmol) in water (60 ml) at rt, was added benzaldehyde (363 μ l, 3.00 mmol) and *N*-methylmorpholine (364 μ l, 3.00 mmol). The pH of the solution was then adjusted to pH 7.0 by adding 1 M HCl or 1 M NaOH solution dropwise. The reaction mixture was stirred at rt for 48 h, and monitored by TLC. The solvent was removed *in vacuo* and the crude product dry loaded onto a flash silica chromatography column (EtOAc:hexane, 1:1) affording **30Ar1** (0.05 g, 10%) as an colorless oil. R_f 0.75; **IR (Neat)** 3429 (b, O-H), 1712 (s, C=O); **¹H NMR (300 MHz; CDCl₃)** δ 4.20 (1H, d, *J* 19.0, CHHOH), 4.33 (1H, d, *J* 19.0, CHHOH), 5.23 (1H, s, HOCH), 7.20-7.43 (5H, m, Ar). **¹³C NMR (75 MHz; CDCl₃)** δ 65.1 (CH₂), 77.7 (CHO), 128.5, 129.3, 130.2, 137.3, 209.1 (C=O); ***m/z* (ES⁺)** 167.6 (M⁺, 94%), 77.7 (C₆H₆⁺, 10%), 58.9 (C₂H₂O₂⁺, 25%).

Biotransformation product generated in a 50 mM TK reaction using D469E gave (5 mg, 3%) as an oil; $[\alpha]_D^{20} = +74.0$ (c 0.5, CHCl₃). The spectral assignment is the same as above.

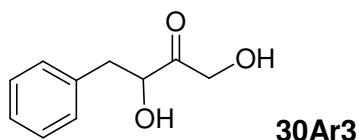
1-Furan-2-yl-1, 3-dihydroxy-propan-2-one⁴⁵



To a stirred solution of **Li-27** (0.111 g, 1.00 mmol) in water (5 ml) and THF (5 ml) at rt, was added furfural (83 μ l, 1.00 mmol) and *N*-methylmorpholine (101 μ l, 1.00 mmol). The pH of the solution was then adjusted to pH 7.0 by adding 1 M HCl or 1 M NaOH solution added dropwise. The reaction mixture was stirred at rt for 24 h, and monitored by TLC. The solvent was removed *in vacuo* and the crude product dry loaded onto a flash silica chromatography column (EtOAc:hexane, 1:1) affording compound **30Ar2** (0.006 g, 4%) as a brown oil; R_f 0.40; **IR (Neat)** 3391 (s, O-H), 1708 (C=O), 694 (Ar-H); **¹H NMR (300 MHz; CDCl₃)** δ 3.39 (2H, s, OH), 4.28 (1H, d, *J* 19.5, CHHOH), 4.43 (1H, d, *J* 19.5, CHHOH), 5.30 (1H, s, HOCH), 6.35 – 6.47 (2H, m), 7.41 (1H, m), **¹³C NMR (125 MHz; CDCl₃)** δ 66.1 (CH₂), 71.0 (CHOH), 110.5, 111.0, 143.6, 149.6 (CCHOH), 207.8 (C=O); ***m/z* (CI)** calcd for C₇H₉O₄ [M+Na]⁺ requires 157.05008, found 157.04964.

Biotransformation product (S)-30Ar2 generated in a 50 mM TK reaction using D469E gave (8 mg, 5%) as an oil; $[\alpha]_{\text{D}}^{20} = +54.0$ (c 0.4, CHCl₃). The spectral assignment is the same as above.

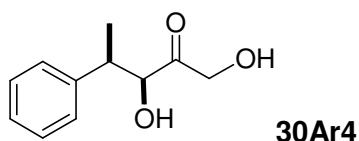
1,3-dihydroxy-4-phenylbutan-2-one⁵¹



To a stirred solution of **Li-27** (0.112 g, 1.00 mmol) in water (5 ml) and THF (5 ml) at rt, was added phenylacetaldehyde (120 μ l, 1.00 mmol) and *N*-methylmorpholine (101 μ l, 1.00 mmol). The reaction mixture was stirred at rt for 24 h, and monitored by TLC. The solvent was removed *in vacuo* and the crude product dry loaded onto a flash silica chromatography column (EtOAc:hexane, 1:1) affording compound **30Ar3** (0.018 g, 10%) as a colourless crystals, R_f 0.30; **M.p.** 122-130; **IR (Neat)** 3262 (br, O-H), 2966-2883 (C-H); 1720 (s, C=O); **¹H NMR (500 MHz; CDCl₃)** δ 2.43 (2H, s, OH), 2.84 (1H, dd, *J* 13.9 and 8.1, CHHPh) 3.08 (1H, dd, *J* 13.9 and 4.5, CHHPh), 4.28 (1H, d, *J* 18.0, CHHOH), 4.38 (1H, d, *J* 18.0, CHHOH), 4.42 (1H, m, CHOH), 7.18-7.34 (5H, m, Ar); **¹³C NMR (125 MHz; CDCl₃)** δ 40.4 (CH₂Ph), 66.2 (CH₂OH), 76.0 (CHOH), 127.2, 128.8, 129.4, 135.9, 211.6 (C=O); ***m/z* (FTMS + p NSI)** calcd [2M+Na]⁺ for C₂₀H₂₄O₆Na requires 383.1471, found 383.1454.

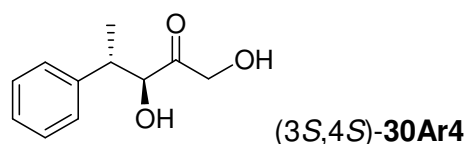
Biotransformation Product (S)-30Ar3: The *ees* was determined from the HPLC benzoylated method (See **123**). The 50 mM TK reaction using WT-TK gave **30Ar3** (9 mg, 5%) in 93% *ee* (1*S*-isomer), G6-TK gave **30Ar3** (90 mg, 50%) in 92% *ee* (1*S*-isomer), D469T-TK gave **30Ar3** (90 mg, 50%) in 96% *ee* (1*S*-isomer); D469K-TK gave **30Ar3** (81 mg, 45%) in 95% *ee* (1*S*-isomer), H26Y-TK gave **30Ar3** (9 mg, 5%) in 88% *ee* (1*S*-isomer), and D469E-TK generated **30Ar3** gave (77 mg, 43%) in 90% *ee* (1*S*-isomer), $[\alpha]_{\text{D}}^{20} = +30.0$ (c 0.5, CHCl₃). The absolute stereochemistry with D469E-TK was determined using the Mosher's derivatisation method (See **126**).

1,3-Dihydroxy-4-phenyl-pentan-2-one



To a stirred solution of **Li-27** (0.11 g, 1.00 mmol) in water (5 ml) and THF (5 ml) at rt, was added 2-phenylpropanal (134 μ l, 1.00 mmol) and *N*-methylmorpholine (101 μ l, 1.00 mmol). The reaction mixture was stirred at rt for 24 h, and monitored by TLC. The solvent was removed *in vacuo* and the crude product dry loaded onto a flash silica chromatography column (EtOAc:hexane, 1:1) affording compound **30Ar4** (0.020 g, 10%) as a colourless crystals, R_f 0.30; **M.p.** 120-130; **IR (Neat)** 3407 (br, O-H), 2925-2855 (C-H); 1720 (s, C=O); **$^1\text{H NMR}$ (500 MHz; CDCl_3)** δ 1.28 (0.6H, d, J 4.3 Hz, CH_3), 1.43 (2.4H, d, J 4.3, CH_3) 3.19-3.24 (1H, m, CHCH_3), 4.22 (1H, d, J 12.0, CHHOH), 4.26 (1H, d, J 12.0, CHHOH), 4.38 (0.2H, m, CHOH); 4.42 (0.8H, m, CHOH); 7.21-7.37 (5H, m, Ar); **$^{13}\text{C NMR}$ (125 MHz; CDCl_3)** δ 14.2 (CH_3), 43.6 (CHCH_3), 67.1 (CH_2OH), 79.5 (CHOH), 127.4, 127.7, 129.0, 142.0, 211.5 (C=O); **m/z (FTMS + p NSI) calcd** $[\text{M}+\text{Na}]^+$ for $\text{C}_{11}\text{H}_{14}\text{O}_3$ requires 217.0835, found 217.0836. The 2-isomer mixture of (3*RS*,4*R*)-1,3-dihydroxy-4-phenylpentan-2-one (4*R*)-**30Ar4** (0.019 g, 10%) was prepared using an identical method and **131**

(3*S*,4*S*)-1,3-Dihydroxy-4-phenyl-pentan-2-one

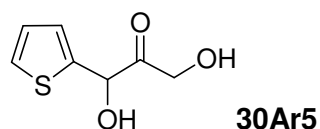


ThDP (23 mg, 48 μ mol) and $\text{MgCl}_2 \cdot 6\text{H}_2\text{O}$ (40 mg, 180 μ mol) were dissolved in H_2O (10 ml) and the pH adjusted to 7 with 0.1 M NaOH. To this stirred solution, at 25 $^\circ\text{C}$, was added D469T-TK clarified lysate (2 ml) and the mixture stirred for 20 min. In another flask, **Li-27** (110 mg, 1 mmol) and 2-phenylpropanal (134 μ l, 1 mmol) were dissolved in H_2O (8 ml) and the pH adjusted to 7 with 0.1 M NaOH. Following the 20 min enzyme/cofactor pre-incubation, the **Li-27**/2-phenylpropanal mixture was added to the enzyme solution and the mixture stirred at 25 $^\circ\text{C}$ for 24 h. During this time, the pH was maintained at 7.0 by addition of 1 M HCl using a pH stat. Silica was added and the reaction mixture concentrated to dryness before dry loading onto a flash silica gel column. Following column purification (EtOAc: CH_3OH , 1:1), compound (3*S*,4*S*)-**30Ar4** was isolated as colorless crystals (0.080 g, 40%). R_f 0.30; **Mp** ($^\circ\text{C}$) 120-130;

$[\alpha]_{\text{D}}^{25} = +30.9$ (*c* 0.22, CHCl_3); **IR (Neat)**: 3407 (b, O-H), 2925-2855 (C-H); 1720 (s, C=O); **$^1\text{H NMR}$ (300 MHz; CDCl_3)** δ 1.26 (0.25H, d, *J* 7.1, CH_3), 1.42 (2.75H, d, *J* 7.1, CH_3) 3.19-3.24 (1H, m, CHCH_3), 4.19 (1H, d, *J* 19.8, CHHOH), 4.27 (1H, d, *J* 19.8, CHHOH), 4.33 (1H, d, *J* 4.5, CHOH); 4.40 (0.92H, m, CHOH); 4.42 (0.08H, m, CHOH), 7.21-7.37 (5H, m, Ar) **$^{13}\text{C NMR}$ (75 MHz; CDCl_3)** δ 14.2 (CH_3), 43.6 (CHCH_3), 67.1 (CH_2OH), 79.5 (CHOH), 127.4, 127.7, 129.0, 142.0, 211.5 (C=O); ***m/z* (FTMS + p NSI)** calcd $[\text{M}+\text{Na}]^+$ for $\text{C}_{11}\text{H}_{14}\text{O}_3$ requires 217.0835, found 217.0836.

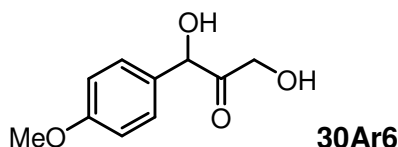
Other TK mutants: The 50 mM TK reaction using WT-TK gave (3*S*,4*S*)-**30Ar4** (68 mg, 35%) (58 mg, 30%) in 76% *de*, H26Y-TK no reaction, and D469K-TK gave (3*S*,4*S*)-**30Ar4** (74 mg, 38%) in 89% *de*, G6-TK gave (3*S*,4*S*)-**30Ar4** (74 mg, 38%) in 88% *de*, and D469E-TK gave (3*S*,4*S*)-**30Ar4** (57 mg, 30%) in 90% *de*. The absolute stereochemistry of (3*S*,4*S*)-**30Ar4** was determined using the Mosher's derivatisation method.

1,3-dihydroxy-1-(thiophen-2-yl)propan-2-one



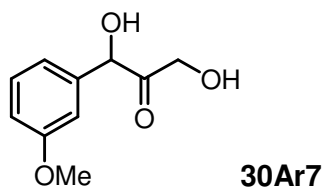
To a stirred solution of **Li-27** (0.110 g, 1.00 mmol) in water (5 ml) and THF (5 ml) at rt, was added 2-thiophenecarboxaldehyde (93 μl , 1.00 mmol) and *N*-methylmorpholine (101 μl , 1.00 mmol). The pH of the solution was then adjusted to pH 7.0 by adding 1 M HCl or 1 M NaOH solution added dropwise. The reaction mixture was stirred at rt for 24 h, and monitored by TLC. The solvent was removed *in vacuo* and the crude product dry loaded onto a flash silica chromatography column (EtOAc:hexane, 1:1) affording compound **30Ar5** (0.006 g, 4%) as a brown oil, **IR (Neat)** 3391 (s, O-H), 1708 (C=O), 694 (Ar-H); **R_f** 0.40; **$^1\text{H NMR}$ (300 MHz; CDCl_3)** δ 3.86 (2H, s, OH), 4.36 (1H, d, *J* 19.5, CHHOH), 4.42 (1H, d, *J* 19.5, CHHOH), 5.52 (1H, s, HOCH), 7.01-7.10 (2H, m), 7.35 (1H, m); **$^{13}\text{C NMR}$ (125 MHz; CDCl_3)** δ 65.2 (CH_2), 73.1 (CHO), 126.6, 127.1, 127.5, 140.1, 207.8, (C=O); ***m/z* (CI)**: calcd $[\text{M}]^+$ for $\text{C}_7\text{H}_9\text{O}_3\text{S}$ requires 173.02724, found 173.02695.

1,3-Dihydroxy-1-(4-methoxy-phenyl)-propan-2-one



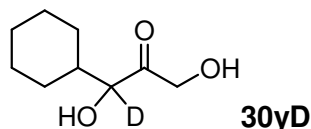
To a stirred solution of **Li-27** (0.113 g, 1.04 mmol) in water (5 ml) and THF (5 ml) at rt, was added *p*-anisaldehyde (122 μ l, 1.00 mmol) and *N*-methylmorpholine (101 μ l, 1.00 mmol). The reaction mixture was stirred at rt for 24 h, and monitored by TLC. The solvent was removed *in vacuo* and the crude product dry loaded onto a flash silica chromatography column (EtOAc: hexane, 1:1) affording compound **30Ar5** (9 mg, 5%) as a colorless oil. R_f 0.40; **IR (Neat)** 3391 (s, O-H), 1708 (C=O), 694 (Ar-H); **¹H NMR (300 MHz; CDCl₃)** δ 3.81 (3H, s), 3.85 (2H, s, OH), 4.21 (1H, d, *J* 19.4, CHHOH), 4.33 (1H, d, *J* 19.4, CHHOH), 5.19 (1H, s, CHOH), 6.90 (2H, d, *J* 6.0, Ar), 7.23 (2H, d, *J* 6.0, Ar); **¹³C NMR (125 MHz; CDCl₃)** δ 55.4 (OCH₃), 65.2 (CH₂), 77.2 (CHO), 114.8, 129.4, 147.4, 160.4, 209.3 (C=O); ***m/z* (HRMS)** [M+Na]⁺ calcd for C₁₀H₁₃O₄Na requires 219.06333, found 219.06239.

1,3-Dihydroxy-1-(3-methoxy-phenyl)-propan-2-one



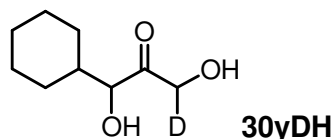
To a stirred solution of **Li-27** (0.110 g, 1.00 mmol) in water (5 ml) and THF (5 ml) at rt, was added *m*-anisaldehyde (122 μ l, 1.00 mmol) and *N*-methylmorpholine (101 μ l, 1.00 mmol). The reaction mixture was stirred at rt for 24 h, and monitored by TLC. The solvent was removed *in vacuo* and the crude product dry loaded onto a flash silica chromatography column (EtOAc: hexane, 1:1) affording compound **30Ar6** (0.008 g, 5%) as a colorless oil; **IR (Neat)** 3391 (s, O-H), 1708 (C=O), 694 (Ar-H); **¹H NMR (300 MHz; CDCl₃)** δ 3.78 (3H, s, OCH₃), 3.76 (2H, s, OH), 4.21 (1H, d, 19.5, CHH), 4.33 (1H, d, 19.5, CHH), 5.18 (1H, s), 6.81 (3H, m, Ar), 7.27 (1H, m, Ar), **¹³C NMR (125 MHz; CDCl₃)** δ 55.6 (OCH₃), 65.5 (CH₂), 77.6 (CHOH), 113.0, 114.8, 119.3, 130.4, 138.5, 160.1, 209.0 (C=O); ***m/z* (HRMS)** [M+Na]⁺ calcd for C₁₀H₁₃O₄Na requires 219.06333, found 219.06239.

[1-²H]-1-Cyclohexyl -1,3-dihydroxy-2-propanone



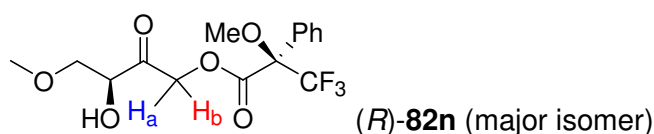
To a stirred solution of **Cs-27** (0.71 g, 3.00 mmol) in water (60 ml) at rt, was added [1-²H]-1-cyclohexanecarboxaldehyde (363 μ l, 3.00 mmol) and *N*-methylmorpholine (364 μ l, 3.00 mmol). The reaction mixture was stirred and adjusted to pH 8, and maintained at pH 8 for 48 h at rt. The solvent was removed *in vacuo* and the crude product dry loaded onto a flash silica chromatography column (EtOAc:hexane, 1:1) affording the product **30yD** (0.202 g, 40%) as a white solid. **R_f** 0.21; **IR (KBr)** 3429 (br, O-H), 1712 (s, C=O), 2925-2855 (C-H); **¹H NMR (300 MHz; CDCl₃)** δ 0.89 -1.30 (11H, m), 4.35 (1H, d, *J* 19.5, CHHOH), 4.45 (1H, d, *J* 19.5, CHHOH); **¹³C NMR (75 MHz; CDCl₃)** δ 25.9, 26.5, 29.5, 42.0, 66.2 (CH₂OH), 80.8 (t, *J*_{CD} 25.0, CDOH), 211.7 (C=O); ***m/z* (HRMS)** C₉H₁₆O₃D requires 174.12404, found 174.12394.

[1-²H]-Cyclohexyl -1,3-dihydroxy-2-propanone



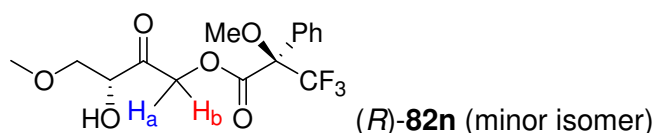
To a stirred solution of **Cs-27** (0.71 g, 3.00 mmol) in D₂O (60 ml) at rt, was added cyclohexanecarboxaldehyde (363 μ l, 3.00 mmol) and *N*-methylmorpholine (364 μ l, 3.00 mmol). The reaction mixture was stirred and adjusted to pH 8, and maintained at pH 8.0 for 48 h at rt. The solvent was removed *in vacuo* and the crude product dry loaded onto a flash silica chromatography column (EtOAc:hexane, 1:1) affording a mixture of products **30yDH** (0.202 g, 40 %) as a white solid, **R_f** 0.21; **M.p.** 110-120; **IR (KBr)** 3429 (br, O-H), 1712 (s, C=O); **¹H NMR (300 MHz; CDCl₃)** δ 0.89 -1.30 (11H, m), 4.35 (1H, d, *J* 19.5, CHHOH), 4.45 (1H, d, *J* 19.5, CHHOH); **¹³C NMR (75 MHz; CDCl₃)** δ 25.9, 26.5, 29.5, 42.0, 66.2 (t, *J*_{CD} 25.0, CHDOH), 80.8 (CHOH), 211.7 (C=O); ***m/z* (HRMS):** calcd [M+H]⁺ for C₉H₁₆DO₃ requires 174.12559, found 174.12632 (100%);

(2*R*,3'*S*)-3,3,3-Trifluoro-2-methoxy-2-phenyl propionic acid 3'-hydroxy-4'-methoxy-2'-oxo-butyl ester¹⁰⁰



The reaction was carried out under anhydrous conditions. To a stirred solution of (*S*)-**30n** (0.010 g, 0.07 mmol) in CH₂Cl₂ (3 ml) was added triethylamine (34 μl, 0.25 mmol) and (*S*)-MTPA chloride (20 μl, 0.08 mmol) in CH₂Cl₂ (2 ml) and the reaction was stirred for 12 h at rt. The product was dry loaded onto silica gel and purified using flash chromatography (EtOAc:hexane, 1:1) to afford (*R*)-**82n** as a colourless oil (0.015 g, 61%), (*2R,3S*) 57% *ee* (from integrations of H_a and H_b ¹H NMR signals of (*R*)-**82n**). **R_f** 0.40; [α]_D²⁰ = +23.2 (*c* 0.25, CHCl₃); **IR (Neat)** 3415 (br, O-H), 2923 (s, C-H), 1727 (s, ester); **¹H NMR (300 MHz; CDCl₃)** δ 3.38 (3H, s, OCH₃), 3.61 (3H, s, OCH₃), 3.57–3.70 (2H, m, CH₂), 4.36 (1H, m, CHOH), 5.13 (1H, d, *J* 17.5, CHHO (*2R,3'S*)), 5.17 (1H, d, *J* 17.5, CHHO (*2R,3'S*)), 7.42 (3H, m, Ph), 7.62 (2H, m, Ph). **¹³C NMR (150 MHz; CDCl₃)** δ 55.8 (OCH₃), 59.5 (OCH₃), 68.1, 72.8, 75.0, 84.5 (q, *J*_{CF} 27, CCF₃), 123.1 (q, *J*_{CF} 285, CF₃), 127.5, 128.5, 129.8, 131.5, 166.1 (C=O ester), 202.9 (C=O, ketone); **¹⁹F NMR (282 MHz; CDCl₃)** δ -72.2.

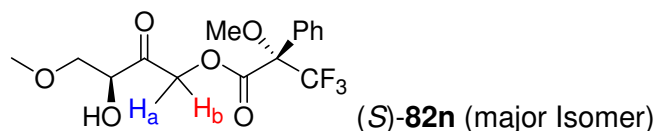
(2*R*,3'*R*)-3,3,3-Trifluoro-2-methoxy-2-phenyl propionic acid 3'-hydroxy-4'-methoxy-2'-oxo-butyl ester¹⁰⁰



The reaction was carried out under anhydrous conditions. To a stirred solution of (*S*)-**30n** (0.010 g, 0.07 mmol) in CH₂Cl₂ (3 ml) was added triethylamine (34 μl, 0.25 mmol) and (*S*)-MTPA chloride (20 μl, 0.08 mmol) in CH₂Cl₂ (2 ml) and the reaction was stirred for 12 h at rt. The product was dry loaded onto silica gel and purified using flash chromatography (EtOAc:hexane, 1:1) to afford (*R*)-**82n** as a colourless oil (0.015 g, 61%). **R_f** 0.40; [α]_D²⁰ = +23.2 (*c* 0.25, CHCl₃); **IR (Neat)** 3415 (br, O-H), 2923 (s, C-H), 1727 (s, ester); **¹H NMR (300 MHz; CDCl₃)** δ 3.38 (3H, s, OCH₃), 3.61 (3H, s, OCH₃), 3.57–3.70 (2H, m, CH₂), 4.36 (1H, m, CHOH), 5.02 (1H, d, *J* 17.5, CHHO (*2R,3'R*)), 5.29 (1H, d, *J* 17.5, CHHO (*2R,3'R*)), 7.42 (3H, m, Ph), 7.62 (2H, m, Ph). **¹³C NMR (150 MHz; CDCl₃)** δ 55.8 (OCH₃), 59.5 (OCH₃), 68.1, 72.8, 75.0, 84.5 (q, *J*_{CF} 27, CCF₃),

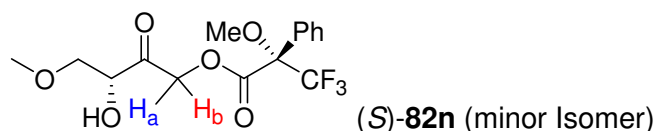
123.1 (q, J_{CF} 285, CF_3), 127.5, 128.5, 129.8, 131.5, 166.1 (C=O ester), 202.9 (C=O, ketone); ^{19}F NMR (282 MHz; $CDCl_3$) δ -72.2.

(2*S*,3'*S*)-3,3,3-Trifluoro-2-methoxy-2-phenyl propionic acid 3'-hydroxy-4'-methoxy-2'-oxo-butyl ester¹⁰⁰



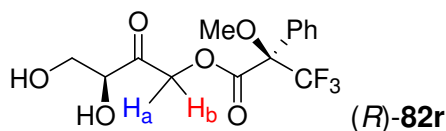
The same procedure was used as that described above for (*R*)-**82n** using (*R*)-MTPA to give (*S*)-**82n** as a colourless oil (0.010 g, 40%) (2*S*,3'*S*) 57% *ee* (from integrations of H_a and H_b 1H NMR signals of (*S*)-**82n**). R_f 0.45; $[\alpha]_D^{20}$ = -10.6 (*c* 0.25, $CHCl_3$); 1H NMR (500 MHz; $CDCl_3$) δ 3.38 (3H, s, OCH_3), 3.61 (3H, s, OCH_3) 3.57–3.70 (2H, m, CH_2), 4.36 (1H, m, $CHOH$), 5.02 (1H, d, J 17.5, $CHHO$ (2*S*,3'*S*)), 5.29 (1H, d, J 17.5, $CHHO$ (2*S*,3'*S*)), 7.42 (3H, m, Ph), 7.62 (2H, m, Ph); ^{13}C NMR (150 MHz; $CDCl_3$) δ 55.8 (OCH_3), 59.5 (OCH_3), 68.1, 72.8, 75.0, 84.5 (q, J_{CF} 27, CCF_3), 123.1 (q, J_{CF} 285, CF_3), 127.5, 128.5, 129.8, 131.5, 166.1 (C=O ester), 202.9 (C=O, ketone); ^{19}F NMR (282 MHz; $CDCl_3$) δ -72.2.

(2*S*,3'*R*)-3,3,3-Trifluoro-2-methoxy-2-phenyl propionic acid 3'-hydroxy-4'-methoxy-2'-oxo-butyl ester¹⁰⁰



The same procedure was used as that described above for (*R*)-**82n** using (*R*)-MTPA to give (*S*)-**82n** as a colourless oil (0.010 g, 40%) (2*S*,3'*S*) 57% *ee* (from integrations of H_a and H_b 1H NMR signals of (*S*)-**82n**). R_f 0.45; $[\alpha]_D^{20}$ = -10.6 (*c* 0.25, $CHCl_3$); 1H NMR (500 MHz; $CDCl_3$) δ 3.38 (3H, s, OCH_3), 3.61 (3H, s, OCH_3) 3.57–3.70 (2H, m, CH_2), 4.36 (1H, m, $CHOH$), 5.13 (1H, d, J 17.5, $CHHO$ (2*S*,3'*R*)), 5.17 (1H, d, J 17.5, $CHHO$ (2*S*,3'*R*)), 7.42 (3H, m, Ph), 7.62 (2H, m, Ph); ^{13}C NMR (150 MHz; $CDCl_3$) δ 55.8 (OCH_3), 59.5 (OCH_3), 68.1, 72.8, 75.0, 84.5 (q, J_{CF} 27, CCF_3), 123.1 (q, J_{CF} 285, CF_3), 127.5, 128.5, 129.8, 131.5, 166.1 (C=O ester), 202.9 (C=O, ketone); ^{19}F NMR (282 MHz; $CDCl_3$) δ -72.2.

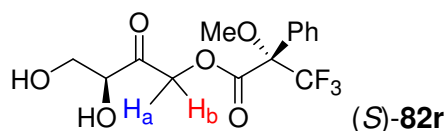
(2*R*,3'*S*)-3,3,3-Trifluoro-2-methoxy-2-phenyl propionic acid 3',4'-dihydroxy-2'-oxo-butyl ester¹⁰⁰



The reaction was carried out under anhydrous conditions. To a stirred solution of L-erythrulose (0.03 g, 0.25 mmol) in CH₂Cl₂ (5 ml) was added triethylamine (34 μl, 0.25 mmol) and (*S*)-MTPA chloride (20 μL, 0.17 mmol) in CH₂Cl₂ (2 ml) and the reaction was stirred for 12 h at rt. The product was dry loaded onto silica gel and purified using flash chromatography (EtOAc) to afford (*R*)-**82r** as a colourless oil (0.054 g, 63%), (*2R,3'S*) >95% *ee* (from integrations of H_a and H_b ¹H NMR signals (*R*)-**82r**). **R_f** 0.45 (EtOAc); [**α**]_D²⁰ = +10.2 (*c* 0.4, CHCl₃); **IR (Neat)** 3429 (b, O-H), 2925, 1712 (s, C=O); **¹H NMR (300 MHz; CDCl₃)** δ 3.64 (3H, s, OMe), 3.89 (1H, dd, *J* 10.6 and 3.8, CHHOH), 3.95 (1H, dd, *J* 10.6 and 3.8, CHHOH), 4.35 (1H, dd, *J* 3.8 and 3.8, CHOH), 5.11 (1H, d, *J* 17.0, CHHO (*2R,3'S*)), 5.19 (1H, d, *J* 17.0, CHHO (*2R,3'S*)), 7.43 (3H, m, Ph), 7.62 (2H, m, Ph), no (*2R,3'R* isomer detected); **¹³C NMR (75 MHz; CDCl₃)** δ 55.9 (OCH₃), 63.5, 68.0, 76.4, 84.6 (q, *J*_{CF} 28, CCF₃), 123.1 (q, *J*_{CF} 288, CF₃), 127.5, 128.6, 129.9, 131.7, 166.5 (C=O ester), 203.3 (C=O, ketone); **¹⁹F NMR (282 MHz; CDCl₃)** δ -72.2; ***m/z* (FTMS) [M+NH₄]** calcd for C₁₄H₁₉F₃O₆N requires 354.1159; found 354.1162.

129.9, 131.7, 166.5 (C=O ester), 203.3 (C=O, ketone); **¹⁹F NMR (282 MHz; CDCl₃)** δ -72.2; ***m/z* (FTMS) [M+NH₄]** calcd for C₁₄H₁₉F₃O₆N requires 354.1159; found 354.1162.

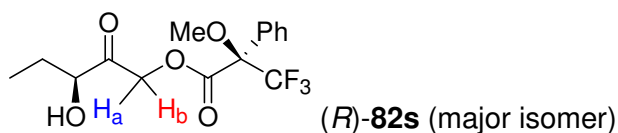
(2*S*,3'*S*)-3,3,3-Trifluoro-2-methoxy-2-phenyl propionic acid 3',4'-dihydroxy-2'-oxo-butyl ester¹⁰⁰



The same procedure was used as that described above for (*R*)-**82r** using (*R*)-MTPA to give (*S*)-**82r** as a colourless oil (0.044 g, 51%) (*2S,3'S*) >95% *ee* (from integrations of H_a and H_b ¹H NMR signals of (*S*)-**82r**). **R_f** 0.45 (EtOAc); [**α**]_D²⁰ = -14.4 (*c* 0.5, CHCl₃), **¹H NMR (500 MHz; CDCl₃)** δ 3.63 (3H, s, OMe), 3.92 (2H, m, CH₂OH), 4.35 (1H, dd, *J* 4.0 and 3.8, CHOH), 5.05 (1H, d, *J* 17.0, CHHO (*2S,3'S*)), 5.23 (1H, d, *J* 17.0, CHHO (*2S,3'S*)), 7.43 (3H, m, Ph), 7.62 (2H, m, Ph), no (*2S,3'R* isomer detected); **¹³C NMR (125 MHz; CDCl₃)** δ 55.8 (OCH₃), 63.5 (CH₂OH), 67.9 (CH₂C=O), 76.3 (CHOH), 84.6

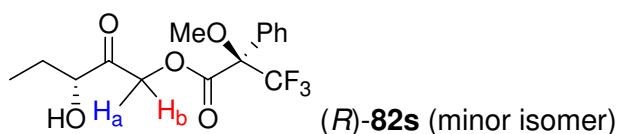
(q, J_{CF} 28, CCF_3), 123.1 (q, J_{CF} 288, CF_3), 127.5, 128.5, 129.9, 131.7, 166.4 ($C=O$ ester), 203.1 ($C=O$, ketone); ^{19}F NMR (282 MHz; $CDCl_3$) δ -72.2.

(2*R*,3'*S*)-3,3,3-Trifluoro-2-methoxy-2-phenyl propionic acid 3'-hydroxy-2'-oxo-pentyl ester¹⁰⁰



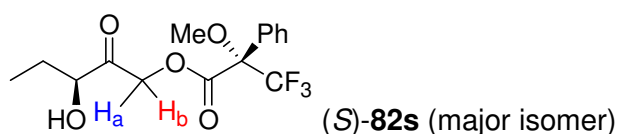
The reaction was carried out under anhydrous conditions. To a stirred solution of (*S*)-**30s** (0.03 g, 0.25 mmol) in CH_2Cl_2 (5 ml) was added DCC (0.06 g, 0.28 mmol) and DMAP (0.01 g, 0.02 mmol) in CH_2Cl_2 (10 ml) at 0 °C and the reaction was stirred for 2 min. (*S*)-MTPA (0.03 g, 0.08 mmol) was added and the reaction stirred for 30 min, then further (*S*)-MTPA (0.02 g, 0.08 mmol) added and the mixture stirred for 48 h at rt. The solvent was removed *in vacuo*, the crude product dry loaded onto silica gel and purified using flash chromatography (EtOAc:hexane, 3:2) to afford (*R*)-**82s** as a colourless oil (0.035 g, 59%), (*2R,3'S*)-55% *ee* (from the integrations of H_a and H_b 1H NMR signals from (*R*)-**82s**). R_f 0.45; $[\alpha]_D^{20}$ +13.3 (*c* 0.15, $CHCl_3$); IR (Neat) 3429br s, 2925s, 1712s; 1H NMR (500 MHz; $CDCl_3$) δ 1.00 (3H, m, CH_3), 1.65 (1H, m, $CHHCH_3$) 1.89 (1H, m, $CHHCH_3$), 2.86 (1H, d, J 6.0, OH), 3.64 (3H, s, OMe), 4.29 (1H, m, $CHOH$), 5.05 (1H, s, CH_2O (*2R,3'S*)), 7.54 (3H, m, Ph), 7.61 (2H, m, Ph); ^{13}C NMR (125 MHz; $CDCl_3$) δ 8.8 (CH_3), 27.2 (CH_2CH_3), 55.8 (OCH₃), 67.2, 76.2, 123.2 (q, J_{CF} 283, CF_3), 127.6, 128.6, 129.9, 131.8, 166.3 ($C=O$ ester), 204.2 ($C=O$, ketone); ^{19}F NMR (282 MHz; $CDCl_3$) δ -72.2; *m/z* (FTMS) calcd [M+NH₄] for $C_{15}H_{21}F_3O_5N$ requires 352.1366; found 352.1371.

(2*R*,3'*R*)-3,3,3-Trifluoro-2-methoxy-2-phenyl propionic acid 3'-hydroxy-2'-oxo-pentyl ester¹⁰⁰



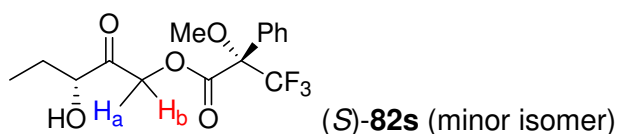
The reaction was carried out under anhydrous conditions. To a stirred solution of (*S*)-**30s** (0.03 g, 0.25 mmol) in CH₂Cl₂ (5 ml) was added DCC (0.06 g, 0.28 mmol) and DMAP (0.01 g, 0.02 mmol) in CH₂Cl₂ (10 ml) at 0 °C and the reaction was stirred for 2 min. (*S*)-MTPA (0.03 g, 0.08 mmol) was added and the reaction stirred for 30 min, then further (*S*)-MTPA (0.02 g, 0.08 mmol) added and the mixture stirred for 48 h at rt. The solvent was removed *in vacuo*, the crude product dry loaded onto silica gel and purified using flash chromatography (EtOAc:hexane, 3:2) to afford (*R*)-**82s** as a colourless oil (0.035 g, 59%). *R*_f 0.45; [α]_D²⁰ = +13.3 (*c* 0.15, CHCl₃); **IR (Neat)** 3429br s, 2925s, 1712s; **¹H NMR (500 MHz; CDCl₃)** δ 1.00 (3H, m, CH₃), 1.65 (1H, m, CHHCH₃) 1.89 (1H, m, CHHCH₃), 2.86 (1H, d, *J* 6.0, OH), 3.64 (3H, s, OMe), 4.29 (1H, m, CHOH), 4.93 (1H, d, *J* 17.0, CHHO (2*R*,3'*R*)), 5.17 (1H, d, *J* 17.0, CHHO (2*R*,3'*R*)), 7.54 (3H, m, Ph), 7.61 (2H, m, Ph); **¹³C NMR (125 MHz; CDCl₃)** δ 8.8 (CH₃), 27.2 (CH₂CH₃), 55.8 (OCH₃), 67.2, 76.2, 123.2 (q, *J*_{CF} 283, CF₃), 127.6, 128.6, 129.9, 131.8, 166.3 (C=O ester), 204.2 (C=O, ketone); **¹⁹F NMR (282 MHz; CDCl₃)** δ -72.2; *m/z* (FTMS) calcd [M+NH₄] for C₁₅H₂₁F₃O₅N requires 352.1366; found 352.1371.

(2*S*,3'*S*)-3,3,3-Trifluoro-2-methoxy-2-phenyl propionic acid 3'-hydroxy-2'-oxo-pentyl ester¹⁰⁰



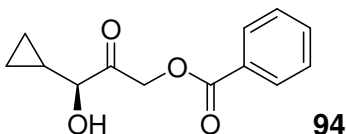
The same procedure was used as that described above for (*S*)-**30s** using (*S*)-MTPA to give (*S*)-**82s** as a colourless oil (0.030 g, 57%) (2*S*,3'*S*)-55% *ee* (from integrations of H_a and H_b ¹H NMR signals from (*S*)-**82s**). *R*_f 0.45; [α]_D²⁰ = -37.0 (*c* 0.1, CHCl₃); **¹H NMR (300 MHz; CDCl₃)** δ 1.00 (3H, t, *J* 7.4, CH₃), 1.69 (1H, m, CHHCH₃) 1.89 (1H, m, CHHCH₃), 2.87 (1H, d, *J* 5.3, OH), 3.64 (3H, s, OMe), 4.29 (1H, m, CHOH), 4.93 (1H, d, *J* 17.0, CHHO (2*S*,3'*S*)), 5.17 (1H, d, *J* 17.0, CHHO (2*S*,3'*S*)), 7.54 (3H, m, Ph), 7.61 (2H, m, Ph); **¹³C NMR (75 MHz; CDCl₃)** δ 8.7 and 8.8 (CH₃), 27.2, 55.8 (OCH₃), 67.2, 76.2, 123.2 (q, *J*_{CF} 283, CF₃), 127.6, 128.5, 128.7, 129.9, 166.2 (C=O ester), 204.2 (C=O, ketone); **¹⁹F NMR (282 MHz; CDCl₃)** δ -72.2.

(2*S*,3'*R*)-3,3,3-Trifluoro-2-methoxy-2-phenyl propionic acid 3'-hydroxy-2'-oxo-pentyl ester¹⁰⁰



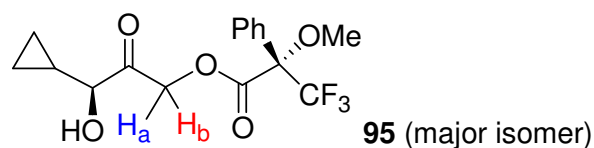
The same procedure was used as that described above for (*S*)-**30s** using (*S*)-MTPA to give (*S*)-**82s** as a colourless oil (0.030 g, 57%) R_f 0.45; $[\alpha]_D^{20} = -37.0$ (c. 0.1, CHCl_3); $^1\text{H NMR}$ (300 MHz; CDCl_3) δ 1.00 (3H, t, J 7.4, CH_3), 1.69 (1H, m, CHHCH_3) 1.89 (1H, m, CHHCH_3), 2.87 (1H, d, J 5.3, OH), 3.64 (3H, s, OMe), 4.29 (1H, m, CHOH), 5.05 (1H, s, CH_2O (2*S*,3'*R*)), 7.54 (3H, m, Ph), 7.61 (2H, m, Ph); $^{13}\text{C NMR}$ (75 MHz; CDCl_3) δ 8.7 and 8.8 (CH_3), 27.2, 55.8 (OCH_3), 67.2, 76.2, 123.2 (q, J_{CF} 283, CF_3), 127.6, 128.5, 128.7, 129.9, 166.2 ($\text{C}=\text{O}$ ester), 204.2 ($\text{C}=\text{O}$, ketone); $^{19}\text{F NMR}$ (282 MHz; CDCl_3) δ -72.2.

(3*S*)-3-Cyclopropyl-3-hydroxy-2-oxopropyl benzoate¹⁰⁶



The reaction was carried out under anhydrous conditions. To a stirred solution of (*S*)-**30v** (0.010 g, 0.06 mmol) in CH_2Cl_2 (1 ml) was added triethylamine (34 μl , 0.25 mmol) and benzoyl chloride (10 μl , 0.04 mmol) the reaction was stirred for 12 h at rt. The product was dry loaded onto silica gel and purified using flash chromatography (Hexane: EtOAc, 4:1) to afford **94** as a colourless oil (0.010 g, 71%). R_f 0.45; $[\alpha]_D^{25} = +74.0$ (c 0.35, CHCl_3); IR (Neat) 3442 (br, O-H) 2931s, 1722 (s, $\text{C}=\text{O}$, ester); $^1\text{H NMR}$ (300 MHz; CDCl_3) δ 1.20-1.72 (4H, m), 1.55 (1H, OH), 2.32 (1H, m), 3.05 (1H, d, J 5.0 Hz, OH) 4.45 (1H, d, J 4.0 Hz, CHOH), 4.97 (1H, d, CHH , J 17.0 Hz), 5.16 (1H, d, CHH , J 17.0 Hz), 7.26-7.48 (2H, m, Ar), 7.58 (1H, m, Ar), 8.02 (1H, m, Ar); $^{13}\text{C NMR}$ (125 MHz; CDCl_3) δ 25.5, 25.9 (signal overlap), 29.2, 66.4 (CH_2O), 77.3 (CHOH), 128.5, 129.0, 130.0, 133.5, 165.2 ($\text{C}=\text{O}$ ester), 205.5 ($\text{C}=\text{O}$, ketone); m/z (HRMS) calcd $[\text{M}+\text{H}]^+$ for $\text{C}_{13}\text{H}_{14}\text{O}_4$ requires 234.12145, found 234.19234; HPLC conditions: chiralpak AD column, hexane:*i*-PrOH, 97:3, 1 ml min^{-1} , retention times: 34.9 min (*S*-isomer, >99% ee), with no *R*-isomer was detected.

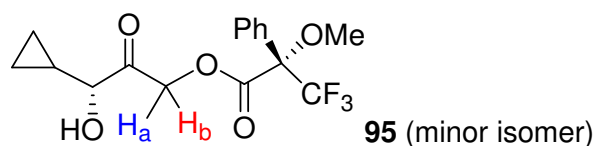
(2*S*,3'*S*)-3,3,3-Trifluoro-2-methoxy-2-phenyl propionic acid 3'-cyclopropyl-3'-hydroxy-2'-oxo-propyl ester¹³³



The reaction was carried out under anhydrous conditions. To a stirred solution of (*S*)-**30v** (0.010 g, 0.08 mmol) in CH₂Cl₂ (1 ml) was added triethylamine (34 μl, 0.25 mmol) and (*R*)-MTPA chloride (10 μl, 0.04 mmol) in CH₂Cl₂ (2 ml) and the reaction was stirred for 12 h at rt. The product was dry loaded onto silica gel and purified using flash chromatography (Hexane:EtOAc, 4:1) to afford **95** as a colourless oil (0.013 g, 87%), (*2S,3S*) 92% *ee* (from integrations of H_a and H_b ¹H NMR signals of **95**). *R_f* 0.45; [α]²⁵_D = +45.0 (*c* 0.2, EtOH); **IR (Neat)** 3420 (b, O-H), 2930, 2855, 1734 (s, C=O);

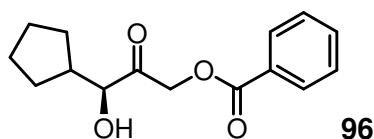
¹H NMR (300 MHz; CDCl₃) δ 0.55 (2H, m), 0.71 (2H, m), 1.03 (1H, m), 3.09 (1H, d, *J* 4.3 Hz), 3.60 (3H, s, OCH₃), 3.63 (1H, m), 4.95 (1H, d, *J* 15.0 Hz, CHHO (*2S,3'S*)), 5.37 (1H, d, *J* 15.0, CHHO (*2S,3'S*)), 7.43 (3H, m, Ph), 7.63 (2H, m, Ph); **¹³C NMR (125 MHz; CDCl₃)** δ 14.7, 55.8 (OCH₃), 66.9, 78.1, 127.6, 128.5, 129.9, 131.8, 166.2 (C=O ester), 203.0 (C=O, ketone); **¹⁹F NMR (282 MHz; CDCl₃)** δ -72.3; ***m/z* (FTMS)** calcd [M+NH₄]⁺ for C₁₆H₂₁F₃O₅N requires 364.1366, found 364.1364.

(2*S*,3'*R*)-3,3,3-Trifluoro-2-methoxy-2-phenyl propionic acid 3'-cyclopropyl-3'-hydroxy-2'-oxo-propyl ester¹³³



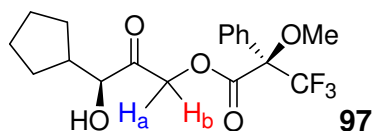
The reaction was carried out under anhydrous conditions. To a stirred solution of (*S*)-**30v** (0.010 g, 0.08 mmol) in CH₂Cl₂ (1 ml) was added triethylamine (34 μl, 0.25 mmol) and (*R*)-MTPA chloride (10 μl, 0.04 mmol) in CH₂Cl₂ (2 ml) and the reaction was stirred for 12 h at rt. The product was dry loaded onto silica gel and purified using flash chromatography (Hexane:EtOAc, 4:1) to afford **95** as a colourless oil (0.013 g, 87%). *R_f* 0.45; [α]²⁵_D = +45.0 (*c* 0.2, EtOH); **IR (Neat)** 3420 (b, O-H), 2930, 2855, 1734 (s, C=O); **¹H NMR (300 MHz; CDCl₃)** δ 0.55 (2H, m), 0.71 (2H, m), 1.03 (1H, m), 3.09 (1H, d, *J* 4.3 Hz), 3.60 (3H, s, OCH₃), 3.63 (1H, m), 5.05 (1H, d, *J* 18.0 Hz, CHHO (*2S,3'R*)), 5.17 (1H, d, *J* 18.0 Hz, CHHO (*2S,3'R*)), 7.43 (3H, m, Ph), 7.63 (2H, m, Ph); **¹³C NMR (125 MHz; CDCl₃)** δ 14.7, 55.8 (OCH₃), 66.9, 78.1, 127.6, 128.5, 129.9, 131.8, 166.2 (C=O ester), 203.0 (C=O, ketone); **¹⁹F NMR (282 MHz; CDCl₃)** δ -72.3; ***m/z* (FTMS)** calcd [M+NH₄]⁺ for C₁₆H₂₁F₃O₅N requires 364.1366, found 364.1364.

(3S)-3-Cyclopentyl-2-oxobutyl benzoate¹⁰⁶



The reaction was carried out under anhydrous conditions. To a stirred solution of (*S*)-**30x** (0.01 g, 0.06 mmol) in CH₂Cl₂ (1 ml) was added triethylamine (34 μl, 0.25 mmol) and benzoyl chloride (10 μl, 0.04 mmol) the reaction was stirred for 12 h at rt. The product was dry loaded onto silica gel and purified using flash chromatography (Hexane:EtOAc, 4:1) to afford **96** as a colourless oil (0.013 g, 79%), *R_f* 0.45; [α]_D²⁵ = +26.6 (*c* 0.3, CHCl₃); IR (Neat) 3484 (br, O-H), 2931s, 1722 (s, C=O, ester); ¹H NMR (300 MHz; CDCl₃) δ 1.25-1.84 (10H, m), 2.32 (1H, m), 3.05 (1H, d, *J* 5.0, OH) 4.45 (1H, d, *J* 3.6, CHOH), 5.04 (1H, d, CHH, *J* 17.0), 5.16 (1H, d, CHH, *J* 17.0), 7.29-7.35 (1H, m), 7.46 (2H, t, *J* 7.8, Ar), 7.61 (1H, t, *J* 7.4, Ar); 8.08 (1H, d, *J* 9.0, Ar); ¹³C NMR (125 MHz; CDCl₃) δ 25.5, 25.9 (signal overlap), 26.0, 29.2, 42.7, 66.4 (CH₂O), 77.3 (CHOH), 128.6, 129.1, 130.0, 133.6, 165.9 (C=O ester), 205.5 (C=O, ketone); *m/z* (HRMS) calcd [M+H]⁺ for C₁₅H₁₉O₄ requires 263.12833, found 263.12787; HPLC conditions: chiralpak AD column, hexane:*i*-PrOH, 97:3, 1 ml min⁻¹, retention times: 31.8 min (*S*-isomer, >99% ee) with no *R*-isomer detected.

(2*R*,3'*S*)-3,3,3-Trifluoro-2-methoxy-2-phenyl propionic acid 3'-cyclopentyl-3'-hydroxy-2'-oxo-propyl ester¹⁰⁶



The reaction was carried out under anhydrous conditions. To a stirred solution of (*S*)-**30x** (0.010 g, 0.05 mmol) in CH₂Cl₂ (1 ml) was added triethylamine (34 μl, 0.25 mmol) and (*R*)-MTPA chloride (10 μl, 0.04 mmol) the reaction was stirred for 12 h at rt. The product was dry loaded onto silica gel and purified using flash chromatography (EtOAc:hexane:, 1:4) to afford **97** as a colourless oil (0.020 g, 87%), (*2S*,3'*S*) >99% *ee* (from integrations of H_a and H_b ¹H NMR signals of **97**). *R_f* 0.50; [α]_D²⁵ = +30.0 (*c* 0.1, CHCl₃); IR (Neat) 3420 (br, O-H), 2930, 2855, 1734 (s, ester); ¹H NMR (600 MHz; CDCl₃) δ 1.34-1.78 (8H, m), 2.23 (1H, m) 2.90 (1H, d, *J* 5.1, OH) 3.64 (3H, s, OCH₃) 4.31 (1H, d, *J* 4.2), 5.05 (1H, d, *J* 16.9, CHHO (*2R*,3*S*)), 5.08 (1H, d, *J* 16.9, CHHO (*2R*, 3*S*)), no (*2S*, 3*S*) isomer detected, 7.43 (3H, m, Ph), 7.63 (2H, m, Ph); ¹³C NMR (150 MHz; CDCl₃) δ 25.7, 25.8, 25.9, 29.1, 42.8, 55.9 (OCH₃), 67.4, 77.0 (CHOH), 84.7 (q, *J*_{CF} 27, CCF₃), 123.2 (d, *J*_{CF} 287, CF₃), 127.6, 128.6, 130.0, 131.9, 166.2 (C=O ester), 204.0 (C=O, ketone); ¹⁹F NMR (282 MHz; CDCl₃) δ -72.2; *m/z* (FTMS) calcd [M+NH₄]⁺ for C₁₈H₂₁F₃O₅NH₄ requires 393.1712 found 393.1712.

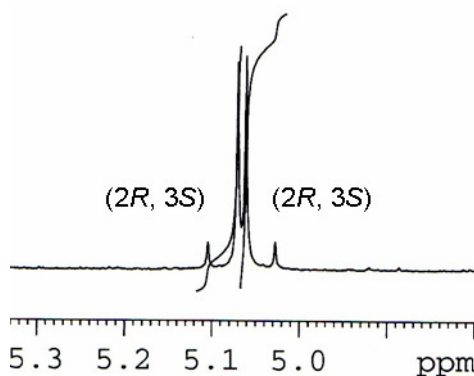
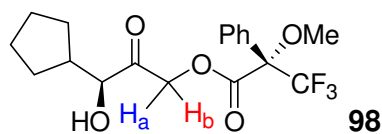


Figure 75 ¹H NMR spectra of compound **97**

(2*S*,3'*S*)-3,3,3-Trifluoro-2-methoxy-2-phenyl propionic acid 3'-cyclopentyl-3'-hydroxy-2'-oxo-propyl ester¹⁰⁶



The reaction was carried out under anhydrous conditions. To a stirred solution of (*S*)-**30x** (0.01 g, 0.05 mmol) in CH₂Cl₂ (1 ml) was added triethylamine (34 μ l, 0.25 mmol) and (*R*)-MTPA chloride (10 μ l, 0.04 mmol) the reaction was stirred for 12 h at rt. The product was dry loaded onto silica gel and purified using flash chromatography (EtOAc:hexane, 1:4) to afford **98** as a colourless oil (0.018 g, 78%), (2*S*,3*S*) >99% *ee* (from integrations of H_a and H_b ¹H NMR signals of **98**). *R*_f 0.50; [α]_D²⁵ = -60.0 (*c* 0.1, CHCl₃); IR (Neat) 3430 (b, O-H), 2930, 1732 (s, C=O, ester); ¹H NMR (600 MHz; CDCl₃) δ 1.17-1.95 (8H, m), 2.23 (1H, m) 2.91 (1H, m) 3.65 (3H, s, OCH₃) 4.31 (1H, d, *J* 3.6), 4.92 (1H, d, *J* 12.0, CHHO (2*S*,3'*S*)), 5.20 (1H, d, *J* 12.0, CHHO (2*R*, 3'*S*)), no (2*R*, 3'*S*) isomer detected, 7.43 (3H, m, Ph), 7.62 (2H, m, Ph); ¹³C NMR (150 MHz; CDCl₃) δ 25.1, 25.7, 25.9, 29.1, 41.9, 55.9 (OCH₃), 67.4, 77.2 (CHOH), 84.7 (q, *J*_{CF} 27, CCF₃), 123.2 (d, *J*_{CF} 287, CF₃), 127.6, 128.6, 130.0, 131.9, 166.2 (C=O ester), 204.0 (C=O, ketone); ¹⁹F NMR (282 MHz; CDCl₃) δ -72.2; *m/z* (FTMS) calcd [M+NH₄]⁺ for C₁₈H₂₁F₃O₅NH₄ requires 393.1712, found 393.1712 (Fig. 74).

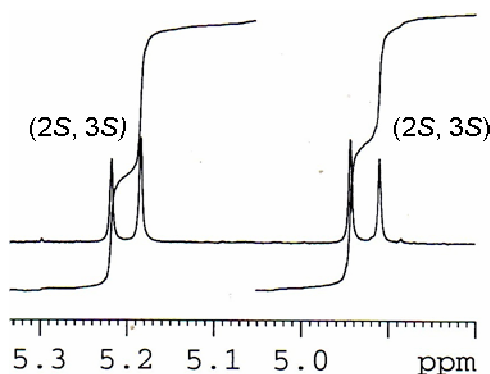
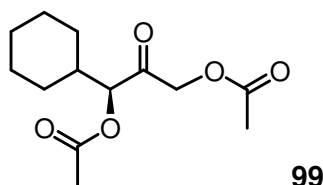


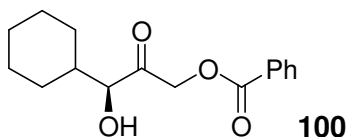
Figure 76 ¹H NMR of spectra of compound **98**

(3S)-3-(Acetyloxy)-3-cyclohexyl-2-oxopropyl acetate



To a stirred solution of **30y** (0.03 g, 0.17 mmol) in anhydrous pyridine (3 ml) at rt was added acetic anhydride (1 ml) under an argon atmosphere. The volatile solvents were removed *in vacuo*. The remaining residue was dissolved in 50 ml EtOAc and was washed with 0.3 M KHSO₄ (2 × 50 ml) and sat. NaHCO₃ (2 × 50 ml). The organic layer was dried under magnesium sulfate and the solvent removed *in vacuo* affording a brown oil **99** (0.043 g, >99 %). *R_f* 0.40 (EtOAc:hexane, 1:4); **IR (Neat)** 3420 (b, O-H), 2930, 2855, 1734 (s, C=O, ester); **¹H NMR (300 MHz; CDCl₃)** δ 0.91-1.89 (11H, m), 2.10 (3H, s), 2.11 (3H, s), 4.71 (1H, d, *J* 18.0), 4.79 (1H, d, *J* 18.0), 4.91 (1H, d, *J* 6.0); **¹³C NMR (75 MHz; CDCl₃)** δ 20.4 (CH₃), 20.5 (CH₃), 25.8, 27.3, 28.9, 39.6, 67.0 (CH₂O), 80.3 (CHO), 170.1 (C=O), 170.5 (C=O), 200.8 (C=O); ***m/z* (CI)** calcd [MH]⁺ for C₁₃H₂₁O₅ requires 257.13890 found 257.13790. **HPLC** conditions: chiralpak AD column, hexane:*i*-PrOH, 97:3, 1 ml min⁻¹, retention times: 12.0 min and 13.6 min (racemic mixtures).

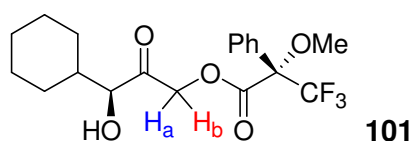
(3S)-3-Cyclohexyl-3-hydroxy-2-oxopropyl benzoate¹⁰⁶



To a stirred solution of (*S*)-**30y** (0.100 g, 0.58 mmol) in 20 ml dry CH₂Cl₂ at rt was added triethylamine (177 μl, 1.27 mmol) and benzoyl chloride (147 μl, 1.27 mmol) under an argon atmosphere. The reaction was heated under reflux for 6 h, and monitored by TLC. The reaction mixture was poured into 30 ml CH₂Cl₂ and washed successively with 0.3 M KHSO₄ (2 × 20 ml), sat. NaHCO₃ (2 × 20 ml) and brine (2 × 20 ml). The organic layer was dried over anhydrous magnesium sulfate and was removed *in vacuo* to obtain the crude product. The residue was further purified by silica gel column chromatography (EtOAc:hexane, 1:4) to afford the dibenzoate product as a colorless oil (0.072 g, 45 %). *R_f* 0.35; **IR (Neat)** 3420 (br, O-H), 2930, 1734 (s, ester); **¹H NMR (300 MHz; CDCl₃)** δ 0.64-1.83 (11H, m), 4.25 (1H, d, *J* 2.8), 5.00 (1H, d, *J* 17.1, CHHO), 5.15 (1H, d, *J* 17.1, CHHO), 7.25-8.18 (5H, m); **¹³C NMR (150 MHz;**

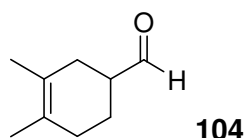
CDCl₃) 25.5, 25.9 (signal overlap), 26.5, 29.8, 66.7 (CH₂O), 79.5 (CHOH), 128.6, 129.1, 130.2, 133.7, 166.0 (C=O ester), 205.7 (C=O, ketone); **m/z (CI)** calcd [M+H]⁺ for C₁₆H₂₀O₄ requires 277.14398, found 277.14335. **HPLC** conditions: Chiracel-OD column; mobile phase hexane:*i*-PrOH, 98:2, 1 m min⁻¹, retention times: 28.5 min (*S*-isomer, >99% *ee*) with no *R*-isomer detected.

(2*S*,3'*S*)-3,3,3-Trifluoro-2-methoxy-2-phenyl propionic acid 3'-cyclohexyl-3'-hydroxy-2'-oxo-propyl ester¹⁰⁶



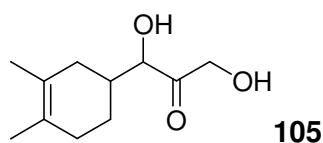
The reaction was carried out under anhydrous conditions. To a stirred solution of (*S*)-**30y** (0.010 g, 0.05 mmol) in CH₂Cl₂ (1 ml) was added triethylamine (34 μl, 0.25 mmol) and (*R*)-MTPA chloride (10 μl, 0.04 mmol) the reaction was stirred for 12 h at rt. The product was dry loaded onto silica gel and purified using flash chromatography (EtOAc:hexane, 1:4) to afford **101** as a colourless oil (0.018 g, 78%), (*2S,3S*) >98% *ee* (from integrations of H_a and H_b ¹H NMR signals of **101**). **R_f** 0.45; **[α]_D²⁵** = -26.0 (*c* 0.2, CHCl₃); **IR (Neat)** 3420 (br, O-H), 2930, 2855, 1734 (s, ester); **¹H NMR (300 MHz; CDCl₃)** δ 0.89-1.76 (1H, m), 2.80 (1H, d, *J* 3.0, OH) 3.65 (3H, s, OCH₃), 4.16 (1H, m), 4.90 (1H, d, *J* 9.0, CHHO (*2S,3'S*)), 5.19 (1H, d, *J* 9.0, CHHO (*2R, 3'S*)) negligible (*2R, 3'S* isomer detected), 7.43 (3H, m, Ph), 7.63 (2H, m, Ph); **¹³C NMR (125 MHz; CDCl₃)** δ 25.5, 25.9 (signal overlap), 26.4, 29.7, 41.9, 55.8 (OCH₃), 67.8, 79.7 (CHOH), 127.5, 128.5, 129.9, 131.9, 166.2 (C=O ester), 204.2 (C=O, ketone); **¹⁹F NMR (282 MHz; CDCl₃)** δ -72.2; **m/z (FTMS)** calcd [M+NH₄]⁺ for C₁₉H₂₇F₃NO₅ requires 406.1836, found 406.1831.

3,4-Dimethyl-cyclohex-3-enecarbaldehyde¹⁰²



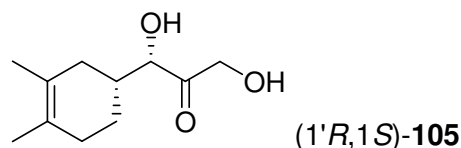
A zinc chloride (5.45 g, 40 mmol,) and choline chloride (2.70 g, 20 mmol) mixture was heated to 150 °C and stirred for 10 min, then left to cool to 26 °C. 2,3 Dimethyl, 1-3-butadiene (800 μ l, 12 mmol) and acrolein (800 μ l, 12 mmol) was added to this ionic liquid and was left to stir for 2 h. The aldehyde was pipetted from the ionic liquid and clear colorless oil **104** was obtained (1.423 g, 84%); **IR (Neat)** 2923, 1720; **¹H NMR (300 MHz; CDCl₃)** δ 1.54 (3H, s, CH₃), 1.61 (3H, s, CH₃), 1.87-2.44 (7H, m), 9.67 (1H, s, CHO); **¹³C NMR (75 MHz; CDCl₃)** δ 18.9 (CH₃), 19.1 (CH₃), 22.8, 30.1, 30.5, 46.9, 123.4, 125.8, 204.7 (C=O); **m/z (CI)** calcd [MH]⁺ for C₉H₁₆O requires 139.11229, found 139.11298.

(1*RS*,1'*RS*)-1-(3',4'-Dimethyl-cyclohex-3'-enyl)-1,3-dihydroxypropan-2-one



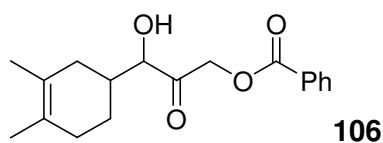
To a stirred solution of **Li-27** (0.33 g, 3.00 mmol) in water (60 ml) at rt, was added **104** (0.414 g, 3.00 mmol) and *N*-methylmorpholine (0.33 ml, 3.00 mmol). The reaction mixture was stirred at rt for 48 h. The solvent was removed *in vacuo* and the crude product dry loaded onto a flash silica chromatography column (EtOAc:hexane, 1:1) to afford **105** as a colourless oil (0.060 g, 10%). **R_f** 0.49, **M.p.** 150-160; **IR (Neat)** 3456 (b, O-H), 2893m, 1721 (s, C=O); **¹H NMR (300 MHz; CDCl₃)** δ 1.40–2.08 (13H, m), 2.93 (2H, m, OH), 4.26 (1H, m, CHOH), 4.36 (1H, br d, *J* 19.3, CHHOH) 4.49 (1H, dd, *J* 19.3 and 4.2, CHHOH); **¹³C NMR (75 MHz; CDCl₃)** δ 18.8 (CH₃), 19.1 (CH₃), 23.5, 31.5, 34.3, 38.9, 66.1 (CH₂OH), 78.2 (CHOH), 125.4, 130.4, 211.6 (C=O); **m/z (FAB⁺)** 221 (MNa⁺, 35%), 199 (MH⁺, 100); **(HRFAB⁺)** calcd for C₁₁H₁₉O₃ (MH)⁺ requires 199.13341 found 199.13381. The 2-isomer mixture of (1*RS*,1'*R*)-1-(3',4'-dimethylcyclohex-3'-enyl)-1,3-dihydroxypropan-2-one (1'*R*)-**105** (0.06 g, 10%) was prepared using an identical method with (1*R*)-**104**

(1'R,1S)-3-(3',4'-Dimethyl-cyclo-3-enyl)-1,3-dihydroxypropan-2-one



The TK conversion protocol using **104** and D469T performed gave (1'R,1S)-**105** (0.06 g, 10%). $[\alpha]_{20}^D = +140$ (c 0.5, CHCl₃); **M.p.** 150-160; **¹H NMR (300 MHz; CDCl₃)** δ 1.38 (2H, m), 1.59 (3H, s, CH₃), 1.61 (3H, s, CH₃), 1.96 (4H, m), 2.12 (1H, m), 2.98 (1H, m) 4.22 (1H, *J* 2.6, CHOH), 4.30 (1H, d, *J* 18.8, CHHOH) 4.48 (1H, d, *J* 18.8, CHHOH); **¹³C NMR (125 MHz; CDCl₃)** δ 18.8 (CH₃), 19.1 (CH₃), 23.3, 31.5, 34.3, 38.9 (CH), 66.1 (CH₂OH), 78.2 (CHOH), 125.4, 130.4, 211.6 (C=O). The HPLC analysis (1'R, 1S)-**105** was formed as the major isomer in 97% ee (minor isomer (1'R, 1R)-**105**).

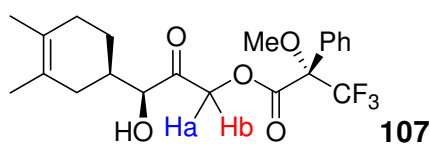
(1RS,1'RS)-3-(3,4-dimethylcyclohex-3-en-1-yl)-3-hydroxy-2-oxopropyl benzoate



To a stirred solution of **105** (0.030 g, 0.10 mmol) in CH₂Cl₂ (3 ml) was added triethylamine (20 μ l, 0.20 mmol) and benzoyl chloride (28 μ l, 0.20 mmol). The reaction was then heated under reflux for 6 h, cooled and added to CH₂Cl₂ (30 ml) and washed with 0.3 M KHSO₄ (2 \times 20 ml), sat. NaHCO₃ (2 \times 20 ml) and brine (2 \times 20 ml). The organic layer was dried using magnesium sulfate and was evaporated to obtain the crude product. The residue was purified using silica gel column chromatography (EtOAc:hexane, 1:4) to afford the benzoate product as a colourless oil **106** (0.040 g, 70%). **R_f** 0.34; **IR (Neat)** 3429 (br, O-H) 2925s, 1785 (s, C=O, ester), 1724s (C=O), 1452m; **¹H NMR (300 MHz; CDCl₃)** δ 1.23–2.04 (13H, m), 3.00 (1H, br s, OH), 4.26 (1H, d, *J* 2.7, CHOH), 5.01 (1H, d, *J* 17.1, CHHOH), 5.15 (1H, d, *J* 17.1, CHHOH), 7.60 (3H, m, Ar), 8.13 (2H, m, Ar); **¹³C NMR (75 MHz; CDCl₃)** δ 18.8 (signals superimposed), 19.2 (CH₃), 22.6 (CH₃), 31.6, 31.9, 34.5, 38.4, 38.5, 66.6 (CH₂C=O), 78.3 (CHOH), 78.7 (CHOH), 124.6, 128.5, 129.9, 133.6, 165.8 (C=O ester), 205.5 (C=O, ketone); **(HRFAB⁺)** calcd for C₁₈H₂₃O₄ (M)⁺ requires 303.15963, found 303.15995. **HPLC:** Chiracel-AD column; mobile phase, *i*-PrOH:hexane (3:97), flow rate, 0.8 ml/min, detection, UV 214 nm. Retention times; 28.6 min, 30.8 min, 34.0 min, 43.1 min.

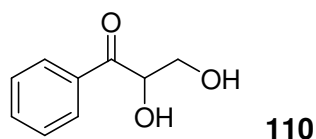
The 2-isomer mixture of benzoic acid (3'*RS*,1''*R*)-3'-(3'',4''-dimethylcyclohex-3''-enyl)-3'-hydroxy-2-oxo-propyl ester (1'*R*)-**106** was prepared using an identical method. Chiral HPLC as above, retention times 28.6 min and 34.0 min. The D469T-TK product (1*S*)-**105** was also converted to the monobenzoate as described above. $[\alpha]_{\text{D}}^{20} = +7.6$ (*c* 0.5, CHCl₃). Chiral HPLC as above, retention times 28.6 min (1%), 30.8 min (1%), 34.0 min (96.5%), 43.1 min (1.5%) to give (1*S*,1'*R*)-**105** of 93% *de*.

(2*S*,3'*S*,1''*R*)-3,3,3-Trifluoro-2-methoxy-2-phenylpropionic acid 3'-(3'',4''-dimethylcyclohex-3''-enyl)-3'-hydroxy-2-oxo-propyl ester



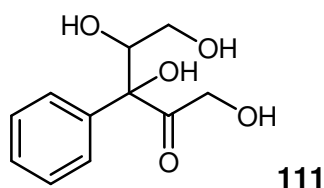
To a stirred solution of the biotransformation (1'*S*,1'*R*)-**105** (0.01 g, 0.05 mmol) in CH₂Cl₂ (5 ml) was added triethylamine (20 μl, 0.25 mmol) and (*R*)-MTPA chloride (15 μl, 0.08 mmol) in CH₂Cl₂ (2 ml) and the reaction was stirred for 12 h at rt. The product was dry loaded onto silica gel and purified using flash chromatography (EtOAc:hexane, 1:4) to afford **107** as a colourless oil (0.015 g, 75%), (2*S*,3'*S*) >98% *ee*. *R_f* 0.45; $[\alpha]_{\text{D}}^{20} = +7.6$ (*c* 0.5, CHCl₃); **IR (Neat)**: 3429 (br, O-H), 2925s, 1758 (s, C=O, ester), 1734 (s, C=O, ketone), 1170s; **¹H NMR (500 MHz; CDCl₃)** δ 1.38 (2H, m), 1.60 (3H, s, CH₃), 1.62 (3H, s, CH₃), 1.98 (4H, m), 2.12 (1H, m), 3.65 (3H, s, OMe), 4.23 (1H, m), 4.91 (1H, d, *J* 17.0, CHHO (2*S*,3'*S*)), 5.18 (1H, d, *J* 17.0, CHHO (2*S*,3'*S*)), 7.42 (3H, m, Ph), 7.63 (2H, m, Ph), (trace 2*S*,3'*R* isomer detected); **¹³C NMR (125 MHz; CDCl₃)** δ 18.8, 19.1, 22.7, 31.6, 34.3, 38.6, 55.8 (OCH₃), 67.7 (O=CCH₂), 78.6 (CHOH), 124.5, 125.5, 127.5, 128.5, 129.9, 131.9, 166.2 (C=O ester), 204.2 (C=O, ketone); **¹⁹F NMR (282 MHz; CDCl₃)** δ -71.0; ***m/z* (FAB⁺)** 437 (MNa⁺-H, 43%), 415 (M⁺, 56), 307 (65), 189 (100), (**+HRFAB**) calcd for C₂₁H₂₆O₅F₃ (M)⁺ requires 415.17322, found 415.17372.

2, 3-Dihydroxypropiofenone¹³⁷



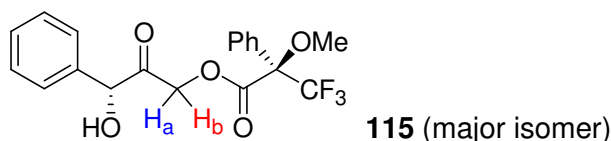
To a stirred solution of **Cs-27** (0.328 g, 3.00 mmol) in water (60 ml) at rt, was added benzaldehyde (363 μ l, 3.00 mmol) and *N*-methylmorpholine (364 μ l, 3.00 mmol). The reaction mixture was stirred at rt for 48 h, and monitored by TLC. The solvent was removed *in vacuo* and the crude product dry loaded onto a flash silica chromatography column (EtOAc: hexane, 1:1) affording **110** (0.025 g, 5%) as a colourless oil. R_f 0.53; **IR (Neat)** 3391 (s, O-H), 1684 (C=O), 691 (Ar-H); **¹H NMR (300 MHz; MeOD)** δ 3.73 (2H, dd, *J* 11.7 and 5.0, CHHOH), 3.88 (2H, dd, *J* 11.7 and 3.7, CHHOH), 5.15 (1H, m, HOCH), 7.51 (2H, t, *J* 6.0, Ar), 7.61 (1H, t, *J* 6.0, Ar), 8.00 (2H, d, *J* 6.0, Ar); **¹³C NMR (75 MHz; CDCl₃)** δ 64.2 (CH₂), 87.2 (CHOH), 128.4, 129.2, 130.2, 137.2, 209.5 (C=O); ***m/z* (ES⁺)**: 167.6 (M⁺, 94%), 77.7 (C₆H₆⁺, 10%), 58.9 (C₂H₂O₂⁺, 25%)

(3*RS*,4*RS*)-1,3,4,5-Tetrahydroxy-3-phenyl-pentan-2-one



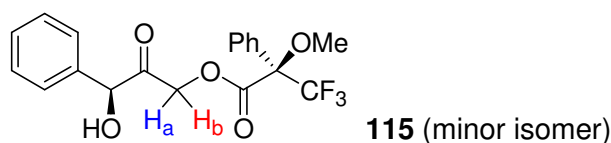
Biotransformation side product (see **30Ar1**) generated in a 50 mM TK reaction using D469E gave (10 mg, 6%) as an oil; $[\alpha]_D^{20} = +18.0$ (c 0.5, CHCl₃); **IR (Neat)** 3391 (s, O-H), 1684 (C=O), 691 (Ar-H); **¹H NMR (600 MHz; MeOD)** δ 3.05 (1H, d, *J* 11.1, OH), 3.72-3.98 (2H, m, CH₂OH), 4.60 (1H, d, *J* 19.4, CHHOH), 4.65 (1H, d, *J* 19.4, CHHOH), 4.81 (1H, m, CHOH); **¹³C NMR (150 MHz; MeOD)** Diastereomers: δ 67.0 (CH₂), 67.4 (CH₂), 68.8 (CH₂), 69.1 (CH₂), 76.6 (CH), 76.7 (CH), 86.2, 86.8, 128.8, 128.9, 129.0, 141.2, 214.6 (C=O), 215.4 (C=O); ***m/z* (ES⁺)**: calcd [M+Na]⁺ for C₁₁H₁₄O₅Na requires 249.2012, found 249.2114.

(2*R*,3'*R*)-3,3,3-Trifluoro-2-methoxy-2-phenyl-propionic acid 3'-hydroxy-2'-oxo-3'-phenyl-propyl ester



The reaction was carried out under anhydrous conditions. To a stirred solution of (*R*)-**3a** (0.008 g, 0.05 mmol) in CH₂Cl₂ (1 ml) was added triethylamine (34 μl, 0.25 mmol) and (*R*)-MTPA chloride (10 μl, 0.04 mmol) the reaction was stirred for 12 h at rt. The product was dry loaded onto silica gel and purified using flash chromatography (EtOAc:hexane, 1:4) to afford **115** as a colourless oil (0.016 g, 84%), (*2R,3'R*) 87% *ee* (from integrations of H_a and H_b ¹H NMR signals of **115**). *R*_f 0.40; [α]²⁵_D = +30.0 (*c* 0.5, CHCl₃); **IR (Neat)** 3420 (br, O-H), 2930, 2855, 1734 (s, ester); **¹H NMR (300 MHz; CDCl₃)** δ 3.61 (3H, s, OCH₃), 4.68 (1H, d, *J* 18.0, CHHO (*2R,3'R*)), 5.02 (1H, d, *J* 18.0, CHHO (*2R, 3'R*)), 4.84 (1H, d, *J* 18.0, CHHO (*2S,3'R*)), 4.91 (1H, d, *J* 18.0, CHHO (*2S,3'R*)), 5.25 (1H, s), 7.25-7.60 (8H, m, Ar), 7.59 (2H, m, Ar); **¹³C NMR (150 MHz; CDCl₃)** δ 55.9 (OCH₃), 66.5, 78.1 (CHOH), 127.4 (signal overlap), 127.5, 128.6, 129.5, 129.6, 130.0, 131.8, 136.7, 166.3 (C=O ester), 201.7 (C=O, ketone); **¹⁹F NMR (282 MHz; CDCl₃)** δ -72.2; ***m/z* (CI)** calcd [M+H]⁺ for C₁₉H₁₈F₃O₅ requires 383.11063, found 383.11154.

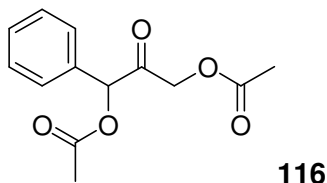
(2*R*,3'*S*)-3,3,3-Trifluoro-2-methoxy-2-phenyl-propionic acid 3'-hydroxy-2'-oxo-3'-phenyl-propyl ester



The reaction was carried out under anhydrous conditions. To a stirred solution of (*R*)-**3a** (0.008 g, 0.05 mmol) in CH₂Cl₂ (1 ml) was added triethylamine (34 μl, 0.25 mmol) and (*R*)-MTPA chloride (10 μl, 0.04 mmol) the reaction was stirred for 12 h at rt. The product was dry loaded onto silica gel and purified using flash chromatography (EtOAc:hexane, 1:4) to afford **115** as a colourless oil (0.016 g, 84%). *R*_f 0.40; [α]²⁵_D = +30.0 (*c* 0.5, CHCl₃); **IR (Neat)** 3420 (br, O-H), 2930, 2855, 1734 (s, ester); **¹H NMR (300 MHz; CDCl₃)** δ 3.61 (3H, s, OCH₃), 4.68 (1H, d, *J* 18.0, CHHO (*2R,3'R*)), 4.84 (1H, d, *J* 18.0, CHHO (*2R,3'S*)), 4.91 (1H, d, *J* 18.0, CHHO (*2R,3'S*)), 5.25 (1H, s), 7.25-7.60 (8H, m, Ar), 7.59 (2H, m, Ar); **¹³C NMR (150 MHz; CDCl₃)** δ 55.9 (OCH₃), 66.5, 78.1 (CHOH), 127.4 (signal overlap), 127.5, 128.6, 129.5, 129.6, 130.0, 131.8,

136.7, 166.3 (C=O ester), 201.7 (C=O, ketone); ^{19}F NMR (282 MHz; CDCl_3) δ -72.2; m/z (CI) calcd $[\text{M}+\text{H}]^+$ for $\text{C}_{19}\text{H}_{18}\text{F}_3\text{O}_5$ requires 383.11063, found 383.11154.

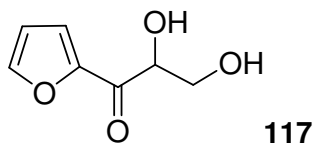
Acetic acid 3-acetoxy-2-oxo-1-phenyl-propyl ester¹³⁸



To a stirred solution of **30Ar1** (0.060, 0.36 mmol) in dry CH_2Cl_2 (15 ml) was added a CH_2Cl_2 solution (10 ml) of DCC (0.082 g, 0.40 mmol) at 0°C under an argon atmosphere. After 5 min the reaction mixture was gently warmed to rt and acetic acid (23 μl , 0.40 mmol) was added to reaction mixture and was left for 12 h under argon. The solvent was removed *in vacuo* and the crude product dry loaded onto a flash silica chromatography column (EtOAc: hexane, 1:4). Colourless oil was isolated **116** (0.075 g, 83 %). R_f 0.38; IR (Neat) 3400 (br, O-H), 2950 (s, CH_2), 1720 (s, C=O); ^1H NMR (300 MHz; CDCl_3) δ 2.04 (3H, s), 2.23 (3H, s), 4.62 (1H, d, J 18.0, CHH), 4.82 (1H, d, J 18.0, CHH), 4.61 (1H, s, OCH), 7.40 (5H, s); ^{13}C NMR (75 MHz; CDCl_3) δ 21.0 (CH_3), 21.2 (CH_3), 68.2 (CH_2), 78.7 (CHO), 128.5, 129.6, 132.2, 137.3, 209.9 (C=O); m/z (HRMS): calcd $[\text{MH}]^+$ for $\text{C}_{13}\text{H}_{14}\text{O}_5$ requires 251.0354, found 251.0923.

The isomers were separated via HPLC conditions: chiralpak AD column, hexane: *i*-PrOH, 98:2, 1 ml min^{-1} , retention times: 24.8 min and 28.8 min (racemic mixtures).

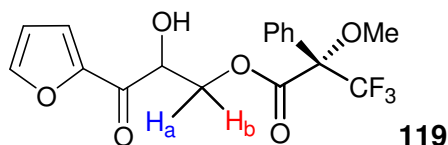
1-Furan-2-yl-2, 3-dihydroxy-propan-1-one



To a stirred solution of **Li-27** (0.113 g, 1.04 mmol) in water (5 ml) and THF (5 ml) at rt, was added furfural (83 μl , 1.00 mmol) and *N*-methylmorpholine (101 μl , 1.00 mmol). The reaction mixture was stirred at rt for 24 h, and monitored by TLC. The solvent was removed *in vacuo* and the crude product dry loaded onto a flash silica chromatography column (EtOAc: hexane, 1:1) affording compound **117** (0.006 g, 4%) as a brown oil. R_f 0.40; IR (Neat) 3391 (s, O-H), 1708 (C=O), 694 (Ar-H); ^1H NMR (300 MHz; CDCl_3) δ 3.93 (1H, dd, J 11.8 and 4.5, CHHOH), 4.06 (1H, dd, J 11.8 and 3.3, CHHOH), 4.91 (1H, m, CHOH), 6.60 (1H, m, Ar), 7.37 (1H, m, Ar), 7.64 (1H, m, Ar); ^{13}C NMR (125

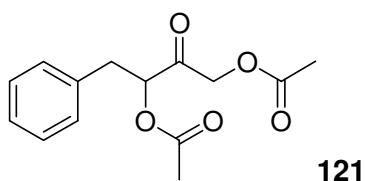
MHz; CDCl₃) δ 64.9 (CH₂), 74.8 (CHO), 112.8, 119.5, 147.4, 150.3, 187.7 (C=O); **m/z (CI)** [M+Na]⁺ calcd for C₇H₉O₄ requires 157.05008, found 157.04964.

(2S)-3,3,3-Trifluoro-2-methoxy-2-phenyl-propionic acid 3-furan-2-yl-2-hydroxy-3-oxo-propyl ester



To a stirred solution of the biotransformation **117** (0.01 g, 0.05 mmol) in CH₂Cl₂ (1 ml) was added triethylamine (20 μ l, 0.25 mmol) and (*R*)-MTPA chloride (15 μ l, 0.08 mmol) in CH₂Cl₂ (1 ml) and the reaction was stirred for 12 h at rt. The product was dry loaded onto silica gel and purified using flash chromatography (EtOAc:hexane, 1:4) to afford **119** as a colourless oil (0.019 g, 70%). **R_f** 0.40; **[α]²⁰_D** = +30.6 (c 0.5, CHCl₃); **IR (Neat)**: 3429 (br, O-H), 2925s, 1750 (s, C=O, ester), 1734 (s, C=O, ketone), 1170s; **¹H NMR (600 MHz; CDCl₃)** δ 3.06 (0.5H, m, CHHO-), 3.30 (1H, m, CH₂O-), 3.48 (0.5H, m, CHHO-), 3.68 (3H, s, OMe), 4.20 (1H, m, CHOH), 6.61 (1H, d, *J* 2.0, Ar), 7.37 (1H, m, Ar), 7.51 (1H, m, Ar); **¹³C NMR (150 MHz; CDCl₃)** δ 18.8, 19.1, 22.7, 31.6, 34.3, 38.6, 55.8 (OCH₃), 68.2 (O=CCH₂), 77.3 (CHOH), 113.2, 126.8 (d, *J*_{CF} 287, CF₃), 128.9, 129.2, 134.4, 149.5, 164.9 (C=O ester), 204.2 (C=O, ketone); **¹⁹F NMR (282 MHz; CDCl₃)** δ -71.0; **m/z (+HRCI)** calcd for C₁₇H₁₅O₆F₃ (M)⁺ requires 373.08990, found 373.08821.

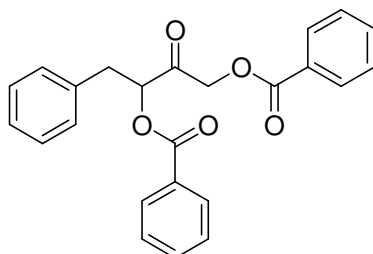
4-(acetyloxy)-3-oxo-1-phenylbutan-2-yl acetate



To a stirred solution of **30Ar4** (0.02 g, 0.11 mmol) in anhydrous pyridine (3 ml) at rt was added acetic anhydride (1 ml) under an argon atmosphere. The reaction was left to stir at rt for 6 h, and monitored by TLC. The volatile solvents were removed *in vacuo*. The remaining residue was dissolved in EtOAc (50 ml) and was washed with 0.3 M KHSO₄ (2 \times 50 ml) and sat. NaHCO₃ (2 \times 50 ml). The organic layer was dried over MgSO₄ and the solvent removed *in vacuo* affording a brown oil **121** (0.029 g, 100%). **R_f** 0.45; **IR (Neat)** 3400 (br, O-H), 2950 (s, CH₂), 1722 (s, C=O); **¹H NMR (300 MHz; CDCl₃)** δ 2.08 (3H, s), 2.18 (3H, s), 3.05 (1H, dd, *J* 14.3 and 8.1, PhCHH), 3.36 (1H, dd, *J* 14.3 and 5.1, PhCHH), 4.64 (1H, d, *J* 18.0, CHHO), 4.72 (1H, d, *J* 18.0, CHHO), 5.32 (1H,

dd, J 8.0 and 5.2, $CHOH$), 7.26 (5H, m), ^{13}C NMR (125 MHz; $CDCl_3$) δ 20.5 (CH_3), 20.6 (CH_3), 36.9, 66.6 ($CH_2C=O$), 77.3 ($CHC=O$), 127.3, 128.7, 129.0, 129.4, 170.1 ($C=O$, ester), 170.2 ($C=O$ ester), 200.7 ($C=O$, ketone); m/z (HRMS) calcd for $C_{14}H_{17}O_5$ $[M+H]^+$ requires 265.10759, found 265.10797.

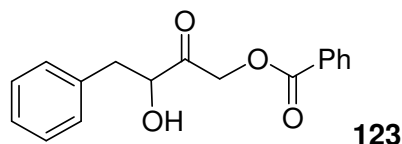
3-(Benzoyloxy)-2-oxo-4-phenylbutyl benzoate



122

To a stirred solution of **30Ar4** (0.01 g, 0.04 mmol) in CH_2Cl_2 (1 ml) was added triethylamine (34 μ l, 0.25 mmol) and benzoyl chloride (20 μ l, 0.08 mmol) the reaction was stirred for 12 h at rt. The product was dry loaded onto silica gel and purified using flash chromatography (Hexane:EtOAc, 4:1) to afford **122** as a colourless oil (0.012 g, 80%). R_f 0.55; IR (Neat) 3484 (br, O-H), 2931, 1722 (s, ester), 694 (Ar-H); 1H NMR (300 MHz; $CDCl_3$) δ 3.28 (1H, dd, J 14.4 and 8.0, PhCHH), 3.36 (1H, dd, J 14.4 and 4.9, PhCHH), 4.98 (1H, d, J 17.2, CHHO), 5.05 (1H, d, J 17.2, CHHO), 5.65 (1H, m, $CHOH$), 7.29 (3H, m, Ar), 7.45 (2H, t, J 7.9), 7.55 (2H, m), 8.01 (2H, d, J 8.1, Ar), 8.07 (2H, d, J 8.1, Ar), 8.16 (2H, d, J 8.1, Ar), 8.32 (2H, d, J 8.1, Ar); ^{13}C NMR (125 MHz; $CDCl_3$) δ 37.1 (CH_2Ar), 67.0 (CH_2O), 77.7 ($CHOH$), 127.3, 128.5, 128.9, 129.0, 129.6, 129.9, 130.0, 130.7, 133.5, 134.6, 135.5, 162.4 ($C=O$, ester), 166.0 ($C=O$ ester), 205.1 ($C=O$, ketone); m/z (HRMS) $[MH]^+$ calcd for $C_{24}H_{20}O_5Na$ requires 411.1208, found 411.1194.

3-Hydroxy-2-oxo-4-phenylbutyl benzoate



123

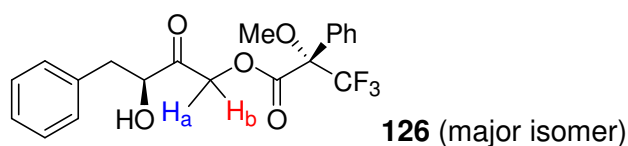
To a stirred solution of (*S*)- **30Ar4** (0.01 g, 0.04 mmol) in CH_2Cl_2 (1 ml) was added triethylamine (34 μ l, 0.25 mmol) and benzoyl chloride (10 μ l, 0.04 mmol) the reaction was stirred for 12 h at rt. The product was dry loaded onto silica gel and purified using flash chromatography (Hexane:EtOAc, 4:1) to afford **123** as a colourless oil (0.010 g, 91%). R_f 0.45; IR (Neat) 3400 (br, O-H), 2950 (s, CH_2) 1722 (s, $C=O$); 1H NMR (300 MHz; $CDCl_3$) δ 2.97 (1H, dd, J 14.0 and 8.1, PhCHH), 3.25 (1H, dd, J 14.0 and 4.5, PhCHH), 4.61 (1H, dd, J 8.0 and 4.6, $CHOH$) 5.02 (1H, d, J 18.0, CHHO), 5.10 (1H, d,

J 18.0, $CHHO$), 7.29 (5H, m), 7.43 (3H, t, J 7.3), 7.59 (1H, m), 8.09 (1H, m); ^{13}C NMR (125 MHz; CDCl_3) δ 40.3, 66.7 (CH_2O), 76.4 (CHOH), 127.3, 127.3, 128.6, 129.1, 129.5, 130.0, 133.6, 136.0, 166.0 ($\text{C}=\text{O}$ ester), 205.1 ($\text{C}=\text{O}$, ketone); m/z (HRMS) calcd for $[\text{M}+\text{H}]^+$ for $\text{C}_{17}\text{H}_{15}\text{O}_4$ requires 283.0958, found 283.0970.

HPLC: Chiracel-AD column; mobile phase *i*-PrOH:hexane (3:97); flow rate, 0.8 ml min^{-1} , detection, UV 214 nm. Retention times at 45.2 min (3*R*)-**123** and 57.0 min (3*S*)-**123**.

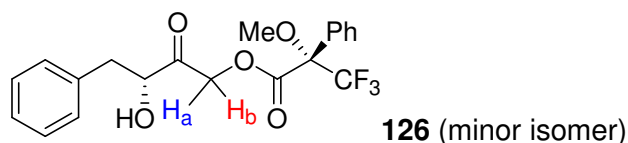
Benzoylated TK mutants: WT-TK gave (3*S*,4*S*)-**127** (10 mg, 91%), H26Y-TK gave (9 mg, 81%) reaction, D469K-TK gave (3*S*,4*S*)-**127** (11 mg, 100%) G6-TK gave (3*S*,4*S*)-**127** (11 mg, 100%) and D469E-TK gave (3*S*,4*S*)-**30Ar4** (10 mg, 91%), and D469T-TK gave (3*S*,4*S*)-**127** (11 mg, 100%), $[\alpha]_{\text{D}}^{25} = -2.0$ (c 0.6, CHCl_3); The spectral assignments are the same as above.

(2*S*,3'*S*)- 3,3,3-Trifluoro-2-methoxy-2-phenyl-propionic acid 3'-hydroxy-1,1-dimethyl-2'-oxo-4'-phenyl-butyl ester



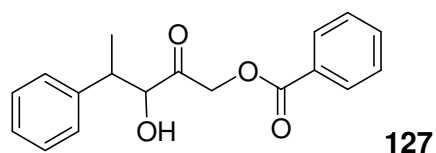
The reaction was carried out under anhydrous conditions. To a stirred solution of synthesized D469E **30Ar3** (0.01 g, 0.04 mmol) in CH_2Cl_2 (1 ml) was added triethylamine (34 μl , 0.25 mmol) and (*R*)-MTPA chloride (10 μl , 0.04 mmol) the reaction was stirred for 12 h at rt. The product was dry loaded onto silica gel and purified using flash chromatography (EtOAc:hexane, 1:4) to afford **126** as a colourless oil (0.015 g, 85%), (2*S*,3*S*) 90% *ee* (from integrations of H_a and H_b ^1H NMR signals of **126**). R_f 0.40; $[\alpha]_{\text{D}}^{25} = -30.0^\circ$ (c 0.3, CHCl_3); **IR (Neat)** 3600 (br, O-H), 2932 (s, CH_2) 1759 (s, $\text{C}=\text{O}$); **^1H NMR (300 MHz; CDCl_3)** δ 2.59 (1H, d, J 4.0 Hz, OH) 2.91 (1H, dd, J 14.1 and 8.6, PhCHH,) 3.17 (1H, dd, J 14.1 and 4.4, PhCHH) 3.66 (1H, s, OCH_3), 4.50 (1H, m, CHOH) 4.95 (1H, d, J 17.4, CHHO (2*S*,3'*S*)), 5.06 (1H, d, J 9.5, (2*S*, 3'*S*)), 7.21-7.42 (5H, m), 7.43 (3H, m, Ar), 7.63 (2H, m, Ar); **^{13}C NMR (125 MHz; CDCl_3)** δ 40.2 (CH_2Ar), 55.8 (OCH_3), 67.8 (CH_2O -), 76.7 (CHOH), 127.5, 127.6, 128.5, 129.0, 129.5, 129.9, 131.9, 135.6, 166.3 ($\text{C}=\text{O}$ ester), 203.5 ($\text{C}=\text{O}$, ketone); **^{19}F NMR (282 MHz; CDCl_3)** δ -72.2; m/z (HRMS) calcd $[\text{M}+\text{H}]^+$ for $\text{C}_{20}\text{H}_{19}\text{F}_3\text{O}_5$ requires 395.1106, found 395.1119.

(2*S*,3'*R*)- 3,3,3-Trifluoro-2-methoxy-2-phenyl-propionic acid 3'-hydroxy-1,1-dimethyl-2'-oxo-4'-phenyl-butyl ester



The reaction was carried out under anhydrous conditions. To a stirred solution of synthesized D469E **30Ar3** (0.01 g, 0.04 mmol) in CH₂Cl₂ (1 ml) was added triethylamine (34 μl, 0.25 mmol) and (*R*)-MTPA chloride (10 μl, 0.04 mmol) the reaction was stirred for 12 h at rt. The product was dry loaded onto silica gel and purified using flash chromatography (EtOAc:hexane, 1:4) to afford **126** as a colourless oil (0.015 g, 85%). **R_f** 0.40; [**α**]_D²⁵ = -30.0° (*c* 0.3, CHCl₃); **IR (Neat)** 3600 (br, O-H), 2932 (s, CH₂) 1759 (s, C=O); **¹H NMR (300 MHz; CDCl₃)** δ 2.59 (1H, d, *J* 4.0 Hz, OH) 2.91 (1H, dd, *J* 14.1 and 8.6, PhCHH,) 3.17 (1H, dd, *J* 14.1 and 4.4, PhCHH) 3.66 (1H, s, OCH₃), 4.50 (1H, m, CHOH), 5.16 (1H, d, *J* 17.4, CHHO (2*S*, 3'*R*)), 7.21-7.42 (5H, m), 7.43 (3H, m, Ar), 7.63 (2H, m, Ar); **¹³C NMR (125 MHz; CDCl₃)** δ 40.2 (CH₂Ar), 55.8 (OCH₃), 67.8 (CH₂O-), 76.7 (CHOH), 127.5, 127.6, 128.5, 129.0, 129.5, 129.9, 131.9, 135.6, 166.3 (C=O ester), 203.5 (C=O, ketone); **¹⁹F NMR (282 MHz; CDCl₃)** δ -72.2; ***m/z* (HRMS)** calcd [M+H]⁺ for C₂₀H₁₉F₃O₅ requires 395.1106, found 395.1119.

(3*RS*,4*RS*)-3-Hydroxy-2-oxo-4-phenylpentyl benzoate

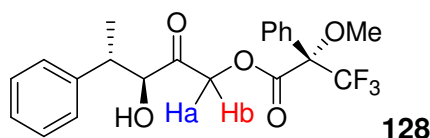


The reaction was carried out under anhydrous conditions. To a stirred solution of **30Ar4** (0.01 g, 0.05 mmol) in CH₂Cl₂ (1 ml) was added triethylamine (34 μl, 0.25 mmol) and benzoyl chloride (10 μl, 0.04 mmol) the reaction was stirred for 12 h at rt. The product was dry loaded onto silica gel and purified using flash chromatography (hexane:EtOAc, 4:1) to afford **127** as a colourless oil (0.012 g, 83%). **R_f** 0.45; **IR (Neat)** 3484 (br, O-H), 2931 (s, CH₂) 1722 (s, C=O); **¹H NMR (300 MHz; CDCl₃)** δ 1.33 (3H, d, *J* 7.1), 2.95 (1H, s, OH), 3.28 (1H, m, CHCH₃), 4.49 (1H, d, *J* 3.8, CHOH,), 4.95 (1H, d, *J* 3.8, CHOH), 7.29-7.35 (5H, m, Ar), 7.46 (2H, t, *J* 7.8, Ar), 7.61 (1H, t, *J* 7.4, Ar); 8.08 (2H, d, *J* 9.0, Ar); **¹³C NMR (125 MHz; CDCl₃)** δ 14.2 (CH₃), 43.2 (CHCH₃), 67.3 (CH₂O), 79.6 (CHOH), 127.3, 127.8, 128.9, 129.5, 130.0, 133.6, 142.5, 166.9 (C=O ester), 205.3 (C=O, ketone); ***m/z* (HRMS)** calcd for C₁₈H₁₇O₄ [M+H]⁺ requires 297.1127,

found 297.1133; **HPLC** conditions: Chiracel-OD column; mobile phase, *i*-PrOH:hexane (3:97); flow rate, 0.8 ml min⁻¹, detection UV 214 nm. Retention times at 28.6 min (3*R*,4*S*)-**127**, 30.8 min (3*R*,4*R*)-**127**, 34.0 min (3*S*,4*R*)-**127**, 43.1 min (3*S*,4*S*)-**127**. The 2-isomer mixture of (3*RS*,4*R*)-3,4-dihydroxy-2-oxo-4-phenylbutyl benzoate (4*R*)-**132** (0.01 g, 71%) was prepared using an identical method and **127**. Retention times; 25.1 min (major peak), 27.3 min (major peak), 30.4 min (minor peak), 45.2 min (minor peak).

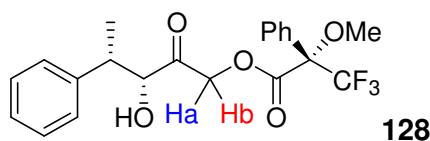
Benzoylated TK mutants: WT-TK gave (3*S*,4*S*)-**127** (13 mg, 87%), H26Y-TK no reaction, D469K-TK gave (3*S*,4*S*)-**127** (10 mg, 67%) G6-TK gave (3*S*,4*S*)-**127** (13 mg, 87%) and D469E-TK gave (3*S*,4*S*)-**30Ar4** (10 mg, 67%), and D469T-TK gave (3*S*,4*S*)-**127** (13 mg, 87%), $[\alpha]_{\text{D}}^{25} = +37.4$ (*c* 1.4, CHCl₃). The spectral assignment same as above with retention times at 30.8 min (3*R*,4*R*)-**127**, 34.0 min (3*S*,4*S*)-**127**.

(2*S*,3'*S*,4'*S*)-3'-hydroxy-2'-oxo-4' phenylpentyl 3,3,3-trifluoro-2-methoxy-2-phenylpropanoate



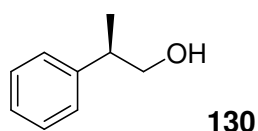
The reaction was carried out under anhydrous conditions. To a stirred solution of (1'*R*,1*S*)-**105** (0.012 g, 0.06 mmol) in CH₂Cl₂ (1 ml) was added triethylamine (34 μl, 0.25 mmol) and (*R*)-MTPA chloride (10 μl, 0.04 mmol) the reaction was stirred for 12 h at rt. The product was dry loaded onto silica gel and purified using flash chromatography (Hexane: EtOAc, 4:1) to afford **128** as a colourless oil (0.018 g, 75%), (2*S*,3*S*) 91% *ee* (from integrations of H_a and H_b ¹H NMR signals of **128**). **R_f** 0.45; $[\alpha]_{\text{D}}^{25} = -37.2$ (*c* 0.25, CHCl₃); **IR (Neat)** 3471 (b, O-H), 2954s, 1759 (s, C=O, ester), 1735s 1170 (C-F); **¹H NMR (300 MHz; CDCl₃)** δ 2.59 (1H, d, *J* 4.0, OH) 2.91 (1H, dd, *J* 8.6, 14.1, PhCHH,) 3.17 (1H, dd, *J* 14.1 and 4.4, PhCHH) 3.66 (1H, s, OCH₃), 4.50 (1H, m, CHOH), 4.86 (1H, d, 17.3, CHHO (2*S*,3*S*)), 5.04 (1H, d, *J* 17.3, CHHO (2*S*, 3*S*)), 7.21-7.42 (5H, m), 7.43 (3H, m, Ph), 7.63 (2H, m, Ph); **¹³C NMR (125 MHz; CDCl₃)** δ 13.8, 43.2, 55.8 (OCH₃), 68.5 (CH₂), 80.1 (CHOH), 127.4, 127.6, 127.8, 128.5, 129.0, 129.9, 129.9, 131.9, 142.0, 166.2 (C=O ester), 203.7 (C=O, ketone); **¹⁹F NMR (282 MHz; CDCl₃)** δ -72.3; ***m/z* (HRMS)** calcd [M+H]⁺ for C₂₁H₂₁F₃O₅ requires 433.1239, found 433.1234.

(2*S*,3'*R*,4'*S*)-3'-hydroxy-2'-oxo-4' phenylpentyl 3,3,3-trifluoro-2-methoxy-2-phenylpropanoate



The reaction was carried out under anhydrous conditions. To a stirred solution of (1'*R*,1*S*)-**105** (0.012 g, 0.06 mmol) in CH₂Cl₂ (1 ml) was added triethylamine (34 μl, 0.25 mmol) and (*R*)-MTPA chloride (10 μl, 0.04 mmol) the reaction was stirred for 12 h at rt. The product was dry loaded onto silica gel and purified using flash chromatography (Hexane: EtOAc, 4:1) to afford **128** as a colourless oil (0.018 g, 75%). **R_f** 0.45; **[α]²⁵_D** = -37.2 (*c* 0.25, CHCl₃); **IR (Neat)** 3471 (b, O-H), 2954s, 1759 (s, C=O, ester), 1735s 1170 (C-F); **¹H NMR (300 MHz; CDCl₃)** δ 2.59 (1H, d, *J* 4.0, OH) 2.91 (1H, dd, *J* 14.1 and 8.6, PhCHH,) 3.17 (1H, dd, *J* 14.1 and 4.4, PhCHH) 3.66 (1H, s, OCH₃), 4.50 (1H, m, CHOH), 4.95 (1H, s, (2*S*, 3*R*)), 7.21-7.42 (5H, m), 7.43 (3H, m, Ph), 7.63 (2H, m, Ph); **¹³C NMR (125 MHz; CDCl₃)** δ 13.8, 43.2, 55.8 (OCH₃), 68.5 (CH₂), 80.1 (CHOH), 127.4, 127.6, 127.8, 128.5, 129.0, 129.9, 129.9, 131.9, 142.0, 166.2 (C=O ester), 203.7 (C=O, ketone); **¹⁹F NMR (282 MHz; CDCl₃)** δ -72.3; ***m/z* (HRMS)** calcd [M+H]⁺ for C₂₁H₂₁F₃O₅ requires 433.1239, found 433.1234.

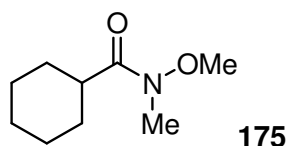
(2*R*)-Phenylpropan-1-ol¹⁰⁸



To a cold stirred solution of LiAlH₄ (0.30 g, 7.48 mmol) in anhydrous THF (10 ml) was added slowly 2-phenylpropionic acid (6.67 mmol, 1.00 g) under argon at 0 °C. The mixture was stirred for 60 min at 0 °C and gently raised to rt for 2 h. The reaction was cooled with an ice-water bath and quenched with sat. NaSO₄ (10 ml) and poured into brine (10 ml). Diethyl ether (50 ml) was added, the layers were separated and the aqueous layer was extracted with diethyl ether (3 × 20 ml). The combined ethereal layers were washed successively with 3 M HCl (2 × 25) ml, sat. NaHCO₃ (2 × 25 ml), and of brine (2 × 20 ml). The organic phase was dried over magnesium sulfate and the solvent was removed *in vacuo* to obtain the aldehyde as pale colourless oil **130** (0.753 g, 84%), **[α]²⁵_D** = -72.0° (*c* 0.4, CHCl₃); **IR (Neat)** 3400 (br, O-H), 2950s; **¹H NMR (500 MHz; CDCl₃)** δ 1.28 (1H, d, *J* 10.0, CH₃) 1.47 (1H, s, OH), 2.95 (1H, sextet, *J* 9.0, CH) 3.69 (1H, d, *J* 10.0, CH₂), 7.23 (3H, m), 7.33 (2H, m); **¹³C NMR (125**

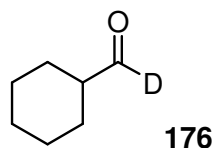
MHz; CDCl₃) δ 42.5 (CH₃), 68.8 (CHCH₃), 77.3 (CH₂), 126.8, 127.0, 127.6, 127.9, 128.7; **m/z (HRMS)** calcd [MH]⁺ for C₉H₁₂O requires 136.08827, found 136.08876.

Cyclohexanecarboxylic acid methoxy-methyl-amide¹³⁹



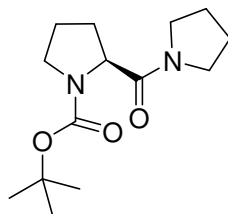
To a stirred solution of *N,O*-dimethylhydroxylamine hydrochloride (0.49 g, 5.00 mmol) in dry CH₂Cl₂ (40 ml) was added *N,N*-diisopropylethylamine DIEA (1.93 ml, 15 mmol) at rt and the reaction was stirred for 5 mins. Cyclohexanecarbonyl chloride (710 μ l, 5 mmol) was added and the mixture a was stirred at rt for 12 h. The reaction mixture was poured into 30 ml CH₂Cl₂ and washed successively with 0.3 mol KHSO₄ (2 \times 20 ml), sat. NaHCO₃ (2 \times 20 ml) and brine (2 \times 20 ml). The organic layer was dried over anhydrous magnesium sulfate and the solvent was removed *in vacuo* to obtain the pure product **175** as yellow oil (0.845, >99%). **R_f** 0.56; **IR (KBr)** 2930-2855 (s, C-H), 1663 (s, C=O); **¹H NMR (300 MHz; CDCl₃)** δ 1.16-1.92 (10H, m, 5 \times CH₂), 2.67 (1H, m, CHCO), 3.24 (3H, s, N-CH₃), 3.68 (3H, s, OCH₃); **¹³C NMR (75 MHz; CDCl₃)** δ 25.4, 25.7 (2C signal overlap), 28.9, 39.9 (CH₃N-), 61.4 (CH₃O-), 172.0 (amide); **m/z (CI)**: 172 ([M+H]⁺, 100%), 111 ([M-C₂H₆NO], 100%), 156 ([M-CH₃O], 10%).

[1-²H]-Cyclohexancarboxyaldehyde



To a cold stirred solution of LiAlD₄ (0.30 g, 7.48 mmol) in anhydrous THF (10 ml) was added slowly **175** (1.01 g, 6.80 mmol) under argon at 0 °C. The mixture was stirred for 60 min at 0 °C and raised to rt for 2 h. The reaction was cooled with an ice-water bath and hydrolysed with sat. citric acid (10 ml) and poured into brine (10 ml). Diethyl ether (50 ml) was added, the layers were separated and the aqueous layer was extracted with diethyl ether (3 \times 20 ml). The combined ether layers were washed successively with 3 M HCl (2 \times 25 ml), sat. NaHCO₃ (2 \times 25 ml), and of brine (2 \times 20 ml). The organic phase was dried over magnesium sulfate and the solvent was removed *in vacuo* to obtain the aldehyde as pale yellow oil **176** (0.412 g, 54%). **IR (KBr)** 1721 (s, C=O); **¹H NMR (300 MHz; CDCl₃)** δ 0.83-2.23 (11H, m); **¹³C NMR (75 MHz; CDCl₃)** δ 24.9, 25.1, 25.9, 49.7 (CHCO), 204.6 (C=O, t, J_{CD} 25.0) **m/z (CI)**: *pending*.

Tert-butyl (2S)-2-[(pyrrolidin-1-yl)carbonyl]pyrrolidine-1-carboxylate¹²⁹

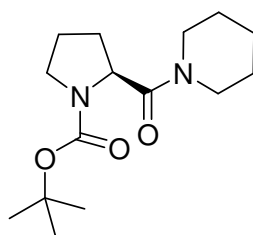


187a

To a CH₂Cl₂ suspension (20 ml) of (*S*)-Boc-proline (1.00 g, 4.00 mmol) was added DCC (1.05 g, 5.00 mmol) in CH₂Cl₂ (5 ml) at 0 °C under an argon atmosphere and the reaction mixture was stirred for 15 min at that temperature. To this reaction mixture was added a CH₂Cl₂ solution (2 ml) of pyrrolidine (410 μl, 4.65 mmol) slowly at 0 °C, and was increased to rt after 10 min and left stirred over 24 h. After removal of CH₂Cl₂ *in vacuo*, EtOAc (20 ml) was then added to the residue. After insoluble materials had been removed by filtration, the filtrate was washed with 1 M HCl (10 ml), saturated NaHCO₃ solution (20 ml) and brine sequentially, then drying over anhydrous Na₂SO₄. The EtOAc was removed *in vacuo*, and the residue was purified by silica gel column chromatography, (CHCl₃:MeOH, 9:1) to afford the amide **187a**; yield 1.06 g (85%).

R_f 0.45; **[α]²⁵_D** = -83.1 (*c* 0.5, EtOH); **IR (Neat)** 1697.5, 1658.2 (amide); **¹H NMR (300 MHz; CDCl₃)** δ 1.45 (9H, s), 1.81-2.09 (5H, m), 3.41-3.75 (9H, m) 4.57 (1H, m, *CH*); **¹³C NMR (125 MHz; CDCl₃)** rotamers δ 23.0, 23.3, 29.5 (CH₃)₃, 29.3, 30.6, 42.0, 45.7, 46.0, 46.5, 46.8, 56.1, 56.2, 66.6, 67.5, 76.6, 153.2 (carbamate), 173.4 (amide); ***m/z* (ES⁺)** 285 (M+H⁺, 50%), 185 (M-Boc⁺, 100%).

Tert-butyl (2S)-2-[(2,3-dihydro-1H-isoindol-2-yl)carbonyl]pyrrolidine-1-carboxylate hydrate^{140,130}

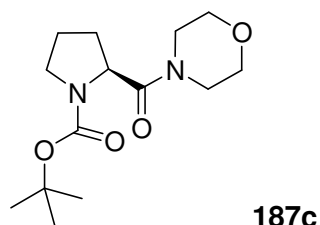


187b

To a CH₂Cl₂ suspension (20 ml) of (*S*)-Boc-proline (1.02 g, 4.00 mmol) was added a CH₂Cl₂ (5 ml) of DCC (1.04 g, 5.00 mmol) at 0 °C under an argon atmosphere and the reaction mixture was stirred for 15 min at that temperature. To this reaction mixture was added a CH₂Cl₂ solution (2 ml) of piperidine (457 μl, 4.66 mmol) slowly at 0 °C, and was increased to rt after 10 min and left stirred over 24 h. CH₂Cl₂ was then removed *in vacuo*, and EtOAc (20 ml) was added to the residue. After insoluble materials had been removed by filtration, the filtrate was washed with 1 M HCl (10 ml),

saturated NaHCO₃ solution (20 ml) and brine sequentially, then drying over anhydrous Na₂SO₄. The EtOAc was removed *in vacuo*, and the residue was purified by silica gel column chromatography, (CHCl₃:MeOH, 9:1) to afford the amide **187b**; yield 1.16 g (89%). **R_f** 0.45; [α]_D²⁵ = -43.4 (*c* 0.5, EtOH); **IR (Neat)** 1697.5 (carbamate), 1658.2 (amide); **¹H NMR (300 MHz; CDCl₃)** rotamers; δ 1.40 (4.5H, s, CH₃), 1.47 (4.5H, s, CH₃), 1.56-2.03 (10H, m, CH₂), 3.35-3.69 (6H, m, CH₂), 4.53 (0.5H, dd, *J* 8.7 and 3.7, CH), 4.66 (0.5H, dd, *J* 8.2 and 2.2, CH); **¹³C NMR (125 MHz; CDCl₃)** rotamers δ 23.4, 24.1, 26.5, 28.5 (CH₃)₃, 29.8, 30.5, 56.5 (CH), 56.9 (CH), 79.3, 154.5 (carbamate), 171.2 (amide); ***m/z* (ES⁺)** 283 (M+H⁺, 100%), 183 (M-Boc⁺, 50%).

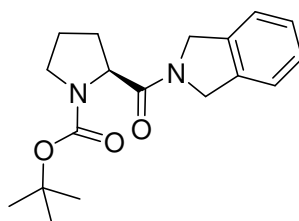
Tert-butyl (2S)-2-[(morpholin-4-yl)carbonyl]pyrrolidine-1-carboxylate¹³⁰



To a CH₂Cl₂ suspension (20 ml) of (*S*)-Boc-proline (1.04 g, 4.00 mmol) was added a CH₂Cl₂ (5 ml) of DCC (1.05 g, 5.00 mmol) at 0 °C under an argon atmosphere and the reaction mixture was stirred for 15 min at that temperature. To this reaction mixture was added a CH₂Cl₂ solution (2 ml) of morpholine (405 μ l, 4.66 mmol) slowly at 0 °C, and was increased to rt after 10 min and left stirred over 24 h. After removal of CH₂Cl₂ *in vacuo*, EtOAc (20 ml) was then added to the residue. After insoluble materials had been removed by filtration, the filtrate was washed with 1 M HCl (10 ml), saturated NaHCO₃ solution (20 ml) and brine sequentially, then drying over anhydrous Na₂SO₄. The EtOAc was removed *in vacuo*, and the residue was purified by silica gel column chromatography, (CHCl₃:MeOH, 9:1) to afford the amide **187c**; yield 1.10 g (83%).

R_f 0.45; [α]_D²⁵ = -83.1 (*c* 0.5, EtOH); **IR (Neat)** 1697.5, 1658.2 (amide); **¹H NMR (300 MHz; CDCl₃)** δ 1.45 (9H, s), 1.81-2.09 (5H, m), 3.41-3.75 (9H, m) 4.57 (1H, m, CH); **¹³C NMR (125 MHz; CDCl₃)** rotamers δ 23.6, 24.3, 28.5 (CH₃)₃, 29.8, 30.6, 42.4, 45.7, 46.0, 46.6, 46.8, 56.1, 56.7, 66.6, 67.0, 76.6, 154.0 (carbamate), 171.0 (amide); ***m/z* (ES⁺)** 285 (M+H⁺, 50%), 185 (M-Boc⁺, 100%).

Tert-butyl (2S)-2-[(2,3-dihydro-1H-isoindol-2-yl)carbonyl]pyrrolidine-1-carboxylate hydrate¹⁴¹

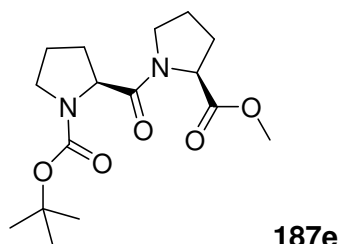


187d

To a CH₂Cl₂ suspension (20 ml) of (*S*)-Boc-proline (1.02 g, 4.00 mmol) was added a CH₂Cl₂ (5 ml) of DCC (1.03 g, 5.00 mmol) at 0 °C under an argon atmosphere and the reaction mixture was stirred for 15 min at that temperature. To this reaction mixture was added a CH₂Cl₂ solution (2 ml) of isoindoline (554 μl, 4.65 mmol) slowly at 0 °C, and was increased to rt after 10 min and left stirred over 24 h. CH₂Cl₂ was removed *in vacuo*, and EtOAc (20 ml) was added to the residue. After insoluble materials had been removed by filtration, the filtrate was washed with 1 M HCl (10 ml), saturated NaHCO₃ solution (20 ml) and brine sequentially, then drying over anhydrous Na₂SO₄. The EtOAc was removed *in vacuo*, and the residue was purified by silica gel column chromatography, (CHCl₃:MeOH, 9:1) to afford the amide **187d**; yield 1.32 g (90%).

R_f 0.45; **[α]²⁵_D** = -103.1 (*c* 0.5, MeOH); **IR (Neat)** 1697.5, 1658.2 (amide); **¹H NMR (300 MHz; CDCl₃)** δ 1.24 (4.5H, s, CH₃), 1.45 (4.5H, s, CH₃), 1.57-1.97 (5H, m), 3.12 (2H, m), 3.42 (1H, m), 3.59 (1H, m), 4.09-4.84 (3H, m), 6.91 (1H, m), 7.08 (1H, m), 8.16 (1H, m); **¹³C NMR (125 MHz; CDCl₃)** rotamers; δ 23.7, 24.2, 28.3, 28.5 (CH₃)₃, 29.5, 30.4, 58.5 (CH), 58.7 (CH), 79.5, 79.6, 117.2, 123.6, 123.7, 124.5, 127.3, 127.5, 130.9, 131.1, 142.9, 143.1, 153.7 (carbamate), 154.5 (carbamate), 170.9 (amide), 171.2 (amide); ***m/z* (ES⁺)** 316 (M+H⁺, 100%), 216 (M-Boc⁺, 50%).

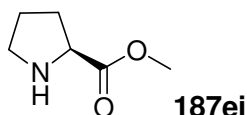
Tert-butyl(2S)-2-[[[(2S)-2-(hydroxymethyl)pyrrolidin-1-yl] carbonyl]pyrrolidine-1-carboxylate¹³¹



To a CH₂Cl₂ suspension (20 ml) of (S)-Boc-proline (1.02 g, 4.00 mmol) was added a CH₂Cl₂ (5 ml) of DCC (1.03 g, 5.00 mmol) at 0 °C under an argon atmosphere and the reaction mixture was stirred for 15 min at that temperature. To this reaction mixture was added a CH₂Cl₂ solution (2 ml) of **187ei** (0.63 g, 4.65 mmol) slowly at 0 °C, and was increased to rt after 10 min and left stirred over 24 h. CH₂Cl₂ was removed *in vacuo*, and EtOAc (20 ml) was added to the residue. After insoluble materials had been removed by filtration, the filtrate was washed with 1 M HCl (10 ml), saturated NaHCO₃ solution (20 ml) and brine sequentially, then drying over anhydrous Na₂SO₄. The EtOAc was removed *in vacuo*, and the residue was purified by silica gel column chromatography, (CHCl₃:MeOH, 9:1) to afford the amide **187e**; yield 1.15 g (76%).

R_f 0.43; **[α]_D²⁵** +42.1 (c 0.5, CHCl₃); **IR** 1705.5, 1658.2 (amide); **¹H NMR (300 MHz; CDCl₃)** δ 1.38 (4.5H, s, CH₃), 1.43 (4.5H, s, CH₃), 1.85-2.19 (8H, m), 3.40-3.78 (7H, m), 4.48-4.57 (2H, m, CH); **¹³C NMR (125 MHz; CDCl₃)** rotamers; δ 23.7, 24.2, 28.3, 28.5 (CH₃)₃, 29.5, 30.4, 58.5 (CH), 58.7 (CH), 79.5, 79.6, 117.2, 123.6, 123.7, 124.5, 127.3, 127.5, 130.9, 131.1, 142.9, 143.1, 153.7 (carbamate), 154.5 (carbamate), 170.9 (amide), 171.2 (amide); **m/z (ES⁺)** 327 (M+H⁺, 100%), 102 (Boc+H⁺, 100%).

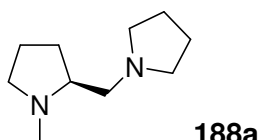
(2S)- Pyrrolidine-2-carboxylic acid methyl ester¹³¹



To 12 ml (0.30 mol) methanol cooled to 0 °C was added dropwise 3 ml (0.04 mol) thionyl chloride. To this solution 1.5 g (0.013 mol) L-proline was added and stirred for 1 h. The mixture was then allowed to warm to rt and stirred for 48 h. After evaporation of methanol, the crystalline product was suspended in 8 ml diethyl ether and was added 2.5 ml (0.018 mol) triethylamine at rt and stirred for 2 h. The white precipitate was filtered and washed with (2x10 ml) diethyl ether. The ethereal layers were combined and evaporated *in vacuo* to afford a pale yellow liquid 1.50 g (90%).

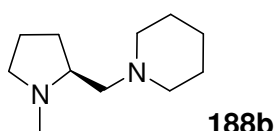
$[\alpha]_{D}^{25} = +19.8$ (*c* 1.4, EtOH); IR (Neat) $\bar{\nu}$ 3385 br, 2971, 1740, 1630; $^1\text{H NMR}$ (300 MHz; CDCl_3) δ 1.74 (3H, m), 2.08 (2H, m), 2.90 (0.5H, m), 3.08 (0.5H, m), 3.73 (3H, s) 3.76 (1H, m), 4.2 (1H, s, NH); $^{13}\text{C NMR}$ (125 MHz; CDCl_3) δ 25.5, 30.2, 47.1, 52.1 (CH_3), 59.7 (CH); m/z (ES^+) 130 ($\text{M}+\text{H}^+$, 20%).

(2S)-1-methyl-2-(pyrrolidin-1-ylmethyl)pyrrolidine¹³⁰



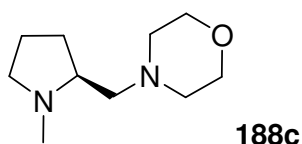
To a THF suspension (10 ml) of LiAlH_4 (0.312 g, 8.22 mmol) was added a THF solution (10 ml) of **187a** (1.02 g, 3.81 mmol) at 0 °C and the temperature of the reaction mixture was raised to rt. Following the complete addition of **187a**, the reaction mixture was refluxed for 4 h. Saturated Na_2SO_4 solution was added to the reaction mixture at 0 °C until the evolution of H_2 ceased. After filtration of the inorganic materials, volatile solvent was removed in *vacuo* to afford the diamine **188a** as a colourless oil; yield 0.52 g (81%). $[\alpha]_{D}^{25} = -83.1$ (*c* 0.5, EtOH); IR (Neat) 2980s, 2950, 1422 ; $^1\text{H NMR}$ (300 MHz; CDCl_3) δ 1.40-2.59 (16H, m), 2.34 (3H, s, $\text{CH}_3\text{-N}$), 2.99 (1H, m, CH); $^{13}\text{C NMR}$ (125 MHz; CDCl_3) δ 22.5, 23.4, 31.0, 41.3 ($\text{CH}_3\text{-N}$), 54.9, 57.5, 61.5, 64.9 (CHNCH_3); m/z (HRMS) calcd for $\text{C}_{10}\text{H}_{20}\text{O}_2\text{Na}$ $[\text{MH}]^+$ 1911.1208, found 191.1324.

1-[[2S)-1-methylpyrrolidin-2-yl]methyl]piperidine¹³⁰



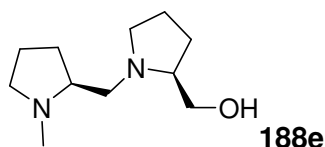
To a THF suspension (10 ml) of LiAlH_4 (0.310 g, 8.22 mmol) was added a THF solution (10 ml) of **187b** (1.06 g, 3.76 mmol) at 0 °C and the temperature of the reaction mixture was raised to rt. Following the complete addition of **187b**, the reaction mixture was refluxed for 4 h. Saturated Na_2SO_4 solution was added to the reaction mixture at 0 °C until the evolution of H_2 ceased. After filtration of the inorganic materials, volatile solvent was removed in *vacuo* to afford the diamine **188b** as a colourless oil; yield 0.53 g (78%). $[\alpha]_{D}^{25} = -83.1$ (*c* 0.5, EtOH); IR (Neat) 2980s, 2950s, 1722; $^1\text{H NMR}$ (300 MHz; CDCl_3) δ 1.22-2.51 (18H, m), 2.39 (3H, s $\text{CH}_3\text{-N}$), 3.03 (1H, m, CH); $^{13}\text{C NMR}$ (125 MHz; CDCl_3) δ 22.7, 24.5, 26.0, 31.3, 41.5 ($\text{CH}_3\text{-N}$), 54.4, 57.7, 63.0 ($-\text{CHNCH}_3$), 64.9; m/z (ES^+) 183 ($\text{M}+\text{H}^+$, 10%).

4-[[**(2S)**-1-methylpyrrolidin-2-yl]methyl]morpholine¹³⁰



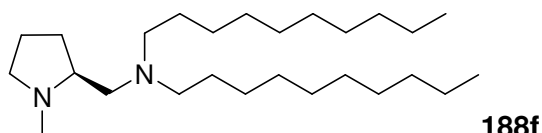
To a THF suspension (10 ml) of LiAlH₄ (0.314 g, 8.22 mmol) was added a THF solution (10 ml) of **187c** (1.05 g, 3.67 mmol) at 0 °C and the temperature of the reaction mixture was raised to rt. Following the complete addition of **187c**, the reaction mixture was refluxed for 4 h. Saturated Na₂SO₄ solution was added to the reaction mixture at 0 °C until the evolution of H₂ ceased. After filtration of the inorganic materials, volatile solvent was removed in *vacuo* to afford the diamine **188c** as a colourless oil; yield 0.57 g (84%). [α]_D²⁵ = -64.5 (*c* 0.8, EtOH); IR (Neat) 3387, 2953, 1739; ¹H NMR (300 MHz; CDCl₃) δ 1.59-2.52 (8H, m), 2.41 (3H, s, CH₃-N), 2.45 (4H, t, *J* 4.5, CH₂NCH₂), 3.04 (1H, m, CH), 3.69 (4H, t, *J* 4.5, CH₂OCH₂); ¹³C NMR (125 MHz; CDCl₃) δ 22.6, 30.8, 41.6 (CH₃-N), 54.4, 57.9, 62.5 (-CH₂NCH₂), 64.4 (CH₂OCH₂), 67.0; *m/z* (ES⁺) 185 (M+H⁺, 100%).

[(**3R**)-1-[[**(2S)**-1-methylpyrrolidin-2-yl]methyl]pyrrolidin-3-yl]methanol amine¹³¹



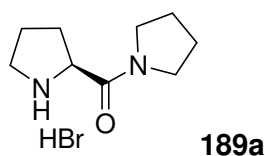
To a THF suspension (10 ml) of LiAlH₄ (0.312 g, 8.22 mmol) was added a THF solution (10 ml) of **187e** (1.03 g, 3.16 mmol) at 0 °C and the temperature of the reaction mixture was raised to rt. Following the complete addition of **187e**, the reaction mixture was refluxed for 4 h. Saturated Na₂SO₄ solution was added to the reaction mixture at 0 °C until the evolution of H₂ ceased. After filtration of the inorganic materials, volatile solvent was removed in *vacuo* to afford the diamine **188e** as a colourless oil; yield 0.57 g (90%). [α]_D²⁵ = -53.1 (*c* 0.8, EtOH); IR (Neat) 3364 (br, OH), 2951, 1738; ¹H NMR (300 MHz; CDCl₃) δ 1.62-1.88 (9H, m), 2.18-2.67 (5H, m), 2.33 (3H, s), 3.06 (1H, m, CH), 3.16 (1H, m, CHCH₂OH), 3.33 (1H, dd, *J* 10.8 and 3.9), 3.54 (1H, dd, *J* 10.8 and 3.1); ¹³C NMR (125 MHz; CDCl₃) δ 22.8, 24.2, 27.7, 29.5, 41.1 (CH₃-N), 56.5, 57.4, 58.4, 63.4, 65.9 (-CHNCH₃), 66.5 (-CHCH₂OH); *m/z* (ES⁺) 199 (M+H⁺, 100%).

bis(decyl){[(2S)-1-methylpyrrolidin-2-yl]methyl}amine¹³¹



To a THF suspension (10 ml) of LiAlH_4 (0.312 g, 8.22 mmol) was added a THF solution (10 ml) of **187f** (1.02 g, 2.02 mmol) at 0 °C and the temperature of the reaction mixture was raised to rt. Following the complete addition of **187f**, the reaction mixture was refluxed for 4 h. Saturated Na_2SO_4 solution was added to the reaction mixture at 0 °C until the evolution of H_2 ceased. After filtration of the inorganic materials, volatile solvent was removed in *vacuo* to afford the diamine **188f** as a colourless oil; yield 0.60 g (81%). $[\alpha]_{\text{D}}^{25} = -94.5$ (*c* 1.1, EtOH); IR (Neat) 2922, 2852, 1456; $^1\text{H NMR}$ (300 MHz; CDCl_3) δ 1.20-2.56 (50H, m), 2.39 (3H, s, $\text{CH}_3\text{-N}$), 3.13 (1H, m, CHNCH_3); $^{13}\text{C NMR}$ (125 MHz; CDCl_3) δ 22.3, 24.1, 25.0, 25.3 (signals superimposed), 26.1, 31.3, 41.5 ($\text{CH}_3\text{-N}$), 54.4, 57.7, 63.0 (-CHNCH_3), 64.9; m/z (ES^+) 395 ($\text{M}+\text{H}^+$, 100%).

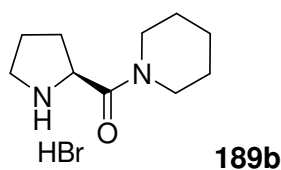
(2S)-2-[(pyrrolidin-1-yl)carbonyl]pyrrolidine hydrobromide¹³²



A mixture of **187a** (1.02 g, 3.81 mmol) and 33% solution of HBr in acetic acid (3 ml) was stirred for 3 h. The reaction was stopped by distillation of acetic acid *in vacuo* and the crude product was purified using a silica chromatography column ($\text{CH}_3\text{Cl}:\text{MeOH}$; 9:1) affording compound **189a** as a brown liquid; yield 0.61 g (97%).

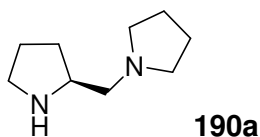
$[\alpha]_{\text{D}}^{25} = -24.1$ (*c* 0.3, EtOH); IR (Neat) 3380br, 2942s, 1632s; $^1\text{H NMR}$ (300 MHz; D_2O) δ 1.77-2.00 (7H, m), 2.42-2.52 (1H, m), 3.28-3.50 (6H, m), 4.46 (1H, t, *J* 7.5, CH); $^{13}\text{C NMR}$ (125 MHz; D_2O) δ 24.0, 24.4, 25.7, 28.7, 47.0, 59.6 (CH), 167.7 (NHC=O); m/z (ES^+) 169 ($\text{M}+\text{H}^+$, 100%).

1-[[**(2S)**-pyrrolidin-2-yl]carbonyl]piperidine hydrobromide¹³²



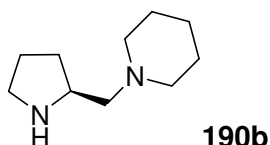
A mixture of **187b** (1.02 g, 3.81 mmol) and 33% solution of HBr in acetic acid (3 ml) was stirred for 3 h. The reaction was stopped by distillation of acetic acid *in vacuo* and the crude product was purified using a silica chromatography column (CH₂Cl:MeOH; 9:1) affording compound **189b** as a brown liquid; yield 0.60 g (94%); [α]_D²⁵ = -63.1 (c 1.2, EtOH); IR (Neat) 3400br, 2950s, 1722s; ¹H NMR (300 MHz; D₂O) δ 1.51-1.61 (6H, m), 1.81-2.07 (3H, m), 2.43 (1H, m), 3.34-3.54 (6H, m), 4.75 (1H, J 8.4, CH); ¹³C NMR (125 MHz; D₂O) δ 24.3, 25.6, 26.2, 30.4, 44.0, 46.4, 46.9, 57.9 (CH), 168.5 (NHC=O); *m/z* (ES⁺) 183 (M+H⁺, 10%).

(2S)-2-(pyrrolidin-1-ylmethyl)pyrrolidine¹³³



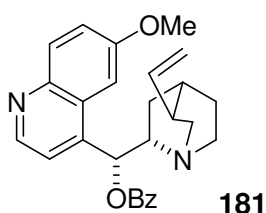
To a THF suspension (10 ml) of LiAlH₄ (0.301 g, 8.00 mmol) was added a THF solution (10 ml) of **189a** (0.61 g, 3.63 mmol) at 0 °C and the temperature of the reaction mixture was raised to rt. Following the complete addition of **189a**, the reaction mixture was refluxed for 4 h. Saturated Na₂SO₄ solution was added to the reaction mixture at 0 °C until the evolution of H₂ ceased. After filtration of the inorganic materials, volatile solvent was removed in *vacuo* to afford the diamine **190a** as a brown oil; yield 0.52 g (93%). [α]_D²⁵ = +8.2 (c 2.0, EtOH); IR (neat) 3250, 1460, 1400; ¹H NMR (300 MHz; CDCl₃) δ 1.25-2.04 (8H, m), 2.32-2.57 (6H, m), 2.83-3.21 (3H, m); ¹³C NMR (125 MHz; CDCl₃) δ 23.5, 25.1, 30.2, 46.2, 54.6, 57.5 (CH), 62.2 (NCH₂CHN), *m/z* (ES⁺) 155 (M+H⁺, 60%), 154 (M⁺, 50%).

1-[(2S)-pyrrolidin-2-ylmethyl]piperidine¹³⁴



To a THF suspension (10 ml) of LiAlH_4 (0.270 g, 7.25 mmol) was added a THF solution (10 ml) of **189b** (0.60 g, 3.30 mmol) at 0 °C and the temperature of the reaction mixture was raised to rt. Following the complete addition of **189b**, the reaction mixture was refluxed for 4 h. Saturated Na_2SO_4 solution was added to the reaction mixture at 0 °C until the evolution of H_2 ceased. After filtration of the inorganic materials, volatile solvent was removed in *vacuo* to afford the diamine **190b** as a brown oil; yield 0.45 g (81%). $[\alpha]_{\text{D}}^{25} = +19.6$ (c 1.2, EtOH); IR (neat) 3250, 2960, 1440, 1300; $^1\text{H NMR}$ (300 MHz; CDCl_3) δ 1.32-2.00 (10H, m), 2.23-2.45 (8H, m), 3.63 (1H, t, J 6.0, CH); $^{13}\text{C NMR}$ (125 MHz; CDCl_3) δ 24.5, 25.0, 26.1, 30.1, 46.1, 55.1, 55.6 (CH), 65.0 (NCH₂CHN), m/z (ES^+) 169 ($\text{M}+\text{H}^+$, 100%)

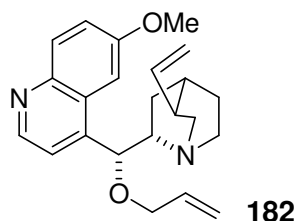
Benzoic acid (6-methoxy-quinolin-4-yl)-(5-vinyl-1-aza-bicyclo[2.2.2]oct-2-yl)-methyl ester¹²⁵



To a solution of quinine **180** (2.05 g, 6.2 mmol) in anhydrous DMF (20 ml) was added triethylamine (863 μl , 12.4 mmol) and the reaction mixture was stirred at rt under an argon atmosphere for 2 h. Then benzoyl chloride (1.0 ml, 6.8 mmol) was added dropwise over 15 min and the reaction mixture was stirred overnight. After starting material had been consumed, brine (20 ml) was added to the reaction mixture and was extracted with EtOAc (100 ml). The organic layer was washed with H_2O (4 x 20 ml), brine (50 ml) and dried over Na_2SO_4 . The solvent was removed *in vacuo* to afford the crude oil which was purified using silica gel chromatography (CHCl_3 :MeOH, 9:1) to afford **181**, as yellow crystals (1.31 g, 50%). **M.p.** 190-200; $[\alpha]_{\text{D}}^{25} = +110$ (c 0.5, CHCl_3); IR (Neat) 2941, 2855, 1711 (s, ester), 1621 (m, Ar), 1504; $^1\text{H NMR}$ (300 MHz; CDCl_3) δ 1.46-1.57 (2H, m), 1.69-1.73 (1H, m), 1.77 (1H, m, br), 1.97-2.04 (1H, m), 2.21 (1H, m), 2.47-2.52 (2H, m), 2.80-2.88 (1H, m), 3.17 (1H), 3.46-3.52 (1H, m), 3.92 (3H, s, OCH_3), 4.97-5.05 (2H, m), 5.93-6.04 (1H, m), 6.52 (1H, d, J 8.4), 7.42 (1H, dd, J 9.0 and 2.4), 7.68 (1H, t, J 7.5), 7.52-7.60 (4H, m), 7.91 (1H, d, J 9.3), 8.04 (2H, d, J 7.2),

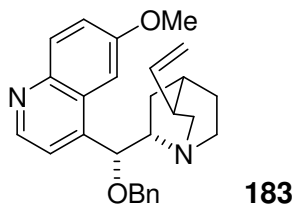
8.67 (1H, d, *J* 4.5); ^{13}C NMR (125 MHz; CDCl_3) δ 24.1, 27.7, 27.9, 39.7 (OCH_3), 42.6, 55.8, 56.8, 59.5, 74.5, 101.5, 114.7, 118.7, 122.1, 127.0, 128.0, 128.7, 129.7, 131.9, 133.6, 141.7, 143.7, 144.9, 147.5, 158.1 (ester), 165.6 (ketone), *m/z* (CI^+) 429 ($\text{M}+\text{H}^+$, 100%).

4-[Allyloxy-(5-vinyl-1-aza-bicyclo[2.2.2]oct-2-yl)-methyl]-6-methoxy-quinoline¹²⁵



To a solution of quinine **180** (2.05 g, 6.2 mmol) in anhydrous DMF (20 ml) was added triethylamine (863 μl , 12.4 mmol) and the reaction mixture was stirred at rt under an argon atmosphere for 2 h. Then benzoyl chloride (1 ml, 6.8 mmol) was added dropwise over 15 min and the reaction mixture was stirred overnight. After starting material had been consumed, brine (20 ml) was added to the reaction mixture and was extracted with EtOAc (100 ml). The organic layer was washed with H_2O (4 x 20 ml), brine (50 ml) and dried over Na_2SO_4 . The solvent was removed *in vacuo* to afford the crude oil which was purified using silica gel chromatography, (CHCl_3 :MeOH, 9:1) to afford a yellow oil **182**; yield 2.52 g (93%). $[\alpha]_{\text{D}}^{25} = +116$ (c. 0.6, CHCl_3); IR (Neat) 2935, 2865, 1620, 1590, 1508, 1240; ^1H NMR (500 MHz; CDCl_3) δ 1.45-1.57 (2H, m), 1.70-1.77 (3H, m), 1.97-2.04 (1H, m), 2.22 (1H, m), 2.57-2.67 (2H, m), 3.03-3.08 (2H, m), 3.45 (1H, m), 3.90 (3H, s, OCH_3), 3.81-3.94 (2H, m), 4.85-4.92 (2H, m), 5.13-5.29 (3H, m), 5.68 (1H, m), 5.90 (1H, m, $\text{CHC}=\text{C}$), 7.30-7.35 (2H, m), 7.40 (1H, d, *J* 4.5), 8.00 (2H, d, *J* 10.2), 8.70 (1H, d, *J* 5.0); ^{13}C NMR (125 MHz; CDCl_3) δ 22.1, 27.5, 28.1, 39.7 (OCH_3), 43.8, 53.1, 55.4, 56.9, 59.8, 69.7 (OCH_2), 80.5 (CHOally), 102.7, 113.9 ($\text{CH}=\text{CH}_2$), 116.8, 118.5, 121.3, 127.0, 127.1 134.1, 141.6, 144.4, 147.3, 157.4; *m/z* (EI) 363 (M^+ , 100%).

4-[Allyloxy-(5-vinyl-1-aza-bicyclo[2.2.2]oct-2-yl)-methyl]-6-methoxy-quinoline¹²⁵



To a solution of quinine **180** (2.00 g, 6.2 mmol) in anhydrous DMF (20 ml) was added triethylamine (863 μ l, 12.4 mmol) and the reaction mixture was stirred at rt under an argon atmosphere for 2 h. Then benzyl chloride (780 μ l, 6.8 mmol) was added dropwise over 15 min and the reaction mixture was stirred overnight. After starting material had been consumed, brine (20 ml) was added to the reaction mixture and was extracted with EtOAc (100 ml). The organic layer was washed with H₂O (4 x 20 ml), brine (50 ml) and dried over Na₂SO₄. The solvent was removed *in vacuo* to afford the crude oil which was purified using silica gel chromatography, (CHCl₃:MeOH, 9:1) to afford brown oil **183**; yield 2.45 g (95%). [α]_D²⁵ = +132 (*c* 0.90, CHCl₃); IR (Neat) 2935, 2865, 1619, 1590, 1507, 1240; ¹H NMR (500 MHz; CDCl₃) δ 1.46-1.80 (5H, m), 2.23 (1H, m), 2.58-2.68 (2H, m), 3.04-3.16 (2H, m), 3.41 (1H, m), 3.91 (3H, s, OCH₃), 4.39 (1H, d, *J* 12.0), 4.46 (1H, d, *J* 12.0), 4.89-4.97 (1H, m, CHO), 5.19 (1H, m), 5.68-5.80 (1H, m), 5.90 (1H, m, CHC=C), 7.28-7.40 (7H, m), 7.47 (1H, d, *J* 4.5 Hz), 8.05 (1H, d, *J* 9.0 Hz), 8.75 (1H, d, *J* 4.5); ¹³C NMR (125 MHz; CDCl₃) δ 22.5, 27.5, 28.1, 39.7 (OCH₃), 43.3, 55.4, 56.9, 59.8, 70.8 (OCH₂), 80.7 (CHOBn), 101.0, 113.9 (CH=CH₂), 116.9, 121.5, 127.4, 127.7, 127.9, 128.3, 131.6, 137.6, 140.9 (CH=CH₂), 144.4, 144.7, 147.3, 157.5; *m/z* (CI) 415 (M+H⁺, 100%).

Publications from PhD research

'Stereoselectivity of an ω -transaminase-mediated amination of 1,3-dihydroxy-1-phenylpropane-2-one'

Smithies, K.; Smith, M.E.B.; Kaulmann, U.K.; Galman, J.L.; Ward, J.M.; Hailes, H.C. *Tetrahedron Asymmetry*. **2009**, *20*, 570.

'Application of a modified Mosher's method for the determination of enantiomeric ratio and absolute configuration at C-3 of chiral 1,3-dihydroxy ketones'

Galman, J.L.; Hailes, H.C. *Tetrahedron: Asymmetry*, **2009**, *20*, 1828.

'Non- α -hydroxylated aldehydes with evolved transketolase enzymes'

Cázares, A.; Galman, J.L.; Crago, L.G.; Smith, M.E.B.; Strafford, J.; Ríos-Solís, L.; Lye, G.L.; Dalby, P.A.; Hailes, H.C. *Org. Biomol. Chem.* **2010**, *6*, 1301.

'A Multidisciplinary Approach Toward the Rapid and Preparative-Scale Biocatalytic Synthesis of Chiral Amino Alcohols: A Concise Transketolase-/ ω -Transaminase-Mediated Synthesis of (2S,3S)-2-Aminopentane-1,3-diol'

Smith, M. E. B.; Chen, B. H.; Hibbert, E. G.; Kaulmann, U.; K. Smithies, Galman, J. L.; Baganz, F.; Dalby, P.A.; Hailes, H.C.; Lye, G.J.; Ward, J.M.; Woodley, J.M.; Micheletti, M. *Org. Process Res. Dev.*, **2010**, *14*, 99

' α,α' -Dihydroxyketone formation using aromatic and heteroaromatic aldehydes with evolved transketolase enzymes'

Galman, J.L.; Steadman, D.; Bacon, S.; Morris, P.; Smith, M.E.B.; Ward, J.M.; Dalby, P.A.; Hailes, H.C. *Chem. Commun.*, **2010**, *46*, 7608



Contents lists available at ScienceDirect

Tetrahedron: Asymmetry

journal homepage: www.elsevier.com/locate/tetasy



Stereoselectivity of an ω -transaminase-mediated amination of 1,3-dihydroxy-1-phenylpropane-2-one

Kirsty Smithies^a, Mark E. B. Smith^a, Ursula Kaulmann^b, James L. Galman^a, John M. Ward^b, Helen C. Hailes^{a,*}

^aDepartment of Chemistry, University College London, 20 Gordon Street, London WC1H 0AJ, UK

^bResearch Department of Structural and Molecular Biology, University College London, Gower Street, London WC1E 6BT, UK

ARTICLE INFO

Article history:

Received 15 December 2008

Accepted 16 March 2009

Available online 22 April 2009

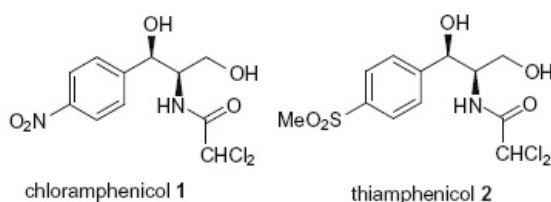
ABSTRACT

The stereoselectivity of a recently isolated ω -transaminase from *Chromobacterium violaceum* in the amination of 1,3-dihydroxy-1-phenylpropane-2-one has been determined. The enzyme is not enantioselective towards a racemic mixture of 1,3-dihydroxy-1-phenylpropane-2-one but is highly stereoselective forming (2*S*)-2-amino-1-phenyl-1,3-propanediols in >99% ee.

© 2009 Elsevier Ltd. All rights reserved.

1. Introduction

The chiral aminodiols motif is present in many pharmacologically important compounds such as antiviral glycosidase inhibitors^{1,2} and sphingolipids.^{3,4} Specifically, the broad spectrum antibiotics chloramphenicol **1** and thiamphenicol **2** contain the 2-amino-1-phenyl-1,3-propanediol functionality.^{5,6}

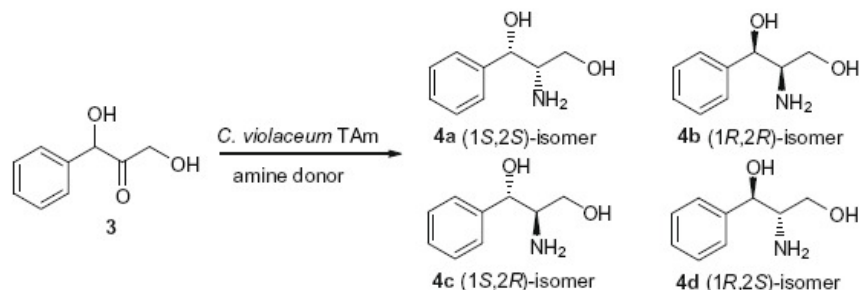


The development of efficient, stereoselective methodology to chiral aminodiols remains a major challenge. There are a wide range of synthetic strategies to chiral amines, however it has recently been highlighted that green chemistry approaches to chiral amines are highly desirable, particularly via ketones or aldehydes.⁷ Biocatalytic routes to chiral amines predominantly focus on the kinetic resolution of racemic mixtures. In particular, *N*-acyl amides may be resolved using amidases, lipases or peptidases.⁸ Although much of this methodology has been developed for use on an industrial scale, it is limited by the fact that the maximum yield of con-

version is 50%. Biocatalytic asymmetric syntheses of amines are therefore highly desirable and a deracemization approach using racemic amines has been reported.⁹ Recently, the use of ω -transaminases (TAM) to generate chiral amines has received increasing attention.^{10–12} Practical difficulties relating to unfavourable thermodynamic parameters have been addressed and a coupled enzyme system incorporating ω -transaminase, α -amino acid dehydrogenase and formate dehydrogenase has been reported.^{13,14}

As part of a multidisciplinary project aiming to develop biocatalytic routes to pharmacologically interesting targets, we are currently investigating the biocatalytic and chemoenzymatic synthesis of aminodiols. We have recently reported the one-pot synthesis of aminoalcohols using an engineered *de novo* transketolase (TK) and β -alanine TAM pathway in *Escherichia coli*.¹⁵ We have also reported *Chromobacterium violaceum* DSM30191 ω -transaminase (*C. violaceum* TAM) that accepts a range of ketones and aldehydes as well as a ketoalcohol as substrates.¹⁶ Our aim was now to establish the stereoselectivity of *C. violaceum* TAM when using an α,α' -dihydroxyketone, notably the aromatic substrate 1,3-dihydroxy-1-phenylpropane-2-one **3** to give 2-amino-1-phenyl-1,3-propanediol **4** (Scheme 1, four possible diastereoisomers shown). Previous work had indicated that when *C. violaceum* TAM was used with **3** to generate **4**, two products were formed which when analysed by HPLC and LC/MS were believed to be the *syn*- and *anti*-isomers. Based upon previous work describing the selectivity of ω -TAMs where (*S*)- α -methylbenzylamine was the amine donor, these were postulated to be the (1*S*,2*S*)- and (1*R*,2*S*)-isomers **4a** and **4d**. However, the 1,3-dihydroxyketone could adopt an alternative orientation in the active site via hydrogen-bonding interactions, or a non-stereoselective amination with TAM could give **4b** and **4c**. These studies set out to establish the absolute stereochemistries resulting from the biocon-

* Corresponding author. Tel.: +44 (0)20 7679 4654; fax: +44 (0)20 7679 7463. E-mail address: h.c.hailes@ucl.ac.uk (H.C. Hailes).

Scheme 1. @-TAM-catalysed conversion of **3** to diastereoisomers **4a–4d**.

version, which is crucial for synthetic applications with this enzyme. Notably, it was important to determine whether one of the enantiomers of **3** is non-stereoselectively transformed to **4**, or if both enantiomers of **3** are stereoselectively converted to **4**.

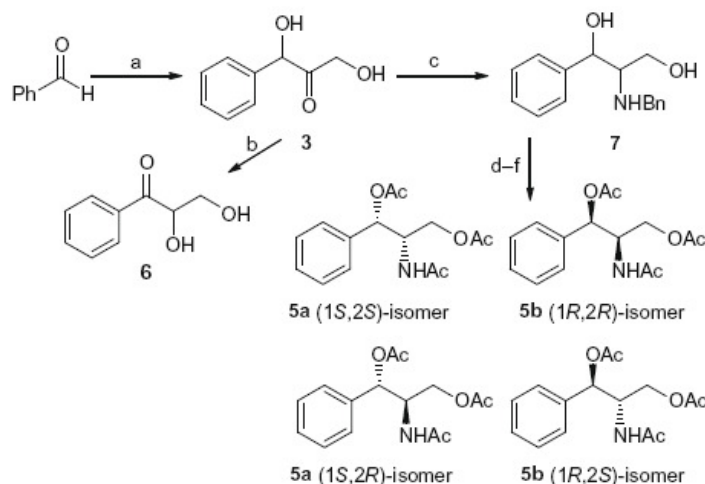
2. Results and discussion

In order to establish the selectivity of the *C. violaceum* TAM, chemically derived analytical standards were required. Both **4a** (the (1*S*,2*S*)-isomer) and **4b** (the (1*R*,2*R*)-isomer) are commercially available and samples of both were readily triacetylated in quantitative yield to give (1*S*,2*S*)-**5a** and (1*R*,2*R*)-**5b** for chiral HPLC method development.¹⁷ A sample of all four of the possible diastereoisomers **4a–4d** was synthesised which could be conveniently prepared from the dihydroxyketone **3** (Scheme 2). Racemic **3** was synthesised via the tertiary amine-catalysed condensation of benzaldehyde with lithium hydroxypyruvate (LiHPA) which has been reported recently in our laboratory.¹⁸ In addition it was noted that if extended reaction times were used, or the product **3** was stored in water for several days, a new product was generated which was postulated to be **6**, formed by the tautomerisation of **3**. The rearranged product was confirmed to be 2,3-dihydroxy-1-phenylpropan-1-one **6**, which was readily prepared via a crossed acyloin condensation between glycolaldehyde and benzaldehyde with catalytic 3-benzyl-5-(2-hydroxyethyl)-4-methyl thiazolium chloride.¹⁹ It was therefore decided to investigate the regioselectivity of the TAM reaction by establishing whether **6** was also a

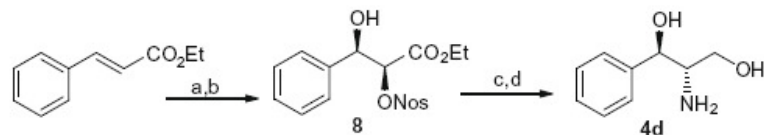
substrate which would generate an isomer of **4**, the 1-amino-2,3-diol.

For synthesis of the triacetylated 2-amino-1,3-diol **5**, the reductive amination of **3** was achieved using sodium cyanoborohydride to give compound **7** in 63% yield, which was converted to the hydrochloride salt. Hydrogenation of the hydrochloride salt gave the desired four diastereoisomers mixture of **4** as a 2:5 mixture of *syn*-**4a** and *syn*-**4b**: *anti*-**4c** and *anti*-**4d** isomers. These were directly acetylated as before to give the mixture **5a–5d**, which was used for chiral HPLC method development.

To establish the absolute stereochemistry of reaction products, synthesis of one of the *anti*-isomers was also required. Compound **4d**, the (1*R*,2*S*)-isomer was synthesised (Scheme 3) via modification of a procedure described by Nicolau et al.²⁰ Sharpless asymmetric dihydroxylation of ethyl cinnamate yielded the *syn*-diol (2*S*,3*R*)-ethyl-2,3-dihydroxy-3-phenylpropanoate. This was selectively converted to the monosylate (2*S*,3*R*)-**8** using stoichiometric quantities of nosyl chloride. Although some epimerisation and generation of the (2*R*,3*R*)-isomer of **8** was observed (70% de by NMR spectroscopy) this was not problematical as the material was required for analytical purposes. Subsequent S_N2 displacement with NaN₃ yielded the azide (in 70% de), then simultaneous reduction of both azide and ester functionalities using LiAlH₄ gave the desired *anti*-isomer **4d** in 44% yield over the four steps and in 70% de (1*R*,2*R*-diastereoisomer **4b** also present). A sample of **5d**-(1*R*,2*S*) was obtained by acetylation in 70% de.¹⁷



Scheme 2. Synthesis of the four diastereoisomers of **4**. Reagents and conditions: (a) LiHPA, 3-(4-morpholino)propanesulfonic acid (MOPS), 25%; (b) extended reaction time for (a) or slow conversion in water; (c) BnNH₂, NaBH₃CN, AcOH, MeOH, 17 h, 63%; (d) 1 M HCl, MeOH, 100%; (e) H₂, Pd/C, MeOH, 48 h, 71%; (f) Ac₂O, pyridine, 100%.



Scheme 3. Synthesis of **4d**. Reagents and conditions: (a) AD- β , MeSO₂NH₂, tBuOH/H₂O (1:1), rt, 18 h, 72%; (b) NosCl, Et₃N, CH₂Cl₂, 0 °C, 5 h, 82%; (c) NaN₃, DMF, 55 °C, 17 h, 75%; (d) LiAlH₄, THF, reflux, 5 h, 100%.

Using the standards synthesised, both standard reverse-phase (RP)-HPLC and chiral HPLC assays were established using **4** (*syn*- and *anti*-isomers) and **5a–5d**. Transamination reactions were performed, using *C. violaceum* TAM and cofactor pyridoxal 5'-phosphate (PLP), with ketodiols **3** and **6**, and (*S*)-(α)-methylbenzylamine as the amine donor. Interestingly, no conversion of **6** to 1-amino-2,3-dihydroxy-1-phenylpropane was observed, highlighting the regioselectivity of the transaminase for 1,3-dihydroxy-1-phenylpropan-2-one **3** rather than for 2,3-dihydroxy-1-phenylpropan-1-one **6**. This was also interesting because acetophenone is aminated, and suggested that the 2,3-hydroxy group is unable to fit into one of the binding pockets.

Compound **3** was readily biotransformed and the reactions were monitored by RP-HPLC and LC-MS. After 24 h, the reaction was complete and two products were evident by RP-HPLC in a 1:1 ratio. A series of RP-HPLC experiments with the synthesised analytical standard **4d** and commercially available **4a** and **4b** confirmed that the two products were *syn*- and *anti*-**4**. The transaminase reaction mixture was purified by HPLC to give a sample of *syn*- and *anti*-**4**. Triacetylation as previously described gave **5**, and analysis by chiral HPLC and comparison to **5a**, **5b** and **5d** showed the TAM products to be exclusively (1*S*,2*S*)-**5a** and (1*R*,2*S*)-**5d**, establishing the TAM products as **4a** and **4d** (Scheme 4). No **5b** or **5c** was detectable by chiral HPLC. This indicated that the transaminase could accept either the (*R*)- or (*S*)-1,3-dihydroxy ketone but formed the (2*S*)-amine (in >99% ee by HPLC) in **4**. This is consistent with previous work describing the stereoselectivity of a pyruvate TAM, for which a two-binding site model was proposed, where (*S*)- α -methylbenzylamine was the amine donor.²¹

3. Conclusion

Using chemically derived standards we have shown that a recently reported ω -transaminase, isolated from *C. violaceum*, exhibits very high (>99% ee) (*S*)-stereoselectivity in transforming 1,3-dihydroxy-1-phenylpropan-2-one **3** to 2-amino-1-phenyl-1,3-propanediol **4**. The enzyme was not enantioselective for either (*R*)- or (*S*)-**3**, but both enantiomers were readily bioconverted to give a mixture of **4a** and **4d**. The TAM was also regioselective for **3** rather than for **6**. These results are important for applications of the ω -TAM with other α,α' -dihydroxyketones.

The versatility of *C. violaceum* to accept either 1,3-dihydroxyketone enantiomer will also enhance its potential use in applications

with enantiomeric precursors such as for two-enzyme step TK-TAM applications.¹⁵ Indeed we have recently reported TK single-point active site mutants that have improved substrate specificities towards propanal, and generate (3*R*)- and (3*S*)-1,3-dihydroxypentan-2-one in high ees.^{22,23} Such substrates could be used with TAM to give *syn*- and *anti*-aminodiols in high optical purities. Further studies are now underway using TAM with alternative substrates.

4. Experimental

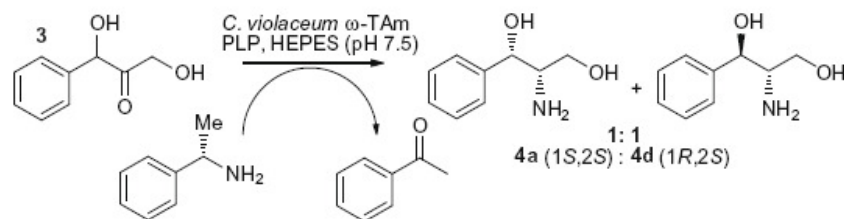
4.1. General information

Unless otherwise noted, solvents and reagents were of reagent grade from commercial suppliers (Sigma–Aldrich) and were used without further purification. Benzaldehyde was distilled prior to use. Dry THF was obtained using anhydrous alumina columns.²⁴ All moisture-sensitive reactions were performed under a nitrogen or argon atmosphere using oven-dried glassware. Reactions were monitored by TLC on Kieselgel 60 F₂₅₄ plates with detection by UV, potassium permanganate and phosphomolybdic acid stains. Flash column chromatography was carried out using silica gel (particle size 40–63 μ m). ¹H NMR and ¹³C NMR spectra were recorded at the field indicated using a Bruker AMX300 MHz and AMX500 MHz machine. Coupling constants are measured in hertz (Hz) and unless otherwise specified, NMR spectra were recorded at 298 K. Mass spectra were recorded on a Thermo Finnegan MAT 900XP spectrometer. Infrared spectra were recorded on a Shimadzu FTIR-8700 infrared spectrophotometer. Optical rotations were recorded on an Optical Activity Limited PolAAR2000 polarimeter at 589 nm, and were quoted in deg cm² g⁻¹ and conc (*c*) was quoted in g/100 mL.

Lithium hydroxypyruvate was synthesised as previously described.²⁵ The ω -transaminase from *C. violaceum* was cloned, over-expressed in *E. coli* and obtained as a clarified lysate as reported elsewhere.¹⁶ Compounds **4a** and **4b** were commercially available. The acetylation of compound **4** was carried out as previously described.¹⁷ Compounds **3**,¹⁸ **6**¹⁹ and (2*S*,3*R*)-ethyl-2,3-dihydroxy-3-phenylpropanoate²⁶ were prepared as previously reported.

4.2. (1*S*,2*S*)- and (1*R*,2*R*)-2-Acetamido-1-phenylpropane-1,3-diyl diacetates **5a** and **5b**

Compounds **4a** and **4b** were acetylated as previously described¹⁷ to give **5a** and **5b** in quantitative yield for HPLC analysis.



Scheme 4. Formation of **4a** and **4d** from **3** using *C. violaceum* TAM, PLP and (*S*)- α -methylbenzylamine as the amine donor.

Compound **5a** $[\alpha]_D^{20} = +47.1$ (c 2.0, CHCl₃); **5b** $[\alpha]_D^{20} = -61.1$ (c 2.0, CHCl₃); ¹H NMR (300 MHz; CDCl₃) δ 1.92 (3H, s, NHAc), 2.01 (3H, s, CH₂OAc), 2.06 (3H, s, CHOAc), 3.82 (1H, dd, J 11.5 and 5.0, CHHOAc), 4.03 (1H, dd, J 11.5 and 4.8, CHHOAc), 4.62 (1H, m, CHNHAc), 5.90 (1H, d, J 7.1, CHOAc), 6.03 (1H, d, J 9.2, NH), 7.30 (5H, m, Ph); ¹³C NMR (75 MHz; CDCl₃) δ 20.6, 20.9 and 23.0 (OAc and NHAc), 52.0 (CHNHAc), 63.1 (CH₂OAc), 74.1 (CHOAc), 126.7, 128.6, 136.5, 149.4, 169.9 (C=O), 170.2 (C=O), 170.6 (C=O); *m/z* (+HRFAB) [MNa] calcd for C₁₅H₁₉NNaO₅, 316.11609; found 316.11550.

4.2.1. 2-Benzylamino-1-phenyl-1,3-propanediol 7

Compound **3**¹⁸ (85 mg, 0.512 mmol) and benzylamine (112 μL, 1.024 mmol) were dissolved in MeOH (5 mL). NaCNBH₃ (96 mg, 1.536 mmol) was added, the pH was adjusted to 6 with acetic acid and the reaction mixture was stirred at rt for 17 h. The reaction mixture was concentrated to dryness in vacuo and the residue was partitioned between CH₂Cl₂ (50 mL) and NaHCO₃ (satd) (50 mL). The product was extracted with further CH₂Cl₂ (2 × 50 mL), dried (MgSO₄) and concentrated, and was then purified using flash silica chromatography (EtOAc) to yield **7** (83 mg, 63%) as a colourless oil. The product was obtained as a 2.6:1 mixture of *anti:syn*²⁷ isomers. ¹H NMR (300 MHz; CDCl₃) δ 2.65 (3H, br s, NH and OH), 2.80 (0.28H, dt, J 7.1 and 3.7, CHCH₂OH), 2.86 (0.72H, m), 3.38 (0.28H, dd, J 11.2 and 3.7, CHHOH), 3.50 (0.72H, dd, 11.2 and 4.1, CHHOH), 3.60 (0.72H, dd, 11.2 and 5.3, CHHOH), 3.67 (0.28H, m, CHHOH), 3.83 (2H, s, CH₂Ph), 4.66 (0.28H, d, J 7.1, CHOHPh), 4.88 (0.72H, d, J 5.0, CHOHPh), 7.31 (10H, m, 2 × Ph); ¹³C NMR (75 MHz; CDCl₃) δ 51.3 and 51.5 (CH₂Ph), 60.0 and 60.3 (CH₂OH), 62.7 and 64.0 (CHCH₂OH), 73.4 and 73.6 (CHOHPh), 125.9, 126.6, 127.3, 127.7, 127.8, 128.1, 128.5, 128.6, 139.6, 139.7, 141.3, 141.9; *m/z* (+HRFAB) [MH] calcd for C₁₆H₁₉NO₂, 258.149400; found 258.149645.

4.3. Diastereoisomeric mixture of 5a–d

Diol **7** (83 mg, 0.323 mmol) was dissolved in MeOH (5 mL) and the pH was adjusted to 1 by the addition of 1 M HCl. The mixture was concentrated to dryness in vacuo to yield a foam which was redissolved in fresh MeOH (5 mL). Pd/C (50 mg, 10% wt) was added and the mixture was subjected to hydrogenation for 2 days. The catalyst was removed by filtration through Celite and the organics were concentrated to yield crude 2-amino-1-phenyl-1,3-propanediol hydrochloride salt which was used without further purification. The crude salt was dissolved in pyridine (3 mL) and Ac₂O (1 mL) and then DMAP (cat.) was added. The reaction mixture was stirred at rt for 17 h, and was then concentrated to dryness in vacuo. The residue was partitioned between EtOAc (20 mL) and 0.3 M KHSO₄ (20 mL), washed with NaHCO₃ (satd; 20 mL) and dried (MgSO₄). Concentration in vacuo gave a residue which was purified using flash silica chromatography (EtOAc/hexane, 1:1) to yield **5a–d** as a colourless oil (67 mg, 71% over 3 steps). The product was obtained as a 2.6:1 mixture of *anti:syn* isomers and the spectral data were in agreement with those reported for **5** above and in the literature.^{17b}

4.4. (2S,3R) Ethyl 3-hydroxy-2-(4-nitrophenylsulfonyloxy)-3-phenylpropanoate 8

To a solution of (2S,3R) ethyl-2,3-dihydroxy-3-phenylpropanoate (4.23 g, 20.1 mmol) in CH₂Cl₂ (100 mL) at 0 °C were added triethylamine (5.60 mL, 40.2 mmol) and then 4-nitrobenzenesulfonyl chloride (4.45 g, 20.1 mmol). The reaction mixture was stirred for 5 h and was then quenched with the addition of saturated NH₄Cl (18 mL). The organic layer was washed with 1 M HCl (35 mL), water (35 mL) and saturated NaCl solution (35 mL) and was dried (MgSO₄). Concentration in vacuo yielded a residue which was puri-

fied using flash silica chromatography (EtOAc/petroleum ether 60–80, 1:4 to 1:1 gradient) to give the desired compound (6.53 g, 82%). $[\alpha]_D^{24} = -42.5$ (c 3.9, CHCl₃); ¹H NMR (300 MHz; CDCl₃) δ 1.19 (3H, t, J 7.2, CH₃), 2.58 (1H, d, J 5.8, OH), 4.18 (2H, q, J 7.2, CH₂), 5.02 (1H, d, J 3.9, CHONs), 5.22 (1H, dd, J 5.8 and 3.9, CHOH), 7.22 (5H, m, ArH), 7.81 (2H, d, J 9.0, ArH), 8.20 (2H, d, J 9.0, ArH); ¹³C NMR (125 MHz; CDCl₃) δ 13.9 (CH₂CH₃), 62.7 (CH₂CH₃), 73.6 (CHOH), 82.4 (CHONs), 124.2, 126.2, 128.5, 128.7, 129.1, 137.6, 141.5, 150.6, 166.5 (C=O); *m/z* (+HRCI) [MC₂H₅] calcd for C₁₉H₂₂NO₈S, 424.10661; found 424.10582.

4.5. (1R,2S)-2-Amino-1-phenyl-1,3-propanediol (1R,2S)-4d

Nosylate **8** (8.94 g, 22.6 mmol) was dissolved in DMF (90 mL) and sodium azide was (2.20 g, 33.9 mmol) added. The mixture was stirred at 55 °C for 17 h and was then cooled, diluted with water (200 mL) and extracted with EtOAc (3 × 200 mL). The combined organics were washed with water (200 mL) and then with saturated NaCl solution (200 mL) and were dried (MgSO₄). Concentration in vacuo yielded a residue which was purified using flash silica chromatography (EtOAc/petroleum ether 40–60, 5:95 to 1:4 gradient) to give the azide as a yellow oil (4.01 g, 75%) which was directly used in the next step. $[\alpha]_D^{24} = +9.4$ (c 11.1, CHCl₃); ¹H NMR (300 MHz; CDCl₃) δ 1.24 (3H, t, J 7.1, CH₃), 3.21 (1H, br s, OH), 4.08 (1H, d, J 6.9, CHCO₂Et), 4.22 (2H, q, J 7.1, CH₂CH₃), 5.00 (1H, dd, J 6.9 and 4.7, CHOH), 7.33 (5H, m, ArH); ¹³C NMR (75 MHz; CDCl₃) δ 14.0, 62.2, 66.8, 74.1, 126.7, 128.6, 128.7, 139.1, 168.9 (C=O). To lithium aluminium hydride (0.820 g, 21.7 mmol) in THF (100 mL) was added the azide (0.850 g, 3.61 mmol) in THF (50 mL) cautiously. The reaction mixture was heated under reflux for 5 h before being quenched with water and filtered. The solvent was removed in vacuo to give **4d** as a yellow oil (0.600 g, 100%). $[\alpha]_D^{24} = -14.9$ (c 2.0, MeOH); ¹H NMR (300 MHz; D₂O) δ 3.04 (1H, m, CHNH₂), 3.51 (1H, dd, J 11.2 and 6.8, CH₂OH), 3.70 (1H, dd, J 11.2 and 3.4, CH₂OH), 4.46 (1H, d, J 7.8, CHOHPh); ¹³C NMR (75 MHz; D₂O) 56.9 (CHNH₂), 63.4 (CH₂OH), 75.2 (CHPh), 126.9, 128.7, 129.1, 141.1; *m/z* (+HRES) [MNa] calcd for C₉H₁₃NO₂Na, 190.0844; found 190.0917.

4.6. (1R,2S)-2-Acetamido-1-phenylpropane-1,3-diyl diacetate 5d

Compound **4d** was acetylated as described above to give **5d** in quantitative yield. $[\alpha]_D^{20} = -19.4$ (c 1.0, CHCl₃); ¹H NMR (300 MHz; CDCl₃) δ 1.88 (3H, s, NHAc), 2.01 (3H, s, CH₂OAc), 2.10 (3H, s, CHOAc), 3.98 (1H, dd, J 11.6 and 4.1, CH₂OAc), 4.32 (1H, dd, J 11.6 and 6.4, CH₂OAc), 4.65 (1H, m, CHNHAc), 5.80 (1H, d, J 9.1, NH), 5.88 (1H, d, J 5.8, CHOAc); ¹³C NMR (75 MHz; CDCl₃) δ 20.8, 21.0, 23.2 (OAc and NHAc), 51.6 (CHNHAc), 62.4 (CH₂OAc), 74.6 (CHOAc), 126.6, 128.6, 136.5, 141.8, 169.7, 169.8, 171.0 (C=O); Found (+HRFAB) MNa⁺, 316.11654. C₁₅H₁₉NNaO₅ requires 316.11609.

4.7. RP HPLC assay for TAm-mediated synthesis of 4

The transaminase reaction was analysed using an ACE 5 C18 reverse phase column (150 mm × 4.6 mm, 5 μm particle size; Advanced Chromatography techniques, Aberdeen). A gradient was used from 5% CH₃CN/95% 0.1% (v/v) TFA in water to 20% CH₃CN/80% 0.1% (v/v) TFA in water, over 8 min followed by a re-equilibration step for 2 min (oven temperature 30 °C, flow rate 1 mL/min). UV detection was carried out at 210 and 250 nm. The retention times were: **4a/4b** 5.73 min; **4c/4d** 5.25 min. All samples were quenched with 0.2% TFA and were briefly centrifuged prior to HPLC analysis.

4.8. Chiral HPLC assay for 5

HPLC analysis was performed on a Varian Prostar instrument equipped with a Chiracel AD chiral column (Daicel, 25 cm × 0.46 cm). HPLC conditions: injection volume, 10 µL; mobile phase, ¹PrOH–hexanes, 3:97; flow rate, 0.6 mL/min; detection, 210 nm. Retention times of **5**: (1*R*,2*R*)-**5b**, 74.4 min; (1*S*,2*S*)-**5a**, 77.1 min; (1*R*,2*S*)-**5d**, 99.8 min; (1*S*,2*R*)-**5c**, 105.4 min.

4.9. Transaminase-mediated synthesis of 4

1,3-Dihydroxy-1-phenylpropan-2-one¹⁸ (33 mg, 0.20 mmol) and (*S*)- α -methylbenzylamine (24 mg, 0.20 mM) were dissolved in HEPES buffer containing pyridoxal-5'-phosphate (7.5 mL, HEPES 100 mM, PLP 0.2 mM, pH 7.5). To this was added *C. violaceum* TAM clarified lysate (2.5 mL, TAM 8.5 mg/mL, HEPES 50 mM, PLP 0.2 mM, pH 7.5) and the reaction mixture was incubated for 24 h at 37 °C without agitation. A portion of the product mixture was purified by C18 RP-HPLC to yield the desired product as a white solid (1 mg) (*m/z* (+HCl) [MH] calcd for C₉H₁₄NO₂, 168.10245; found 168.10212). The product **4** was redissolved in pyridine (600 µL) and Ac₂O (200 µL) and then DMAP (cat.) was added. After 17 h, the solvent was removed in vacuo and the sample of **5** was analysed by chiral HPLC without further purification. The product was shown to be exclusively a 1:1 mixture of (1*S*,2*S*)-**5a** and (1*R*,2*S*)-**5d**.

Acknowledgements

The authors would like to thank the UK Engineering and Physical Sciences Research Council (EPSRC) for support (K.S., M.E.B.S., U.K.) of the multidisciplinary Bioconversion Integrated with Chemistry and Engineering (BiCE) programme. Financial support from the 13 industrial partners is also acknowledged. The EPSRC is also thanked for a DTA studentship to J.L.G.

References

- Hughes, A. B.; Rudge, A. J. *Nat. Prod. Rep.* **1994**, *11*, 135–162.
- Liang, P. H.; Cheng, W. C.; Lee, Y. L.; Yu, H. P.; Wu, Y. T.; Lin, Y. L.; Wong, C. H. *ChemBioChem* **2006**, *7*, 165–173.
- Hannun, Y. A.; Obeid, L. M. *J. Biol. Chem.* **2002**, *277*, 25847–25850.
- Nakamura, T.; Shiozaki, M. *Tetrahedron* **2001**, *57*, 9087–9092.
- Cutler, R. A.; Stenger, R. J.; Suter, C. M. *J. Am. Chem. Soc.* **1952**, *74*, 5475–5481.
- Hajra, S.; Karmakar, A.; Maji, T.; Medda, A. K. *Tetrahedron* **2006**, *62*, 8959–8965.
- Constable, D. J. C.; Dunn, P. J.; Hayler, J. D.; Humphrey, G. R.; Leazer, J. L.; Linderman, R. J.; Lorenz, K.; Manley, J.; Pearlman, B. A.; Wells, A.; Zaks, A.; Zhang, T. Y. *Green Chem.* **2007**, *9*, 411–420.
- Bornscheur, U. T.; Kazlauskas, R. J. *Hydrolases in Organic Synthesis*, 2nd ed.; Wiley-VCH: Weinheim, 2006.
- Turner, N. J. *Curr. Opin. Biotechnol.* **2003**, *14*, 401–406.
- Shin, J. S.; Kim, B. G. *Biosci. Biotechnol. Biochem.* **2001**, *65*, 1782–1788.
- Shin, J. S.; Kim, B. G. *Biotechnol. Bioeng.* **1999**, *65*, 206–211.
- Koszelewski, D.; Lavandera, I.; Clay, D.; Rozzell, D.; Kroutil, W. *Adv. Synth. Catal.* **2008**, *350*, 2761–2766.
- Hohne, M.; Kuhl, S.; Robins, K.; Bornscheur, U. T. *ChemBioChem* **2008**, *9*, 363–365.
- Koszelewski, D.; Lavandera, I.; Clay, D.; Guebitz, G. M.; Rozzell, D.; Kroutil, W. *Angew. Chem., Int. Ed.* **2008**, *120*, 9477–9480.
- Ingram, C. U.; Bommer, M.; Smith, M. E. B.; Dalby, P. A.; Ward, J. M.; Hailes, H. C.; Lye, G. *J. Biotechnol. Bioeng.* **2007**, *96*, 559–569.
- Kaulmann, U.; Smithies, K.; Smith, M. E. B.; Hailes, H. C.; Ward, J. M. *Enzyme Microb. Technol.* **2007**, *41*, 628–637.
- (a) Boruwa, J.; Borah, J. C.; Gogoi, S.; Barua, N. C. *Tetrahedron Lett.* **2005**, *46*, 1743–1746; (b) Effenberger, F.; Gutterer, B.; Syed, J. *Tetrahedron: Asymmetry* **1995**, *6*, 2933–2943.
- Smith, M. E. B.; Smithies, K.; Senussi, T.; Dalby, P. A.; Hailes, H. C. *Eur. J. Org. Chem.* **2006**, *5*, 1121–1123.
- Heck, R.; Henderson, A. P.; Kohler, B.; Retej, J.; Golding, B. T. *Eur. J. Org. Chem.* **2001**, *14*, 2623–2627.
- Nicolaou, K. C.; Boddy, C. N. C.; Li, H.; Koumbis, A. E.; Hughes, R.; Natarajan, S.; Jain, N. F.; Ramanjulu, J. M.; Brase, S.; Solomon, M. E. *Chem. Eur. J.* **1999**, *5*, 2602–2621.
- Shin, J. S.; Kim, B. G. *J. Org. Chem.* **2002**, *67*, 2848–2853.
- Pangborn, A. B.; Giargello, M. A.; Grubbs, R. H.; Rosen, R. K.; Timmers, F. J. *Organometallics* **1996**, *15*, 1518–1520.
- Hibbert, E. G.; Senussi, T.; Smith, M. E. B.; Costelloe, S. J.; Ward, J. M.; Hailes, H. C.; Dalby, P. A. *J. Biotechnol.* **2008**, *134*, 240–245.
- Smith, M. E. B.; Hibbert, E. G.; Jones, A. B.; Dalby, P. A.; Hailes, H. C. *Adv. Synth. Catal.* **2008**, *350*, 2631–2638.
- Dickens, F. *Biochem. Prep.* **1962**, *9*, 86–91.
- (a) Sharpless, K. B.; Amberg, W.; Bennani, Y. L.; Crispino, G. A.; Hartung, J.; Jeong, K. S.; Kwong, H. L.; Morikawa, K.; Wang, Z. M.; Xu, D.; Zhang, X. L. *J. Org. Chem.* **1992**, *57*, 2768–2771; (b) Kuang, Y. Q.; Zhang, S. H.; Wei, L. L. *Synth. Commun.* **2003**, *33*, 3545–3550.
- Rozwadowska, M. D. *Tetrahedron* **1997**, *53*, 10615–10622.



Application of a modified Mosher's method for the determination of enantiomeric ratio and absolute configuration at C-3 of chiral 1,3-dihydroxy ketones

James L. Galman, Helen C. Hailes*

Department of Chemistry, University College London, 20 Gordon Street, London WC1H 0AJ, UK

ARTICLE INFO

Article history:
Received 17 June 2009
Accepted 16 July 2009
Available online 21 August 2009

ABSTRACT

The enantiomeric ratio and absolute configuration of products of the transketolase reaction are typically determined by comparison of the specific rotation or derivatisation and HPLC or GC. A Mosher's ester method has been developed via ester formation at the primary alcohol C-1 which can be used to determine the stereoselectivity of the reaction, as well as the absolute configuration of the product at C-3.

© 2009 Elsevier Ltd. All rights reserved.

1. Introduction

Several methods are available for determining the absolute stereochemistries of compounds including comparison of specific rotation data to reported values, chiral HPLC and GC with correlation to known or synthesised compounds,¹ X-ray crystallography, and NMR spectroscopy via the use of lanthanide shift reagents² or chiral derivatising agents.^{3,4} The latter approach, in particular the application of the Mosher's method using 2-methoxy-2-(trifluoromethyl) phenylacetic acid (MTPA) has been extensively used:^{4–6} it should be noted that it has been reliably utilised for determining the absolute configuration of secondary alcohols and primary amines.^{5,6} For example, chiral secondary alcohols have typically been coupled in two separate, analogous experiments using each enantiomer of the Mosher's acid. The chemical shift differences of the ester protons at R¹ and R² (Fig. 1) were then calculated ($\Delta\delta = \delta_{S\text{-MTPA}} - \delta_{R\text{-MTPA}}$) and assigned. Protons at R¹ in the (R)-MTPA diastereoisomer were observed upfield relative to the (S)-MTPA ester due to the diamagnetic effect of the aromatic ring.⁴

α,α' -Dihydroxy ketone functionalities are found in several biologically important compounds, and can be used as synthons in further structural elaboration to a range of compounds including ketosugars and aminodiols.^{7–10} The enzyme transketolase (TK) (EC 2.2.1.1) has been shown to catalyse in vitro the condensation of hydroxypyruvate (Li-HPA, **1**) with a range of aldehydes to stereoselectively generate α,α' -dihydroxy ketones **2** (Scheme 1); a biomimetic route to these compounds has also been reported.^{8–13} In addition, asymmetric routes to such chiral dihydroxyacetones have been established using Ender's chiral auxiliary methodology.¹⁴

Several assays have been described which detect α,α' -dihydroxy ketones in biocatalytic conversions including spectrophotometric and colorimetric methods.^{11,15} However, chiral assays that both establish the enantiomeric purity and determine the absolute stereochemistry of these structural motifs are most important. For TK-generated products this has predominantly been carried out by comparison of the specific rotation, and enantiomeric purities have frequently not been determined. Recently, an acetate derivatisation and chiral HPLC and GC method has been reported, together with Ender's SAMP methodology to confirm absolute stereochemistries.¹² The use of chiral auxiliaries and a six-step procedure to determine absolute stereochemistries however is time consuming, and although suitable for a range of compounds, the reaction fails to accommodate derivatives when R is Ar. A more convenient and

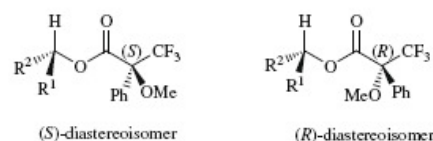
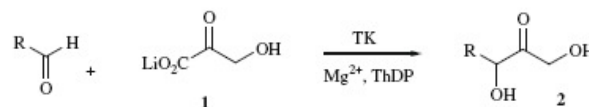


Figure 1. Two Mosher conformers showing the (S)-MTPA and (R)-MTPA derivatives.



Scheme 1. TK-catalysed reaction with cofactors Mg²⁺ and thiamine diphosphate (ThDP) to generate α,α' -dihydroxy ketones.

* Corresponding author. Tel.: +44 (0) 20 7679 4654; fax: +44 (0) 20 7679 7463.
E-mail address: h.c.hailes@ucl.ac.uk (H.C. Hailes).

rapid approach would be the application of the modified Mosher's method for determining both the enantiomeric purity and absolute stereochemistry at the C-3 carbinol stereocentre. To date, a modified Mosher's method has been applied to 1,3-diol motifs via derivatisation as di-MTPA esters which was successfully used with acyclic *syn*-diols and cyclic diols, however irregularities in the $\Delta\delta$ of acyclic *anti*-1,3-diols made this method not applicable in all cases.¹⁶ Interestingly, the modified Mosher's method has been used to determine the absolute configuration of primary alcohols with chiral methyl groups at C-2: chemical shifts of the oxymethylene protons in each MTPA ester (attached at C-1) were noted, and a larger chemical shift difference was observed in the (2*S*,2'*S*)- and (2*R*,2'*R*)-isomers compared to the (2*S*,2'*R*)- and (2*R*,2'*S*)-isomers.¹⁷ This was attributed to restricted rotation along the C2–C3 bond. Due to the presence of the ketone at C-2 in **2**, and the conformational restriction this may confer, application of the modified Mosher's method, via coupling at C-1, to α,α' -dihydroxy ketones was investigated to establish whether it could be used to determine the absolute configuration and ee at C-3.

2. Results and discussion

The absolute stereochemistry and enantiomeric purity of (3*S*)-1,3-dihydropentan-2-one **2a** have been established previously,¹² and so were used in the initial studies for the attachment of MTPA at the primary hydroxyl position. The diastereotopic protons H_a and H_b in **2a** are normally observed at 4.59 and 4.70 ppm, and may be shifted in each MTPA ester as described previously for C-2 methyl primary alcohol systems.¹⁷ Compound **2a** was prepared using wild-type (WT)-TK.¹² Coupling of **2a** to either (*R*)- or (*S*)-MTPA was performed under standard conditions (Scheme 2), and after purification to remove the remaining starting materials, urea side products and di-MTPA esters which were formed in low yields, the MTPA esters **4a** and **5a** were analysed by ¹H NMR spectroscopy in CDCl₃. The ¹H NMR signals for diastereotopic protons H_a and H_b in the (*R*)-MTPA ester **4a** for the major isomer (2*R*,3'*S*) were at δ_H 5.05 ppm ($\Delta\delta_H^{2*R*,3'*S*} = 0$) and for the minor isomer were at δ_H 4.93 and 5.17 ppm ($\Delta\delta_H^{2*R*,3'*R*} = 0.24$) (Fig. 2, spectrum A). For the (*S*)-MTPA ester **5a** the major isomer (2*S*,3'*S*) signals for H_a and H_b were at δ_H 4.93 ppm and 5.17 ppm ($\Delta\delta_H^{2*S*,3'*S*} = 0.24$) and the minor isomer (2*S*,3'*R*) signals were at δ_H 5.05 ppm ($\Delta\delta_H^{2*S*,3'*R*} = 0$) (Fig. 2, spectrum B). Averaging of the two ee values calculated from the integration of H_a, H_b signals in spectra A and B gave an ee of 55% which was comparable to that of 58% determined by GC methods.¹²

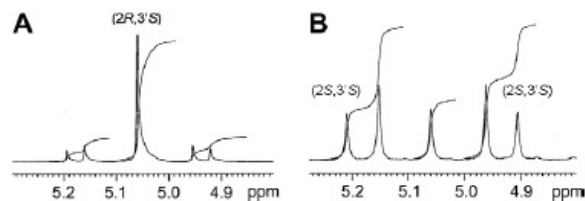
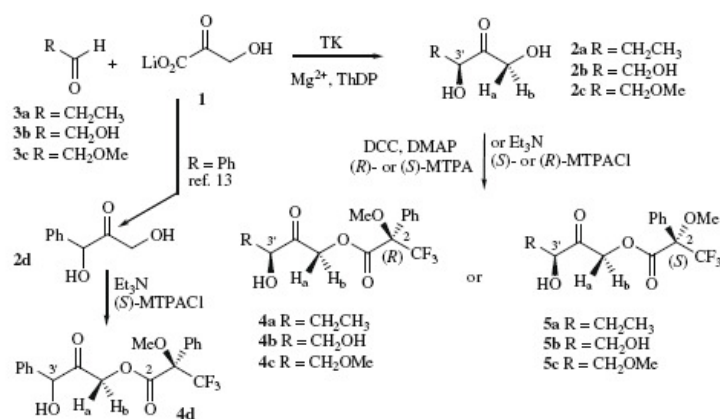


Figure 2. ¹H NMR signals for diastereotopic protons H_a and H_b in the (*R*)-MTPA ester **4a** (spectrum A) and (*S*)-MTPA ester **5a** (spectrum B).

As with the work of Kobayashi et al. on chiral primary alcohols with methyl groups at C-2, the oxymethylene proton separation varied and $\Delta\delta_H^{2*R*,3'*R*}$ and $\Delta\delta_H^{2*S*,3'*S*}$ > $\Delta\delta_H^{2*R*,3'*S*}$ and $\Delta\delta_H^{2*S*,3'*R*}$. The ee could be determined to within 5% of the value from GC analysis. α,α' -Dihydroxyketones with reported absolute configurations were then used to investigate the validity of the method.

First, commercially available *L*-erythrose **2b**, prepared from **1** and glycolaldehyde **3b** using TK, was converted into the corresponding (*R*)- and (*S*)-MTPA esters using MTPA chloride. The ¹H NMR analysis revealed that H_a and H_b in the (*R*)-MTPA ester **4b** (major isomer (2*R*,3'*S*)) were at δ_H 5.11 and 5.19 ppm ($\Delta\delta_H^{2*R*,3'*S*}$ is 0.08) and negligible signals for the minor isomer were observed. For the (*S*)-MTPA ester **5b**, the major isomer (2*S*,3'*S*) signals for H_a and H_b were observed at δ_H 5.05 and 5.23 ppm ($\Delta\delta_H^{2*S*,3'*S*}$ is 0.18) while no minor isomer was detected. Integration of the signals for H_a and H_b as before indicated *L*-erythrose to be of >95% ee. Again for the oxymethylene protons $\Delta\delta_H^{2*S*,3'*S*}$ > $\Delta\delta_H^{2*R*,3'*S*}$ enabling, by formation of both MTPA esters, confirmation of absolute stereochemistry as well as the enantiomeric purity.

2-Methoxy ethanal **3c** has been described as an aldehyde acceptor in the TK reaction with spinach TK, where an ee of 60% was observed (*S*-major isomer).¹⁸ This transformation was performed using WT *Escherichia coli* TK to validate Mosher's method for stereochemical determination. Compound **2c** was formed in 30% yield and coupling to the MTPA chlorides gave **4c** and **5c** with H_a and H_b for the major isomers at 5.13 and 5.17 ppm (2*R*,3'*S*) and 5.02 and 5.29 ppm (2*S*,3'*S*), respectively. Again $\Delta\delta_H^{2*S*,3'*S*}$ (0.27) > $\Delta\delta_H^{2*R*,3'*S*}$ (0.04) (Table 1), confirming the application of the method, and integration of H_a and H_b for both esters **4c** and **5c** as before gave an average value for the ee of 57%, which was comparable to that reported for spinach-TK.¹⁸ The synthesis of the 1,3-dihydroxy-1-phenylpropan-2-one **2d** has been described previously and the MTPA method was also explored with this aromatic analogue to



Scheme 2. TK-catalysed reactions using **3** to generate ketones **2** and the formation of MTPA esters **4** and **5**.

Table 1
Chemical shifts for MTPA esters and absolute stereochemistries

R	MTPA ester	$\Delta\delta_{\text{H}}$ H _a H _b (major isomer)	ee ^a of 2	Lit. ee
CH ₂ CH ₃	4a (R)	0 (2 <i>R</i> ,3' <i>S</i>)	55% 2a	58% (S) ¹²
CH ₂ CH ₃	5a (S)	0.24 (2 <i>S</i> ,3' <i>S</i>)		
CH ₂ OH	4b (R)	0.08 (2 <i>R</i> ,3' <i>S</i>)	>95% 2b	>98% (S) ¹²
CH ₂ OH	5b (S)	0.18 (2 <i>S</i> ,3' <i>S</i>)		
CH ₂ OMe	4c (R)	0.04 (2 <i>R</i> ,3' <i>S</i>)	57% 2c	60% (S) ¹⁸
CH ₂ OMe	5c (S)	0.27 (2 <i>S</i> ,3' <i>S</i>)		

^a Determined from the integration of ¹H NMR signals for H_a and H_b from both the (R)- and (S)-MTPA esters.

establish whether the separation of H_a and H_b was similar to that for the aliphatic series.^{13,19} Compound **2d** was prepared using the biomimetic TK reaction described previously¹³ and was converted to the mono-MTPA diastereoisomeric esters **4d** using (S)-MTPA chloride. Protons H_a and H_b were observed as before and by analogy to the assignment for the aliphatic series, $\Delta\delta_{\text{H}}^{2*R*,3'*R*}$ was 0.31 while $\Delta\delta_{\text{H}}^{2*S*,3'*R*}$ was 0.05, highlighting the potential application of this approach with aromatic analogues.

3. Conclusion

The stereoselectivity of *E. coli* WT-TK using 2-methoxy ethanal as a substrate was comparable to that observed with spinach TK, and was consistent with previous reports indicating a preference for formation of the (S)-isomer in the biotransformation. In addition, by using (R)- and (S)-MTPA we have demonstrated that the ees of α,α' -dihydroxyketones can routinely be determined, to within 5% of values determined using GC or HPLC method, as well as the absolute stereochemistries. The method can be used with a range of aliphatic α,α' -dihydroxyketones **2** with lipophilic and polar R groups. Determination of the absolute stereochemistries is more convenient than the multistep chiral auxiliary procedures described previously, and is also applicable to a wider range of compounds including aromatic systems (R is Ar). This is important for future work using chemical or biocatalytic routes to α,α' -dihydroxyketones.

4. Experimental

4.1. General information

Unless otherwise noted, solvents and reagents were of reagent grade from commercial suppliers (Sigma–Aldrich) and were used without further purification. Dry CH₂Cl₂ was obtained using anhydrous alumina columns.²⁰ All moisture-sensitive reactions were performed under a nitrogen or argon atmosphere using oven-dried glassware. Reactions were monitored by TLC on Kieselgel 60 F₂₅₄ plates with detection by UV, potassium permanganate and phosphomolybdic acid stains. Flash column chromatography was carried out using silica gel (particle size 40–63 μm). ¹H NMR and ¹³C NMR spectra were recorded at the field indicated using Bruker AMX300 MHz and Avance 500 and 600 MHz machines. Coupling constants are measured in hertz (Hz) and unless otherwise specified, NMR spectra were recorded at 298 K. Mass spectra were recorded on a LTQ Orbitrap XL. Infrared spectra were recorded on a Shimadzu FTIR-8700 infrared spectrophotometer. Optical rotations were recorded on an Optical Activity Limited PoLAAR2000 polarimeter at 589 nm, quoted in deg cm² g⁻¹ and concn (c) in g/100 mL.

Lithium hydroxypyruvate was synthesised as described previously.²¹ (3*S*)-1,3-Dihydroxypentan-2-one **2a** (58% ee) was prepared as described previously using WT *E. coli* TK,¹² and L-erythrose **2b** was commercially available.

4.2. (2*R*,3'*S*)-3,3,3-Trifluoro-2-methoxy-2-phenyl propionic acid 3'-hydroxy-2'-oxo-pentyl ester **4a**

The reaction was carried out under anhydrous conditions. To a stirred solution of **2a** (0.030 g, 0.25 mmol) in CH₂Cl₂ (5 mL) were added DCC (0.057 g, 0.28 mmol) and DMAP (0.012 g, 0.02 mmol) in CH₂Cl₂ (10 mL) at 0 °C and the reaction mixture was stirred for 2 min. (S)-MTPA (0.030 g, 0.08 mmol) was added and the reaction mixture was stirred for 30 min, after which further (S)-MTPA (0.020 g, 0.08 mmol) was added and the mixture was stirred for 48 h at rt. The solvent was removed in vacuo, and the crude product was dry loaded onto silica gel and purified using flash chromatography (EtOAc/hexane, 3:2) to afford **5a** as a colourless oil (0.035 g, 59%), (2*R*,3'*S*)-55% ee (from the integrations of H_a and H_b ¹H NMR signals from **4a** and **5a**). *R*_f = 0.45 (EtOAc/hexane, 3:2); $[\alpha]_{\text{D}}^{20} = +13.3$ (c 0.15, CHCl₃); ν_{max} (KBr)/cm⁻¹ 3429br s, 2925s, 1712s; ¹H NMR (500 MHz; CDCl₃) δ 1.00 (3H, m, CH₃), 1.65 (1H, m, CHHCH₃) 1.89 (1H, m, CHHCH₃), 2.86 (1H, d, *J* 6.0, OH), 3.64 (3H, s, OMe), 4.29 (1H, m, CHOH), 4.93 (0.26H, d, *J* 17.0, CHHO (2*R*,3'*R*)), 5.05 (1.48H, s, CH₂O (2*R*,3'*S*)), 5.17 (0.26H, d, *J* 17.0, CHHO (2*R*,3'*R*)), 7.54 (3H, m, Ph), 7.61 (2H, m, Ph); ¹³C NMR (125 MHz; CDCl₃) δ 8.8 (CH₃), 27.2 (CH₂CH₃), 55.8 (OCH₃), 67.2, 76.2, 123.2 (q, *J*_{CF} 283, CF₃), 127.6, 128.6, 129.9, 131.8, 166.3 (C=O ester), 204.2 (C=O, ketone); ¹⁹F NMR (282 MHz; CDCl₃) δ -72.2; *m/z* (FTMS) [M+NH₄] calcd for C₁₅H₂₁F₃O₅N, 352.1366; found 352.1371.

4.3. (2*S*,3'*S*)-3,3,3-Trifluoro-2-methoxy-2-phenyl propionic acid 3'-hydroxy-2'-oxo-pentyl ester **5a**

The same procedure was used as that described above for **4a** using (S)-MTPA to give **5a** as a colourless oil (0.030 g, 57%) (2*S*,3'*S*)-55% ee (from integrations of H_a and H_b ¹H NMR signals from **4a** and **5a**). *R*_f = 0.45 (EtOAc/hexane, 3:2); $[\alpha]_{\text{D}}^{20} = -37.0$ (c 0.1, CHCl₃); ¹H NMR (300 MHz; CDCl₃) δ 1.00 (3H, t, *J* 7.4, CH₃), 1.69 (1H, m, CHHCH₃) 1.89 (1H, m, CHHCH₃), 2.87 (1H, d, *J* 5.3, OH), 3.64 (3H, s, OMe), 4.29 (1H, m, CHOH), 4.93 (0.82H, d, *J* 17.0, CHHO (2*S*,3'*S*)), 5.05 (0.36H, s, CH₂O (2*S*,3'*R*)), 5.17 (0.82H, d, *J* 17.0, CHHO (2*S*,3'*S*)), 7.54 (3H, m, Ph), 7.61 (2H, m, Ph); ¹³C NMR (75 MHz; CDCl₃) δ 8.7 and 8.8 (CH₃), 27.2, 55.8 (OCH₃), 67.2, 76.2, 123.2 (q, *J*_{CF} 283, CF₃), 127.6, 128.5, 128.7, 129.9, 166.2 (C=O ester), 204.2 (C=O, ketone); ¹⁹F NMR (282 MHz; CDCl₃) δ -72.2.

4.4. (2*R*,3'*S*)-3,3,3-Trifluoro-2-methoxy-2-phenyl propionic acid 3',4'-dihydroxy-2'-oxo-butyl ester **4b**

The reaction was carried out under anhydrous conditions. To a stirred solution of **2b** (0.030 g, 0.25 mmol) in CH₂Cl₂ (5 mL) were added triethylamine (34 μL , 0.25 mmol) and (S)-MTPA chloride (34 μL , 0.18 mmol) in CH₂Cl₂ (2 mL) and the reaction mixture was stirred for 12 h at rt. The product was dry loaded onto silica gel and purified using flash chromatography (EtOAc) to afford **4b** as a colourless oil (0.054 g, 63%), (2*R*,3'*S*) >95% ee (from integrations of H_a and H_b ¹H NMR signals of **4b** and **5b**). *R*_f = 0.45 (EtOAc); $[\alpha]_{\text{D}}^{20} = +10.2$ (c 0.4, CHCl₃); ν_{max} (KBr)/cm⁻¹ 3429br s, 2925s, 1712s; ¹H NMR (300 MHz; CDCl₃) δ 3.64 (3H, s, OMe), 3.89 (1H, dd, *J* 10.6 and 3.8, CHHOH), 3.95 (1H, dd, *J* 10.6 and 3.8, CHHOH), 4.35 (1H, dd, *J* 3.8 and 3.8, CHOH), 5.11 (1H, d, *J* 17.0, CHHO (2*R*,3'*S*)), 5.19 (1H, d, *J* 17.0, CHHO (2*R*,3'*S*)), 7.43 (3H, m, Ph), 7.62 (2H, m, Ph), no (2*R*,3'*R* isomer detected); ¹³C NMR (75 MHz; CDCl₃) δ 55.9 (OCH₃), 63.5, 68.0, 76.4, 84.6 (q, *J*_{CF} 28, CCF₃), 123.1 (q, *J*_{CF} 288, CF₃), 127.5, 128.6, 129.9, 131.7, 166.5 (C=O ester), 203.3 (C=O, ketone); ¹⁹F NMR (282 MHz; CDCl₃) δ -72.2; *m/z* (FTMS) [M+NH₄] calcd for C₁₄H₁₉F₃O₆N, 354.1159; found 354.1162.

4.5. (2*S*,3'*S*)-3,3,3-Trifluoro-2-methoxy-2-phenyl propionic acid 3',4'-dihydroxy-2'-oxo-butyl ester **5b**

The same procedure was used as that described above for **4b** using (*R*)-MTPA chloride to give **5b** as a colourless oil (0.044 g, 51%) (2*S*,3'*S*) >95% ee (from integrations of H_a and H_b ¹H NMR signals of **4b** and **5b**). *R*_T = 0.45 (EtOAc); [α]_D²⁰ = −14.4 (c 0.5, CHCl₃); ¹H NMR (500 MHz; CDCl₃) δ 3.63 (3H, s, OMe), 3.92 (2H, m, CH₂OH), 4.35 (1H, dd, *J* 4.0 and 3.8, CHOH), 5.05 (1H, d, *J* 17.0, CHHO (2*S*,3'*S*)), 5.23 (1H, d, *J* 17.0, CHHO (2*S*,3'*S*)), 7.43 (3H, m, Ph), 7.62 (2H, m, Ph), no (2*S*,3'*R* isomer detected); ¹³C NMR (125 MHz; CDCl₃) δ 55.8 (OCH₃), 63.5, 67.9, 76.3, 84.6 (q, *J*_{CF} 28, CCF₃), 123.1 (q, *J*_{CF} 288, CF₃), 127.5, 128.5, 129.9, 131.7, 166.4 (C=O ester), 203.1 (C=O, ketone); ¹⁹F NMR (282 MHz; CDCl₃) δ −72.2.

4.6. 1, 3-Dihydroxy-4-methoxy-butan-2-one **2c**

ThDP (22 mg, 48 μmol) and MgCl₂·6H₂O (39 mg, 180 μmol) were dissolved in H₂O (10 mL) and the pH was adjusted to 7 with 0.1 M NaOH. To this stirred solution, at 25 °C, was added WT-TK clarified lysate (2 mL)^{11c,12} and the mixture was stirred for 20 min. In another flask, **1** (110 mg, 1 mmol) and **3c** (74 mg, 1 mmol) were dissolved in H₂O (8 mL) and the pH was adjusted to 7 with 0.1 M NaOH. Following the 20-min enzyme/cofactor pre-incubation, the **1/3c** mixture was added to the enzyme solution and the mixture was stirred at 25 °C for 24 h. During this time, the pH was maintained at 7.0 by addition of 1 M HCl using a pH stat (Stat Titro, Metrohm). Silica was added and the reaction mixture was concentrated to dryness before dry loading onto a flash silica gel column. Following column purification (EtOAc/CH₃OH, 80:20), **2c** was isolated as an oil (40 mg, 30%). [α]_D²⁰ = +2.0 (c 2.0, CHCl₃), lit.¹⁸ [α]_D²⁵ = +3.0 (c 0.017, MeOH); ν_{max} (KBr)/cm^{−1} 3415br s, 2923s, 1727s; ¹H NMR (300 MHz; CDCl₃) δ 3.36 (3H, s, OCH₃), 3.61 (1H, dd, *J* 9.9 and 4.4, CHHOMe), 3.70 (1H, dd, *J* 9.9 and 4.4, CHHOMe), 4.38 (1H, dd, *J* 4.4 and 4.4, CHOH), 4.43 (1H, d, *J* 19.7, CHHOH), 4.53 (1H, d, *J* 19.7, CHHOH); ¹³C NMR (75 MHz; CDCl₃) δ 59.5 (OCH₃), 66.7 (CH₂), 73.4 (CH₂), 74.8 (CHOH) 210.8 (C=O); *m/z* (FTMS) [M+NH₄]⁺ calcd for C₅H₁₄O₄N, 152.0917; found 152.0919.

4.7. (2*R*,3'*S*)-3,3,3-Trifluoro-2-methoxy-2-phenyl propionic acid 3'-hydroxy-4'-methoxy-2'-oxo-butyl ester **4c**

The reaction was carried out under anhydrous conditions. To a stirred solution of **2c** (0.010 g, 0.07 mmol) in CH₂Cl₂ (3 mL) were added triethylamine (34 μL, 0.25 mmol) and (*S*)-MTPA chloride (20 μL, 0.11 mmol) in CH₂Cl₂ (2 mL) and the reaction mixture was stirred for 12 h at rt. The product was dry loaded onto silica gel and purified using flash chromatography (EtOAc/hexane, 1:1) to afford **4c** as a colourless oil (0.015 g, 61%), (2*R*,3'*S*) 57% ee (from integrations of H_a and H_b ¹H NMR signals of **4c** and **5c**). *R*_T = 0.40 (EtOAc/hexane, 1:1); [α]_D²⁰ = +23.2 (c 0.25, CHCl₃); ν_{max} (KBr)/cm^{−1} 3415br s, 2923s, 1727s; ¹H NMR (300 MHz; CDCl₃) δ 3.38 (3H, s, OCH₃), 3.61 (3H, s, OCH₃) 3.57–3.70 (2H, m, CH₂), 4.36 (1H, m, CHOH), 5.02 (0.16H, d, *J* 17.5, CHHO (2*R*,3'*R*)), 5.13 (0.84H, d, *J* 17.5, CHHO (2*R*,3'*S*)), 5.17 (0.81H, d, *J* 17.5, CHHO (2*R*,3'*S*)), 5.29 (0.16H, d, *J* 17.5, CHHO (2*R*,3'*R*)), 7.42 (3H, m, Ph), 7.62 (2H, m, Ph); *m/z* (FTMS) [M+NH₄]⁺ calcd for C₁₅H₂₁F₃O₆N, 368.1315; found 368.1318.

4.8. (2*S*,3'*S*)-3,3,3-Trifluoro-2-methoxy-2-phenyl propionic acid 3'-hydroxy-4'-methoxy-2'-oxo-butyl ester **5c**

The same procedure was used as that described above for **4c** using (*R*)-MTPA chloride to give **5c** as a colourless oil (0.010 g, 40%) (2*S*,3'*S*) 57% ee (from integrations of H_a and H_b ¹H NMR sig-

nals of **4c** and **5c**). *R*_T = 0.45 (EtOAc/hexane, 1:1); [α]_D²⁰ = −10.6 (c 0.25, CHCl₃); ¹H NMR (500 MHz; CDCl₃) δ 3.38 (3H, s, OCH₃), 3.61 (3H, s, OCH₃) 3.57–3.70 (2H, m, CH₂), 4.36 (1H, m, CHOH), 5.02 (0.74H, d, *J* 17.5, CHHO (2*S*,3'*S*)), 5.13 (0.81H, d, *J* 17.5, CHHO (2*S*,3'*R*)), 5.17 (0.38H, d, *J* 17.5, CHHO (2*S*,3'*R*)), 5.29 (0.81H, d, *J* 17.5, CHHO (2*S*,3'*S*)), 7.42 (3H, m, Ph), 7.62 (2H, m, Ph); ¹³C NMR (150 MHz; CDCl₃) δ 55.8 (OCH₃), 59.5 (OCH₃), 68.1, 72.8, 75.0, 84.5 (q, *J*_{CF} 27, CCF₃), 123.1 (q, *J*_{CF} 285, CF₃), 127.5, 128.5, 129.8, 131.5, 166.1 (C=O ester), 202.9 (C=O, ketone); ¹⁹F NMR (282 MHz; CDCl₃) δ −72.2.

4.9. (2*R*,3'*RS*)-3,3,3-Trifluoro-2-methoxy-2-phenyl propionic acid 3'-hydroxy-2'-oxo-3'-phenylpropyl ester **4d**

The same procedure was used as that described above for **4c** using (*S*)-MTPA chloride and **2d**.¹³ The product was purified using flash silica chromatography (EtOAc/hexane, 1:4) to give **4d** as a colourless oil (0.014 g, 61%). ¹H NMR (500 MHz; CDCl₃) δ 3.62 (3H, s, OCH₃), 4.71 (0.25H, d, *J* 16.9, CHHO (2*R*,3'*R*)), 4.86 (0.25H, d, *J* 16.9, CHHO (2*R*,3'*S*)), 4.91 (0.25H, d, *J* 16.9, CHHO (2*R*,3'*S*)), 5.02 (0.25H, d, *J* 16.9, CHHO (2*R*,3'*R*)), 5.25 (1H, m, CHOH), 7.34–7.54 (6H, m, Ph), 7.70 (2H, m, Ph), 8.01 (2H, *J* 8.6, Ph).

Acknowledgements

We thank the EPSRC for a DTA studentship to J.L.G. and Abil Aliev for helpful discussions. We thank the EPSRC National Mass Spectrometry Service Centre, Swansea University, for the provision of high resolution MS data.

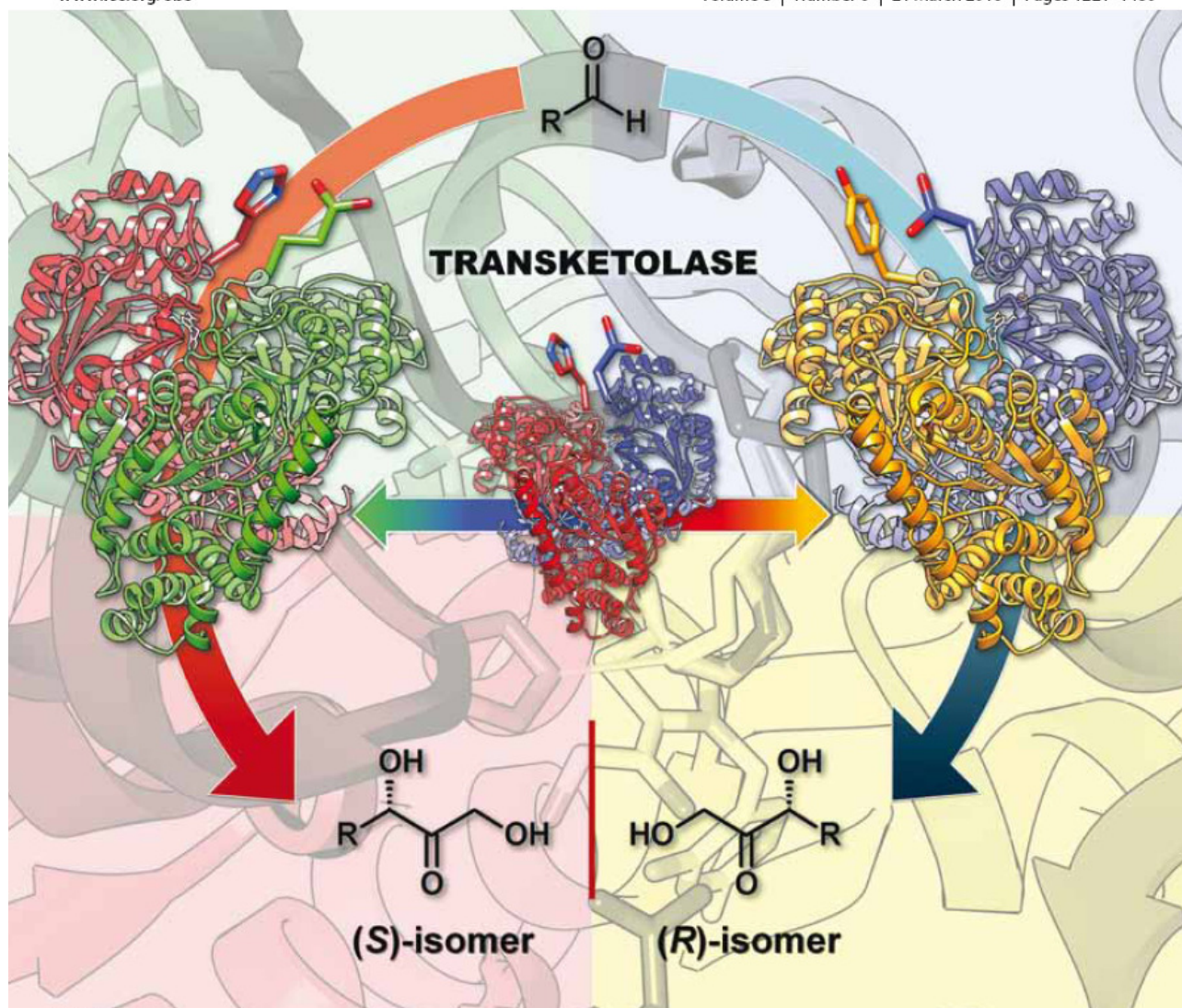
References

- For example: (a) Lindner, W. *Chromatographia* **1987**, *24*, 97–107; (b) Hailes, H. C.; Madden, J. *Synlett* **1999**, 105–107.
- Wenzel, T. J.; Morin, C. A.; Brechtel, A. A. *J. Org. Chem.* **1992**, *57*, 3594–3599.
- Dale, J. A.; Mosher, H. S. *J. Am. Chem. Soc.* **1973**, *95*, 512–519.
- Pehk, T.; Lippmaa, E.; Lopp, M.; Paju, A.; Borer, B. C.; Taylor, R. J. K. *Tetrahedron: Asymmetry* **1993**, *4*, 1527–1532.
- Ohtani, I.; Kusumi, T.; Kashman, Y.; Kakisawa, H. *J. Am. Chem. Soc.* **1991**, *113*, 4092–4096.
- Allen, D. A.; Tomaso, A. E.; Priest, O. P.; Hindson, D. F.; Hurlburt, J. L. *J. Chem. Educ.* **2008**, *85*, 698–700.
- Satoh, T.; Onda, K.; Yamakawa, K. *J. Org. Chem.* **1991**, *56*, 4129–4134.
- Kobori, Y.; Myles, D. C.; Whitesides, G. M. *J. Org. Chem.* **1992**, *57*, 5899–5907.
- Ingram, C. U.; Bommer, M.; Smith, M. E. B.; Dalby, P. A.; Ward, J. M.; Hailes, H. C.; Lye, G. J. *Biotechnol. Bioeng.* **2007**, *96*, 559–569.
- (a) Kaulmann, U.; Smithies, K.; Smith, M. E. B.; Hailes, H. C.; Ward, J. M. *Enzyme Microb. Technol.* **2007**, *41*, 628–637; (b) Smithies, K.; Smith, M. E. B.; Kaulmann, U.; Galman, J. L.; Ward, J. M.; Hailes, H. C. *Tetrahedron: Asymmetry* **2009**, *20*, 570–574.
- For example: (a) Hobbs, G. R.; Lilly, M. D.; Turner, N. J.; Ward, J. M.; Willets, A. J.; Woodley, J. M. *J. Chem. Soc., Perkin Trans. 1* **1993**, 165–166; (b) Hecquet, L.; Bolte, J.; Demuyck, C. *Tetrahedron* **1994**, *50*, 8677–8684; (c) Hibbert, E. G.; Senussi, T.; Costelloe, S. J.; Lei, W.; Smith, M. E. B.; Ward, J. M.; Hailes, H. C.; Dalby, P. A. *J. Biotechnol.* **2007**, *131*, 425–432; (d) Hibbert, E. G.; Senussi, T.; Smith, M. E. B.; Costelloe, S. J.; Ward, J. M.; Hailes, H. C.; Dalby, P. A. *J. Biotechnol.* **2008**, *134*, 240–245.
- Smith, M. E. B.; Hibbert, E. G.; Jones, A. B.; Dalby, P. A.; Hailes, H. C. *Adv. Synth. Catal.* **2008**, *350*, 2631–2638.
- Smith, M. E. B.; Smithies, K.; Senussi, T.; Dalby, P. A.; Hailes, H. C. *Eur. J. Org. Chem.* **2006**, 1121–1123.
- Enders, D.; Voith, M.; Ince, S. J. *Synthesis* **2002**, 1775–1779.
- Smith, M. E. B.; Kaulmann, U.; Ward, J. M.; Hailes, H. C. *Bioorg. Med. Chem.* **2006**, *14*, 7062–7065.
- Konno, K.; Fujishima, T.; Liu, Z.; Takayama, H. *Chirality* **2002**, *13*, 72–80.
- (a) Yasuhara, F.; Yamaguchi, S.; Kasai, R.; Tanaka, O. *Tetrahedron Lett.* **1986**, *27*, 4033–4034; (b) Tsuda, M.; Toriyabe, Y.; Endo, T.; Kobayashi, J. *Chem. Pharm. Bull.* **2003**, *51*, 448–451; (c) Akiyama, K.; Kawamoto, S.; Fujimoto, H.; Ishibashi, M. *Tetrahedron Lett.* **2003**, *44*, 8427–8431; (d) Czuba, I. R.; Zammit, S.; Rizzacasa, M. A. *Org. Biomol. Chem.* **2003**, *1*, 2044–2056.
- Dalmas, V.; Demuyck, C. *Tetrahedron: Asymmetry* **1993**, *4*, 2383–2388.
- Petizon, M.; Goulaouic, P.; Hanna, I. *Tetrahedron Lett.* **1985**, *26*, 4925–4927.
- Fangborn, A. B.; Giardello, M. A.; Grubbs, R. H.; Rosen, R. K.; Timmers, F. J. *Organometallics* **1996**, *15*, 1518–1520.
- Dickens, F. *Biochem. Prep.* **1962**, *9*, 86–91.

Organic & Biomolecular Chemistry

www.rsc.org/obc

Volume 8 | Number 6 | 21 March 2010 | Pages 1221–1480

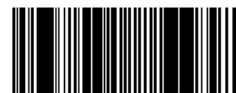


ISSN 1477-0520

RSC Publishing

FULL PAPER
Helen C. Hailes *et al.*
Non- α -hydroxylated aldehydes with
evolved transketolase enzymes

PERSPECTIVE
Marino Petrini *et al.*
Synthesis of 3-substituted indoles
via reactive alkylideneindolenine
intermediates



1477-0520(2010)8:6;1-E

Non- α -hydroxylated aldehydes with evolved transketolase enzymes†Armando Cázares,^a James L. Galman,^a Lydia G. Crago,^{a,b} Mark E. B. Smith,^a John Strafford,^b Leonardo Ríos-Solis,^b Gary J. Lye,^b Paul A. Dalby^b and Helen C. Hailes^{*a}

Received 18th November 2009, Accepted 9th January 2010

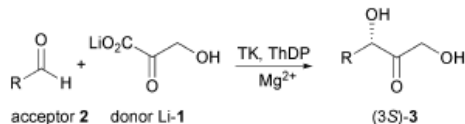
First published as an Advance Article on the web 5th February 2010

DOI: 10.1039/b924144b

Transketolase mutants previously identified for use with the non-phosphorylated aldehyde propanal have been explored with a series of linear and cyclic aliphatic aldehydes, and excellent stereoselectivities observed.

Introduction

The use of biocatalysis as a sustainable, atom efficient strategy in organic synthesis is of increasing importance, and is particularly attractive due to the high stereoselectivities that can be achieved.¹ Transketolase (TK) (EC 2.2.1.1) is an essential thiamine diphosphate (ThDP) dependent enzyme, which provides a link between the glycolytic and pentose phosphate pathways.² *In vivo* it catalyses the reversible transfer of a ketol unit to D-ribose-5-phosphate or D-erythrose-4-phosphate.² The TK reaction is made irreversible using the donor β -hydroxy pyruvate (HPA 1),³ which has been used with acceptors 2 such as α -hydroxyaldehydes where it is stereospecific for the (2*R*)-hydroxyaldehyde to give (S)- α,α' -dihydroxyketones 3 (Scheme 1).^{4,5} The substrate tolerance of TK towards a range α -hydroxyaldehydes has led to interest in industrial applications.⁶ *E. coli* TK, which has been over-expressed,⁷ shows increased specific activity towards 1 compared to yeast and spinach TKs.⁸



Scheme 1 Formation of α,α' -dihydroxy ketones (3*S*)-3 using TK.

α,α' -Dihydroxyketone functionalities (3) are present in a range of natural products and are also important compounds for further conversion into other synthons, including ketosugars and 2-amino-1,3-diols.^{4d,9,10} TK shows high specificity towards the donor substrates but is more tolerant towards the acceptor aldehyde: several non- α -hydroxylated aldehydes have been used but lower relative rates of reaction (5–35% compared to hydroxylated aldehydes) were noted.⁵

With a view to enhancing the use of TK in synthetic applications with a wider range of aldehydes, we used saturation mutagenesis that was targeted to the TK active site residues. Mutants with improved activity towards glycolaldehyde (Scheme 1, R =

CH_2OH), and enhanced specificity to propanal 2a (R = CH_2CH_3) such as D469T, were identified.¹¹ In addition, when propanal was used with wild-type (WT) TK, the *ee* of the product 3a (R = CH_2CH_3) was only 58% (Table 1) and therefore chiral assays were developed to identify mutants with improved stereoselectivities.^{12,13} Notable variants leading to high stereoselectivities were D469E (90% *ee*, 3*S*-isomer) and H26Y (88% *ee*, 3*R*-isomer), which remarkably with a single point active site mutation reversed the stereoselectivity.¹²

The D469E mutant TK has also been reported to reduce the acceptance of glycolaldehyde and formaldehyde,¹⁴ and the D469 residue has been highlighted as a key residue involved in enantioselection with α -hydroxylated aldehydes: a yeast TK structure with the adjunct erythrose-4-phosphate, indicated it hydrogen bonds to the C-2 hydroxy group of 2-hydroxylated aldehydes in the active site.¹⁵ In view of the interesting substrate tolerances exhibited by the TK mutants, a more systematic study was carried out using linear and cyclic aliphatic aldehydes, with the aim of understanding substrate tolerance and limitations with selected mutants.

Results and discussion

Stereoselectivity of *E. coli* WT TK

Linear aliphatic aldehydes (C_4 – C_8) and cyclopropane-, cyclopentane- and cyclohexanecarboxaldehyde were selected for use with WT-TK and TK mutants to determine the influence of chain length and ring size on reaction selectivities. Initially racemic α,α' -dihydroxyketones 3b–3i were prepared for chiral assay development. The commercially available aldehydes 2b–2i were converted into 3b–3i in yields of 2–35% using *N*-methylmorpholine and the previously described TK biomimetic reaction in water (Scheme 2).¹⁶ In general, lower yields were observed with the more lipophilic aldehydes, which may reflect poor substrate solubilities in water.

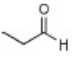
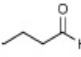
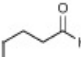
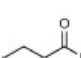

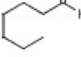
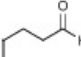

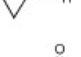
Methods were established for the determination of *ees* in 3 *via* monobenzylation at the primary alcohol of 3g–3i and chiral HPLC. Compounds 3b–3f required dibenzylation for satisfactory peak resolution by chiral HPLC. Then WT-TK and 1 were reacted with 2b–2f (C_4 – C_8) to determine product stereoselectivities and yields (Table 1). As well as establishing *ees via* derivatisation and chiral HPLC, the selected ketodiols 3b and 3d were coupled to (S)-MTPACI to give the corresponding Mosher's esters: application of

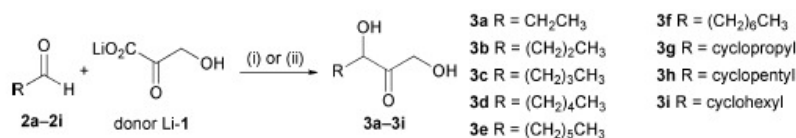
^aDepartment of Chemistry, University College London, 20 Gordon Street, London, UK WC1H 0AJ. E-mail: h.c.hailes@ucl.ac.uk; Fax: +44 (0)20 7679 7463; Tel: +44 (0)20 7679 7463

^bDepartment of Biochemical Engineering, University College London, Torrington Place, London, UK WC1E 7JE

† Electronic supplementary information (ESI) available: Colorimetric assay plates for the cyclic aldehydes. See DOI: 10.1039/b924144b

Table 1 Stereoselectivities and yields for WT-TK and TK mutant reactions using linear aliphatic and cyclic aldehydes

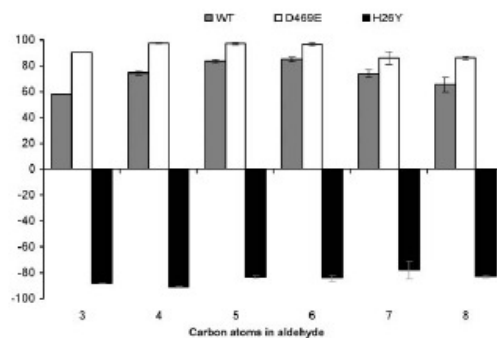
Aldehyde	Product	WT-TK <i>ee</i> (yield)	D469E <i>ee</i> (yield)	D469T <i>ee</i> (yield)	D469K <i>ee</i> (yield)	D469L <i>ee</i> (yield)	H26Y <i>ee</i> (yield)
2a 	3a ¹²	58% (3 <i>S</i>) (36%) ¹²	90% (3 <i>S</i>) (70%) ¹²	64% (3 <i>S</i>) ¹² (68%) ¹⁷	—	12% (3 <i>S</i>) (nd)	88% (3 <i>R</i>) (63%) ¹²
2b 	3b	75% (3 <i>S</i>) (36%)	98% (3 <i>S</i>) (44%)	—	—	—	92% (3 <i>R</i>) (16%)
2c 	3c	84% (3 <i>S</i>) (16%)	97% (3 <i>S</i>) (58%)	—	—	—	84% (3 <i>R</i>) (7%)
2d 	3d	85% (3 <i>S</i>) (25%)	97% (3 <i>S</i>) (47%)	—	—	—	84% (3 <i>R</i>) (12%)
2e 	3e	74% (3 <i>S</i>) (7%)	86% (3 <i>S</i>) (14%)	—	—	—	78% (3 <i>R</i>) (4%)
2f 	3f	66% (3 <i>S</i>) (<3%)	86% (3 <i>S</i>) (18%)	—	—	—	83% (3 <i>R</i>) (21%)
2g 	3g	72% (1 <i>S</i>) (<3%)	>99% (1 <i>S</i>) (10%)	99% (1 <i>S</i>) (10%)	99% (1 <i>S</i>) (<3%)	99% (1 <i>S</i>) (<3%)	no reaction
2h 	3h	0% (<3%)	>99% (1 <i>S</i>) (40%)	99% (1 <i>S</i>) (30%)	25% (1 <i>S</i>) (10%)	no reaction	30% (1 <i>R</i>) (<3%)
2i 	3i	0% (<3%)	97% (1 <i>S</i>) (10%)	99% (1 <i>S</i>) (<3%)	25% (1 <i>S</i>) (<3%)	no reaction	no reaction

**Scheme 2** Reagents and conditions: (i) *N*-methylmorpholine, pH 8, H₂O; (ii) TK, ThDP, Mg²⁺, pH 7.

a recently reported NMR method indicated the major enantiomers formed were (3*S*)-**3b** and (3*S*)-**3d**.¹³

As in previous work using propanal, WT-TK leads to the formation of the (3*S*)-isomer as the major enantiomer, and the *ees* are given in Table 1: by analogy, the major isomers of **3c**, **3e** and **3f** were assigned as (3*S*). Interestingly, the degree of stereoselectivity of the transformation varied with the length of the aliphatic chain of the aldehyde, reaching a maximum of 84% and 85% *ee* for pentanal and hexanal (Fig. 1), which are similar in size to the *in vivo* substrates of TK. In addition, increasing lipophilicity of the aldehyde acceptor resulted in lower conversion yields, probably due to decreasing aqueous solubilities.

WT-TK was then used with the cyclic aldehydes **2g–2i**. The conversion yields were low (<3%) and for the cyclopropane analogue **3g** the *ee* was 72%. The major isomer formed was determined using the modified Mosher's ester method as again the (1*S*)-isomer.¹³ However, for the cyclopentane and cyclohexane analogues **3h** and **3i**, racemic products were formed. The substrate

**Fig. 1** Variation in stereoselectivities for linear aliphatic aldehydes using WT-TK, D469E-TK and H26Y-TK.

cyclopropane carboxaldehyde may be able to adopt a similar conformation to butanal in the active site leading to a similar

level of stereoselectivity in the product; however, the larger-ringed cyclic analogues cannot.

Molecular modelling: WT TK

With a view to rationalising the stereoselectivities with WT-TK and the linear aliphatic aldehydes, which demonstrated a clear experimental relationship between chain length and *ee* in the product, molecular docking experiments were carried out using the X-ray crystal structure of WT-TK (PDB ID: 1QGD).¹⁸ Initially, in order to validate the method, direct docking of D-erythrose-4-phosphate, a natural substrate of TK, was carried out using AutoDock.¹⁹ The predominant conformations obtained were compared with an existing X-ray crystal structure of a noncovalent complex of *E. coli* TK with the aldose (PDB ID: 1NGS) and co-factor.²⁰ Most docked conformations coincided with the conformation of the ligand in the crystal structure in terms of hydrogen bonding and consequently orientation. Despite the dynamic nature of proteins, the conformation generated *in silico* reproduced the experimental findings suggesting a molecular docking method would be a useful model to adopt.

Direct docking of the linear aliphatic aldehydes (C_3 – C_8) was performed into the TK active site containing a modelled ThDP-enamine intermediate and the results compared, firstly in terms of cluster populations, and then the hydrogen bonding and orientation. The conformations obtained populated one cluster preferentially in all cases, except for butanal, which occupied two energetically similar conformations. For all the C_3 – C_8 aldehydes, docks were obtained in which the aldo oxygen atom is bound to two histidine residues (His26 and His261), bringing the substrates into close proximity with the coenzyme for nucleophilic attack.

The longer C_5 – C_8 aldehydes docked with the aliphatic chain bound to a hydrophobic region around the lip of the entrance to the ThDP-containing cavity (Fig. 2, magenta model). This presented neither face of the aldehyde preferentially towards the ThDP enamine intermediate. Interestingly, the smallest aliphatic chain (C_3) of **2a** docked in an alternative orientation with the aliphatic chain occupying the narrow entrance to the cofactor containing cavity (Fig. 2, white model), marginally rendering the *Re*-face of the carbonyl exposed to the ThDP-enamine $C\alpha$ atom.

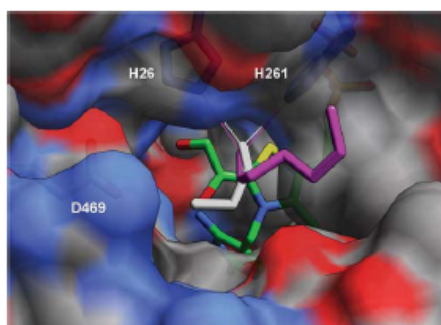


Fig. 2 Aldehydes **2a** (grey) and **2d** (magenta) docked into the TK active site containing the modelled ThDP-enamine intermediate (green). A surface plot is shown with D469, H26 and H261 highlighted as sticks beneath the surface.

This is reflected in the low *ee* (58%) in favour of the (*3S*)-isomer product for reaction with **2a**. The slightly larger C_4 aldehyde was

found to dock in two different conformations, with the first similar to that for C_3 , and the second similar to the C_5 – C_8 aldehydes. This transition of docking conformations at C_4 in the series from C_3 to C_8 mirrors the observed increase in *ee* from 58% for C_3 , through 73% for C_4 to 84% and 85% for C_5 and C_6 respectively. However, the increased *ee* resulting from the alternative conformations adopted by the C_4 – C_8 aldehydes is not easily rationalised. One possibility is that as the aldo O-atom moves closer to H26 and H261 during the reaction, and the Van der Waals contacts between the aliphatic chains and the lipophilic region of the active site are weakened, allowing the chain to move further into the active site and more freedom to rotate the carbonyl with the *Re*-face of the carbonyl exposed to the ThDP-enamine $C\alpha$ atom. The decrease in *ee* observed for C_7 and C_8 may be due to an increase in the Van der Waals interactions with the active-site wall and therefore, less flexibility in the re-orientation of the substrate.

Finally docking of the cyclic aldehydes **2g**–**2i** was carried out; however, they docked preferentially in a lip at the entrance to the active site in non-productive conformations, which could explain the low yielding reactions observed. Only the cyclopropyl analogue **2g** docked in a similar conformation to propanal **2a**, which gave **3g** in 72% *ee*. Modelling with the mutant TKs was not performed as we do not have the crystal structures of the mutants at present, and modelling both the protein mutation and the substrate binding simultaneously would be less informative.

Stereoselectivity of selected single-point TK mutants

In previous mutant screening studies using propanal as the acceptor, two active-site single-point mutant TKs exhibited marked improved and reversed stereoselectivity, Asp469Glu (D469E) and His26Tyr (H26Y). Variant D469E had led to the formation of (*3S*)-**3a** in 90% *ee*, while H26Y gave (*3R*)-**3a** in 88% *ee* (Table 1).¹² With the aim of understanding substrate tolerances, and enhancing and reversing stereoselectivities compared to WT-TK with the C_4 – C_8 linear aldehydes, reactions were carried out using these high performing mutants: others screened with propanal were not explored due to the lower stereoselectivities achieved. D469E gave products in 14–58% isolated yield, with decreasing yield upon increasing chain length, but enhanced yields compared to WT-TK. Notably, high stereoselectivities (97–98% *ee*) were observed when using butanal, pentanal and hexanal, and the highest *ees* were when using aldehydes of a similar size to *in vivo* substrates for TK. As shown in Fig. 1, the greatest enhancement in *ee* between WT and D469E was for the C_3 and C_4 aldehydes. The use of H26Y gave products in generally lower yields (4–21%), with the highest (*3R*)-stereoselectivities observed in **3b** using butanal (92% *ee*), decreasing to 78% *ee* for **3e**. The reversal in *ee* was observed across the whole series of linear aldehydes used, although a smaller change in *ee* was observed in going from C_3 to C_8 (Fig. 1). The lower yields with some longer chain length analogues reflect a lower turnover of substrate and may be due to steric interactions in the active site.

The selection of TK-mutants for use with cyclic aldehydes was less clear, and very low yields were observed using WT-TK. A recently developed tetrazolium red-based colorimetric assay was therefore used with the three substrates **2g**–**2i** against the D469X library, which had led to the identification of several improved mutants when using propanal.^{12,21} From this, three

mutants were selected, which were able to accept one or more of the cyclic aldehydes, D469T, D469K and D469L. These were used together with mutants D469E and H29Y, which gave high selectivities with the linear series. The results indicated that high stereoselectivities could be achieved with D469E: the cyclopropane and cyclopentane adducts, **3g** and **3h**, were formed in >99% *ee*, and cyclohexane analogue **3i** formed in 97% *ee* (by HPLC) (Table 1). In all cases, the major isomer was the (1*S*)-product. When using D469T similar results were observed, with all products **3g**–**3i** formed in 99% *ee* (the (1*S*)-isomer). Similar yields were observed with both mutants, with **3g** and **3i** formed in 3–10% yields, while the cyclopentane product was formed in a higher 30–40% yield. This possibly reflects the comparable ring size of **2h** and the natural substrate, ribose-5-phosphate (furanose form). Mutants D469K and D469L gave the cyclopropane product in 99% *ee* in low yields, but when using **2h** and **2i** either low *ees* (D469K) or no reaction (D469L) were observed. The use of H26Y-TK gave no product with the cyclopropane and cyclohexane aldehydes, but when using cyclopentanecarboxaldehyde, **3h** was formed in 30% *ee*, and the major isomer was the (1*R*)-product. Overall, these results suggest that when using cyclic substrates D469E and D469T may be suitable mutants to achieve bioconversions. The smallest cyclic substrate **2g** appeared to have greater activity with a larger range of mutants (leading to high *ees*), presumably because it causes less steric problems. Most mutants gave (1*S*)-products, other than the low *ee* for the (1*R*)-isomer observed with H26Y-TK. The generally lower yields for the cyclic series may reflect poor substrate solubilities and/or product inhibition.

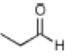
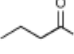
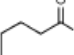
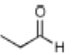
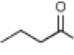
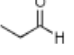
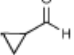
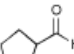
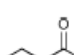
Initial relative rates were also determined for selected reactions using D469E, H26Y and D469T for the cyclic series (Table 2). Relative activities are given compared to propanal for each particular mutant: for comparison the wild-type specific activity towards glycolaldehyde was previously reported as 0.65 $\mu\text{mol mg}^{-1}\text{min}^{-1}$.¹¹

Previous work highlighted that when using propanal, higher relative activities for D469E, H26Y and D469T compared to WT were observed. Here, relative rates decreased with increasing aldehyde size in all cases, although was most marked for H26Y. Interestingly, butanal had a higher initial rate with D469E than pentanal, although the isolated yield for the reaction was higher for the pentanal-derived product **3c**. This may be due to product inhibition by **3b**, limiting the overall reaction. For the cyclic aldehydes and D469T, increasing ring size also had less of an effect on initial rates, than increasing the linear chain length with D469E, although it decreased slightly as the ring size increased. This may result from lower conformational flexibilities of cyclic substrates, compared to aliphatic substrates, resulting in a smaller and more favourable entropy loss on binding. The small increase in conformational flexibility as the ring size increases may also lead to a less favourable loss of entropy upon binding.

Conclusions

Ideally, for use in synthesis, enzymes should have good substrate tolerance and demonstrate high stereoselectivities. In this work transketolase mutants able to accept lipophilic longer chain and cyclic aldehydes have been identified, which gives significant potential for further synthetic applications. With several substrate/mutant combinations very high stereoselectivities were observed, with moderate to low conversion yields. Future work is

Table 2 Initial relative rates for selected reactions with the aldehyde indicated

Aldehyde	Mutant	Initial rate/ mM h^{-1}	TK/ mg mL^{-1}	Spec. activity/ $\mu\text{mol mg}^{-1}\text{min}^{-1}$	Initial rel. rate ^a
	D469E	8.14	0.45	0.30	1
	D469E	2.14	0.45	0.08	0.3
	D469E	0.89	0.45	0.03	0.1
	H26Y	8.00	1.01	0.13	1
	H26Y	0.41	1.01	0.007	0.05
	D469T	12.5	0.30	0.69	1
	D469T	7.45	0.30	0.41	0.6
	D469T	4.47	0.30	0.25	0.4
	D469T	3.46	0.30	0.19	0.3

^a Relative rates are given for substrates compared to propanal with the selected mutant.

under way to investigate strategies to improve yields with lipophilic aldehyde acceptors.

Experimental

General methods

Unless otherwise noted, solvents and reagents were reagent grade from commercial suppliers (Sigma-Aldrich) and used without further purification. Dry CH_2Cl_2 was obtained using anhydrous alumina columns.²² All moisture-sensitive reactions were performed under a nitrogen or argon atmosphere using oven-dried glassware. Reactions were monitored by TLC on Kieselgel 60 F₂₅₄ plates with detection by UV, potassium permanganate and phosphomolybdic acid (PMA) [PMA hydrate (12 g) and ethanol (250 ml)] stains. Flash column chromatography was carried out using silica gel (particle size 40–63 μm). ¹H NMR and ¹³C NMR spectra were recorded at the field indicated using Bruker AMX300 MHz, AMX400 Avance-500 MHz and Avance-600 MHz machines. Coupling constants are measured in Hertz (Hz) and unless otherwise specified, NMR spectra were recorded at 298 K. Mass spectra were recorded on a Thermo Finnegan MAT 900XP and Micro Mass Quattro LC electrospray mass spectrometers VG ZAB 2SE. Infrared spectra were recorded on

a Shimadzu FTIR-8700 and Perkin Elmer Spectrum 100 FTIR spectrometer. Optical rotations were recorded on a Perkin Elmer model 343 polarimeter at 589 nm, quoted in $\text{deg cm}^2 \text{g}^{-1}$ and conc (c) in $\text{g}/100 \text{ mL}$. Chiral HPLC analysis was performed on a Varian Prostar instrument equipped with a Chiralcel AD chiral column (Daicel; Chiral Technologies Europe, France) $25 \text{ cm} \times 0.46 \text{ cm}$.

Lithium hydroxypyruvate was synthesised as previously described.² 1,3-Dihydroxypentan-2-one **3a** was prepared as previously described.¹²

Synthesis of racemic α,α' -dihydroxyketones. The corresponding aldehyde (3.00 mmol) was added to a solution of Li-1 (336 mg, 3.00 mmol) and *N*-methylmorpholine (330 μL , 3.00 mmol) in water (60 mL) at pH 8 (adjusted with 10% HCl). The reaction was stirred for 24–48 h at rt and monitored by TLC analysis. Upon concentration *in vacuo*, the crude material was dry loaded and purified using flash silica chromatography.

Chiral HPLC analysis of **3b–3i to determine *ees*.** Compounds **3b–3f** were dibenzoylated (monobenzoylated compounds were not separable by chiral HPLC columns used) and the products analysed by chiral HPLC to determine *ees*. Ketodiols **3g–3i** were monobenzoylated at the primary alcohol for chiral HPLC analysis. HPLC analysis was carried out using a Chiralpak AD column and the hexane–2-propanol solvent system given.

Monobenzoylation procedure. To the ketodiol (30 μmol) in CH_2Cl_2 (5 mL) triethylamine (1.5 eq, 45 μmol) and benzoyl chloride (1.5 eq, 45 μmol) were added. The reaction was stirred for 2 h at rt, quenched by the addition of saturated NaHCO_3 solution (5 mL), and the organic phase was dried (MgSO_4). Upon removal of the solvent *in vacuo*, the resulting monobenzoylated material was dissolved in hexane–2-propanol (1 : 1) to a final concentration of 1 mg mL^{-1} .

Dibenzoylation procedure. To the ketodiol (30 μmol) in CH_2Cl_2 (5 mL) triethylamine (5 eq, 150 μmol) and benzoyl chloride (5 eq, 150 μmol) were added. The reaction was stirred for 2 h at rt, quenched by the addition of saturated NaHCO_3 solution (5 mL), and the organic phase was dried (MgSO_4). Upon removal of the solvent *in vacuo*, the resulting dibenzoylated material was dissolved in hexane–2-propanol (1 : 1) to a final concentration of 1 mg mL^{-1} .

1,3-Dihydroxyhexan-2-one (3b**).** The reaction was carried out for 24 h and the product purified using flash silica chromatography (EtOAc–hexane, 1 : 1) to give **3b** as a white powder (47 mg, 12%). Mp 109–112 °C (EtOAc); $\nu_{\text{max}}(\text{neat})/\text{cm}^{-1}$ 3413, 2960, 2935, 2874, 1719; $^1\text{H NMR}$ (500 MHz; CDCl_3) δ 4.49 (1H, d, *J* 20.1, *CHHOH*), 4.38 (1H, d, *J* 20.1, *CHHOH*), 4.31 (1H, dd, *J* 8.0 and 3.9, *CHOH*), 2.70 (br, *OH*), 1.75 (1H, m, 4-*HH*), 1.57 (1H, m, 4-*HH*), 1.46 (2H, m, CH_2CH_3), 0.95 (3H, t, *J* 7.3, CH_3); $^{13}\text{C NMR}$ (125 MHz; CDCl_3) δ 211.9 (C-2), 74.8 (C-3), 65.6 (C-1), 36.3 (C-4), 18.1 (C-5), 13.8 (C-6); *m/z* (CI) 133 (MH^+ , 100%), 115 ($[\text{MH} - \text{H}_2\text{O}]^+$, 30), 85 (47); Found (HRCI) MH^+ 133.08611. $\text{C}_6\text{H}_{12}\text{O}_5$ requires 133.08647. Racemic **3b** was dibenzoylated and HPLC analysis (97 : 3, 1 mL min^{-1}) gave retention times of 20.4 min (*R*-isomer) and 24.5 min (*S*-isomer).

1,3-Dihydroxyheptan-2-one (3c**).** The reaction was carried out for 24 h and the product purified using flash silica chromatography (EtOAc–hexane, 1 : 1) to give **3c** as a white powder (152 mg, 35%). Mp 110–125 °C (EtOAc); $\nu_{\text{max}}(\text{neat})/\text{cm}^{-1}$ 3430, 3263, 2956, 2929,

2872, 1720; $^1\text{H NMR}$ (500 MHz; CDCl_3) δ 4.49 (1H, d, *J* 19.4, *CHHOH*), 4.39 (1H, d, *J* 19.4, *CHHOH*), 4.31 (1H, dd, *J* 7.9 and 3.9, *CHOH*), 2.89 (br, *OH*), 1.80 (1H, m, 4-*HH*), 1.20–1.75 (5H, m, 4-*HH*, $(\text{CH}_2)_2\text{CH}_3$), 0.91 (3H, t, *J* 6.6, CH_3); $^{13}\text{C NMR}$ (125 MHz; CDCl_3) δ 211.7 (C-2), 75.0 (C-3), 65.6 (C-1), 34.0 (C-4), 26.8 (C-5), 22.5 (C-6), 13.9 (C-7); *m/z* (CI) 147 (MH^+ , 100%), 129 ($[\text{MH} - \text{H}_2\text{O}]^+$, 35), 85 (94); Found (HRCI) MH^+ 147.10288. $\text{C}_7\text{H}_{14}\text{O}_5$ requires 147.10212. Racemic **3c** was dibenzoylated and HPLC analysis (97 : 3, 1 mL min^{-1}) gave retention times of 16.6 min (*R*-isomer) and 20.0 min (*S*-isomer).

1,3-Dihydroxyoctan-2-one (3d**).** The reaction was carried out for 24 h and the product purified using flash silica chromatography (EtOAc–hexane, 1 : 1) to give **3d** as a white powder (11 mg, 3%). Mp 106–110 °C (EtOAc); $\nu_{\text{max}}(\text{neat})/\text{cm}^{-1}$ 3406, 2956, 2925, 2858, 1720; $^1\text{H NMR}$ (500 MHz; CDCl_3) δ 4.49 (1H, d, *J* 19.4, *CHHOH*), 4.38 (1H, d, *J* 19.4, *CHHOH*), 4.31 (1H, dd, *J* 7.9 and 3.9, *CHOH*), 2.89 (br, *OH*), 1.77 (1H, m, 4-*HH*), 1.58 (1H, m, 4-*HH*), 1.20–1.34 (6H, m, 5-*H*₂, 6-*H*₂, 7-*H*₂), 0.89 (3H, t, *J* 6.9, CH_3); $^{13}\text{C NMR}$ (125 MHz; CDCl_3) δ 211.7 (C-2), 75.0 (C-3), 65.6 (C-1), 34.3 (C-4), 31.6 (C-5), 24.4 (C-6), 22.5 (C-7), 14.0 (C-8); *m/z* (CI) 161 (MH^+ , 100%); Found (HRCI) MH^+ 161.11823. $\text{C}_7\text{H}_{14}\text{O}_5$ requires 161.11777. Racemic **3d** was dibenzoylated and HPLC analysis (97 : 3, 1 mL min^{-1}) gave retention times of 15.5 min (*R*-isomer) and 19.9 min (*S*-isomer).

1,3-Dihydroxynonan-2-one (3e**).** The reaction was carried out for 24 h and the product purified using flash silica chromatography (EtOAc–hexane, 1 : 1) to give **3e** as a white powder (22 mg, 4%). Mp 104–107 °C (EtOAc); $\nu_{\text{max}}(\text{neat})/\text{cm}^{-1}$ 3406, 2955, 2925, 2857, 1718; $^1\text{H NMR}$ (500 MHz; CDCl_3) δ 4.49 (1H, d, *J* 19.4, *CHHOH*), 4.38 (1H, d, *J* 19.4, *CHHOH*), 4.30 (1H, dd, *J* 7.8, 3.9, *CHOH*), 2.96 (br s, *OH*), 1.78 (1H, m, 4-*HH*), 1.57 (1H, m, 4-*HH*), 1.27–1.50 (8H, m, 5-*H*₂, 6-*H*₂, 7-*H*₂, 8-*H*₂), 0.88 (3H, t, *J* 6.9, CH_3); $^{13}\text{C NMR}$ (125 MHz; CDCl_3) δ 211.7 (C-2), 75.0 (C-3), 65.6 (C-1), 34.3 (C-4), 31.7 (C-5), 29.0 (C-6), 24.7 (C-7), 22.6 (C-8), 14.1 (C-9); *m/z* (CI) 175 (MH^+ , 100%), 139 (62), 113 (97), 97 (100); Found (HRCI) MH^+ 175.13360. $\text{C}_9\text{H}_{18}\text{O}_5$ requires 175.13342. Racemic **3e** was dibenzoylated and HPLC analysis (97 : 3, 1.2 mL min^{-1}) gave retention times of 11.6 min (*R*-isomer) and 15.4 min (*S*-isomer).

1,3-Dihydroxydecan-2-one (3f**).** The reaction was carried out for 24 h and the product purified using flash silica chromatography (EtOAc–hexane, 1 : 1) to give **3f** as a white powder (2%, 3 mg). Mp 100–103 °C (EtOAc); $\nu_{\text{max}}(\text{neat})/\text{cm}^{-1}$ 3420, 2959, 2928, 2873, 1721; $^1\text{H NMR}$ (500 MHz; CDCl_3) δ 4.49 (1H, d, *J* 19.4, *CHHOH*), 4.38 (1H, d, *J* 19.4, *CHHOH*), 4.31 (1H, m, *CHOH*), 2.93 (br s, *OH*), 1.77 (1H, m, 4-*HH*), 1.20–1.61 (11H, m, 4-*HH*, 5-*H*₂, 6-*H*₂, 7-*H*₂, 8-*H*₂, 9-*H*₂), 0.88 (3H, t, *J* 7.0, CH_3); $^{13}\text{C NMR}$ (125 MHz; CDCl_3) δ 211.7 (C-2), 75.0 (C-3), 65.6 (C-1), 34.3 (C-4), 31.8 (C-5), 29.3 (C-6), 29.1 (C-7), 24.7 (C-8), 22.7 (C-9), 14.1 (C-10); *m/z* (CI) 189 (MH^+ , 100%), 153 (93), 127 (97); Found (HRCI) MH^+ 189.14971. $\text{C}_{10}\text{H}_{20}\text{O}_5$ requires 189.14907. Racemic **3f** was dibenzoylated and HPLC analysis (97 : 3, 1.2 mL min^{-1}) gave retention times of 10.5 min (*R*-isomer) and 13.9 min (*S*-isomer).

1-Cyclopropyl-1,3-dihydroxy-2-propanone (3g**).** The reaction was carried out for 48 h and the product purified using flash silica chromatography (EtOAc) to give **3g** as an oil (0.013 g, 10%). *R*_f 0.50 (EtOAc). $\nu_{\text{max}}(\text{KBr})/\text{cm}^{-1}$ 3380, 3007, 2924, 1724; $^1\text{H NMR}$ (300 MHz; CDCl_3) δ 4.50 (1H, d, *J* 19.3, *CHHOH*), 4.37

(1H, d, *J* 19.3, CHHOH), 4.30 (1H, d, *J* 4.2, CHOH), 2.19 (1H, m), 1.30–1.80 (4H, m, 2 × CH₂); ¹³C NMR (75 MHz; CDCl₃) δ 211.4 (C-2), 77.0 (CHOH), 65.9 (CH₂OH), 43.0, 29.1, 25.8 and 25.6; *m/z* (CI) 161 (MH⁺, 100%); *m/z* (FTMS) found [M + NH₄]⁺ 148.0969. C₆H₁₄O₃N requires 148.0968. Racemic **3g** was monobenzoyleated and HPLC analysis (97:3, 1 mL min⁻¹) gave retention times of 31.1 min (*S*-isomer) and 33.6 min (*R*-isomer).

1-Cyclopentyl-1,3-dihydroxy-2-propanone (3h). The reaction was carried out for 48 h and the product purified using flash silica chromatography (EtOAc–hexane, 1:1) to give **3h** as a white solid (0.119 g, 25%). *R_f* 0.21 (EtOAc–hexane, 1:1). Mp 110–112 °C (EtOAc–hexane, 1:1); *v*_{max}(KBr)/cm⁻¹ 3411, 2953, 2870, 1718; ¹H NMR (300 MHz; CDCl₃) δ 4.50 (1H, d, *J* 19.4, CHHOH), 4.36 (1H, d, *J* 19.4, CHHOH), 4.30 (1H, m, CHOH), 3.04 (2H, s, 2 × OH), 2.18 (1H, m), 1.31–1.75 (8H, m, 4 × CH₂); ¹³C NMR (75 MHz; CDCl₃) δ 211.5 (C-2), 76.9 (CHOH), 65.8 (CH₂OH), 42.9, 29.0, 25.7 and 25.6; *m/z* (FTMS) found [M + NH₄]⁺ 176.1281. C₉H₁₆O₃N requires 176.1281. Racemic **3h** was monobenzoyleated and HPLC analysis (97:3, 1 mL min⁻¹) gave retention times of 32.1 min (*R*-isomer) and 34.8 min (*S*-isomer).

1-Cyclohexyl-1,3-dihydroxy-2-propanone (3i). The reaction was carried out for 48 h and the product purified using flash silica chromatography (EtOAc–hexane, 1:1) to give **3i** as a white solid (0.088 g, 17%). *R_f* 0.21 (EtOAc–hexane, 1:1). Mp 115–118 °C (EtOAc–hexane, 1:1); *v*_{max}(KBr)/cm⁻¹ 3429, 2940, 1712; ¹H NMR (300 MHz; CD₃OD) δ 4.45 (1H, d, *J* 19.3, CHHOH), 4.34 (1H, d, *J* 19.3, CHHOH), 3.96 (1H, d, *J* 4.4, CHOH), 1.45–1.87 (6H, m), 1.16–1.30 (5H, m); ¹³C NMR (75 MHz; CD₃OD) δ 214.3 (C-2), 80.7 (CHOH), 67.4 (CH₂OH), 43.0, 30.3, 27.7, 27.3 (signals superimposed); *m/z* (CI) 173 (MH⁺, 100%), 155 (45), 137 (86), 95 (100); Found (HRCI) MH⁺ 173.11736. C₉H₁₇O₃ requires 173.11722. Racemic **3i** was monobenzoyleated and HPLC analysis of the product (97:3, 1 mL min⁻¹) gave retention times of 17.0 min (*R*-isomer) and 18.5 min (*S*-isomer).

Biocatalytic synthesis of 3b-3i

TK Cell-free lysate preparation. Cells from a single colony of *Escherichia coli* XL10 transformed with the plasmid containing the appropriate TK mutant gene were inoculated in 10 mL of sterile Luria-Bertani medium containing ampicillin (150 mg mL⁻¹). The culture was incubated overnight (14 h) with orbital shaking at 200 rpm and 37 °C. The overnight culture was inoculated in 90 mL of fresh medium and incubated until the absorbance at 600 nm was greater than 4. The culture was pelleted by centrifugation at 4000 rpm for 20 min at 4 °C and then resuspended in cold phosphate buffer (5 mM, pH 7) to a final suspension of 1 g cell paste/10 mL buffer. The suspension was sonicated for 3 min in total at 4 °C, and centrifuged at 4500 rpm for 20 min at 4 °C. The supernatant cell-free lysate was aliquoted and stored at –20 °C until needed.

TK conversions. ThDP (22 mg, 48 μmol) and MgCl₂·6H₂O (39 mg, 180 μmol) were dissolved in H₂O (10 mL) and the pH adjusted to 7 using 0.1 M NaOH. To this stirred solution, at 25 °C, was added TK clarified lysate (2 mL) and the mixture stirred for 20 min. In another flask, Li-1 (110 mg, 1.00 mmol) and the aldehyde (1.00 mmol) were dissolved in H₂O (8 mL) and the pH adjusted to 7 with 0.1 M NaOH. Following the 20 min enzyme/cofactor pre-incubation, the 1-aldehyde mixture

was added to the enzyme solution and the mixture stirred at rt for 24 h. During this time, the pH was maintained at 7.0 by addition of 1 M HCl using a pH stat (Stat Titrimo, Metrohm) and the reactions were followed by TLC analysis. Silica was added and the reaction mixture concentrated to dryness, dry loaded onto a flash silica gel column, and purified as before.

Determination of initial rates for selected reactions

Linear series. Data for selected compounds was determined as detailed below. Aliquots of the biotransformation reaction (200 μL) were collected and diluted with 0.1% TFA (200 μL) and stored at –20 °C after various reaction times (0, 0.25, 0.50, 0.75, 1, 1.5, 2, 3, 4, 12, 24 and 48 h). Samples were centrifuged at 13,000 rpm for 5 min and the supernatant transferred to a clean microcentrifuge tube. The samples were diluted accordingly for the absorbance to be within the range of the calibration curve and then analysed by HPLC. Separation of the biotransformation components was achieved by HPLC (Dionex, UK) using a Bio-Rad Amines HPX-87H reverse phase column (300 × 7.8 mm) and 0.2% TFA in water as the mobile phase at 60 °C. Detection of the products was carried out *via* UV absorption at 210 nm. Retention times for **3a**, **3b**, and **3c** were 15.4, 18.5 and 23.4 min, respectively.

Cyclic series. Data was determined *via* application of the colorimetric assay²¹ as poor separation was observed using HPLC methods. D469T TK lysate, 60 μL was incubated with 100 μL cofactor solution (TPP (2.4 mM), and MgCl₂ (9 mM)) for 20 min at 20 °C. Li-1 (7.4 mg, 50 mmol) and aldehyde (50 mmol) were added to the reaction mixture. Aliquots (50 μL) were taken at hourly intervals and the reaction was quenched with 50 μL methanol. The aliquots were transferred onto a microwell plate containing 10 mg MP-Carbonate resin (Biotage AB) and incubated at 20 °C for 3 h. 50 μL of the quenched reaction sample was transferred without resin into a microwell plate. The colour assay was performed as described previously:²¹ 50 μL of each concentration was diluted with 100 μL of water. Automated injection of 20 μL of tetrazolium red solution (0.2% of 2,3,5-triphenyltetrazolium chloride in methanol) and 10 μL 3 M NaOH (aq) with shaking by FLUOstar Optima plate reader (BMG Labtechnologies GmbH), was followed by immediate measurement at OD_{485nm}.

Protein concentrations were determined using determined using a combined Bradford and SDS-PAGE densitometry method as previously described.^{11a}

TK formation of 1,3-dihydroxyhexan-2-one (3b). WT-TK gave **3b** (47 mg, 36%) in 75% *ee* (3*S*-isomer) by HPLC (97:3, 1.0 mL min⁻¹). D469E-TK gave **3b** (58 mg, 44%) in 98% *ee* (3*S*-isomer) by HPLC (97:3, 1.0 mL min⁻¹); [α]_D²⁰ –16.3 (*c* 1.4, CH₃OH). H26Y-TK gave **3b** (21 mg, 16%) in 92% *ee* (3*R*-isomer) by HPLC (97:3, 1.0 mL min⁻¹); [α]_D²⁰ +14.2 (*c* 1.6, CH₃OH). The absolute stereochemistry of **3b** generated using D469E-TK was determined using the Mosher's derivatisation method.¹³

(2*R*,3'*S*)-3,3,3-Trifluoro-2-methoxy-2-phenyl propionic acid 3'-hydroxy-2'-oxo-hexyl ester. The reaction was carried out under anhydrous conditions. Triethylamine (20 μL, 0.13 mmol) and (*S*)-MTPA chloride (5 μL, 0.03 mmol) were added to a stirred solution of **3b** from the D469E-TK reaction (0.018 g, 0.07 mmol) in CH₂Cl₂ (2 mL) and the reaction was stirred for 2 h at rt. The product was dry loaded onto silica gel and purified using flash chromatography

(hexane–EtOAc, 10:1) to afford the Mosher's derivative as a colourless oil (4.6 mg, 43%). ¹H NMR (600 MHz; CDCl₃) δ 7.64 (2H, m, Ph), 7.45 (3H, m, Ph), 5.21 (d, *J* 18.0, CHHO (2*R*,3'*R*-trace)), 5.11 (1H, d, *J* 18.0, CHHO (2*R*,3'*S*)), 5.07 (1H, d, *J* 18.0, CHHO (2*R*,3'*S*)), 4.96 (1H, d, *J* 18.0, CHHO (2*R*,3'*R*-trace)), 4.33 (1H, m, CHOH), 3.66 (3H, s, OCH₃), 2.90 (1H, d, *J* 5.4, OH), 1.79 (1H, m, CHH), 1.46–1.65 (3H, m, CHH and CH₂), 0.97 (3H, t, *J* 7.0, CH₂CH₃); ¹³C NMR (150 MHz; CDCl₃) δ 204.3 (C-2'), 166.2 (C=O ester), 131.7, 129.9, 128.5, 127.5, 123.0 (q, *J*_{CF} 290, CF₃), 75.1 (CHOH), 67.0 (CH₂OH), 55.8 (OCH₃), 36.0, 29.7, 13.8 (CH₂CH₃); ¹⁹F NMR (282 MHz; CDCl₃) δ -72.2; *m/z* (ES+) 371 (MNa⁺, 100%); Found (HRES) MNa⁺ 371.1096. C₁₆H₁₉O₅F₃Na requires 371.1106.

TK formation of 1,3-dihydroxyheptan-2-one (3c). WT-TK gave **3c** (24 mg, 16%) in 84% *ee* (3*S*-isomer) by HPLC (97:3, 1.0 mL min⁻¹). D469E-TK gave **3c** (84 mg, 58%) in 97% *ee* (3*S*-isomer) by HPLC (97:3, 1.0 mL min⁻¹); [α]_D²⁰ -38.5 (c 1.4, CH₃OH). H26Y-TK gave **3c** (10 mg, 7%) in 84% *ee* (3*R*-isomer) by HPLC (97:3, 1.0 mL min⁻¹); [α]_D²⁰ +18.6 (c 1.4, CH₃OH).

TK formation of 1,3-dihydroxyoctan-2-one (3d). WT-TK gave **3d** (40 mg, 25%) in 85% *ee* (3*S*-isomer) by HPLC (97:3, 1.0 mL min⁻¹). D469E-TK gave **3d** (75 mg, 47%) in 97% *ee* (3*S*-isomer) by HPLC (97:3, 1.0 mL min⁻¹); [α]_D²⁰ -32.5 (c 1.4, CH₃OH). H26Y-TK gave **3d** (20 mg, 12%) in 84% *ee* (3*R*-isomer) by HPLC (97:3, 1.0 mL min⁻¹); [α]_D²⁰ +16.0 (c 1.4, CH₃OH). The absolute stereochemistry of **3d** generated using D469E-TK was determined using the Mosher's derivatisation method.¹³

(2*R*,3'*S*)-3,3,3-Trifluoro-2-methoxy-2-phenyl propionic acid 3'-hydroxy-2'-oxo-octyl ester. The reaction was carried out under anhydrous conditions. To a stirred solution of **3d** from the D469E-TK reaction (0.015 g, 0.06 mmol) in CH₂Cl₂ (2 mL) was added triethylamine (20 μL, 0.13 mmol) and (*S*)-MTPA chloride (5 μL, 0.03 mmol) and the reaction was stirred for 2 h at rt. The product was dry loaded onto silica gel and purified using flash chromatography (hexane–EtOAc, 10:1) to afford the Mosher's derivative as a colourless oil (3.2 mg, 28%). ¹H NMR (600 MHz; CDCl₃) δ 7.64 (2H, m, Ph), 7.45 (3H, m, Ph), 5.20 (d, *J* 16.8, CHHO (2*R*,3'*R*-trace)), 5.10 (1H, d, *J* 16.8, CHHO (2*R*,3'*S*)), 5.07 (1H, d, *J* 16.8, CHHO (2*R*,3'*S*)), 4.96 (1H, d, *J* 16.8, CHHO (2*R*,3'*R*-trace)), 4.32 (1H, dd, *J* 8.0 and 3.9, CHOH), 3.66 (3H, s, OCH₃), 2.85 (1H, br s, OH), 1.05–1.80 (8H, m, 4 × CH₂), 0.89 (3H, t, *J* 7.3, CH₂CH₃); ¹³C NMR (150 MHz; CDCl₃) δ 204.3 (C-2'), 166.2 (C=O ester), 131.7, 129.9, 128.5, 127.5, 75.3 (CHOH), 67.0 (CH₂OH), 55.8 (OCH₃), 33.9, 32.0, 29.5, 22.7, 14.0 (CH₂CH₃); ¹⁹F NMR (282 MHz; CDCl₃) δ -72.2; *m/z* (ES+) 399 (MNa⁺, 100%); Found (HRES) MNa⁺ 399.1338. C₁₈H₂₃O₅F₃Na requires 399.1395.

TK formation of 1,3-dihydroxynonan-2-one (3e). WT-TK gave **3e** (13 mg, 7%) in 74% *ee* (3*S*-isomer) by HPLC (97:3, 1.2 mL min⁻¹). D469E-TK gave **3e** (25 mg, 14%) in 86% *ee* (3*S*-isomer) by HPLC (97:3, 1.2 mL min⁻¹); [α]_D²⁰ -22.7 (c 1.1, CH₃OH). H26Y-TK gave **3e** (6 mg, 4%) in 78% *ee* (3*R*-isomer) by HPLC (97:3, 1.2 mL min⁻¹); [α]_D²⁰ +36.7 (c 0.9, CH₃OH).

TK formation of 1,3-dihydroxydecan-2-one (3f). WT-TK gave **3f** (3 mg, 2%) in 66% *ee* (3*S*-isomer) by HPLC (97:3, 1.2 mL min⁻¹). D469E-TK gave **3f** (34 mg, 18%) in 86% *ee*

(3*S*-isomer) by HPLC (97:3, 1.2 mL min⁻¹); [α]_D²⁰ -13.3 (c 1.1, CH₃OH). H26Y-TK gave **3f** (39 mg, 21%) in 83% *ee* (3*R*-isomer) by HPLC (97:3, 1.2 mL min⁻¹); [α]_D²⁰ +9.1 (c 0.6, CH₃OH).

TK formation of 1-cyclopropyl-1,3-dihydroxy-2-propanone (3g). WT-TK gave **3g** (3 mg, 2%) in 72% *ee* (1*S*-isomer) by HPLC (97:3, 1.0 mL min⁻¹). D469E-TK gave **3g** (13 mg, 10%) in >99% *ee* (1*S*-isomer) by HPLC (97:3, 1.0 mL min⁻¹); [α]_D²⁰ +70.0 (c 0.3, CHCl₃). H26Y-TK gave no reaction. D469T-TK gave **3g** (14 mg, 10%) in 99% *ee* (1*S*-isomer), D469K-TK gave **3g** (3 mg, 2%) in 99% *ee* (1*S*-isomer), and D469L gave **3g** (2 mg, 2%) in 99% *ee* (1*S*-isomer). The absolute stereochemistry of **3g** generated using D469E-TK was determined using the Mosher's derivatisation method.¹³

(2*S*,3'*S*)-3,3,3-Trifluoro-2-methoxy-2-phenyl propionic acid 3'-cyclopropyl-3'-hydroxy-2'-oxo-propyl ester. The reaction was carried out under anhydrous conditions. To a stirred solution of **3g** from the D469E-TK reaction (0.010 g, 0.08 mmol) in CH₂Cl₂ (1 mL) was added triethylamine (34 μL, 0.25 mmol) and (*R*)-MTPA chloride (10 μL, 0.04 mmol) in CH₂Cl₂ (2 mL) and the reaction was stirred for 12 h at rt. The product was dry loaded onto silica gel and purified using flash chromatography (hexane–EtOAc, 4:1) to afford the Mosher's derivative as a colourless oil (0.013 g, 87%). *R*_f 0.45 (hexane–EtOAc; 1:1); [α]_D²⁰ +45.0 (c 0.2, EtOH); *v*_{max}(KBr)/cm⁻¹ 3420, 2930, 2855, 1734; ¹H NMR (300 MHz; CDCl₃) δ 7.63 (2H, m, Ph), 7.43 (3H, m, Ph), 5.37 (1H, d, *J* 15.0, CHHO (2*S*,3'*S*)), 5.17 (d, *J* 18.0, CHHO (2*S*,3'*R*-trace)), 5.05 (d, *J* 18.0, CHHO (2*S*,3'*R*-trace)), 4.95 (1H, d, *J* 15.0, CHHO (2*S*,3'*S*)), 4.33 (1H, m, CHOH), 3.60 (3H, s, OCH₃), 3.09 (1H, d, *J* 4.3 Hz), 1.03 (1H, m), 0.71 (2H, m), 0.55 (2H, m); ¹³C NMR (125 MHz; CDCl₃) δ 203.0 (C-2'), 166.3 (C=O ester), 131.8, 129.9, 128.5, 127.6, 78.1 (CHOH), 66.9 (CH₂OH), 55.8 (OCH₃), 14.7, 2.9 and 2.8; ¹⁹F NMR (282 MHz; CDCl₃) δ -72.3; *m/z* (FTMS) found [M + NH₄]⁺ 364.1364. C₁₆H₂₁F₃O₅N requires 364.1366.

TK formation of 1-cyclopentyl-1,3-dihydroxy-2-propanone (3h). WT-TK gave **3h** (2 mg, 1%) as a racemate. D469E-TK gave **3h** (63 mg, 40%) in >99% *ee* (1*S*-isomer) by HPLC (97:3, 1.0 mL min⁻¹); [α]_D²⁰ +33.0 (c 0.5, CHCl₃). H26Y-TK gave **3h** (3 mg, 2%) in 30% *ee* (1*R*-isomer), D469T-TK gave **3h** (47 mg, 30%) in 99% *ee* (1*S*-isomer) and D469K-TK gave **3h** (16 mg, 10%) in 25% *ee* (1*S*-isomer). The absolute stereochemistry of **3h** generated using D469E-TK was determined using the Mosher's derivatisation method.¹³

(2*S*,3'*S*)-3,3,3-Trifluoro-2-methoxy-2-phenyl propionic acid 3'-cyclopentyl-3'-hydroxy-2'-oxo-propyl ester. The reaction was carried out under anhydrous conditions. Triethylamine (34 μL, 0.25 mmol) and (*R*)-MTPA chloride (10 μL, 0.04 mmol) in CH₂Cl₂ (2 mL) were added to a stirred solution of **3h** from the D469E-TK reaction (0.010 g, 0.05 mmol) in CH₂Cl₂ (1 mL) and the reaction was stirred for 12 h at rt. The product was dry loaded onto silica gel and purified using flash chromatography (hexane–EtOAc, 4:1) to afford the Mosher's derivative as a colourless oil (0.018 g, 78%). *R*_f 0.50 (hexane–EtOAc; 4:1); [α]_D²⁵ -60.0 (c 0.1, CHCl₃); *v*_{max}(KBr)/cm⁻¹ 3429, 2930, 2855, 1733; ¹H NMR (600 MHz; CDCl₃) δ 7.62 (2H, m, Ph), 7.43 (3H, m, Ph), 5.20 (1H, d, *J* 16.9, CHHO (2*S*,3'*S*)), 4.92 (1H, d, *J* 16.9, CHHO (2*S*,3'*S*)), 4.31 (1H, d, *J* 3.6, CHOH), 3.65 (3H, s, OCH₃), 2.91 (1H, m), 2.23 (1H, m), 1.27–1.85 (10H, m, 5 × CH₂), no (2*S*,3'*R*)

detected; ^{13}C NMR (150 MHz; CDCl_3) δ 204.0 (C-2'), 166.3 (C=O ester), 131.9, 130.0, 128.6, 127.6, 123.2 (q, J_{CF} 287, CF_3), 84.7 (q, J_{CF} 27, CCF_3), 77.2 (CHOH), 67.4 (CH_2OH), 55.9 (OCH_3), 42.9, 29.1, 25.8 (signals superimposed); ^{19}F NMR (282 MHz; CDCl_3) δ -72.2; m/z (FTMS) found $[\text{M} + \text{NH}_4]^+$ 392.1678. $\text{C}_{18}\text{H}_{25}\text{F}_3\text{O}_5\text{N}$ requires 392.1679.

(2*R*,3'*S*)-3,3,3-Trifluoro-2-methoxy-2-phenyl propionic acid 3'-cyclopentyl-3-hydroxy-2'-oxo-propyl ester. The reaction was carried out under anhydrous conditions. Triethylamine (34 μL , 0.25 mmol) and (*S*)-MTPA chloride (10 μL , 0.04 mmol) in CH_2Cl_2 (2 mL) were added to a stirred solution of **3h** from the D469E-TK reaction (0.010 g, 0.05 mmol) in CH_2Cl_2 (1 mL), and the reaction was stirred for 12 h at rt. The product was dry loaded onto silica gel and purified using flash chromatography (hexane–EtOAc, 4:1) to afford the Mosher's derivative as a colourless oil (0.020 g, 87%). R_f 0.50 (hexane–EtOAc; 4:1); $[\alpha]_{\text{D}}^{25}$ +30.0 (c 0.1, CHCl_3); ν_{max} (KBr)/ cm^{-1} 3430, 2930, 1732; ^1H NMR (600 MHz; CDCl_3) δ 7.63 (2H, m, Ph), 7.43 (3H, m, Ph), 5.08 (1H, d, J 16.9, *CHHO* (2*R*,3'*S*)), 5.05 (1H, d, J 16.9, *CHHO* (2*R*,3'*S*)), 4.31 (1H, t, J 4.2, *CHOH*), 3.64 (3H, s, *OCH*₃), 2.90 (1H, d, J 4.2, *OH*), 2.23 (1H, m), 1.34–1.78 (10H, m, $5 \times \text{CH}_2$), no (2*R*,3'*R*) detected; ^{13}C NMR (150 MHz; CDCl_3) δ 204.0 (C-2'), 166.3 (C=O ester), 131.9, 130.0, 128.6, 127.6, 123.2 (q, J_{CF} 287, CF_3), 84.7 (q, J_{CF} 27, CCF_3), 77.0 (CHOH), 67.4 (CH_2OH), 55.9 (OCH_3), 42.8, 29.1, 25.8 (signals superimposed); ^{19}F NMR (282 MHz; CDCl_3) δ -72.2.

TK formation of 1-cyclohexyl-1,3-dihydroxy-2-propanone (3i). WT-TK gave **3i** (1 mg, 1%) as a racemate. D469E-TK gave **3i** (17 mg, 10%) in 97% *ee* (1*S*-isomer) by HPLC (97:3, 1.0 mL min^{-1}); $[\alpha]_{\text{D}}^{20}$ +33.0 (c 0.5, CHCl_3). H26Y-TK gave no reaction. D469T-TK gave **3i** (5 mg, 3%) in 99% *ee* (1*S*-isomer) and D469K-TK gave **3i** (5 mg, 3%) in 25% *ee* (1*S*-isomer). The absolute stereochemistry with D469E-TK was determined using the Mosher's derivatisation method.¹³

(2*S*,3'*S*)-3,3,3-Trifluoro-2-methoxy-2-phenyl propionic acid 3'-cyclohexyl-3-hydroxy-2'-oxo-propyl ester. The reaction was carried out under anhydrous conditions. To a stirred solution of **3i** from the D469E-TK reaction (0.010 g, 0.05 mmol) in CH_2Cl_2 (1 mL) was added triethylamine (34 μL , 0.25 mmol) and (*R*)-MTPA chloride (10 μL , 0.04 mmol) in CH_2Cl_2 (2 mL) and the reaction was stirred for 12 h at rt. The product was dry loaded onto silica gel and purified using flash chromatography (hexane–EtOAc, 4:1) to afford the Mosher's derivative as a colourless oil (0.018 g, 78%). R_f 0.45 (hexane–EtOAc; 4:1); $[\alpha]_{\text{D}}^{20}$ -26.0 (c 0.2, CHCl_3); ^1H NMR (300 MHz; CDCl_3) δ 7.63 (2H, m, Ph), 7.43 (3H, m, Ph), 5.19 (1H, d, J 17.0, *CHHO* (2*S*,3'*S*)), 5.07 (d, J 17.0, *CHHO* (2*S*,3'*R*-trace)), 5.03 (d, J 17.0, *CHHO* (2*S*,3'*R*-trace)), 4.90 (1H, d, J 17.0, *CHHO* (2*S*,3'*S*)), 4.16 (1H, dd, J 5.2, 3.3, *CHOH*), 3.65 (3H, s, *OCH*₃), 2.80 (1H, d, J 5.2, *OH*), 1.11–1.76 (11H, m); ^{13}C NMR (125 MHz; CDCl_3) δ 204.2 (C-2'), 166.2 (C=O ester), 131.9, 129.9, 128.5, 127.5, 79.7 (CHOH), 67.8 (CH_2OH), 55.8 (OCH_3), 41.9, 29.6, 26.4, 25.9 (signal overlap), 25.5; ^{19}F NMR (282 MHz; CDCl_3) δ -72.2; m/z (FTMS) found $[\text{M} + \text{NH}_4]^+$ 406.1831. $\text{C}_{19}\text{H}_{27}\text{F}_3\text{O}_5\text{N}$ requires 406.1836.

Modelling of substrate binding in WT-TK. The open source Autodock software¹⁹ was used for all substrate docking models in the *E. coli* TK structure 1qgd.pdb with a cubic grid in the active site

of sides 80 Å. Defaults were used for docking each substrate except for the following: the maximum number of energy evaluations was increased to 1 million, the number of genetic algorithm runs was increased from 10 to 200, and the grid spacing used was 0.375 Å. The enamine-ThDP intermediate structure obtained in yeast TK²³ was first docked into the *E. coli* TK, prior to docking of the aldehyde substrates.

Acknowledgements

CONACYT is thanked for a PhD studentship to A.C. and L.R.S. The UK Engineering and Physical Sciences Research Council (EPSRC) are thanked for DTA studentships to J.L.G. and L.G.C, and for support of the multidisciplinary Bioconversion Integrated with Chemistry and Engineering (BiCE) programme (GR/S62505/01). Financial support from the 12 industrial partners supporting the BiCE programme is also acknowledged. J. S. was supported on a Biotechnology and Biological Sciences Research Council (BBSRC) studentship (BBS/S/A/2004/10920). We thank the EPSRC National Mass Spectrometry Service Centre, Swansea University, for the provision of some high resolution MS data.

Notes and references

- 1 A. Schmid, J. S. Dordick, B. Hauer, A. Kiener, M. Wubbolts and B. Witholt, *Nature*, 2001, **409**, 258.
- 2 E. Racker, in *The Enzymes*, ed. P. D. Boyer, H. Lardy and K. Myrzbach, Academic Press, New York, 1961, Vol. 5 pp. 397.
- 3 P. Srere, J. R. Cooper, M. Tabachnick and E. Racker, *Arch. Biochem. Biophys.*, 1958, **74**, 295.
- 4 (a) J. Bolte, C. Demuyneck and H. Samaki, *Tetrahedron Lett.*, 1987, **28**, 5525; (b) F. Effenberger, V. Null and T. Ziegler, *Tetrahedron Lett.*, 1992, **33**, 5157; (c) L. Hecquet, J. Bolte and C. Demuyneck, *Tetrahedron*, 1994, **50**, 8677; (d) Y. Kobori, D. C. Myles and G. M. Whitesides, *J. Org. Chem.*, 1992, **57**, 5899; (e) R. K. Mitra, J. M. Woodley and M. D. Lilly, *Enzyme Microb. Technol.*, 1998, **22**, 64.
- 5 (a) C. Demuyneck, J. Bolte, L. Hecquet and V. Dalmas, *Tetrahedron Lett.*, 1991, **32**, 5085; (b) G. R. Hobbs, M. D. Lilly, N. J. Turner, J. M. Ward, A. J. Willets and J. M. Woodley, *J. Chem. Soc., Perkin Trans. 1*, 1993, 165; (c) K. G. Morris, M. E. B. Smith, N. J. Turner, M. D. Lilly, R. K. Mitra and J. M. Woodley, *Tetrahedron: Asymmetry*, 1996, **7**, 2185.
- 6 (a) N. J. Turner, *Curr. Opin. Biotechnol.*, 2000, **11**, 527; (b) J. Bongs, D. Hahn, U. Schörken, G. A. Sprenger and C. Wandrey, *Biotechnol. Lett.*, 1997, **19**, 213; (c) J. Shaeri, R. Wohlgenuth and J. M. Woodley, *Org. Process Res. Dev.*, 2006, **10**, 605; (d) J. Shaeri, I. Wright, E. B. Rathbone, R. Wohlgenuth and J. M. Woodley, *Biotechnol. Bioeng.*, 2008, **101**, 761.
- 7 M. D. Lilly, R. Chauhan, C. French, M. Gyamerah, G. R. Hobbs, A. Humphrey, M. Isupov, J. A. Littlechild, R. K. Mitra, K. G. Morris, M. Rupperecht, N. J. Turner, J. M. Ward, A. J. Willets and J. M. Woodley, *Recombinant Dna Biotechnology III: the Integration of Biological and Engineering Sciences*, 1996, 782, 513.
- 8 G. A. Sprenger and M. Pohl, *J. Mol. Catal. B: Enzym.*, 1999, **6**, 145.
- 9 D. C. Myles, P. J. Andrusis, III and G. M. Whitesides, *Tetrahedron Lett.*, 1991, **32**, 4835.
- 10 (a) C. U. Ingram, M. Bommer, M. E. B. Smith, P. A. Dalby, J. M. Ward, H. C. Hailes and G. J. Lye, *Biotechnol. Bioeng.*, 2007, **96**, 559; (b) U. Kaulmann, K. Smithies, M. E. B. Smith, H. C. Hailes and J. M. Ward, *Enzyme Microb. Technol.*, 2007, **41**, 628; (c) K. Smithies, M. E. B. Smith, U. Kaulmann, J. L. Galman, Ward and H. C. Hailes, *Tetrahedron: Asymmetry*, 2009, **20**, 570.
- 11 (a) E. G. Hibbert, T. Senussi, S. J. Costelloe, W. Lei, M. E. B. Smith, J. M. Ward, H. C. Hailes and P. A. Dalby, *J. Biotechnol.*, 2007, **131**, 425; (b) E. G. Hibbert, T. Senussi, M. E. B. Smith, S. J. Costelloe, J. M. Ward, H. C. Hailes and P. A. Dalby, *J. Biotechnol.*, 2008, **134**, 240.
- 12 M. E. B. Smith, E. G. Hibbert, A. B. Jones, P. A. Dalby and H. C. Hailes, *Adv. Synth. Catal.*, 2008, **350**, 2631.

-
- 13 J. Galman and H. C. Hailes, *Tetrahedron: Asymmetry*, 2009, **20**, 1828.
- 14 U. Schörken, H. Sahm and G. A. Sprenger, in *Biochemistry and Physiology of Thiamine Diphosphate Enzymes*, ed. H. Bisswanger and A. Schellenberger, Intemann, Prien, 1996, ch. 6, pp 543–554.
- 15 U. Nilsson, L. Meshalkina, Y. Lindqvist and G. Schneider, *J. Biol. Chem.*, 1997, **272**, 1864.
- 16 M. E. B. Smith, K. Smithies, T. Senussi, P. A. Dalby and H. C. Hailes, *Eur. J. Org. Chem.*, 2006, 1121.
- 17 M. E. B. Smith, B. H. Chen, E. G. Hibbert, U. Kaulmann, K. Smithies, J. L. Galman, F. Baganz, P. A. Dalby, H. C. Hailes, G. J. Lye, J. M. Ward, J. M. Woodley and M. Micheletti, *Org. Process Res. Dev.*, 2010, **14**, 99.
- 18 J. Littlechild, N. J. Turner, G. R. Hobbs and M. D. Lilly, *Acta Crystallogr., Sect. D: Biol. Crystallogr.*, 1995, **51**, 1074.
- 19 G. M. Morris, D. S. Goodsell, R. S. Halliday, R. Huey, W. E. Hart, R. K. Belew and A. J. Olson, *J. Comput. Chem.*, 1998, **19**, 1639.
- 20 P. Asztalos, C. Parthier, R. Golbik, M. Kleinschmidt, G. Hübner, M. S. Weiss, R. Friedemann, G. Wille and K. Tittmann, *Biochemistry*, 2007, **46**, 12037.
- 21 M. E. B. Smith, K. Smithies, U. Kaulmann, J. M. Ward and H. C. Hailes, *Bioorg. Med. Chem.*, 2006, **14**, 7062.
- 22 A. B. Pangborn, M. A. Giardello, R. H. Grubbs, R. K. Rosen and F. J. Timmers, *Organometallics*, 1996, **15**, 1518.
- 23 E. Fiedler, S. Thorell, T. Sandalova, R. Golbik, S. König and G. Schneider, *Proc. Natl. Acad. Sci. U. S. A.*, 2002, **99**, 591.

A Multidisciplinary Approach Toward the Rapid and Preparative-Scale Biocatalytic Synthesis of Chiral Amino Alcohols: A Concise Transketolase-/ ω -Transaminase-Mediated Synthesis of (2S,3S)-2-Aminopentane-1,3-diol

Mark E. B. Smith,[†] Bing H. Chen,^{‡¶} Edward G. Hibbert,^{‡□} Ursula Kaulmann,^{§■} Kirsty Smithies,[†] James L. Galman,[†] Frank Baganz,[‡] Paul A. Dalby,[‡] Helen C. Hailes,[†] Gary J. Lye,[‡] John M. Ward,[§] John M. Woodley,[‡] and Martina Micheletti^{*‡}

Department of Chemistry, University College London, 20 Gordon Street, London WC1H 0AJ, U.K., Department of Biochemical Engineering, University College London, Torrington Place, London WC1E 7JE, U.K., Institute of Structural and Molecular Biology, University College London, Gower Street, London WC1E 6BT, U.K., and Department of Chemical and Biochemical Engineering, Technical University of Denmark, 2800 Lyngby, Denmark

Abstract:

Chiral amino alcohols represent an important class of value-added biochemicals and pharmaceutical intermediates. Chemical routes to such compounds are generally step intensive, requiring environmentally unfriendly catalysts and solvents. This work describes a multidisciplinary approach to the rapid establishment of biocatalytic routes to chiral aminodiols taking the original synthesis of (2S,3S)-2-aminopentane-1,3-diol as a specific example. An engineered variant of *Escherichia coli* transketolase (D469T) was used for the initial asymmetric synthesis of (3S)-1,3-dihydroxypentane-2-one from the achiral substrates propanal and hydroxypyruvate. A bioinformatics led strategy was then used to identify and clone an ω -transaminase from *Chromobacterium violaceum* (DSM30191) capable of converting the product of the transketolase-catalysed step to the required (2S,3S)-2-aminopentane-1,3-diol using isopropylamine as an inexpensive amine donor. Experiments to characterize, optimize and model the kinetics of each reaction step were performed at the 1 mL scale using previously established automated microwell processing techniques. The microwell results provided excellent predictions of the reaction kinetics when the bioconversions were subsequently scaled up to preparative scales in batch stirred-tank reactors. The microwell methods thus provide process chemists and engineers with a valuable tool for the rapid and early evaluation of potential synthetic strategies. Overall, this work describes a concise and efficient biocatalytic route to chiral amino alcohols and illustrates an integrated multidisciplinary approach to bioconversion process design and scale-up.

1. Introduction

The pharmaceutical industry today faces significant challenges in bringing new drugs to the market. A key area of interest is in harnessing new technologies to progress from initial

drug discovery to the final manufacturing process as rapidly and cost-effectively as possible. Rising costs related to the development of increasingly complex pharmaceuticals (with multiple chiral centers and functional groups) are compounded by increasingly stringent environmental legislation and the drive toward sustainable processes. Working together with industry these are the technologies and challenges that the multidisciplinary UCL Bioconversion - Chemistry - Engineering interface (BiCE) programme aims to address.

While there are extensive synthetic transformations for which chemical (catalytic) conversions are most appropriate, biocatalytic (enzyme and microbial) strategies have been increasingly adopted where mild conditions and high regio- or stereoselectivity are desired.^{1,2} The majority of biocatalytic processes reported to date have involved the use of a single isolated enzyme. However, recent developments in metabolic engineering and synthetic biology have highlighted the possibility of using multienzyme synthetic pathways to perform more complex syntheses.^{3,4} Furthermore, many of the enzymes that could be used in series do not necessarily exist naturally together in known metabolic pathways. This raises the possibility of creating *de novo* pathways in engineered microorganisms using existing powerful tools such as rDNA technology. As a demonstration of such an approach we have previously devised a synthetic scheme using a transketolase (TK) and a transaminase (TAm) to create an optically enriched 2-amino-1,3-diol using an engineered *Escherichia coli* strain.⁵

Chiral 2-amino-1,3-diols are an important class of pharmaceutically relevant compounds, and their motif is present in antibiotics,^{6–10} antiviral glycosidase inhibitors,^{11,12} and sphingo-

* Corresponding author. E-mail: m.micheletti@ucl.ac.uk.

[†] Department of Chemistry, University College London.

[‡] Department of Biochemical Engineering, University College London.

[§] Institute of Structural and Molecular Biology, University College London.

[¶] Department of Chemical and Biochemical Engineering, Technical University of Denmark.

[□] Current address: Department of Chemical and Biochemical Engineering, College of Chemistry and Chemical Engineering, Xiamen University, Xiamen 361005, China.

[■] Current address: Illumina Cambridge Ltd., Chesterford Research Park, Cambridge CB10 1XL, UK.

[●] Current address: Biotica Ltd., Chesterford Research Park, Cambridge CB10 1XL, UK.

- (1) Pollard, D. J.; Woodley, J. M. *Trends Biotechnol.* **2007**, *25*, 66.
- (2) Woodley, J. M. *Trends Biotechnol.* **2008**, *26*, 321.
- (3) Ro, D. K.; Paradise, E. M.; Ouellet, M.; Fisher, K. J.; Newman, K. L.; Ndungu, J. M.; Ho, K. A.; Eachus, R. A.; Ham, T. S.; Kirby, J.; Chang, M. C.; Withers, S. T.; Shiba, Y.; Sarpong, R.; Keasling, J. D. *Nature* **2006**, *440*, 940.
- (4) Chang, M. C.; Eachus, R. A.; Trieu, W.; Ro, D. K.; Keasling, J. D. *Nat. Chem. Biol.* **2007**, *3*, 274.
- (5) Ingram, C. U.; Bommer, M.; Smith, M. E.; Dalby, P. A.; Ward, J. M.; Hailes, H. C.; Lye, G. J. *Biotechnol. Bioeng.* **2006**, *96*, 559.
- (6) Controulis, J.; Rebstock, M. C.; Crooks, H. M. *J. Am. Chem. Soc.* **1949**, *71*, 2463.
- (7) Wu, G.; Schumacher, D. P.; Tormos, W.; Clark, J. E.; Murphy, B. L. *J. Org. Chem.* **1997**, *62*, 2996.
- (8) Veeresa, G.; Datta, A. *Tetrahedron Lett.* **1998**, *39*, 8503.
- (9) Boruwa, J.; Borah, J. C.; Gogoi, S.; Barua, N. C. *Tetrahedron Lett.* **2005**, *46*, 1743.

lipids.^{13,14} A number of chemical methods exist to produce this class of amino alcohols including those starting from the chiral pool materials serine^{8,15,16} and glucose,¹⁷ Sharpless asymmetric dihydroxylation with subsequent regioselective azide substitution^{18,19} and nucleophilic attack of α,β -epoxy carboxylic esters with azide followed by azide and ester reduction.²⁰ However, these procedures are either step-intensive and/or make use of toxic catalysts. We have recently developed the first nonenzymatic one-pot synthesis of α,α' -dihydroxyketones via a mimetic of the transketolase reaction.²¹ However, no asymmetric variant of this synthesis has been developed to date, and thus reductive amination of the racemic products obtained from this reaction can only be manipulated into mixtures of diastereoisomers. Alternatively, using TK in combination with a TAm potentially offers a highly concise, stereospecific, and benign biocatalytic route to this key class of synthons.

In vivo TK catalyses the transfer of a two-carbon ketol unit from D-xylulose-5-phosphate, to either D-ribose-5-phosphate or D-erythrose-4-phosphate.²² The enantioselective carbon-carbon bond-forming ability of TK, together with the ability to yield an irreversible reaction when using β -hydroxypyruvate (HPA) as the ketol donor, makes it very attractive as a biocatalyst in industrial synthesis.^{23,24} Although nonhydroxylated aliphatic aldehydes can be accepted by TK, the activity is typically very low. Using active-site targeted saturation mutagenesis we have recently identified several mutants with improved activities, notably a novel TK mutant, D469T, with a nearly 5-fold increase in specific activity when screened towards the nonhydroxylated aldehyde acceptor substrate, propionaldehyde (PA), for the production of 1,3-dihydroxypentan-2-one (DHP).²⁵ Other mutants with improved, and even reversed, enantioselectivity have also been described.²⁶ ω -Transaminases, such as that isolated from *Vibrio fluvialis*, have been shown to aminate a wide range of aldehyde and ketone substrates. This is not true for α -transaminases which typically have a strong preference for either α -ketoacids or α -amino acids as substrates.²⁷ However, several transaminases which efficiently aminate an

aromatic α,α' -dihydroxyketone have been described.²⁸ Recently we used the published sequence of the ω -TAm isolated from *V. fluvialis* to conduct a bioinformatics-based search of genome homologues, thereby facilitating the recruitment and characterization of novel ω -TAMs.²⁸ The production of chiral aliphatic 2-amino-1,3-diols from chiral ketodiols using the ω -TAM recruited from *Chromobacterium violaceum* DSM30191 (CV2025) would demonstrate the significant commercial potential of this enzyme and class on bioconversion.

From an engineering perspective, there are several factors contributing to the successful implementation of a multienzymatic process such as a linked TK- ω -TAm bioconversion. In order to achieve a competitive final product yield the reaction rates and initial substrate loading(s) need to be maximised, whilst at the same time overcoming issues of substrate or product inhibition of each enzyme. The identification of the "best" biocatalyst at an early stage is crucial since recent advances in protein engineering have enabled the subsequent modification of enzymes to achieve greater activity, enhanced stability and enantioselectivity, and wider substrate range.²⁹ Ultimately, experiments performed early during development need to provide insight into the most suitable strategies for process optimization and scale-up in order to maximize the yield of product on substrate and catalyst. In this regard we have recently established a range of automated and microscale (100–1000 μ L) experimental techniques to successfully mimic key bioprocess unit operations. An understanding of the engineering fundamentals governing experimentation at this scale underpins the ability to obtain quantitative results capable of predicting larger-scale process performance.^{30–32}

The aim of this work is to demonstrate a challenging and novel example of a two-step stereoselective biocatalytic synthesis of 2-amino-1,3-diols using a multidisciplinary approach that integrates (1) enzymes obtained either by directed evolution or bioinformatics-based cloning strategies, (2) microscale experimentation and robotics for rapid process optimisation and scale-up, (3) advanced high-throughput analytical techniques for small-molecule detection and analysis, and (4) establishment of an enzymatic kinetic model from microscale data for the rapid design of the larger-scale bioconversion process. Specifically, as shown in Scheme 1, we have focused on the TK D469T-catalysed conversion of propanal (**1**) and hydroxypyruvate (HPA) (**2**) to (3*S*)-1,3-dihydroxypentan-2-one (DHP) (**3**) and the subsequent CV2025 ω -TAm-catalysed conversion of DHP to (2*S*,3*S*)-2-aminopentane-1,3-diol (APD) (**4**).

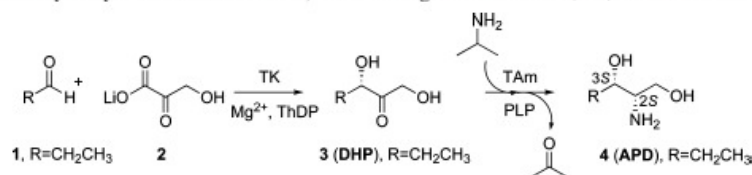
2. Results and Discussion

2.1. Multidisciplinary Approach and Strategy. Taking into account the lack of kinetic information available on the TK D469T and CV2025 ω -TAm-catalyzed reactions, a detailed

- (10) Hajra, S.; Karmakar, A.; Maji, T.; Medda, A. K. *Tetrahedron* **2006**, *62*, 8959.
- (11) Hughes, A. B.; Rudge, A. J. *J. Nat. Prod. Rep.* **1994**, *11*, 135.
- (12) Liang, P. H.; Cheng, W. C.; Lee, Y. L.; Yu, H. P.; Wu, Y. T.; Lin, Y. L.; Wong, C. H. *Chem. Biochem.* **2006**, *7*, 165.
- (13) Nakamura, T.; Shiozaki, M. *Tetrahedron* **2001**, *57*, 9087.
- (14) Hannun, Y. A.; Obeid, L. M. *J. Biol. Chem.* **2002**, *277*, 25847.
- (15) Ndakala, A. J.; Hashemzadeh, M.; So, R. C.; Howell, A. R. *Org. Lett.* **2002**, *4*, 1719.
- (16) Azuma, H.; Takao, R.; Niuro, H.; Shikata, K.; Tamagaki, S.; Tachibana, T.; Ogino, K. *J. Org. Chem.* **2003**, *68*, 2790.
- (17) Chaudhari, V. D.; Kumar, K. S. A.; Dhavale, D. D. *Org. Lett.* **2005**, *7*, 5805.
- (18) He, L.; Byun, H. S.; Bittman, R. *J. Org. Chem.* **2000**, *65*, 7627.
- (19) Smithies, K.; Smith, M. E. B.; Kaulmann, U.; Galman, J. L.; Ward, J. M.; Hailes, H. C. *Tetrahedron: Asymmetry* **2009**, *20*, 570.
- (20) Takanami, T.; Tokoro, H.; Kato, D. I.; Nishiyama, S.; Sugai, T. *Tetrahedron Lett.* **2005**, *46*, 3291.
- (21) Smith, M. E. B.; Smithies, K.; Senussi, T.; Dalby, P. A.; Hailes, H. C. *Eur. J. Org. Chem.* **2006**, 1121.
- (22) Sprenger, G. A.; Schorken, U.; Sprenger, G.; Sahm, H. *Eur. J. Biochem.* **1995**, *2*, 525.
- (23) Hobbs, G. R.; Lilly, M. D.; Turner, N. J.; Ward, J. M.; Willetts, A. J.; Woodley, J. M. *J. Chem. Soc., Perkin Trans. I* **1993**, 165.
- (24) Hibbert, E. G.; Dalby, P. A. *Microb. Cell Fact.* **2005**, *4*, 29.
- (25) Hibbert, E. G.; Senussi, T.; Smith, M. E. B.; Costelloe, S. J.; Ward, J. M.; Hailes, H. C.; Dalby, P. A. *J. Biotechnol.* **2008**, *134*, 240.
- (26) Smith, M. E. B.; Hibbert, E. G.; Jones, A. B.; Dalby, P. A.; Hailes, H. C. *Adv. Synth. Catal.* **2008**, *350*, 2631.

- (27) Okada, K.; Hirotsu, K.; Hayashi, H.; Kagamiyama, H. *Biochemistry* **2001**, *40*, 7453.
- (28) Kaulmann, U.; Smithies, K.; Smith, M. E. B.; Hailes, H. C.; Ward, J. M. *Enzyme Microb. Technol.* **2007**, *41*, 628.
- (29) Dalby, P. A. *Curr. Opin. Struct. Biol.* **2003**, *13*, 500.
- (30) Doig, S. D.; Pickering, S. C. R.; Lye, G. J.; Woodley, J. M. *Biotechnol. Bioeng.* **2002**, *80*, 42.
- (31) Micheletti, M.; Lye, G. J. *Curr. Opin. Biotechnol.* **2006**, *17*, 611.
- (32) Micheletti, M.; Barrett, T.; Doig, S. D.; Baganz, F.; Levy, M. S.; Woodley, J. M.; Lye, G. J. *Chem. Eng. Sci.* **2006**, *61*, 2939.

Scheme 1. Two-step biocatalytic synthesis of 2-amino-1,3-diols using transketolase (TK) and transaminase (TAm)



initial characterization was considered necessary for both enzymes in order to determine the optimal reaction conditions in terms of substrate concentration ratios, enzyme loading, and in the case of the ω -TAm-catalysed step, potential use of a cosolvent. This lack of initial kinetic information is a common feature at the early stages of bioconversion process evaluation and so is typically the starting point for experimental studies. Automated microscale experimentation was initially used for this purpose, and experiments were planned with a view to subsequent integration of the two steps and ultimately process scale-up. Development of a successful and scalable enzymatic synthesis of APD (4) involved specifically: (i) evaluation of the TK D469T-catalysed step (section 2.2), (ii) evaluation of the CV2025 ω -TAm-catalysed step (section 2.3), and (iii) integration of the two enzymatic steps such that a concise synthesis of APD (4) could be successfully modeled and then verified experimentally at preparative scale (section 2.4). Underpinning this approach was the establishment of high-throughput assays to characterize the synthetic potential of the enzymes and to quantitatively determine the influence of process conditions on biocatalyst performance.

2.2. TK Evaluation. Mutants of *Escherichia coli* transketolase with improved substrate specificity towards the non-natural aldehyde substrate propanal have been obtained by directed evolution in a previous study.²⁵ In particular mutant D469T was identified from an active site library of TK mutants as being a likely catalyst, showing a 4.9-fold increase in specific activity with this substrate, compared to wild-type TK. The D469 residue was previously identified as important for substrate binding by Schörken who carried out a kinetic analysis of several *E. coli* transketolase mutants obtained by using site-directed mutagenesis.^{33,34} This mutant enzyme was therefore selected for use in the proposed biocatalytic process demonstration (Scheme 1). The availability of an analytical method for the study of the TK-catalysed reaction was crucial in order to quantify the reaction kinetics. Several TK assays have been reported for product quantification;^{23,35–37} however, an HPLC assay was established²⁵ in order to detect both HPA (2) starting material and the product of the propanal reaction, DHP (3). The assay time and sample loading needed were minimized to increase the throughput in accord with the microscale experi-

mentation strategy. In-house chemical synthesis²¹ of HPA (2) and racemic DHP (3) provided samples for calibration purposes to ensure complete quantitative analysis of this reaction. As propanal is a rather volatile substrate, control experiments were carried out to confirm that no loss was occurring during sampling and that all mass balances were closed.

The TK D469T-catalysed reaction required optimization in order to achieve the highest possible product yield and reaction rate. For simplicity of operation, a batch reaction approach to performing the bioconversion was adopted. The final concentration of both propanal (1) and HPA (2) were dictated to a degree by the necessary requirement to preincubate the enzyme with its cofactors, ThDP and Mg²⁺, prior to the introduction of the substrates. It has been previously documented that aldehyde substrates react with primary amines forming a Schiff base and may therefore react with enzymes exhibiting these functional groups in accessible positions, thus affecting enzyme activity.³⁵ A significant effect of glycolaldehyde on halo- and apo-transketolase activity has been shown at a range of aldehyde concentrations.³⁵ For this reason a strategy of working at an excess of propanal was immediately ruled out. Taking into account the economic implications of working at high HPA concentrations, it was decided on the basis of these observations and requirements to optimize the TK-catalysed step using equimolar and stoichiometric concentrations of propanal and HPA.

All TK D469T evaluation experiments were carried out at 1 mL scale and at room temperature using previously established automated microwell methods.³¹ At this scale the reaction pH was controlled at pH = 7 using appropriate buffers and concentrations. Initial experiments were carried out at 50, 100, 200, and 300 mM concentrations of reagents in stoichiometric amounts with 30% v/v cell-free lysate (Figure 1a). At 200 mM substrate concentration the reaction went to completion in 8–10 h, with reaction rates increasing from 22.2 mmol L⁻¹ h⁻¹ of DHP (3) to 57 mmol L⁻¹ h⁻¹ at 50 and 200 mM initial substrate concentrations, respectively. When the initial substrate concentration was set at 300 mM, an initial rate of 45.3 mmol L⁻¹ h⁻¹ was obtained, indicating the probable effects of aldehyde inhibition and/or toxicity on the enzyme. Increasing the amount of enzyme used increased the final product yield (Figure 1b). Increasing the lysate concentration from 30% to 50% v/v, whilst maintaining the substrate concentration at 300 mM, allowed complete conversion to DHP (3) to be achieved in 5–10 h and with an initial rate of 92.5 mmol L⁻¹ h⁻¹. This set of microwell reaction conditions was therefore selected as the optimum for the TK D469T-catalysed synthesis of the intermediate product (3S)-1,3-dihydroxypentan-2-one (DHP) (3) and was subsequently adopted for the larger-scale reaction (section 2.4).

2.3. TAm Evaluation. The value of the well-known *V. fuvialis* ω -TAm JS17 for synthetic applications has already

(33) Bisswanger, H.; Schellenberger, A., Eds. *Biochemistry and Physiology of Thiamin Diphosphate Enzymes*; A.u.C. Intemann, Wissenschaftlicher Verlag: Prien, Germany, 1996.

(34) Schörken, U. *Investigation of Structure and Function of Transketolase and Transaldolase from Escherichia coli and Biochemical Characterization of the Enzymes*; Institut für Biotechnologie, Jülich, Germany, 1997.

(35) Mitra, R. K.; Woodley, J. M.; Lilly, M. D. *Enzyme Microb. Technol.* **1998**, *22*, 64.

(36) Sevestre, A.; Hélaine, V.; Guyot, G.; Martin, C.; Hecquet, L. *Tetrahedron Lett.* **2003**, *44*, 827.

(37) Smith, M. E. B.; Kaulmann, U.; Ward, J. M.; Hailes, H. C. *Bioorg. Med. Chem.* **2006**, *14*, 7062.

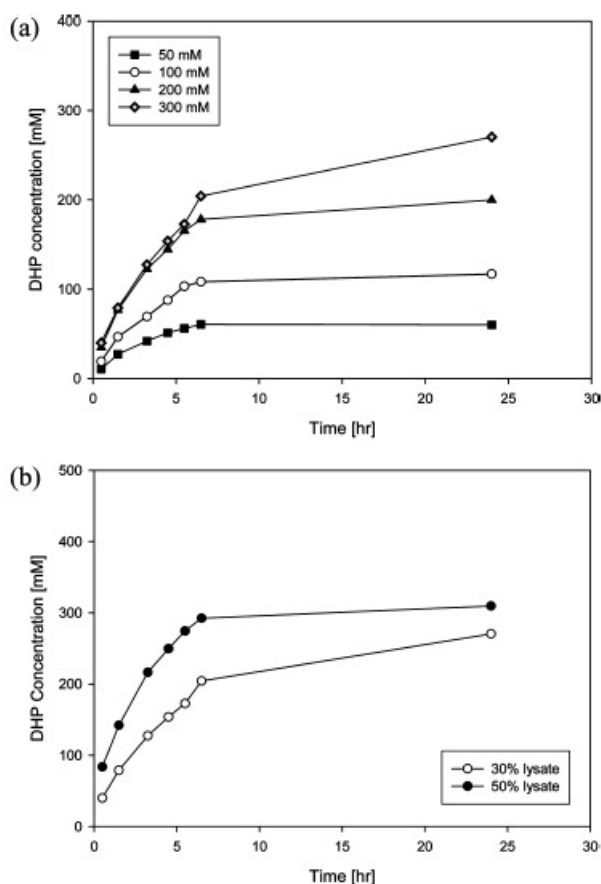


Figure 1. Characterization of the TK D469T reaction step at 1 mL scale. (a) Effect of substrate, propanal and HPA, concentration on product formation kinetics at stoichiometric conditions with 30% v/v lysate. (b) Effect of enzyme concentration on product formation kinetics at stoichiometric conditions and 300 mM substrate concentration.

been widely recognized. Both the ketol 3-hydroxy-2-butanone (acetoin) and the aromatic amino alcohol 2-phenylglycine are reported to be accepted by the enzyme as substrates.³⁸ *V. fluvialis* and related ω -TAMs therefore have the potential to be used as biocatalysts in the preparation of chiral 2-amino-1,3-diols. Since the *V. fluvialis* ω -TAM is not publicly available, a detailed search for homologues of this enzyme was carried out in the genome databases of fully sequenced bacteria using the published protein sequence of the enzyme. This led to the identification, cloning into *E. coli*, and partial characterization of 12e ω -TAMs from a variety of bacteria. The most efficient ω -TAM²⁸ for aminodiol synthesis among all those recruited was that from *C. violaceum* DSM30191 (CV2025). Initial experiments using the CV2025 enzyme with DHP (3) indicated it was converted to APD (4), and so further experiments were performed using this enzyme.

Preliminary experiments to investigate the potential of running a one-pot reaction found that the CV2025 ω -TAM could act upon the TK substrates in the presence of an amine donor (data not shown). Consequently, it was decided to run the synthesis as two sequential steps. Since solvent extraction was

(38) Shin, J. S.; Kim, B. G. *J. Org. Chem.* **2002**, *67*, 2848.

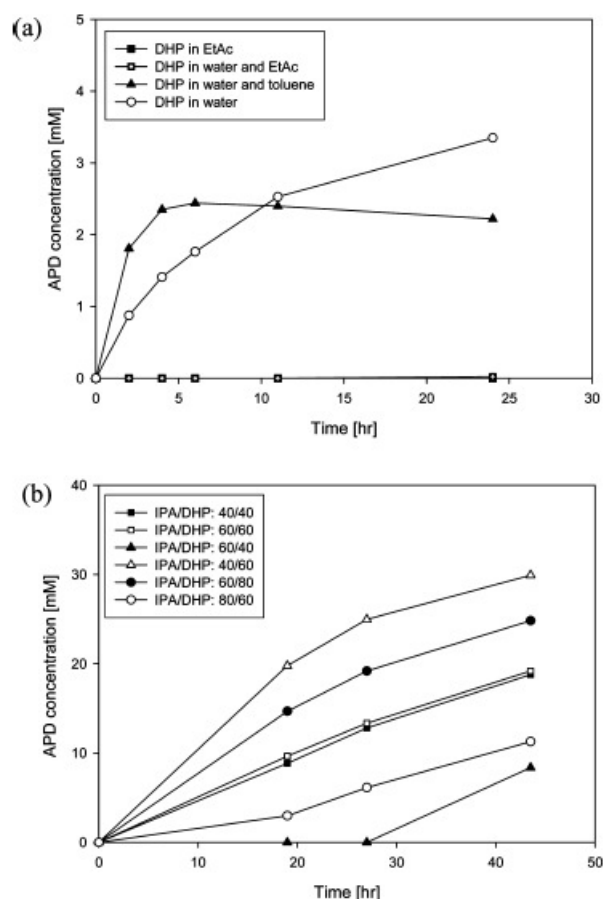


Figure 2. Characterization of the TAM reaction step at 1 mL scale. (a) Effect of cosolvent and type on product formation kinetics using the CV2025 ω -TAM. (b) Effect of substrate, IPA, and DHP ratio on product formation kinetics.

envisaged as the likely method for isolation of the intermediate product DHP (3) from the initial TK D469T-catalysed reaction, an appraisal of solvent tolerance was carried out for the *C. violaceum* ω -TAM. All evaluation experiments were carried out at the 1 mL microwell scale using buffers for pH control as in the TK studies. Ethyl acetate (EtOAc) and toluene were initially evaluated as solvents with differing polarities and physicochemical properties. The influence of these solvents on the kinetics of the CV2025 ω -TAM-catalysed conversion of DHP (3) to APD (4) using isopropylamine (IPA) as the amine donor is illustrated in Figure 2a. When the transamination of DHP (3) in EtOAc was carried out, no aminodiol product was formed. Similarly, no product was detected when the reaction was carried out in a mixture of EtOAc and water. Using toluene as a cosolvent proved to be more positive with an excellent initial rate of reaction observed. However, after a relatively short period of time the reaction ceased, suggesting that the solvent may be having an adverse effect on the CV2025 ω -TAM over time. It was therefore concluded that use of a cosolvent was not appropriate in the TAM-catalysed step. Consequently, it would be necessary to isolate the intermediate DHP product from the TK D469T-catalysed reaction by solvent extraction prior to the second CV2025 ω -TAM step.

Table 1. Characterization of the CV2025 ω -TAM reaction at 1 mL scale: impact of the amount of cell lysate on the extent of APD (4) formation over 24 h based on initial substrate concentrations of 40 mM of IPA and 60 mM of DHP

lysate (enzyme) concentration (% v/v)	[APD] after 6 h (mM)	[APD] after 24 h (mM)
30	8.7	22.7
40	11.8	22.5
50	12.8	19.6
60	13.5	21.5
70	14.3	20.0
80	18.1	22.0

Given that the product yield from the ω -TAM step will depend upon the equilibrium position of the reaction, another crucial variable with regard to process optimization is the ratio of the amine donor to DHP (3). Initial experiments to investigate this were conducted with a number of amine donors (data not shown), systematically varying each of the substrate concentrations while maintaining the other constant. The aim of these experiments was to identify donors with minimal inhibition effects on the enzyme. Preliminary studies conducted with (*S*)-(α)-methylbenzylamine, which has been used in other transaminase systems,³⁹ showed the detrimental effect of using an excess of this amine donor, probably due to its toxicity towards the enzyme. Attempts were made to reduce this effect by carrying out the reaction in the presence of a nonpolar organic solvent, the aim being to diminish the effective concentration of the amine in the ω -TAM-containing aqueous phase whilst ensuring that the DHP (3) remains in the reactive phase. The use of hexadecane allowed for higher concentrations of amine to be present in the reactor; however, the maximum working concentration of (*S*)-(α)-methylbenzylamine was still limited to 40 mM. Alternative amine donors were therefore examined, and similar conversions were achieved with a cheaper, more volatile, and more water-soluble substrate, isopropylamine (IPA). At comparable reaction concentrations the quantity of product 4 formed was similar when using (*S*)-(α)-methylbenzylamine and IPA without the need for additional organic solvent. In addition, any excess IPA (and its product, acetone) could be more easily removed downstream compared to the aromatic amine.

Figure 2a shows the results obtained at different substrate ratios of the selected amine donor, IPA, and DHP (3) using 30% v/v lysate. The highest concentration of APD (4) achieved was 30 mM, obtained with 40 mM of IPA and 60 mM DHP. In order to further increase the reaction rate, increased quantities of cell lysate were used that allowed for the same amount of product to be formed in shorter periods of time. The results of these experiments are shown in Table 1. Approximately the same amount of product formed using 30% v/v cell lysate in 48 h could be obtained in 24 h using 80% v/v cell lysate. The enzyme activity values, based on initial rates, were 10.8 and 15.6 U g⁻¹_{TAM} for 30% and 80% v/v cell-free lysate concentrations, respectively. A compromise is therefore needed between the cost of preparing an increased amount of cell lysate and the overall reaction time when operating conditions for scale-up are selected. It is noteworthy that the reaction could be

(39) Shin, J. S.; Kim, B. G. *Biosci. Biotechnol. Biochem.* 2001, 65, 1782.

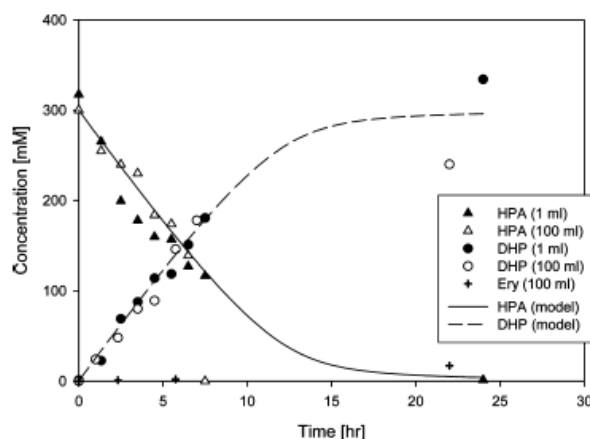


Figure 3. Comparison of TK D469T reaction kinetics at microwell (open symbols) and 100 mL (solid symbols) scales and with the kinetic model predictions (lines). TK reaction performed at 300 mM stoichiometric substrate concentration and 40% v/v lysate. Model predictions are based on eq 1 using the kinetic parameters shown in Table 2 determined from microscale experiments.

potentially driven to completion by feeding of one of the two substrates or by enzymatic⁴⁴ or in situ product removal.⁴⁵

2.4. TK-TAM Reaction Scale-up, Modeling, and Integration. Once the optimal conditions for each biocatalytic step had been assessed, the reactions optimized at microwell scale were scaled to 100 mL scale for the TK D469T reaction and 333 mL for the ω -TAM reaction. Both reactions were performed in laboratory-scale batch stirred-tank reactors. At the 100 mL scale, the pH of the TK-catalysed reaction was maintained at pH 7.0 by the use of automated pH stat addition of 1 M HCl (aq) to minimize the salt concentration in the reactor outlet and waste stream. The kinetic profiles for the TK D469T reactions conducted at both 100 and 1 mL scale, using 300 mM of both HPA and PA and 40% v/v cell lysate, are shown in Figure 3. The results of the microwell optimized conditions have scaled excellently, showing very similar kinetic profiles after a 100-fold scale-up. Calculated values of the initial reaction rates varied by just 15%, confirming the utility of the automated microwell experiments for rapid process optimization and scale-up. The product DHP (3) was extracted from the reaction via multiple solvent extractions into EtOAc. Subsequent removal of the solvent under vacuum gave the product as an oil in 68% yield. The ee of the product was determined by diacetylation and chiral GC to be comparable to that previously reported of 64%.²⁶ No reduction in ee was thus observed during the transition to preparative-scale operation. This crude DHP material was taken forward without further purification as substrate for the following ω -TAM step of the synthesis.

At this stage in process development a reliable enzyme kinetic model for the TK D469T mutant would be desirable in order to predict reaction rate and yield over a range of bioreactor operating conditions. The general TK reaction mechanism is well-known and leads to the following kinetic expression based on competitive substrate inhibition:

$$\frac{d[Q]}{dt} = \frac{k_{\text{cat}}E_i[A][B]}{K_b[A]\left(1 + \frac{[A]}{K_{ia}}\right) + K_a[B]\left(1 + \frac{[B]}{K_{ib}}\right) + [A][B] + \frac{K_a}{K_{iq}}[B][Q] + \frac{K_a K_{ib}}{K_{iq}}[Q]} \quad (1)$$

Solutions to such models are, however, difficult to establish due to the large number of experiments required to determine the specific kinetic constants for a particular enzyme mutant and set of reaction substrates. We have previously reported a model-driven approach to kinetic parameter identification that combines automated microscale experimentation with numerical methods for kinetic parameter estimation from a minimum number of experiments.^{40,41} This approach was used here to rapidly determine the kinetic parameters for the new TK D469T mutant for DHP (**3**) synthesis from propanal (**1**) and HPA (**2**).

The specific reaction kinetic parameters obtained are presented in Table 2. Comparing the model parameters it can be seen that there is a major difference in reaction rate between use of propanal (**1**) as substrate compared to the kinetic parameters previously reported for glycolaldehyde.⁴² Another key difference is that the Michaelis constant for propanal is 6 times that of glycolaldehyde. The consequence of this for process design is that significantly more TK D469T will be required for the propanal/HPA reaction in order to achieve the same bioconversion rate. Using eq 1 and the kinetic parameters listed in Table 2 from microscale experimentation, Figure 3 also shows the predicted preparative-scale bioconversion kinetics (solid and dashed lines). The good agreement between the experimentally determined preparative-scale reaction kinetics and the model predictions confirms the utility of the modeling approach. Such modeling tools can build confidence for process chemists and engineers in process scale-up, reactor sizing, and first approximations of the process costs.

Following the TK D469T-catalysed synthesis of DHP (**4**), the subsequent CV2025 ω -TAm reaction was performed using 40 mM IPA and 60 mM DHP together with cofactor PLP and 30% v/v clarified lysate in HEPES buffer. After 24 h, an Amberlite IRA-410 resin was added with stirring to the final product mixture to remove any HEPES from solution. The filtrate was then passed through an Isolute SCX-2 (Biotage) ion-exchange column which retained the desired APD product

Table 2. Enzyme kinetic parameters for the TK D469T-catalysed conversion of propanal, PROP (**1**), and HPA (**2**) into (3*S*)-1,3-dihydroxypentan-2-one (**3**)^a

kinetic parameters	value
rate constant: K_{cat} (min^{-1})	501
Michaelis constant for HPA: K_a (mM)	12
Michaelis constant for PROP: K_b (mM)	98
inhibition constant for HPA: K_{ia} (mM)	43
inhibition constant for PROP: K_{ib} (mM)	625
inhibition constant for DHP: K_{iq} (mM)	681

^a Kinetic parameters determined using the method described in section 2.4 from 34 microscale (1 mL) experiments at a range of substrate and enzyme concentrations.

(**4**) whilst allowing all other impurities to be washed away. The APD was then released from the column by elution with 4 M ammonia in methanol, giving the product as a solid in 26% isolated yield. Reports using (*S*)-(α)-methylbenzylamine as the amine donor with ω -Tams and our studies using the *C. violaceum* ω -TAm with aromatic α,α' -dihydroxyketones have indicated selectivity for formation of the *S*-amine.^{19,39} The ee of the product **4** at C-2 was determined to be >98% and postulated from previous work to be the 2*S*-isomer. The de of **4** was 61% by chiral HPLC, the impurity being exclusively (2*S*,3*R*)-2-aminopentane-1,3-diol. This indicated that the *C. violaceum* ω -TAm was able to accept both (*R*)- and (*S*)-isomers of **3**, highlighting its potential versatility, and demonstrated excellent stereoselectivity in catalyzing the conversion of the ketone DHP (**3**) to the amine moiety in APD (**4**).

Table 3 provides a summary of the reaction and recovery yields of each step of the TK D469T and CV2025 ω -TAm-catalysed route to APD (**4**). For the TK reaction there is particularly good agreement between the reaction rates (as previously discussed) and yields achieved at the two scales. The isolated yield of the final product at 26% is acceptable at this stage since little attention has been directed toward optimization of the recovery process. This two-step biocatalytic synthesis represents an extremely concise and atom-efficient route to such aminodiols. Indeed, a recent study focused on compound screening for fungicidal activity reported the nine-step synthesis of the *anti*-2*S*,3*R*-isomer of APD.⁴² The biocatalytic route reported here thus represents a significant improvement. On the basis of the process design information obtained at the microwell scale (sections 2.2 and 2.3) and subsequently verified here at the preparative scale, Figure 4 shows a feasible process flowsheet of how the complete two-step biocatalytic synthesis might proceed at a manufacturing scale. Standard geometry stirred tank bioreactor configurations would be best suited for the two bioconversion steps since for the TK reaction at least mass transfer limitations have been reported when performed without mixing or shaking at volumes higher than 10 mL.⁴³ The product of the first biocatalytic reaction, an aqueous mixture of DHP and other lysate components, can be followed by a suitable enzyme recovery step, such as ultrafiltration, from where the TK enzyme could be recycled to the bioreactor. A solvent extraction step using EtOAc in a simple mixer/settler unit is necessary to separate the DHP (**3**) from the other components. After removal of the EtOAc under vacuum, the DHP would then be redissolved in water to the optimal concentration for the following CV2025 ω -TAm reaction. Following enzyme separation the product mixture from this reaction containing ADP (**4**) and unreacted substrates would

(40) Chen, B. H.; Hibbert, E. G.; Dalby, P. A.; Woodley, J. M. *A.I.Ch.E.J.* **2008**, *54*, 2155.

(41) Chen, B. H.; Micheletti, M.; Baganz, F.; Woodley, J. M.; Lye, G. J. *Chem. Eng. Sci.* **2009**, *64*, 403.

(42) Thevissen, K.; Hillaert, U.; Meert, E. M. K.; Chow, K. K.; Cammue, B. P. A.; Van Calenbergh, S.; François, I. E. J. A. *Bioorg. Med. Chem. Lett.* **2008**, *18*, 3728.

(43) Matosevic, S.; Micheletti, M.; Woodley, J. M.; Lye, G. J.; Baganz, F. *Biotechnol. Lett.* **2008**, *30*, 995.

(44) Koszelewski, D.; Lavandera, I.; Clay, D.; Rozzell, D.; Kroutil, W. *Adv. Synth. Catal.* **2008**, *350*, 2761.

(45) Lye, G. J.; Woodley, J. M. *Trends Biotechnol.* **1999**, *17*, 395.

Table 3. Comparison of microscale and preparative-scale yield data for the TK D469T (batch reactor 1) and CV2025 ω -TAm (batch reactor 2) conversions showing reaction conditions, product concentrations, and isolated product yields (N/D = not determined)

reaction scale (mL)	batch reactor R1 [D469T, 300 mM HPA/PA, TK 40% v/v]		batch reactor R2 [CV2025, 40 mM IPA/60 mM DHP, TAm 30% v/v]	
	product [DHP] (mM)	isolated yield (%)	product [APD] (mM)	isolated yield (%)
1	300	N/D	22.7	N/D
100	300	68	37.8	26

undergo a simple resin-based purification step, as described above, prior to a final evaporation step to obtain the dry solid product.

3. Conclusion

The two-step biocatalytic preparative synthesis of (2*S*,3*S*)-2-aminopentane-1,3-diol from the achiral starting substrates, propanal and hydroxypyruvate, and the inexpensive amine donor, isopropylamine, represents a concise and efficient route to this class of compound. The synthesis was facilitated by the ability to engineer the TK enzyme to accept the non-natural substrate propanal and the use of bioinformatics-led strategies to identify a suitable ω -TAm able to accept the intermediate TK product and convert it into the final desired synthon. The use of automated microscale processing techniques facilitated rapid optimisation and initial scale-up of the two biocatalytic steps. Such microscale approaches are particularly useful at the early stages of process development where quantities of key intermediates and information of their reaction kinetics are scarce.

While the TK D469T mutant displays desirable reaction rates and yields, alternative recently identified mutants could be used,²⁵ or the D469T mutant could be further engineered to specifically improve the ee of the product of this reaction step. Similarly, now that a suitable ω -TAm has been cloned and overexpressed, strategies to increase the rate and yield of this step could be explored including directed evolution of the enzyme or the application of techniques to shift the reaction equilibrium to product formation such as enzymatic byproduct removal⁴⁴ or *in situ* product removal.⁴⁵

4. Experimental Section

Materials. Unless otherwise noted, solvents and reagents were reagent grade from commercial suppliers (Sigma-Aldrich)

and used without further purification. ¹H NMR and ¹³C NMR spectra were recorded at the field indicated using a Bruker AMX300 MHz and AMX500 MHz machines. Coupling constants are measured in hertz (Hz) unless otherwise specified, NMR spectra were recorded at 298 K. Mass spectra were recorded on a Thermo Finnegan MAT 900XP spectrometer. LC-MS was performed on a Finnigan LTQ mass spectrometer and an Agilent 1100 HPLC (G1322A degasser, G1311A quaternary pump, and a G1367A autosampler). The data were processed using Xcalibur Quan browser. Lithium hydroxypyruvate was synthesised as previously described.⁴⁶ The TK D469T mutant was engineered, overexpressed in *E. coli*, and obtained as a clarified lysate as reported elsewhere.²⁵ Similarly the CV2025 ω -TAm from *C. violaceum* was cloned, overexpressed in *E. coli*, and obtained as a clarified lysate as reported previously.²⁸

Automated Microscale Bioconversion Methods. TK D469T and CV2025 ω -TAm bioconversions were carried out in 96-deep square well (96-DSW) and 96-standard round well (96-SRW) microplate formats over a range of experimental conditions. Automated microscale process sequences involving bioconversion setup and operation, sample acquisition, and processing were established for both reaction steps shown in Scheme 1. Automation was achieved using a Genesis Workstation (Tecan, Berkshire, UK) equipped with a liquid handling arm and a RoMa arm for plate manipulation. Disposable tips were used for reagent addition. The accuracy and precision of pipetting were determined for the low viscosity liquids and dispense volumes used in this work, and the error was less than 5% in all cases.³² All the experiments were carried out in a Class II robotic containment cabinet.

Analytical Methods. Progress of the TK D469T-catalysed synthesis of (*S*)-1,3-dihydroxypentan-2-one was monitored by HPLC: 100% of 0.1% TFA in water, 0.6 mL/

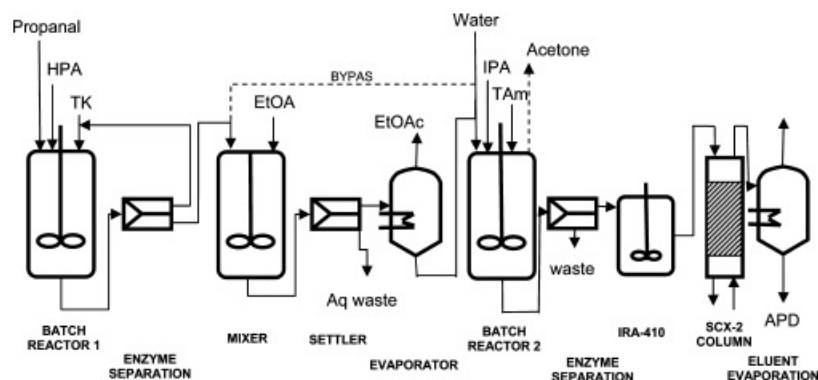


Figure 4. Proposed manufacturing process flow sheet for the large-scale, two-step TK D469T (batch reactor 1) and CV2025 ω -TAm (batch reactor 2) biocatalytic synthesis and purification of (2*S*,3*S*)-2-aminopentane-1,3-diol.

min, a 15 cm C18 column, 0.1% TFA (aq), 0.6 mL/min, UV detection at 210 nm, HPA 2 8.95 min, DHP (3) 15.55 min, propanal 22.53 min.²⁵

The ee of the (*S*)-1,3-dihydroxypentan-2-one was determined by first derivatising the ketodiol to the diacetate as previously described.²⁶ The assay was performed against a racemic sample of the diacetate using chiral GC: β -Dex column (Supelco, 30 m \times 0.25 mm); injection volume, 1 μ L; carrier gas, He; carrier gas pressure, 15 psi; injector temperature, 250 $^{\circ}$ C; oven temperature, 60 $^{\circ}$ C and then increased at 10 $^{\circ}$ C/min to 160 $^{\circ}$ C and held; detector temperature, 300 $^{\circ}$ C; detection, flame-ionised detector (FID). Retention times: (*R*)-isomer, 13.7 min; (*S*)-isomer, 13.9 min.

Progress of the ω -TAm-catalysed synthesis of (2*S*,3*S*)-2-aminopentane-1,3-diol was monitored by LC-MS. Ten microliters of the aminodiol biotransformation reaction mixture was dissolved in 990 μ L acetonitrile. The solutions were then homogenised by vortex for 10 s in a 2 mL centrifuge tube. This was followed by centrifugation at 13000 rpm for 5 min. The supernatant was transferred to a glass autosampler vial and 1 μ L injected into the chromatographic system. For screening the reaction, separation between DHP and APD was achieved using isocratic conditions of 40% 10 mmol NH₄OAc and 60% acetonitrile at a flow rate of 0.2 mL min⁻¹, and the analytical column was a ZIC-HILIC column (50 mm \times 2.1 mm, i.d., 5 μ m particle size) maintained at 20 $^{\circ}$ C. Operating conditions of the ESI interface in positive ion mode: capillary temperature 245 $^{\circ}$ C, capillary voltage 2 kV, spray voltage 4 kV, sheath gas 30, auxiliary gas 0, sweep gas 10 arbitrary units. For LC-MS calibration purposes stock standard solutions (10 mmol) of APD were prepared in water. Six calibration standards were prepared (0.6–12 ng/mL) covering the possible concentration range of the reaction (0–10 mmol conversion) and six point calibration curves were generated. Over the concentration ranges linear regression of observed peak areas against concentration gave correlation coefficients from 0.9935 to 0.9996. Limit of quantitation (LOQ) for APD from the low-level spiked matrix with 1 μ L injected on a 2.1 mm i.d. column was determined (*S/N* = 3) to be 0.6 ng/mL.

The ee and de of the (2*S*,3*S*)-2-aminopentane-1,3-diol (**4**) was determined by first derivatising the aminodiol to the tribenzoate. The assay was performed against a four diastereoisomer sample of the tribenzoate (synthesised as described in the Supporting Information) using chiral HPLC: Chiracel-OD column (Daicel); mobile phase, isopropanol/hexane (5:95); flow rate, 0.8 mL/min, detection, UV 214 nm. Retention times; 26.7 min, 31.5 min, 40.6 min, 47.8 min for the (2*R*,3*S*)-, (2*S*,3*S*)-, (2*S*,3*R*)-, and (2*R*,3*R*)-isomers, respectively.

Preparation of (*S*)-1,3-Dihydroxypentan-2-one. Thiamine diphosphate (111 mg, 240 μ mol) and MgCl₂·6H₂O (183 mg, 900 μ mol) were added to a reaction vessel containing H₂O (6.7 mL), and the pH was adjusted to 7.0 using 0.1 M NaOH (aq). To the stirred solution was added clarified TK D469T lysate (40 mL, XL10:pQR412(D469T), containing 1.37 mg/mL of TK by densitometry), and the mixture stirred for 20 min. In another flask, lithium hydroxypyruvate (3.30 g, 300 mmol) and propanal (2.16 mL, 30 mmol) were dissolved in H₂O (53.3 mL), and

the pH was adjusted to 7.0 using 1 M NaOH (aq). Following the 20 min enzyme incubation, the solution of hydroxypyruvate and propanal was added to the enzyme solution with stirring, and the reaction commenced. The pH of the reaction was maintained at 7.0 using a pH stat (Metrohm Stat Titrimo) *via* addition of 1 M HCl (aq) and the progress of the reaction followed by HPLC. After 22 h, the crude reaction mixture was extracted with EtOAc (10 \times 100 mL), and the combined organics were dried over MgSO₄. Filtration and concentration of the organics yielded the desired compound (2.40 g, 68%). The ee of the product was determined by chiral GC to be 61% (*S*-isomer). Found (+HRCI) MH⁺, 119.07043; C₅H₁₁O₃ requires 119.07082. ¹H NMR (300 MHz; D₂O): δ 0.82 (3H, t, *J* 7.5, CH₃), 1.49–1.76 (2H, m, CH₂CH₃), 4.22 (1H, dd, *J* 7.7 and 4.4, CHOH), 4.37 (1H, d, *J* 19.4, CH₂OH), 4.46 (1H, d, *J* 19.4, CH₂OH); ¹³C NMR (75 MHz; H₂O): δ 8.7, 26.5, 65.3, 76.1, 214.5.

Preparation of (2*S*,3*S*)-2-Aminopentane-1,3-diol. (*S*)-1,3-Dihydroxypentan-2-one (2.36 g; 0.5 M in water, 40 mL) was added to a solution of isopropylamine (1.25 mL; 6.7 M in water, 4.54 mL, pH 7.5) in 1 M HEPES (23.3 mL, pH 7.5) containing and pyridoxal 5'-phosphate hydrate (17.1 mg, 69 μ mol) To this mixture was further added water (165.5 mL) and clarified CV2025 ω -TAm lysate (100 mL). Lysate was obtained in 100 mM HEPES, pH 7.5, containing 0.2 mM PLP, 0.5 mM phenylmethyl sulfonyl fluoride (PMSF), and 8 U of benzonase (Novagen)/mL of cell extract. The reaction was shaken in a 500 mL Erlenmeyer flask at 100 rpm and 37 $^{\circ}$ C for 48 h and monitored exclusively by LC-MS. The enzyme was spun down (4500 rpm, at 4 $^{\circ}$ C for 10 min), and the mixture was additionally filtered through a 0.2 μ m sterile filter. Amberlite IRA-410 resin (50 g) was added to the reaction mixture. After 1 h, the resin was removed by filtration and washed with H₂O (300 mL). The aqueous mixture was then passed through an Isolute SCX-2 (Biotage) ion-exchange column (40 g of resin) and the column washed with MeOH (2 \times 200 mL). The column was then eluted with 4 M NH₃ in MeOH (3 \times 200 mL) and the eluent concentrated to yield the desired product as a solid (410 mg, 26%). The ee of the (2*S*,3*S*)-product was determined to be >98% (*S*-isomer at C-2) and the de determined as 61% by chiral HPLC, the impurity being exclusively (2*S*,3*R*)-2-aminopentane-1,3-diol. Found (+HRCI) MH⁺, 120.10250; C₅H₁₄NO₂ requires 120.10245; ¹H NMR (500 MHz; D₂O): δ 0.93 (2.4H, t, *J* 7.5, CH₃), 0.94 (0.6H, t, *J* 6.5, CH₃), 1.40–1.60 (2H, m, CH₂CH₃), 2.76 (0.8H, ddd, *J* 6.3, 5.1, and 4.6, CHNH₂), 2.81 (0.4H, ddd, *J* 7.5, 5.9, and 4.1, CHNH₂), 3.47–3.76 (3H, m, CH₂OH and CHOH); ¹³C NMR (75 MHz; H₂O): δ (2*S*,3*S*) 10.1, 26.3, 55.8, 64.1, 73.7; (2*S*,3*R*) 9.9, 25.6, 56.2, 63.7, 74.7.

Acknowledgment

We thank the UK Engineering and Physical Sciences Research Council (EPSRC) for support of the multidisciplinary Bioconversion Integrated with Chemistry and Engineering (BiCE) programme (GR/S62505/01). For further information see <http://www.ucl.ac.uk/biochemeng/industry/bice>. Financial

(46) Dickens, F. *Biochim. Prep.* 1962, 9, 86.

support from the 13 industrial partners supporting the BiCE programme is also acknowledged.

ThDP thiamine diphosphate
TK transketolase

NOMENCLATURE

APD (2*S*,3*S*)-2-aminopentane-1,3-diol
DHP 1,3-dihydroxypentan-2-one
EtOAc ethylacetate
HPA β -hydroxypyruvate
IPA isopropylamine
PA propionaldehyde
PLP pyridoxal 5'-phosphate
TAm transaminase
TFA trifluoroacetic acid

Supporting Information Available

Further detail of experimental methods including synthesis and analysis of the four diastereomer mixture of 2-aminopentane-1,3-diol hydrochloride and the chiral HPLC assay for the determination of ee and de of transaminase-derived 2-aminopentane-1,3-diol and synthesis of related standards. This material is available free of charge via the Internet at <http://pubs.acs.org>.

Received for review July 24, 2009.

OP900190Y

α,α' -Dihydroxyketone formation using aromatic and heteroaromatic aldehydes with evolved transketolase enzymes†

James L. Galman,^a David Steadman,^a Sarah Bacon,^b Phattaraporn Morris,^c Mark E. B. Smith,^a John M. Ward,^b Paul A. Dalby^c and Helen C. Hailes^{a*}

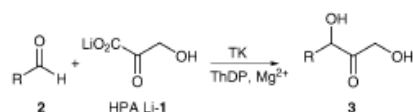
Received 30th July 2010, Accepted 25th August 2010

DOI: 10.1039/c0cc02911d

Transketolase mutants have been identified that accept aromatic acceptors with good stereoselectivities, in particular benzaldehyde for which the wild type enzyme showed no activity.

The advantages of using biocatalysts as a sustainable resource in synthesis are well established and include their potential to achieve high regio- and stereoselectivities.^{1,2} Transketolase (TK) (E.C.2.2.1.1) is a thiamine diphosphate (ThDP) dependent carbon-carbon bond forming enzyme.³ *In vivo* it reversibly transfers a two carbon ketol unit to D-erythrose-4-phosphate and D-ribose-5-phosphate.^{3,4} To render the reaction irreversible *in vitro*, β -hydroxyppyruvic acid (HPA 1) has been used extensively as the ketol donor and *E. coli* TK shows higher specific activity towards 1 than yeast and spinach TKs.^{5,6} TKs have been used with a range of non-phosphorylated α -hydroxyaldehydes, where good conversion rates and stereospecificities for the (2*R*)-hydroxyaldehyde acceptor were observed, to give (*S*)- α,α' -dihydroxyketones 3 (Scheme 1).^{4,7} Wild-type (WT) TKs have been noted to tolerate some non- α -hydroxylated aliphatic aldehydes, but compared to α -hydroxyaldehydes lower substrate activities were reported.⁸ *E. coli* TK has also been overexpressed,⁹ and there is interest in industrial applications.¹⁰

To generate TKs with improved properties towards hydrophobic substrates for synthetic applications, saturation mutagenesis libraries were created, each targeted to one TK active-site residue.¹¹ Single point active-site mutants were identified with improved activity towards propanal (R = CH₂CH₃) that were selective for (3*S*)-3 and (3*R*)-3.¹² Several variants were from the D469X library: D469E with propanal gave 3*S*-3 in 90% ee and D469Y 3*R*-3 in 53% ee.¹² The mutant D469E-TK has also been shown to decrease the acceptance of formaldehyde and glycolaldehyde compared to



Scheme 1 TK catalysed reaction to generate α,α' -dihydroxy ketones 3.

^a Department of Chemistry, University College London, 20 Gordon Street, London WC1H 0AJ, UK.
E-mail: h.c.hailes@ucl.ac.uk; Fax: +44 (0)20 7679 7463;
Tel: +44 (0)20 7679 4654

^b Research Department of Structural & Molecular Biology, University College London, Gower Street, London WC1E 6BT, UK
^c Department of Biochemical Engineering, University College London, Torrington Place, London WC1E 7JE, UK

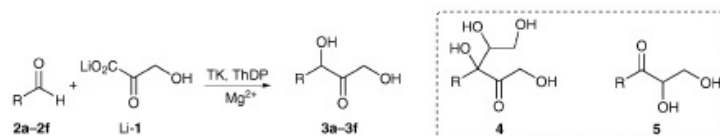
† Electronic supplementary information (ESI) available: Characterisation data for 3a–3f formation. See DOI: 10.1039/c0cc02911d

WT-TK,¹³ while a yeast TK crystal structure showed that the equivalent residue hydrogen bonds to the C-2 hydroxy group of erythrose-4-phosphate in the active site.¹⁴ For these reasons the D469X library was investigated with a series of linear aldehydes (C₄ to C₈) and C₃, C₅ and C₆ cyclic carboxaldehydes.¹⁵ Excellent ees (86–99%) were observed with the D469E mutant and variable yields (10–58%) which were generally lower with the cyclic aldehydes.¹⁵

The α,α' -dihydroxyketones 3 produced by TK are valuable building blocks for conversion to other chiral synthons such as 2-amino-1,3-diols.¹⁶ For example, (*rac*)-1,3-dihydroxy-1-phenylpropane-2-one synthesised non-enzymatically can be converted using a transaminase enzyme to (1*rac*,2*S*)-2-amino-1-phenyl-1,3-propanediol, a motif present in several antibiotics such as thiamphenicol and fluoramphenicol.¹⁷

In the current work the focus was to identify TK variants able to accept aromatic and heteroaromatic aldehydes. Such substrates in terms of their reactivity and structure are far removed from the natural aldoses used *in vivo*. Previous work has highlighted the possible acceptance of aromatic and heteroaromatic substrates. 2-Furaldehyde has been used with *E. coli* TK but very low *V*_{red}s were observed,^{8b} as was the case for benzaldehyde and 2-furaldehyde with yeast TK, although 2-thiophene-carboxaldehyde was more readily accepted.^{8a} *E. coli* variants D469E and D469A have been used with pyridine carboxaldehydes where conversions were observed, but no reaction occurred with benzaldehyde or 2-furaldehyde.¹⁸ However, as previously highlighted, no data corresponding to the TK products have ever been reported, and reactions were typically monitored by determining HPA 1 consumption, which can undergo slow decomposition.^{6,19} The use of aldehydes with aromatic moieties have been reported using WT-TK including phenylacetaldehyde and 2-hydroxy-phenylacetaldehyde, to give products in 26% (isomeric mixture) and 54% yield ((3*S*,4*R*)-isomer), respectively.^{8c,20}

Initially, benzaldehyde 2a and Li-1 were used with WT-TK, but no reaction was observed (Scheme 2, Table 1). Benzaldehyde was then screened against the D469X library utilising the tetrazolium red colorimetric assay for use with non- α -hydroxylated aldehydes.¹⁹ From this several promising mutants were selected: D469E, D469K, D469S, and D469T. Interestingly, D469E, D469K and D469T had also been identified as suitable variants for use with the cyclic aldehydes where D469E and D469T gave (3*S*)-products in > 97% ee.¹⁵ An engineered TK mutant F434A was also selected for investigation as this highly conserved first-shell residue is adjacent to the D469 site and the mutation to alanine was therefore predicted to improve substrate acceptance for larger



Scheme 2 Formation of dihydroxyketones 3 using TK and side products 4 and 5.

Table 1 Stereoselectivities for WT-TK and TK mutant reactions with aromatic aldehydes

Aldehyde	Product	WT-TK ee or isomer (yield)	D469E ee or isomer (yield)	D469T ee or isomer (yield)	D469K ee or isomer (yield)	F434A ee or isomer (yield)
2a 	3a (R = Ph)	No reaction	0% (2%) [4 (5%)]	70% (3R) (2%) [4 (5%)]	82% (3R) (2%) [4 (5%)]	82% (3R) (10%) no 4
2b 	3b (R = furyl)	No reaction	— (5%) [5 (<2%)]	— (3%) [5 (<2%)]	— (3%) [5 (<2%)]	— (1%) [5 (<2%)]
2c 	3c (R = thienyl)	No reaction	— (2%) [5 (<2%)]	— (3%) [5 (<2%)]	— (2%) [5 (<2%)]	— (1%) [5 (<2%)]
2d 	3d (R = CH ₂ Ph)	93% (3S) (5%)	90% (3S) (50%)	96% (3S) (50%)	95% (3S) (50%)	97% (3S) (48%)
2e 	3e (R = CH(CH ₃)Ph)	88% (3S,4R) 12% (3S,4S) (35%)	95% (3S,4R) 5% (3S,4S) (30%)	96% (3S,4R) 4% (3S,4S) (40%)	95% (3S,4R) 5% (3S,4S) (38%)	85% (3S,4R) 15% (3S,4S) (35%)
2f 	3f (R = <i>m</i> -(OH)C ₆ H ₄)	No reaction	No reaction	0% (4%)	—	53% (3R) (6%)

aromatic and heteroaromatic aldehydes by removing hydrophobic and steric interactions within the active site. From the colorimetric assay variant D469S gave significant amounts of product and was explored further. However, product analysis revealed only a trace of **3a**, and instead a double addition product **4** ($R = \text{Ph}$) was isolated, resulting from the aldol addition of **3a** to glycolaldehyde, presumably generated from decarboxylation of the donor HPA *in situ*. An additional experiment was performed using **3a** (prepared using the biomimetic reaction²¹) with Li-I and D469S-TK and no **4** was formed, and was repeated with D469T-TK with the same result. This suggested that the addition to glycolaldehyde might occur in the active site while the intermediate leading to **3a** is still attached to ThDP, or with **3a** when it has been formed. However the formation of **3a**, even as an intermediate product was promising. Benzaldehyde was then used with the other selected mutants and **3a** isolated in yields of 2–10% (Table 1), with variant F434A giving the highest yield. Care was taken when isolating **3a** due to the ease of rearrangement to **5** ($R = \text{Ph}$). For the first time these experiments established that as with several other ThDP dependent enzymes, such as pyruvate decarboxylase (PDC), TK-mutants can accept benzaldehyde even though the yields are low. For D469E, D469K and D469T 5% of **4** ($R = \text{Ph}$) was also generated. By comparison, the mutant F434A gave no double addition product **4**, but **3a** in 10% yield, perhaps reflecting that with increased accessibility to the active site, with the substitution of Phe to Ala, the product **3a** can more readily exit the active site region avoiding glycolaldehyde addition. For HPLC analysis of the optical purities of **3a**, it was

dibenzoylated and determination of the absolute stereochemistry was achieved by the formation of the Mosher's ester at the primary hydroxyl with (*S*)- and (*R*)-MTPACl.²² Mutant D469E gave **3a** as a racemate, in contrast to the high stereoselectivities observed with this mutant for the aliphatic linear and cyclic aldehydes.¹⁵ Variants D469K, D469T and F434A gave **3a** in 82% ee, 70% ee and 82% ee, respectively, and in all cases the 3*R*-isomer was formed predominantly, comparable to the (*R*)-hydroxyketones formed using ThDP dependent PDC and benzaldehyde lyase. By analysis of an alignment of 382 TPP-dependent enzyme sequences described previously,²³ the position equivalent to F434 is always Phe or Tyr, except in phospho- or sulfo-pyruvate decarboxylases (Asn), and most interestingly is Ala only in benzoyl formate decarboxylase and benzaldehyde lyase enzymes, indicating the potential role of the F434A mutation for acceptance of the benzene ring. Position D469 is typically Asp or Asn and occurs naturally as Lys of Thr only in a few PDC and PDC-related enzymes.

With several TK mutants able to accept benzaldehyde, the use of aromatic and heteroaromatic aldehydes **2b–2f** was also investigated. Products **3b–3f** were prepared for chiral assay development from aldehydes **2b–2f** using the biomimetic reaction.²¹ For the determination of ees by chiral HPLC **3d** and **3e** were monobenzoylated at the primary alcohol and **3f** dibenzoylated, and Mosher's ester derivatisation of **3d**, **3e**, and **3f** performed.²² For **2b** and **2c** no conversions to **3b** and **3c** were observed with WT-TK. When using the D469 mutants and F434A products **3b** and **3c** were formed in low yields

< 5%, with < 2% of the rearranged dihydroxyketone **5** and no **4**. Attempts to derivatise **3b** and **3c** as esters for absolute stereochemistry and ee determination were not successful: rearrangement to **5** occurred. Phenylacetaldehyde **2d** and (*rac*)-2-phenylpropionaldehyde **2e** were initially used with WT-TK and **3d** and **3e** formed in 5% and 35% yield, where the more bulky α -methylated aldehyde was accepted more readily. Phenylacetaldehyde has been used with *E. coli* WT-TK to give **3d** and **5** (R = CH₂Ph) as a mixture of isomers, although here only **3d** was formed, possibly due to maintenance of the pH during the reaction. The D469 mutants and F434A led to the formation of **3d** in approximately 50% yield, and **3e** in 30–40% yield. For **3d** ees in the range 90–97% (*3S*-isomer) were determined with the highest stereoselectivity observed with F434A. ¹H NMR analysis of **3e** formed by D469T indicated the presence of two diastereoisomers, one major and one minor. Monobenzylation and chiral HPLC analysis revealed two products in a ratio of 96 : 4. Use of (*2R*)-**2e** in the biomimetic reaction and chiral HPLC peak correlation, together with the Mosher's method indicated that the major product formed using (*rac*)-**2e** with the D469 mutants and F434A was (*3S,4R*)-**3e**, and the minor isomer (*3S,4S*)-**3e**. The D469 mutants were therefore enantioselective for (*2R*)-**2e**, and stereoselectively formed the (*3S*)-isomer. When (*2R*)-**2e** was used with D469T only (*3S,4R*)-**3e** was formed. 2-Hydroxy-phenylacetaldehyde has been used with *E. coli* WT-TK and generates the (*3S,4R*)-isomer.²⁰ Despite removal of the key hydrogen-bonding interaction between the aldehyde C-2 hydroxyl and D469, H100, H26, indicated from yeast TK studies, and replacement with a methyl group this aldehyde enantioselectivity was maintained.^{11,14} To probe whether a hydroxylated benzaldehyde might influence active site hydrogen bonding interactions, the aldehyde **2f** was used. No reaction was observed with WT-TK or D469E, but with D469T racemic **3f** and F434A (*3R*)-**3f** formed (53% ee).

These results are extremely interesting, for the first time it has been shown that selected TK mutants can accept benzaldehyde, however the stereoselectivity observed is the opposite to that reported for the aliphatic series. In addition, phenylacetaldehyde and 2-methyl phenylacetaldehyde gave products in good yields and high ees when using the single point mutants. Higher reactivities with phenylacetaldehydes compared to benzaldehyde may reflect increased conformational flexibilities, less steric interactions, and higher reactivities. The yields for the formation of **3a–3c** and **3f** probably reflect low rates due to poor access to the active site, since the use of F434A clearly enhanced product formation. However, for more productive reactions, the yield may also be influenced by product inhibition or enzyme deactivation: aldehyde solubility is not limiting with these substrates. This work also highlights the importance of product isolation: TK assays based on HPA consumption or colorimetric detection of hydroxyketones cannot distinguish between products **3** and **4**. With identification of the first TK mutants to definitively accept benzaldehyde, further studies are now underway to produce improved combination mutants.

The EPSRC are thanked for DTA studentships to J.L.G. and support of the Bioconversion Integrated with Chemistry

and Engineering (BiCE) programme (GR/S62505/01). The UCL Department of Chemistry are thanked for funding D.S., the Thai government for support to P.M. and the BBSRC for a studentship to S.B.

Notes and references

- 1 A. Schmid, J. S. Dordick, B. Hauer, A. Kiener, M. Wubbolts and B. Witholt, *Nature*, 2001, **409**, 258.
- 2 K. M. Koeller and C. H. Wong, *Nature*, 2001, **409**, 232.
- 3 E. Racker, in *The Enzymes*, ed. P. D. Boyer, H. Lardy and K. Myrzbach, Academic Press, New York, 1961, vol. 5, p. 397.
- 4 N. J. Turner, *Curr. Opin. Biotechnol.*, 2000, **11**, 527.
- 5 P. Srere, J. R. Cooper, M. Tabachnick and E. Racker, *Arch. Biochem. Biophys.*, 1958, **74**, 295.
- 6 G. A. Sprenger and M. Pohl, *J. Mol. Catal. B: Enzym.*, 1999, **6**, 145.
- 7 (a) J. Bolte, C. Demuyck and H. Samaki, *Tetrahedron Lett.*, 1987, **28**, 5525; (b) F. Effenberger, V. Null and T. Ziegler, *Tetrahedron Lett.*, 1992, **33**, 5157; (c) L. Hecquet, J. Bolte and C. Demuyck, *Tetrahedron*, 1994, **50**, 8677; (d) Y. Kobori, D. C. Myles and G. M. Whitesides, *J. Org. Chem.*, 1992, **57**, 5899; (e) R. K. Mitra, J. M. Woodley and M. D. Lilly, *Enzyme Microb. Technol.*, 1998, **22**, 64.
- 8 (a) C. Demuyck, J. Bolte, L. Hecquet and V. Dalmas, *Tetrahedron Lett.*, 1991, **32**, 5085; (b) G. R. Hobbs, M. D. Lilly, N. J. Turner, J. M. Ward, A. J. Willets and J. M. Woodley, *J. Chem. Soc., Perkin Trans. 1*, 1993, 165; (c) K. G. Morris, M. E. B. Smith, N. J. Turner, M. D. Lilly, R. K. Mitra and J. M. Woodley, *Tetrahedron: Asymmetry*, 1996, **7**, 2185.
- 9 M. D. Lilly, R. Chauhan, C. French, M. Gyamerah, G. R. Hobbs, A. Humphrey, M. Isupov, J. A. Littlechild, R. K. Mitra, K. G. Morris, M. Rupperecht, N. J. Turner, J. M. Ward, A. J. Willets and J. M. Woodley, *Ann. N. Y. Acad. Sci.*, 1996, **782**, 513.
- 10 (a) J. Bongs, D. Hahn, U. Schorken, G. A. Sprenger and C. Wandrey, *Biotechnol. Lett.*, 1997, **19**, 213; (b) J. Shaeri, R. Wohlgenuth and J. M. Woodley, *Org. Process Res. Dev.*, 2006, **10**, 605; (c) J. Shaeri, I. Wright, E. B. Rathbone, R. Wohlgenuth and J. M. Woodley, *Biotechnol. Bioeng.*, 2008, **101**, 761.
- 11 (a) E. G. Hibbert, T. Senussi, S. J. Costelloe, W. Lei, M. E. B. Smith, J. M. Ward, H. C. Hailes and P. A. Dalby, *J. Biotechnol.*, 2007, **131**, 425; (b) E. G. Hibbert, T. Senussi, M. E. B. Smith, S. J. Costelloe, J. M. Ward, H. C. Hailes and P. A. Dalby, *J. Biotechnol.*, 2008, **134**, 240.
- 12 M. E. B. Smith, E. G. Hibbert, A. B. Jones, P. A. Dalby and H. C. Hailes, *Adv. Synth. Catal.*, 2008, **350**, 2631.
- 13 U. Schörken, H. Sahn and G. A. Sprenger, in *Biochemistry and Physiology of Thiamine Diphosphate Enzymes*, ed. H. Bisswanger and A. Schellenberger, Intemann, Prien, 1996, ch. 6, pp. 543–554.
- 14 U. Nilsson, L. Meshalkina, Y. Lindqvist and G. Schneider, *J. Biol. Chem.*, 1997, **272**, 1864.
- 15 A. Cázares, J. L. Galman, L. G. Crago, M. E. B. Smith, J. Stafford, L. Ríos-Solis, G. L. Lye, P. A. Dalby and H. C. Hailes, *Org. Biomol. Chem.*, 2010, **8**, 1301.
- 16 (a) C. U. Ingram, M. Bommer, M. E. B. Smith, P. A. Dalby, J. M. Ward, H. C. Hailes and G. J. Lye, *Biotechnol. Bioeng.*, 2007, **96**, 559; (b) U. Kaulmann, K. Smithies, M. E. B. Smith, H. C. Hailes and J. M. Ward, *Enzyme Microb. Technol.*, 2007, **41**, 628; (c) M. E. B. Smith, B. H. Chen, E. G. Hibbert, U. Kaulmann, K. Smithies, J. L. Galman, F. Baganz, P. A. Dalby, H. C. Hailes, G. J. Lye, J. M. Ward, J. M. Woodley and M. Micheletti, *Org. Process Res. Dev.*, 2010, **14**, 99.
- 17 K. Smithies, M. E. B. Smith, U. Kaulmann, J. L. Galman, J. M. Ward and H. C. Hailes, *Tetrahedron: Asymmetry*, 2009, **20**, 570.
- 18 U. Schörken, PhD thesis, University of Düsseldorf, 1997.
- 19 M. E. B. Smith, K. Smithies, U. Kaulmann, J. M. Ward and H. C. Hailes, *Bioorg. Med. Chem.*, 2006, **14**, 7062.
- 20 A. J. Humphrey, N. J. Turner, R. McCague and S. J. C. Taylor, *J. Chem. Soc., Chem. Commun.*, 1995, 2475.
- 21 M. E. B. Smith, K. Smithies, T. Senussi, P. A. Dalby and H. C. Hailes, *Eur. J. Org. Chem.*, 2006, 1121.
- 22 J. Galman and H. C. Hailes, *Tetrahedron: Asymmetry*, 2009, **20**, 1828.
- 23 S. J. Costelloe, J. M. Ward and P. A. Dalby, *J. Mol. Evol.*, 2008, **66**, 36.

References

-
- ¹ a) Anastas, P.T.; Warner, J.C. *Green chemistry: Theory and Practice*; Oxford University Press: Oxford; **1998** b) Anastas, P.T.; Kirchhoff, M.M. *Acc. Chem. Res.* **2002**, *35*, 686.
- ² Ran, N.; Draths K. M.; Frost J. W. *J. Am. Chem. Soc.* **2004**, *126*, 6856.
- ³ Reviews a) Wong, C.H.; *Annu. Rev. Microbiol.* **1997**, *51*, 285; b) Wong, C.H.; Halcomb, R.L.; Ichikawa, Y.; Kajimoto, T. *Angew. Chem.* **1995**, *107*, 453; c) Moris-Veras, F.; Qian, X-N.; Wong, C-H.; *J. Am. Chem. Soc.* **1996**, *118*, 7647.
- ⁴ Lohmann, W.; Schuster, G. *Biochem Z.* **1937**, *294*, 188.
- ⁵ Hegeman, H. *J Bacteriol.* **1966**, *3*, 1140.
- ⁶ a) Reynolds, L.J.; Garcia, G.A.; Kozarich, J.W.; Kenyon, G.L. *Biochem.* **1988**, *27*, 5530 b) Wilcocks, R.; Ward, O.P.; Collins, S.; Dewdney, N.J.; Hong, Y.; Prosen, E. *Appl. Environ. Microbiol.* **1992**, *52*, 1699.
- ⁷ Gijssen, H.J.M.; Qiao, L.; Fitz, W.; Wong, C.H. *Chem. Rev.* **1996**, *184*, 97.
- ⁸ a) Wilcocks, R.; Ward, O.P. *Biotechnol. Bioeng.* **1992**, *39*, 1058. b) Prosen, E.; Ward, O.P. *J. Ind. Microbiol.* **1994**, *13*, 287.
- ⁹ Inding, H.; Dünwald, T.; Griener, L.; Liese, A.; Müller, M.; Siegert, P.; Grötzinger, J.; Demir, AS.; Pohl, M. *Chem. Eur. J.* **2000**, *6*, 1483.
- ¹⁰ Dünwald, T.; Müller, M.; Siegert, P.; Demir, AS.; Pohl, M. *Eur. J. Org. Chem.* **2000**, 2161.
- ¹¹ Dünwald, T.; Müller, M.; Iding, M.; Demir, AS.; Pohl, M. *Tetrahedron: Asymmetry.* **1999**, *10*, 4769.
- ¹² De Maria, P.D.; Pohl, M.; Gocke, D.; Gröger, H.; Trautwein, H.; Stillger, T.; Walter, I.; Müller, M.; *Eur. J. Org. Chem.* **2007**, 2940.
- ¹³ Lingen, B.; Kolter-Jung, P.; Dünkelmann, R.; Feldmann, J.; Grötzinger, T.; Pohl, M.; Müller, M.; *Chembiochem.* **2003**, *4*, 721.
- ¹⁴ Gonzalez, B.; Vicuna, R.; *J. Bacteriol.* **1989**, *171*, 2401.
- ¹⁵ Müller, M.; Jenzen, E.; Pohl, M.; Demir, AS. *J. Chem. Soc. Perkin Trans.1*, **2001**, 633.
- ¹⁶ Jenzen, E.; Pohl, M.; Sesenoglu, Ö.; Eren, B.; Hosrik, M.; Demir, AS.; Kolter, D. *Adv. Synth. Catal.* **2002**, *344*, 96.
- ¹⁷ Gocke, D.; Walter, L.; Gauchenova, E.; Kolter, G.; Knoll, M.; Berthold, C.L.; Schneider, G.; Pleiss, J.; Müller, M.; Pohl, M. *Chembiochem.* **9**, 406.
- ¹⁸ Moshbacher, T.G.; Schulz, G.E.; Müller, M. *FEBS J.* **272**, 6067.

-
- ¹⁹ Engel, S.; Vyazmensky, M.; Berkovich, D.; Barak, Z.; Chipman, D.; *Biotechnol. Bioengin.* **2004**, *88*, 825.
- ²⁰ Auge, C.; Delest, V. *Tetrahedron Asymmetry.* **1995**, *6*, 863.
- ²¹ Kren, V.; Crout, D.H.G.; Dalton, D.W.; Hutchinson, W.; Konig,.; Turner, M.M.; *J. Chem. Soc. Chem. Commun.* **1993**, 341.
- ²² Bornmemann, S.; Crout, D.H.G.; Dalton, H.; Lobell, V.; Kren, M.; Thomson, M.; Turner, M.M. *J. Chem. Perkin Trans. 1.* **1995**, 425.
- ²³ Stryer, Lubert. *Biochemistry.* 4th Ed. **1995**, 561.
- ²⁴ Heinrich, P.C.; Steffan, H.; Janser, P.; Wiss, O.; *Eur. J. Biochem.* **1972**, *30*, 533.
- ²⁵ Voet. *Biochemistry*, 3rd Ed. **2004**, 865.
- ²⁶ Sundatröm, M.; Lindqvist, Y.; Schneider, G.; Hellman, U.; Ronne, H.; *J. Biol. Chem.* **1993**, *268*, 24346.
- ²⁷ Muller, Y.A.; Lindqvist, Y.; Furey, W.; Schulz, G.E.; Jordan, F.; Schneider, G.; *Structure 1.* **1993**, 95.
- ²⁸ Ulrika, N.; Meshalkina, L.; Lindqvist, Y.; Schneider, G.; *J. Biol. Chem.*; **1997**, *272*, 1864.
- ²⁹ Gyamerah. M.; Willetts, A.J. *Enzyme Microb. Technol.* **1997**, *20*, 127.
- ³⁰ Fiedler, E.; Thorell, S.; Sandalova, T.; Golbik, R.; Konig, S.; Schneider, G. **2002**, *Proc. Natl. Acad.Sci. U.S.A.* *99*, 591.
- ³¹ Asztalos, P.; Parthier, C.; Golbik, R.; Kleinschmidt, M.; Hubner, G.; Weiss, M.S.; Friedemann, R.; Wille, G.; Tittmann, K.; *Biochemistry.* **2007**, *46*, 12037.
- ³² Wille, G.; Meyer, D.; Steinmetz, A.; Hinze, E.; Golbik, R.; Tittmann, K. *Nat. Chem. Biol.* **2006**, *2*, 324.
- ³³ Arjunan, P.; Sax, M.; Brunskill, A.; Chandrasekhar, K.; Nemeria, N.; Zhang, S.; Jordan, F.; Furey, W. *J. Biol. Chem.* **2006**, *281*, 15296.
- ³⁴ Lobell, M.; Crout, D.H.G. *J. Am. Chem. Soc.* **1996**, *118*, 1867.
- ³⁵ Friedemann, R.; Breitkopf, C. *Int. J. Quant.Chem.* **1996**, *57*, 943.
- ³⁶ Usmanov, R.A.; Kochetov, G.; *Biochemistry.* **1983**, *48*, 478.
- ³⁷ Myles, D.; Andrulis III, P.J.; Whitesides, G.M. *Tetrahedron Lett.* **1991**, *32*, 4835.
- ³⁸ Nilsson, U.; Hecquet, L.; Gefflaunt, T.; Guerard, C.; Schneider, G. *FEBS Lett.* **1998**, *424*, 49.
- ³⁹ Srere, P.; Cooper, J.; Tabachnick, M.; Racker, E. *Arch. Biochem. Biophys.* **1958**, *74*, 295.
- ⁴⁰ Datta, A. G.; Racker, E.; *J. Biol. Chem.* **1961**, *236*, 617.

-
- ⁴¹ Villafranca, J.; Axelrod, B. *J. Biol. Chem.* **1971**, *246*, 3126.
- ⁴² Kobori, Y.; Myles, D.C.; Whitesides, G. M. *J. Org. Chem.* **1992**, *57*, 5899.
- ⁴³ Humphrey, A.J.; Turner, N.J.; McCague, R.; Taylor, S.C.J. *J. Chem. Soc. Chem. Commun.* **1995**, 2475.
- ⁴⁴ Effenberger, F.; Volker, N.; Ziegler, T. *Tetrahedron Lett.* **1992**, *36*, 5157.
- ⁴⁵ Demuynck, C.; Bolte, J.; Hecquet, L.; Dalmas, V.; *Tetrahedron Lett.* **1991**, *32*, 5085.
- ⁴⁶ Bergmeyer, H.U.; *Methods of Enzymatic Analysis*. Verlag Chemie Academic Press: New-York, **1974**, *3*, 1452.
- ⁴⁷ Fluery, D.; Fluery, M.B.; Platzer, N. *Tetrahedron*, **1981**, *37*, 493.
- ⁴⁸ Cordier, P. *C.R.Hebd.Seances Acad. Sci.* **1936**, *202*, 1440.
- ⁴⁹ Dalmas, V.; Demuynck, C. *Tetrahedron: Asymmetry*. **1993**, *4*, 2185.
- ⁵⁰ Bolte, J.; Demuynck, C.; Samaki, H. *Tetrahedron Lett.* **1987**, *28*, 5525.
- ⁵¹ Hobbs, G.R.; Lilly, M.; Turner, N.J.; Ward, J.M.; Willets, A.J.; Woodley, J.M.; *J. Chem. Soc. Perkin Trans. 1*, **1993**, 165.
- ⁵² Morris, K.; Smith, M.E.B.; Turner, N.J.; Lilly, M.D.; Mitra, R.K.; Woodly J.M.; *Tetrahedron Asymmetry*. **1996**, *7*, 2185.
- ⁵³ Unger, F.M. *Adv. Carbohydr. Chem. Biochem.* **1981**, *38*, 323.
- ⁵⁴ a) Sugai, T.; Shen, G.J.; Ichikawa, Y.; Wong, C.H. *J. Am. Chem. Soc.* **1993**, *115*, 413; b) Auge, C.; Delest, V. *Tetrahedron Asymmetry*. **1995**, *6*, 863.
- ⁵⁵ Crestia, D.; Demuynck, C.; Bolte, J. *Tetrahedron*. **2004**, *60*, 2417.
- ⁵⁶ Hecquet, L.; Lemaire, M.; Bolte, J.; Demuynck, C. *Tetrahedron Lett.* **1994**, *47*, 8791; b) Humphrey, A.J.; Parsons, S.F.; Smith, M.E.B.; Turner, N.J.; Lilly, M.D.; Mitra, R.K.; Woodly J.M.; *Tetrahedron Lett.* **1996**, *7*, 2185.
- ⁵⁷ Fetizon, M.; Goulaouic, P.; Hanna, I.; *Tetrahedron Lett.* **1985**, *26*, 4925.
- ⁵⁸ The detailed two step synthesis of 1-chloroalkyl *p*-tolyl sulfoxide (a) Satoh, T.; Kaneko, Y.; Izawa, T.; Sakata, K.; Yamakawa, K. *Bull Chem. Soc. Jpn.* **1985**, *58*, 1983; b) Satoh, T.; Oohara, T.; Ueda, Y.; Yamakawa, K. *J. Org. Chem.* **1989**, *54*, 3130.
- ⁵⁹ Shing, T.K.M.; Tai, V.W.F.; Tam, E.K.W. *Angew. Chem.* **1994**, *106*, 2408.
- ⁶⁰ Laux, M.; Krause, N. *Synlett*. **1997**, 765.
- ⁶¹ Godfrey, J.D.; Mueller, T.C.; Sedergran, N.; Soundarajan, V.J.C.; *Tetrahedron Lett.* **1994**, *35*, 6405.
- ⁶² a) Hassner, A.; Reuss, R.H.; Pinnick, H.W. *J. Org. Chem.* **1975**, *40*, 3427; b) Horiguchi, Y.; Nakamura, E.; Kuwajima, I. *Tetrahedron Lett.* **1989**, *30*, 3323.
- ⁶³ Hoppe, D.; Schmincke, H.; Kleemann, H.W.; *Tetrahedron*. **1989**, *45*, 687.

-
- ⁶⁴ a) Enders, D.; Bockstiegel, B. *Synthesis*. **1989**, 493; b) Linden, G.B.; Gold, M.H.; *J. Org. Chem.* **1956**, *21*, 1175; c) Araki, Y.; Nagasawa, J-i.; Ishido, Y.; *J. Chem. Soc. Perkin Trans. 1*. **1981**, 12.
- ⁶⁵ a) Enders, D.; Eichenauer, H. *Angew. Chem.* **1976**, *88*, 579; b) Enders, D.; Eichenauer, H. *Tetrahedron Lett.* **1977**, *18*, 191.
- ⁶⁶ Kipphardt, H.; Fey, P; Enders, D. *Org. Synth.* **1987**, *65*, 183.
- ⁶⁷ Hundertmark, T.; Lazny, R.; Enders, D. *Synth. Commun.* **1999**, *29*, 27.
- ⁶⁸ Hundertmark, T.; Lazny, R.; Enders, D. *Synth. Lett.* **1998**, 721.
- ⁶⁹ Voith, M.; Ince, S.J.; Enders, D. *Synth.* **2002**, *12*, 1775.
- ⁷⁰ Breuer, I.; Raabe, G.; Enders, D. *Synth.* **2005**, *20*, 3517.
- ⁷¹ Anon. 'Thalidomide 40 years on' <http://news.bbc.co.uk/1/hi/uk/2031459.stm>
- ⁷² Harada, N.; Nakanishi, K. *Circular Dichronic Spectroscopy – Exciton Coupling in Organic StereoChemistry*; University Science Books: Mill Valley, CA, **1983**.
- ⁷³ Wenzel, T.J.; Morin, C.A.; Brechting, A. A. *J. Org. Chem.* **1992**, *57*, 3594.
- ⁷⁴ Dale, J.A.; Mosher, H.S. *J. Am. Chem. Soc.* **1973**, *95*, 512.
- ⁷⁵ Sullivan, G.R.; Dale, J.A.; Mosher, H.S. *J. Org. Chem.* **1973**, *38*, 2143.
- ⁷⁶ Merckx, E.M.; Vanhoeck, L.; Lepoivre, J.A.; Alderweireidt, F.C.; Van der Veken, B.J.; Tollenacre, J.P.; Raymaekers, L.A. *Spectros. Int. J.* **1982**, *2*, 30.
- ⁷⁷ Doesburg, H.M.; Petit, G.H.; Merckx, E.M. *Acta Crystallogr.* **1982**, *B38*, 1181.
- ⁷⁸ Ohtani, I.; Kusumi, T.; Kashman, Y.; Kakisawa, H.A. *J. Org. Chem.* **1991**, *56*, 1296.
- ⁷⁹ Dale, J.A.; Dull, D.L.; Mosher, H.S. *J. Org. Chem.* **1969**, *34*, 2543.
- ⁸⁰ a) Kusumi, T.; Ohtani, I.; Ishitsuka, O.M.; Kakisawa, H. *Tetrahedron. Lett.* **1989**, *30*, 3147; b) Kusumi, T.; Ohtani, I.; Inouye, I.; Kakisawa, H. *Tetrahedron. Lett.* **1988**, *29*, 4731.
- ⁸¹ Latypov S.K.; Ferreira. M.; Quiñoá, E.; Riguera, R. *J. Am. Chem. Soc.* **1998**, *120*, 4741.
- ⁸² Finnamore, E.; Riccio, R.; Rinaldo, G.; Zollo, F.; Minale, L.; *J. Org. Chem.* **1991**, *56*, 1146.
- ⁸³ Tsuda, M.; Toriyabe, Y.; Endo, T.; Kobayashi, J. *Chem. Pharm. Bull.* **2003**, *51*, 448.
- ⁸⁴ Torres-Valencia, J.; Leon, G.I.; Villagomez-Ibarra, J.R.; Suarez-Castillo, O.R.; Cerda-Garcia-Rojas, C.M.; Joseph-Nathan, P. *Phytochem. Anal.* **2002**, *13*, 329.
- ⁸⁵ Smithies, K.; Smith, M.E.B.; Kaulmann, U.; Galman, J.L.; Ward, J.M.; Hailes, H.C.; *Tetrahedron Asymmetry.* **2009**, *20*, 570.
- ⁸⁶ Konno, K.; Fujishima, T.; Liu, Z.; Takayama, H. *Chirality.* **2002**, *13*, 72.

-
- ⁸⁷ Smith, M.E.B.; Hibbert, E.G.; Jones, A.B.; Dalby, P.A.; Hailes, H.C. *Adv. Synth. Catal.* **2008**, *350*, 2631.
- ⁸⁸ Sprenger, G.A.; Schörken, U.; Sprenger, G.; Sahm, H. *Eur. J. Biochem.* **1995**, *230*, 525.
- ⁸⁹ Littlechild, J.; Turner, N.; Hobbs, G.M.; Lilly, M.; Rawas, A.; Watson, H. *Acta. Cryst.* **1995**, *D51*, 1074.
- ⁹⁰ Hibbert, E.G.; Senussi, T.; Costelloe, S.J.; Lei, W.; Smith, M.E.B.; Ward, J.M.; Hailes, H.C.; Dalby, P.A. *J Biol. Technol.* **2007**, *131*, 425.
- ⁹¹ Hibbert, E.G.; Senussi, T.; Costelloe, S.J.; Smith, M.E.B.; Ward, J.M.; Hailes, H.C.; Dalby, P.A. *J Biol. Technol.* **2008**, *134*, 240.
- ⁹² Smith, M.E.B.; Kaulmann, U.; Ward, J.M.; Hailes, H.C.; *Bioorg. Med. Chem.* **2006**, *14*, 7062.
- ⁹³ Mitra, R.K.; Woodley, J.M.; Lilly, M.D. *Enzyme Microb. Technol.* **1998**, *22*, 64.
- ⁹⁴ Demuynck, C.; Bolte, J.; Hecquet, L.; *Tetrahedron.* **1994**, *50*, 8677.
- ⁹⁵ Sevestre, A.; Hélaïne, V.; Guyot, G.; Martin, C.; Hecquet, L. *Tetrahedron Lett.* **2003**, *44*, 827.
- ⁹⁶ Lee, J-Y.; Cheong, D.E.; Kim, G-J.; *Biotechnol Lett.* **2008**, *30*, 899.
- ⁹⁷ Breuer, M.; Pohl, M.; Hauer, B.; Lingen, B. *Anal. Bioanal. Chem.* **2002**, *374*, 1069.
- ⁹⁸ Smith, M.E.B.; Smithies, K.; Senussi, T.; Dalby, P.A.; Hailes, H.C.; *Eur. J. Org. Chem.* **2006**, 1121.
- ⁹⁹ a) Ingram, C.U.; Bommer, M.; Smith, M.E.B.; Dalby, P.A.; Ward, J.M.; Hailes, H.C.; Lye, G.L. *J. Biotechnol. Bioeng.* **2007**, *96*, 559.
- ¹⁰⁰ Galman, J.L.; Hailes, H.C. *Tetrahedron: Asymmetry*, **2009**, *20*, 1828.
- ¹⁰¹ Abbott, A.; Capper, G.; Davies, D.; Munro, H.; Rasheed, R.; Tamyrajah, V.; *Chem. Comm.* **2001**, 2010.
- ¹⁰² Abbott, A.; Capper, G.; Davies, D.; Rasheed, R.; Tamyrajah, V. *Green Chem.* **2002**, *4*, 24.
- ¹⁰³ Crago, L.G.; Galman, J.L.; Smith, M.E.B.; Woodley, J.M.; Hailes, H.C.; Dalby, P.A.; unpublished results **2010**.
- ¹⁰⁴ Lye, G.J.; Woodley, J.M. *Trends Biotechnol.*, **1999**, *17*, 395.
- ¹⁰⁵ Matsumura, I.; Ellington, A.D. *J. Mol. Biol.* **2001**, *305*, 331.
- ¹⁰⁶ Cázares, A.; Galman, J.L.; Crago, L.G.; Smith, M.E.B.; Strafford, J.; Ríos-Solís, L.; Lye, G.L.; Dalby, P.A.; Hailes, H.C. *Org. Biomol. Chem.* **2010**, *6*, 1301.
- ¹⁰⁷ Bach, R.D., Canepa, C. *J. Org. Chem.*, **1996**, *61*, 6346.
- ¹⁰⁸ Botuha, C.; Haddad, M.; Larcheveque, M. *Tetrahedron Asymmetry.* **1998**, *9*, 1929.

-
- ¹⁰⁹ Iwabuchi, Y.; Nakatani, M.; Yokoyama, N.; Hatakeyama, S. *J. Am. Chem. Soc.* **1999**, *121*, 10219.
- ¹¹⁰ Basavaiah, D.; Rao, A. J.; Satyanarayana, T. *Chem. Rev.* **2003**, *103*, 811.
- ¹¹¹ Preliminary results reported by List, B.; Barbas, C. F.; *J. Am. Chem. Soc.* **2000**, *122*, 2395.
- ¹¹² Ahrendt, K.A.; Borths, C.J.; MacMillan, D.W.C. *J. Am. Chem. Soc.* **2000**, *122*, 4243.
- ¹¹³ F. Dickens, *Biochemical preparations.* **1962**, *9*, 86.
- ¹¹⁴ Bellamy, L.J.; Williams, R.L.; *Biochem. J.*; **1958**, *18*, 81.
- ¹¹⁵ Cooper, A.; Ginos, J.; Meister, A.; *Chem. Rev.* **1983**, *83*, 321.
- ¹¹⁶ Reimer, M.; Howard, M. *J. Am. Chem. Soc.* **1928**, *50*, 2506.
- ¹¹⁷ Reimer, M.; Howard, Tobin, E.; Schaffner, M. *J. Am. Chem. Soc.* **1935**, *57*, 211.
- ¹¹⁸ Baylis, A.B.; Hillman, M.E.D.; *Ger. Offen. 2*, **1972**, *155*, 113.
- ¹¹⁹ Papageorgiou, C.D.; Ley, S.V.; Guant, M.J.; *Angew. Chem. Int. Ed.* **2003**, *42*, 828.
b) Papageorgiou, C.D.; Cubillo de Dios, M.A.; Ley, S.V.; *Angew. Chem. Int. Ed.* **2004**, *43*, 4641.
- ¹²⁰ Fischer, G.; Sieber, M.; Schellenber, A. *Bioorg. Chem.* **1982**, *11*, 478.
- ¹²¹ Bailey, M. *Biochemistry.* **1988**, *27*, 6275.
- ¹²² Nahm, S.; Weinreb, S.M. *Tetrahedron Lett.* **1981**, *22*, 3815.
- ¹²³ Michael, J.P. *The Quinoline Alkaloids, In Rodd's Chemistry of Carbon Compounds* 2nd ed. Elsevier, **1998**, *4*, 432.
- ¹²⁴ De Lucas, N.C.; Netto-Ferreira, J.C.; Andraos, J.; Scaiano, J.C. *J.Org. Chem.* **2001**, *66*, 5016.
- ¹²⁵ a) Mandal, T.; Samanta, S.; Zhao, C.G. *Org Lett.* **2007**, *9*, 943. b) Li, H.; Wang, B.; Deng, L. *J. Am. Chem. Soc.* **2006**, *128*, 732.
- ¹²⁶ Mukaiyama, T. *Challenges in Synthetic Organic Chemistry*, OUP, **1990**
- ¹²⁷ a) Oriyama, T.; Imai, K.; Sano, T.; Hosoya, T. *Tetrahedron Lett.* **1998**, *39*, 3529; b) Oriyama, T.; Imai, K.; Sano, T.; Ohashi, K. *Chem. Lett.* **1999**, *28*, 265.
- ¹²⁸ Mase, N.; Nakai, Y.; Ohara, N.; Yoda, H.; Takabe, K.; Tanaka, F.; Barbas III, C.F. *J. Am. Chem. Soc.* **2006**, *128*, 734.
- ¹²⁹ Hayashi, Y.; Tamura, T.; Shoji, M.; *Adv. Synth. Catal.* **2004**, *346*, 1106.
- ¹³⁰ a) Mukaiyama, T. *Tetrahedron.* **1981**, *37*, 4111; b) Kobayashi, S.; Uchiro, H.; Fujisjita, Y.; Shiina, I.; Makaiyama, T. *J. Am. Chem. Soc.* **1991**, *113*, 4247.
- ¹³¹ Chimni, S.S.; Mahajan, D. *Tetrahedron: Asymmetry.* **2006**, *17*, 2108.

-
- ¹³² Dieter, R.K.; Tokles, M. *J. Am. Chem. Soc.* **1987**, *109*, 2040.
- ¹³³ Hendrie, S.K.; Leonard, J. *Tetrahedron*. **1987**, *43*, 3289.
- ¹³⁴ Kobayashi, S.; Hachiya, I. *J. Org. Chem.* **1994**, *59*, 3590.
- ¹³⁵ Heinrich, P.C.; Steffan, H.; Janser, P.; Wiss, O. *Eur. J. Biochem.* **1972**, *30*, 533.
- ¹³⁶ Smith, L.; Anderson R.; *J. Org. Chem.* **1951**, *16*, 963.
- ¹³⁷ Cahnmann, H. *Bull. Soc. Chim.* **1937**, *4*, 226.
- ¹³⁸ Smith; A. *J. Org. Chem.* **1951**, *16*, 972.
- ¹³⁹ Pippel, D.J; Mapes, C.M.; Mani, N.S. *J. Org. Chem.* **2007**, *72*, 5828.
- ¹⁴⁰ Mukaiyama, T.; Iwasawa, N.; Stevens, R.W.; Haga, T. *Tetrahedron*. **1984**, *40*, 1381.
- ¹⁴¹ Calter, M.; Hollis, T.K.; Overman, L.E.; Ziller, J.; Zipp, G.G. *J. Org. Chem.* **1997**, *62*, 1449.